The Dissertation Committee for Juan Carlos Santos Certifies that this is the approved version of the following dissertation:

Phylogeography and the Evolution of Correlated Traits under Multiple Origins of Aposematism in the Poison Frog Family

Committee:

David Cannatella, Supervisor

Molly Cummings

Harold Zakon

Lauren Ancel Meyers

Michael J. Ryan

Phylogeography and the Evolution of Correlated Traits under Multiple Origins of Aposematism in the Poison Frog Family

by

Juan Carlos Santos, B.A.

Dissertation

Presented to the Faculty of the Graduate School of

The University of Texas at Austin

in Partial Fulfillment

of the Requirements

for the Degree of

Doctor of Philosophy

The University of Texas at Austin

August, 2009

Dedication

To my parents, Ernesto and Sara, for being there every time

To Natalia and Ignacio for smiling, completing, and enlightening my life

To the Poison Frogs for teaching me about humility

Acknowledgements

This dissertation is the result of my interaction with great people at all levels during my career as undergraduate and graduate student. I thank Luis Coloma for his insights in the poison frogs and his uncommon knowledge into the Neotropical natural history of frogs. I thank the David Cannatella and the Cannatella Lab (past and present) for the companionship, support, and criticisms during my years as a graduate student.

I thank Art Woods for a complete and clear introduction to experimental physiology; Richard Ree for sharing his insights in historical biogeography; Janalee Caldwell and Kyle Summers for sharing their knowledge on the biology of poison frogs. I thank N. Biani, J. Brown, E. Lemmon, G. Pauly, and B. Symula for suggestions about data analysis and proofreading my texts. I thank to my friends in EEB for their support, camaraderie, and amity during my years in Texas. I thank specially to Catalina, Samraat, Barrett, Naira, Juanita, Carlos, Christian, Simone, and Monica.

I thank my field companions C. Barrio, N. Biani, R. F. Guerrero, J. Gómez, I. Tapia, E. Tapia, F. Ayala, C. Aguilar, and R. Schulte for their unparallel assistance. I thank the common people of Ecuador, Panamá, Perú,

Venezuela, and Colombia that shared with me their kindness and knowledge of poison frogs that live in their backyards and crop fields.

I thank the Smithsonian Tropical Research Institute, A. Amézquita (Universidad de los Andes, Bogotá), and QCAZ museum for field guidance and lab space. I thank M. Baquero, R. F. Guerrero, and J. Gómez, for her unparallel support and patience during the physiological experiments.

I thank for the research and collection permits to the Dirección Nacional de Áreas Protegidas y Vida Silvestre (Panamá; permit SE/A-4-6), Ministerio de Ambiente (Ecuador; permits 0004-IC-FAU-DNBAP/MA, 0006-IC-FAU-DNBAP/MA, 016-IC-FAU-DNBAP/MA, 027-IC-FAU-DNBAPVS/MA), Instituto Nacional de Recursos Naturales-INRENA (Perú; permits 061-2003-INRENA-IFFS-DCB, 002765-AG-INRENA, 003-2005-INRENA-IFFS-DCB and CITES Permit No. 4326) and the Conselho Nacional de Desenvolvimento Científico e Tecnológico (Brazil; CNPq, Portaria MCT no. 170, de 28/09/94) and the Instituto Brasileiro do Meio Ambiente e dos Recursos Naturais Renováveis (Brazil) (IBAMA, no. 073/94-DIFAS), under a research agreement between the Oklahoma Museum of Natural History and the Museu Paraense Emilio Goeldi.

I thank for the loan of tissue samples to C. Aguilar (Museo de Historia Nacional San Marcos, Lima), I. de la Riva and I. Rey (Museo Nacional de Ciencias Naturales, Madrid), R. Ibañez (Smithsonian Tropical Research Institute), L. Trueb, W. E. Duellman and J. Simmons (University of Kansas), S. B. Hedges (Pennsylvania State University), C. Cicero (Museum of Vertebrate Zoology,

University of California at Berkeley), and D. L. Dittmann (Louisiana State University Museum of Natural Science).

I thank the National Science Foundation, which provided support (DDIG DEB-0710033 under IACUC protocol 05111001), and the University of Texas EEB Graduate Research Fellowships. David Cannatella research grants (EF-0334952) also supported field and lab experiments of this dissertation.

Finally, I thank to my parents, Ernesto and Sara, to my brothers, Mauricio and Fabian, to my wife, Natalia, to my son, Ignacio, and to my grandmother, Teresita, for their enduring and unselfish support.

Phylogeography and the Evolution of Correlated Traits under Multiple Origins of Aposematism in the Poison Frog Family

Publication No._____

Juan Carlos Santos, Ph. D.

The University of Texas at Austin, 2009

Supervisor: David Cannatella

Living organisms are under selection not only for one, but also for several inheritable characters at the same time. Well-sampled and well-supported phylogenies are necessary for the studies of character evolution and their history. The poison frogs (Dendrobatidae) are a well-known example of aposematism in anurans. They include ~270 species of Neotropical frogs with aposematic (toxic and conspicuous) and non-defended (palatable and cryptic) species. The origin of aposematism in poison frogs is puzzling, because of its predicted low probability of establishment due to the prey's increased conspicuousness. Previous studies suggested a single origin of toxicity and warning coloration. By expanding taxon sampling of the group, I reexamined the phylogenetic correlation between the origins of toxicity and warning coloration. I found four or five independent origins of aposematism; by using simulations, I rejected hypotheses of one, two,

or three origins of aposematism ($P < 0.002$). I also found that diet specialization is linked with the evolution of aposematism and has evolved independently at least two times. Poison frogs are endemic to the Neotropic, which is one of the Earth's largest reservoir of biodiversity. I reconstructed the biogeography of the poison frog clade and rejected an Amazonian center-of-origin in favor of a model expanding over the Neotropics. I inferred 14 dispersals into and 18 out of Amazonia to adjacent regions; the Andes were the major source of dispersals into Amazonia. Significant percentage of dendrobatid diversity in Amazonia and Chocó resulted from repeated immigrations, with radiations at <10.0 million years ago. In contrast, the Andes, Venezuelan Highlands, and Guiana Shield have undergone extended in situ diversification at near constant rate since the Oligocene. Poison frogs have significant variation on their physiological characteristics. I measured resting and active metabolic rates of 54 species. I traced metabolic measurements along aposematism, diet specialization, molecular rates, and body mass. I found a synergistic and co-adapted functionality of active metabolic rates with all previous traits that is perhaps the consequence of the increase in complexity in most biological systems. My thesis has expanded the knowledge of the biology, phylogenetic history, and biogeography of the poison frogs.

Table of Contents

List of Tables

List of Figures

Figure 2.1: Biogeographic areas, extension of the floodbasin system or marine incursions (hatched arrows), and possible connections within Cenozoic paleogeographic maps of Central and South America, modified (Hoorn, 1994; Diaz de Gamero, 1995). Panels A-D correspond to paleogeographic reconstruction of northern South America. A: early to late Eocene; B: late Oligocene to middle Miocene; C: middle to late Miocene; and D: early Pliocene to the present. Uncertainties about the limit between biogeographic regions before the Pliocene are indicated by "?". The hypotheses about the spatial configuration of biogeographic areas on the origin of Neotropical diversity are indicated in the panels E-G. E: the null model (H_0: SM0), that assumes no spatial structure and equal rates of dispersal among all areas; F: the center-of-origin model (H_A: SM1), that assumes the Amazonia as the primary center of origin with widespread ancestral ranges constrained to include the Amazon Basin; and G: the stepping-stone model (H_A: SM2), that the assumes the historical spatial arrangement of biogeographic areas and constrains dispersals among geographically adjacent areas. The biogeographic areas used in the dispersal-extinction-cladogenesis (DEC) modeling are the Amazon Basin (C), Guiana Shield (B), Venezuelan Highlands and Trinidad and Tobago Islands (D), North Oriental Andes (E), North Occidental Andes (F), Central Oriental Andes

Figure 2.2: Box Chronogram and major biogeographic events of the poison frogs divided by major regions and inferred from the DEC (dispersal-extinction-cladogenesis) analysis. The green slice of the pie charts is the proportion of the likelihood associated with Amazonian reconstruction using Bayesian analysis of ancestral traits. The test results against the null hypothesis of an Amazonian ancestral state are indicated as * ($p < 0.05$) significant and ** ($p < 0.001$) highly significant. In the chronogram, support values from 200 non-parametric bootstrap replicates (ML), Bayesian posterior probabilities (PP), and the 95% CI of the estimated node age are also indicated. The major geographical events reconstructed using the SM2 model were mapped onto the ML phylogeny. The Amazon Basin subtree includes dispersals into Amazonia (numbered white squares), out of Amazonia (numbered gray squares), major lineage diversifications (5), and a lineage extinction (†). The Andes subtree includes cross-Andean (*ca* boxes) events, Northern-Southern Andean (*ns* boxes) dispersals, and the identification number of each event (Santos et al. 2009). The Guiana-Venezuela subtree includes dispersals toward this region from the Amazon Basin lineages (*ad* boxes) and the identification number of each event (Santos et al. 2009). The Central America-Chocó subtree indicates the three dispersals from Chocó and

Figure 2.3: The genus-supraspecific level tree (GSPF chronogram) of poison frogs with known taxonomic diversity (i.e., numbers within parentheses) and significant diversification rate changes for nodes or lineages from Table 2.3 (🡅 indicates rate increase, and 🡇 indicates rate decrease). Taxonomic diversity is indicated by the species sampled in our study (left number) and the total number of species described per group or genus (right number). The highest diversification increase (node 1) corresponds to the widespread *Ameerega* lineage that rapidly expanded into Amazonian since the late Miocene. The Andean-Amazonian increase (node 2) corresponds to the diversification of clade *Colostethus* 2 in the early Miocene. The Chocoan increases (nodes 3 and 10) correspond to the lowland radiation in western Colombian and Ecuadorian lowlands of *Colostethus* sensu lato, *Epipedobates*, and *Silverstoneia* during the middle Miocene and before the formation of the Panamanian Land Bridge. The Guiana decrease in the early Miocene (node 4) corresponds to the *Allobates* lineage of the Guianan tepuis. The Amazonian rate increases (nodes 5 and 9) correspond the largest radiation of *Allobates* since the Miocene to the Pliocene. The Andean-Amazonian increase (node 6) corresponds to the diversification of clade *Dendrobates* from the eastern Central Andean foothills into Amazonia since the early Miocene. The Andean decreases

Figure 3.5: Maximum likelihood reconstructions and CLSR regression analyses of high aerobic scope, conspicuousness, and alkaloid sequestration in poison frogs. Positive character states are indicated by black boxes at the tips of the phylogeny: metabolic scope (positive residual after mass correction), conspicuousness (bright coloration), alkaloid sequestration (able to sequester), and diet specialization (ant and mite specialist). Unknown states are indicated by dots. The traced reconstructions over the phylogeny correspond to the aerobic scope after mass correction and the fraction of relative likelihood probability of high aerobic capacity (black) or low aerobic capacity (white). Rounded boxes indicate four origins of tandem evolution of bright coloration, alkaloid sequestration, and diet specialization. Two origins of bright coloration were not associated alkaloid sequestration and diet specialization and the conspicuousness icon indicates them. Plots of the CLSR regression including the categorical variables of (A) conspicuousness, and (B) alkaloid sequestration for AMR (circles) and RMR (diamonds) and body mass. Results from the homogeneity of slopes and similar intercept (constant) are indicated in the black box (***, P <0.001; NS, P > 0.05). Plot of the PIC regression analysis (C) of the metabolic scope and body mass independent contrasts. Lettered diamond boxes correspond

Chapter 1: Multiple, recurring origins of aposematism and diet specialization in poison frogs

INTRODUCTION

Aposematism is the association, in a prey organism, of the presence of a warning signal with unprofitability to predators. The origin of aposematism is puzzling, because of its predicted low probability of establishment in a population due to the prey's increased conspicuousness. Aposematism is a widespread trait in invertebrate taxa, but, in vertebrates, it is mostly evident in amphibians, reptiles, and fishes. Poison frogs (Dendrobatidae) are one of the most well known examples of the co-occurrence of warning coloration and toxicity. This monophyletic group of mostly diurnal leaf-litter Neotropical anurans has both toxic/colorful and palatable/cryptic species. Previous studies suggested a single origin of toxicity and warning coloration, dividing the family in two discrete groups of primitively cryptic and more derived aposematic frogs. Recent molecular phylogenetic analyses using mostly aposematic taxa supported this conclusion and proposed a single tandem origin of toxicity and conspicuous warning coloration. By using expanded taxon and character sampling, we reexamined the phylogenetic correlation between the origins of toxicity and warning coloration. At least four or five independent origins of aposematism have occurred within poison frogs; by using simulations, we rejected hypotheses of one, two, or three origins of aposematism ($P < 0.002$). We also found that diet

specialization is linked with the evolution of aposematism. Specialization on prey, such as ants and termites, may have evolved independently at least two times.

Warning signals may inform a predator that the intended prey is toxic, unpalatable, or generally not worth the predator's effort. The association of unprofitability with a warning signal, such as bright or conspicuous coloration, is known as aposematism. Its evolutionary origin has posed a conundrum since the time of Wallace and Darwin (Mallet and Joron 1999). Although aposematism evolves as a predator deterrent, its chance of establishment in a population is predicted to be low, because it would lead to an increased probability of predation (Yachi and Higashi 1998). Aposematism exists in many invertebrates, fishes, amphibians, snakes, and birds (Komárek 1998). Models proposed to explain the origin of aposematism (e.g., individual selection versus kin selection, gregariousness, greenbeard selection) treat trait evolution at only the population level (Fisher 1958; Guilford 1988; Lindström et al. 1999; Servedio 2000). In contrast, a phylogenetic perspective can provide evidence for the likelihood of historical patterns of trait evolution (e.g., does toxicity always evolve before conspicuousness?), but this approach has rarely been examined (Guilford 1988) (Harlin and Harlin 2003; Sillén-Tullberg 1988).

Well supported and well sampled phylogenies are fundamental for comparative biology, and reliable inferences should likely be derived from them (Harlin and Harlin 2003) (Felsenstein 1985). Ancestral character states, and their order of appearance (i.e., character mapping), can be mistakenly reconstructed if taxon sampling is not comprehensive (Pollock et al. 2002). Although most

analyses of aposematism perform tests for predator deterrence based on hypotheses of current utility only, aposematism can be defined within a historical context as the consecutive or prior occurrence of unpalatability, relative to conspicuousness (Harlin and Harlin 2003). The addition of a phylogenetic framework in these tests would facilitate the identification of the sequences of evolutionary transformations in these traits.

Poison frogs (Dendrobatidae) are a well supported monophyletic group (±210 species) distributed in tropical South and Central America (Ford and Cannatella 1993). The family includes both aposematic and cryptic species, all of which are diurnal, with *Aromobates nocturnus* being the one exception (Myers et al. 1991). Some species (primarily *Dendrobates, Phyllobates,* and *Epipedobates*) are brightly colored and possess toxic, lipophilic skin alkaloids (Daly et al. 1999). Some of these substances are of biomedical importance (Daly et al. 2000b), and their source is probably dietary (Daly et al. 2002). Other species (e.g., *Colostethus, Mannophryne,* and *Nephelobates*) are cryptic and nontoxic, lacking lipophilic skin alkaloids, as far as is known (Myers et al. 1991) (Coloma 1995; Daly 1998). Based on the assumption that structurally complex biochemical compounds are difficult to evolve, the possession of alkaloids was believed to have originated once in dendrobatids (Myers et al. 1991). Phylogenetic analyses of characters other than DNA (Myers et al. 1995; Myers et al. 1991) also proposed a single origin of toxicity. These findings were supported by an analysis of DNA sequences (Clough and Summers 2000), although other smaller datasets (Vences et al. 2000) had suggested the possibility of convergence. Here we show,

based on a more comprehensive taxon sample, that the association of conspicuous bright coloration and toxicity appeared not once, but several times, within poison frogs.

Aposematic species (*Dendrobates, Phyllobates*, and some *Epipedobates*) eat mostly ants, termites, and mites (Caldwell 1996; Toft 1981; Toft 1995). Some *Dendrobates* exclusively eat ants or mites and reject other available prey (Toft 1995). The majority of cryptic species (*Colostethus*) eat diverse prey (Caldwell 1996), mostly everything available that is the right size. Natural history and ecological studies suggest that higher degrees of toxicity and toxin diversity are directly associated with a specialized diet (Daly et al. 2002), which has been assumed to have evolved only once within dendrobatids (Caldwell 1996; Toft 1995). Here we present evidence that diet specialization has occurred more than once, and is tightly associated with the multiple origins of conspicuousness and toxicity.

MATERIALS AND METHODS

Phylogeny Estimation

We sampled a broadly representative group of cryptic and aposematic dendrobatids. We sequenced 56 samples, of which six were outgroups [*Bufo variegatus* (Bufonidae), *Centrolene grandisonae* (Centrolenidae), *Pseudacris regilla* (Hylidae), *Pseudis paradoxa* (Pseudidae), *Telmatobius niger*, and *Adenomera* sp. (Leptodactylidae); for brevity, these samples are not shown on the phylogenetic trees]. The remaining 50 samples represented 38 species of

dendrobatids from most species groups of *Colostethus*. Taxonomically, we include *Minyobates* within *Dendrobates*, and *Phobobates* in *Epipedobates* (Clough and Summers 2000). These data included 2,298 characters from the entire 12S, tRNA-val, and almost all of the 16S mitochondrial genes. These data were combined with 22 dendrobatid sequences from GenBank, most of which consist of 900 bases that are completely overlapped by our data. Specimen museum numbers, collection localities, lists of primers used, and GenBank accession nos. can be seen in Tables 1 and 2, which are published as supporting information (Santos et al. 2003).

Preliminary alignment was done with clustalx (Thompson et al. 1997). The ambiguously aligned regions were realigned under various parameters of clustalx, and were finally adjusted by eye to produce a parsimonious alignment; thus, informative sites were minimized. Hypothesized secondary structure diagrams from the Comparative RNA web site (www.rna.icmb.utexas.edu) were consulted to optimize alignments. We analyzed four configurations of the data under parsimony by using paup* (Swofford 2000); a combination of both datasets; (i) including and (ii) excluding regions of doubtful alignment (248 base pairs); (iii) a reduced-character dataset with only the GenBank regions common to all taxa (900 base pairs); and (iv) a reduced-taxon dataset using only our sequences. All shorter GenBank sequences were omitted, as were as the unalignable characters. Likelihood and Bayesian analyses (Huelsenbeck 1991) were performed by using configuration ii. By using a hierarchical test of models (Posada and Crandall 1998) the best fitting model was found to be GTR+G+I, and

parameters for this model were estimated during the likelihood search. In the Bayesian analysis, model parameters were also estimated during the run with starting default values of the 10 Markov chains with 0.2 as the value of the exponential prior. Four independent mrbayes runs were executed; each used a random starting tree for 1 million generations and sampled every 10 generations, resulting in 100,000 sampled trees. We determined whether the Markov chains had reached stationarity by examining plots of likelihood scores of sampled trees against generation time. Log-likelihood scores for the sampled trees stabilized after 60,000 generations. The first 10,000 trees sampled were discarded, and the posterior probabilities were estimated with the remaining trees. The posterior probability of each bipartition was calculated by using a majorityrule consensus tree of the retained trees. A clade was considered significantly supported if its posterior probability was ≥95%. All four Bayesian runs produced concordant results. Parsimony and likelihood analyses yielded almost identical trees.

Hypothesis Testing

For testing hypotheses of multiple origins of aposematism, we compared the optimal tree (alternative hypothesis) to trees constrained to represent null hypotheses of one, two, three, and four origins of conspicuous coloration. Sequence evolution parameters were estimated by using maximum likelihood under the GTR+G+I model. We used parametric bootstrapping procedures (Swofford et al. 1996) to evaluate 500 simulated datasets generated by using seq-gen 1.2.5 (Rambaut and Grassly 1997) for each test. Because the GenBank

sequences were shorter than our sequences (i.e., 900 vs. 2,298 base pairs), only the regions in common (configuration iii above) were used. Thus, the bootstrapping tests are more conservative; with fewer data, the null hypothesis is more difficult to reject (Huelsenbeck et al. 1996).

Phylogenetic analysis with no topological constraints indicated five origins of bright coloration. This tree was compared with other topologies that were constrained to have various number of origins (null hypotheses). For the hypothesis of a single origin, all brightly colored species were constrained to be an exclusive clade. For the hypothesis of two origins, all possible constraints using pairwise combinations of the five brightly colored clades were evaluated, and the shortest resulting tree (i.e., the one least likely to reject the null hypothesis) was used (one constraint for Dendrobates plus Phyllobates and a second for all other brightly colored species). The constraints for three and four origins were determined in a similar fashion by using combinations of three and four clades.

To infer the presence of aposematism, a correlation between conspicuous coloration and toxicity was tested by using the concentrated changes test in macclade 4.0 (Maddison and Maddison 2000). The reconstructed changes of the two traits (conspicuous coloration and presence of toxins) on the optimal tree were compared with a null distribution from 10,000 simulated datasets. Because there is some disagreement as to whether certain species are “conspicuously” colored, we repeated the correlated changes tests under three criteria: (i) the presence of obvious bright coloration on the exposed surfaces; (ii) a published

table of coloration scores (Summers and Clough 2001) for 21 species, with interpolation of additional species based on our field experience with these animals in life, by using field notes and photographs; and (iii) a traditional taxonomic definition, in which species of *Dendrobates, Phyllobates, Allobates, Cryptophyllobates*, and *Epipedobates* are scored as conspicuous, and species of Colostethus are scored as cryptic (Santos et al. 2003). The different criteria affected three species (*Allobates femoralis, Epipedobates boulengeri*, and *Epipedobates* sp. F), but the results of the correlation tests were the same regardless of which definition of conspicuous coloration was used.

RESULTS

The results of parsimony, likelihood, and Bayesian analyses were highly concordant, and four well supported clades were identified (Fig. 1a, clades A–D), each with conspicuously colored species. On the parsimony topology (Fig. 1), the most-parsimonious reconstruction shows five independent origins of warning coloration (species names are bold). A less-parsimonious reconstruction of six changes requires three origins and three losses. On the likelihood and Bayesian topologies (Fig. 2) the reconstruction also requires five origins (shown as gray boxes); a less-parsimonious reconstruction under the assumption of no losses requires seven origins.

With the exception of *Cryptophyllobates azureiventris*, for which no data on toxins are available, each group of conspicuously colored species includes species with toxic skin alkaloids (Santos et al. 2003). The correlated changes test

indicates that the independent appearances of conspicuous coloration and skin alkaloids are significantly correlated ($P < 0.001$), even though data on toxins are missing for many of the cryptic species. Thus, we conclude that aposematism (i.e., an association between defense and warning coloration) evolved de novo four (and probably five) times; this result is independent of the three criteria used to characterize species as conspicuous.

By using parametric bootstrapping, we tested whether the tree requiring five origins of aposematism (null hypothesis) could be distinguished from a tree with fewer origins. The null hypothesis was rejected at $P < 0.002$ for each hypothesis of one, two, or three origins. In each case, the observed tree-length difference was >10 steps longer than the greatest difference from the simulated data. We could not reject the four origins of aposematism ($P = 0.782$), indicating that the two observed origins of aposematism in the *Epipedobates* group within clade C (Fig. 1) cannot be statistically distinguished from one origin. However, the reduced dataset of 900 base pairs used for the simulations diminishes the power of these tests. More extensive analyses, including more *Epipedobates* species and more complete sequences, would be needed to distinguish between four or five independent origins of aposematism within the poison frogs.

The hypothesis of multiple origins of aposematism is more robust than previous hypotheses, because we sampled a broad array of cryptically colored species from throughout the taxonomic diversity of the family. If only aposematic species are analyzed, almost no differences exist between our tree and that of a previous study (Clough and Summers 2000) (compare Fig. 1 a and b). Also, the

current taxonomy is misleading, with respect to evolutionary relationships, because it relied on bright coloration as a diagnostic character. *Colostethus*, a group of inconspicuous species, is paraphyletic with respect to *Allobates*, *Cryptophyllobates*, and *Epipedobates*, with the latter being a polyphyletic assemblage of independent aposematic lineages. Previously, *C. azureiventris* (Lötters et al. 2000) was considered to be an *Epipedobates*. The extensive polyphyly of *Epipedobates* can be reduced by transferring *Epipedobates zaparo* (clade A) to *Allobates*; thus, the name is *Allobates zaparo* (new combination). However, *Colostethus* remains grossly paraphyletic; reducing the degree of polyphyly of *Epipedobates* by recognizing *Allobates* and *Cryptophyllobates* is but a transitional solution toward a classification of dendrobatids based solely on monophyletic taxa. Notwithstanding these taxonomic changes, the remaining *Epipedobates* species in clade C are not monophyletic. Resolution of this clade is crucial for the Linnean taxonomy of dendrobatids, because it contains the type species of *Epipedobates* (*tricolor*) and may also contain the type species of *Colostethus* (*latinasus*), based on morphological similarity (Coloma 1995). Given the current lack of molecular data on the position of *Colostethus latinasus*, a wholesale revision of poison frog taxonomy is beyond the scope of this paper.

A striking feature of the multiple origins is that they occur on different time scales, indicating recurring origins through evolutionary history. Aposematism had a single ancient origin at the base of clade D (*Dendrobates* plus *Phyllobates*) and was not lost in any descendants in this clade. Alkaloid data are available for most species in this clade, and all are toxic. The other origins of

aposematism are much more recent. For example, sequence divergence (uncorrected p-distance) between the cryptically colored *Colostethus machalilla* and its toxic, bright red sister species *Epipedobates tricolor* (Fig. 2) is a mere 0.9–1.0%. The latter species is the natural source of epibatidine, an alkaloid that is an opioid analgesic (Daly 1998). In contrast, divergence in the same genes is 1.7–5.7% among five well differentiated and strikingly variable and brightly colored species of the *Dendrobates pumilio* group (Fig. 1). Such low genetic divergence is not necessarily inconsistent with extreme color divergence, because color pattern in some model organisms is controlled by very few genes (Koch et al. 2000). Nonetheless, the low genetic divergence suggests the microevolutionary lability of defensive signals and toxicity in these frogs.

A significant correlation between evolutionary change in degree of conspicuous coloration and degree of toxicity in poison frogs was demonstrated (Summers and Clough 2001) under the hypothesis of a single origin of aposematism, and this correlation holds under a hypothesis of multiple origins. However, we found no significant correlation between the appearance of each trait under the single-origin hypothesis (correlated changes test; $P = 0.975$). However, as stated above, the independent appearances of conspicuous coloration and toxicity under the multiple-origins hypothesis are significantly correlated ($P < 0.001$). A correlation between coloration and toxicity is not surprising when one considers distantly related groups such as coral snakes, monarch butterflies, and nudibranch molluscs. However, the presence of this correlation within a group of

closely related species invites a consideration of possible mechanisms for the origin of aposematism.

Accumulating evidence suggests that poison frogs sequester toxins from their diet. Most brightly colored and toxic dendrobatids (*Dendrobates*, *Phyllobates*, and *Epipedobates*) are dietary specialists on ants, termites, or mites. Thus, they eat many and smaller prey, whereas the cryptic and nontoxic species (*Colostethus*) have generalized diets of few and larger prey (Caldwell 1996; Toft 1995). Specialized phenotypic traits in diet-specialized dendrobatids (e.g., narrow head and tongue) are recognized as adaptations for foraging on tiny prey (Vences et al. 1998). The aposematic species have probably evolved narrow diets to maximize the accumulation of toxins from diet (Daly et al. 2002). Experiments have shown that at least two poison frog species derive alkaloids from ants, and that *Dendrobates auratus* can sequester certain alkaloids (allopumiliotoxins and izidines) from food supplements (Daly et al. 1994b). When raised on fruit flies, captive *Phyllobates*, *Dendrobates*, and *Epipedobates tricolor* lose much of their toxicity (Daly et al. 2000a; Daly et al. 1992). Nonetheless, despite the demonstration of alkaloid sequestration, the source of the most biologically active alkaloids; i.e., batrachotoxins, histrionicotoxins, epibatidine, and others, remains unknown (Daly 1998).

Based on the available information, our phylogeny demonstrates at least two, and perhaps three, independent origins of dietary specialization (Fig. 2). One origin of diet specialization is in the ancestor of clade D (*Phyllobates* and *Dendrobates*), in which all species are ant, termite, or mite specialists (Caldwell

1996). A second origin is within clade C (*Epipedobates* and *Colostethus*), in which some species have generalist diets (including the brightly colored *E. tricolor*), but *E. parvulus* and its relatives are ant specialists (Caldwell 1996). A possible third origin is in clade A, in which most species, including *A. femoralis*, have generalist diets. However, the limited data (Almendáriz 1987) indicate that *A. zaparo*, its brightly colored sister species (Fig. 1), eats mostly ants. Although there is a clear phylogenetic correlation between bright coloration and toxicity (as demonstrated by the correlated changes test), data sufficient to test the association of diet are lacking for most species.

Under the single-origin hypothesis, dietary specialization and foraging ecology were predicted to be key evolutionary factors in the diversification of poison frogs (Caldwell 1996; Toft 1995; Vences et al. 1998). Under this multiple-origins hypothesis, the evolutionary association between diet and aposematism may be more complex. Although one large clade (D) displays an ancient origin of aposematism, most of the origins are relatively recent and involve one or a few species, suggesting that this homoplasy is dynamic and recurring. The specialization on different prey types (ants, termites, or mites), which may explain the great diversity of alkaloids, suggests selection for specialization per se (Futuyma and Moreno 1988), rather than commitment to a particular food resource. For example, *E. tricolor* is toxic but is not specialized on ants or termites, which suggests that this species might sequester toxins from unrecognized sources, such as larger-prey items.

The association of dietary specialization and sequestration of toxic defensive compounds in aposematic organisms is not novel to frogs. For example, two unrelated lineages of aposematic papilionid butterflies sequester aristocholic acid compounds from pipevines (Aristolochiaceae) (Nishida 2002). *Longitarsus* leaf beetles (Chrysomelidae) have evolved the sequestration of pyrrolizidine alkaloids multiple times (Dobler 2001). However, dendrobatid frogs are unique among vertebrates in their recurring associations of coloration, toxicity, and diet specialization. This observation suggests an as-yet-unidentified physiological mechanism in the ancestor of poison frogs that allowed sequestration of toxic compounds.

Fragmentary but exciting evidence suggests other behavioral traits that may be associated with aposematism and dietary specialization. In contrast to almost all other frogs, both cryptic and aposematic dendrobatids are diurnal, rather than nocturnal, with the apparent exception of *A. nocturnes* (Myers et al. 1991). This change to a diurnal habit, in which visual signals would be favored, may have facilitated repeated adaptive shifts toward novel foraging ecology, dietary specialization, toxicity, and bright coloration. Also, high aerobic and low anaerobic metabolic capacity have been found in the few aposematic dendrobatid species studied (Taigen and Pough 1985). In contrast, cryptic species of other leaf-litter frogs (*Eleutherodactylus*) that co-occur with these dendrobatids have low aerobic and high anaerobic capacity (Taigen and Pough 1985), and are not dietary specialists on ants (Caldwell 1996). This physiological trait in some dendrobatids probably favored a recurring association of these traits. More data

about metabolic rate in dendrobatids are needed within this phylogenetic framework.

Ecological specialization is a widespread evolutionary outcome in many animal systems (Futuyma and Moreno 1988). It is commonly stated that a specialization should derive from a generalized, plesiomorphic trait. This finding appears to be true in the case at hand; the traits of conspicuousness, unpalatability, and narrow diet are derived from crypticity, palatability, and a generalized diet, respectively. In the phylogeny presented here, these derived traits are not statistically independent, and probably reinforce each other, promoting evolutionary specialization. The appearance of toxicity may generally precede the appearance of diet specialization and warning coloration. Evidence for this possibility comes from three cases. First, *A. nocturnus*, the putative sister species of all dendrobatids, has a noxious, mercaptan-like odor, despite the lack of alkaloids (Myers et al. 1991) and its cryptic coloration. Second, although the few *Colostethus* sampled for lipophilic alkaloids show no traces (Daly et al. 1999), *Colostethus inguinalis* has tetrodotoxin (Daly et al. 1994a), a water-soluble (rather than lipophilic) toxin otherwise unknown in dendrobatids. These two cases suggest parallel but isolated origins of defense in obviously cryptic species. Third, certain species are not brightly colored, but have either flash coloration or contrasting patterns on concealed surfaces; these species also have some degree of alkaloid toxicity (*A. femoralis, E. boulengeri*, and its sister species, *E*. sp. F), and are closely related to brightly colored species. These species may represent microevolutionary cases of dynamic intermediate conditions between the cryptic-

palatable and conspicuous-toxic extremes. However, the data are meager and much work at the population level is needed to confirm this hypothesis.

At the other extreme, all conspicuous species (*Dendrobates*, *Phyllobates*, and most *Epipedobates*) surveyed possess diverse and often abundant toxins (Daly et al. 1999); i.e., no Batesian mimics are known. Furthermore, although the degree of diet specialization among the toxic species varies, the diets of the least specialized toxic species are still narrower than those of the cryptic species (Caldwell 1996; Toft 1995).

In summary, a more comprehensive phylogeny reveals the multiple appearances of this complex of traits (visual signals, toxicity, narrow diet, and, perhaps, higher metabolic rate), which suggests parallel and correlated evolutionary trends toward specialization. These multiple occurrences may indicate directional selection for the acquisition of toxins from dietary components, which likely led to aposematic coloration and feeding specializations.

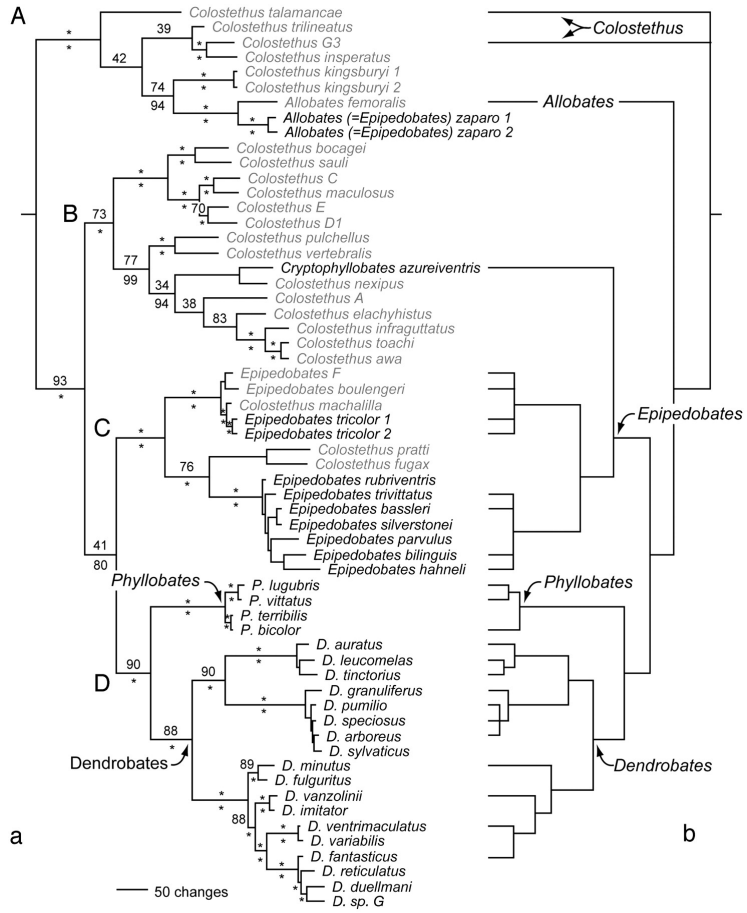

Figure 1.1: (a) Phylogeny of poison frogs. Species names in black refer to conspicuous and (as far as is known) toxic species. Names in gray refer to cryptic and nontoxic species. The tree shown is based on the parsimony analysis, but the likelihood tree (Fig. 1.2) is almost identical. The sister-group relationship of clades C and D was recovered in all three types of analyses. In the parsimony analysis, the sister-group relationship of clades B and C was equally supported, but this topology was not the best estimate under likelihood or Bayesian analysis. Neither alternative (clade C + D vs. clade B + C) is strongly supported by bootstrap proportions or Bayesian posterior probabilities. Parsimony bootstrap proportions are above each branch, and Bayesian posterior probabilities are below. *, a value of ≥95. (b) Previous molecular phylogeny of poison frogs (Summers and Clough 2001). The difference between a and b is due to the degree of taxon sampling.

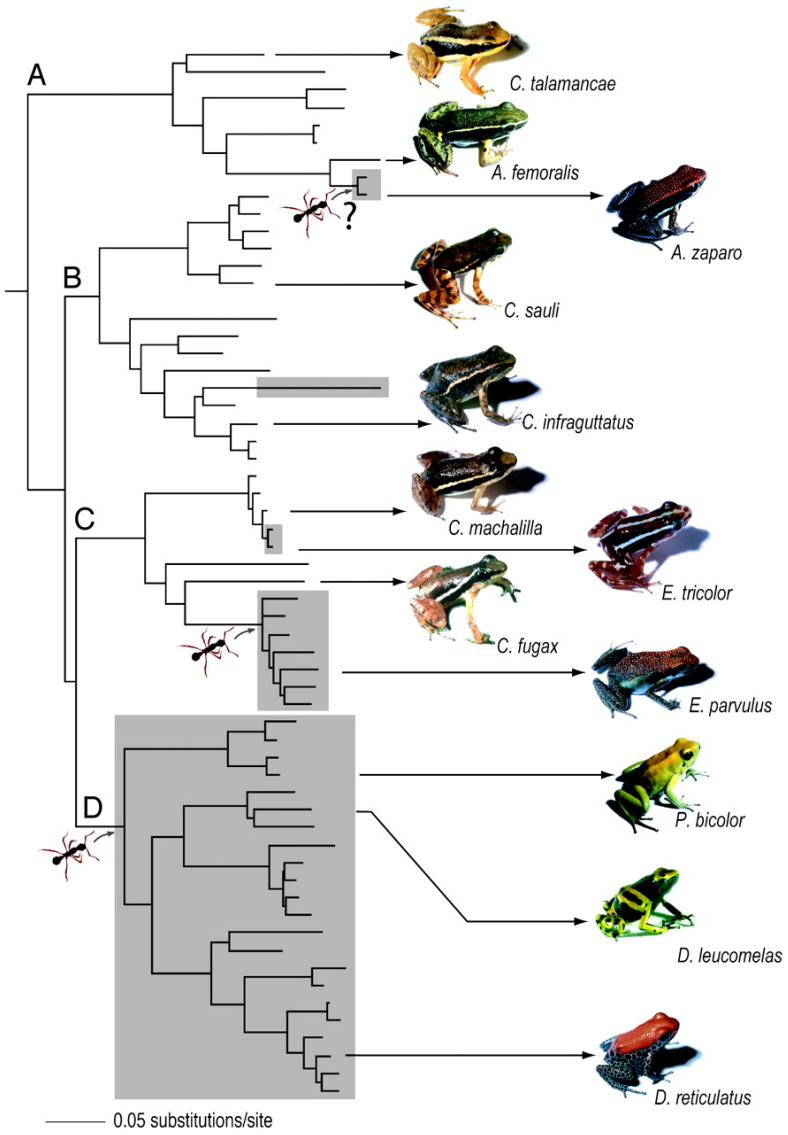

Figure 1.2: The likelihood topology, with gray boxes representing the species names shown in black on Fig. 1.1. The column of photos on the left shows representative cryptic and nontoxic species, and the column on the right shows conspicuous and toxic species (the toxicity of *A. zaparo* is unknown). The ant icons indicate two origins of specialized diet, and a possible third origin is indicated by a question mark.

Chapter 2: Amazonian amphibian diversity is primarily derived from late Miocene Andean lineages

INTRODUCTION

Tropical regions contain more than half of biological diversity on just 7% of the Earth's surface (Myers et al. 2000; Wilson 1988). Differences in biodiversity between tropical and temperate regions have been attributed to contrasting speciation and extinction rates (Moritz et al. 2000). Within the Neotropical realm, the Amazon Basin and the Chocoan region contain half of Earth's remaining rainforests and one of the largest reservoirs of terrestrial biodiversity. However, the impact of pre-Quaternary ecogeographic constraints on Neotropical biodiversity is largely unknown and the mechanisms contributing to species richness are unclear (Burnham and Graham 1999; Moritz et al. 2000). For example, the well-documented high α–diversity (species richness) of the flora and fauna of the Amazon rainforest (Pitman et al. 2001) is usually attributed to local geoclimatic dynamics that promote monotonic accumulation of lineages (Bush 1994; Hubbell 2001). However, the lower β–diversity (species turnover relative to distance) within the Amazon Basin is puzzling (Condit et al. 2002) and vastly underestimated. Current hypotheses are based on restricted, mostly Quaternary, spatiotemporal scales involving paleogeographic or ecological events (e.g., riverine barriers, Pleistocene climate change) (Moritz et al. 2000), persistence of conservative niches (Wiens and Donoghue 2004), and analyses of

phylogeography and endemicity (Patton and da Silva 1998). In addition to speciation/extinction processes (Moritz et al. 2000), major paleogeological events promote diversification, yielding complex phylogenetic patterns of vicariance, dispersal, and secondary sympatry (Bush 1994). Using phylogeographic analyses of the endemic and diverse clade of poison frogs (Dendrobatidae), we reconstruct Neotropical biogeography from the Oligocene to the present and revealed a widespread and highly dynamic pattern of multiple dispersals and radiations during the Miocene.

Major geoclimatic events have shaped the Neotropics. The most important include the isolation and reconnection of South America, the uplift of the Andes, the extensive floodbasin system in the Amazonian Miocene, the formation of Orinoco and Amazon drainages, and the dry–wet climate cycles of the Pliocene–Pleistocene (Fig. 2.1). The Panamanian Land Bridge (PLB) between the Chocó and Central America, which formed progressively until the Pliocene (Coates and Obando 1996), was an important biogeographic catalyst of dispersal and vicariance events at the Miocene–Pliocene boundary (e.g., *Alpheus* shrimps and freshwater teleost fishes) (Bermingham and Martin 1998; Knowlton and Weigt 1998). Similarly, the uplift of the Andes advanced the formation of the Amazon River, converting a widespread, northwest-flowing Miocene floodbasin into the current eastward-running Amazon Basin (Hoorn 1994; Latrubesse et al. 1997). Two Miocene marine incursions into this wetland system isolated several aquatic taxa as living relicts, including the Amazon River dolphin, lineages of marine-derived teleosts and stingrays, and brackish water mollusks (Kaandorp et

al. 2006; Lovejoy et al. 2006). However, controversies exist about the magnitude and duration of these geoclimatic events (Hoorn 2006).

Although well-known for its megadiversity, no studies of the Neotropics have examined diversification patterns in highly speciose and widespread lineages over broad temporal and spatial scales. A general explanation that associates rates of speciation with paleogeographic events is lacking. Here, we test two general hypotheses about the spatial configuration of biogeographic areas on the origin of Neotropical diversity (Fig. 2.1). First, under the center-of-origin hypothesis, lineages from the currently most diverse area (i.e., Amazon Basin) dispersed to other areas (Fig. 2.1, H_A: SM1). Second, under the stepping-stone hypothesis, paleogeographic events constrained the patterns of lineage diversification in the Neotropics among geographically adjacent areas (Fig. 2.1, H_A: SM2). Using a recently developed maximum likelihood procedure that estimates geographic range evolution, we tested both hypotheses against a null biogeographic model (Fig. 2.1 H_0: SM0) using a well-sampled Neotropical clade, the poison frogs (Dendrobatidae). We sampled 223 of the ~353 (264 described and 34-89 undescribed) species, distributed from Central America and Guiana Shield to southeast Brazil and from Andean páramos (4000 meters above sea level, masl) to lowland rainforests (<300 masl). However, ~40% of the species diversity remains unsampled (Santos et al. 2009). Because the true diversity (i.e., described, undescribed, and extinct species) cannot be accurately assessed (Alroy 2002; Sepkoski 1997), macroevolutionary inference should account for missing diversity. Our goals are to (1) infer how geographic range evolution yielded

current species distributions, (2) estimate the general patterns of speciation and extinction under necessarily incomplete taxon sampling, and (3) synthesize these findings with paleogeographic events to explain current patterns of species richness.

MATERIALS AND METHODS

Data Collection and Species Sampled

Because there are no fossil poison frogs, a large phylogeny of amphibians was constructed to calibrate the age of the root of the dendrobatid tree. We used a total of 89 terminals including 80 species of anurans (30 families), 3 species of salamanders (3 families), 3 species of caecilians (3 families), and 3 outgroups (lungfish, human, and chicken) (Santos et al. 2009). The amphibian classification partially follows that of Frost *et al*. (Frost et al. 2006). Conflicts with Frost *et al*. (Frost et al. 2006) are indicated as paraphyletic families (e.g., Dicroglossidae 1 and 2).

Molecular data include the mitochondrial rRNA genes (12S and 16S sequences; ~2400 bp) and the nuclear protein-coding gene RAG-1 (approximately 495 bp). Sequences were retrieved from GenBank (74 terminals) or sequenced (15 terminals) from total genomic DNA (Santos et al. 2009). The primers and protocols for amplification, purification and sequencing of PCR products are provided in previous studies (Bossuyt et al. 2006; Darst and Cannatella 2004; Santos et al. 2003). PCR products were sequenced in both directions and compared to GenBank sequences using BLAST

(http://www.ncbi.nlm.nih.gov/BLAST/). By this procedure, we were also able to validate sequences in GenBank and exclude contaminated or mislabeled submissions. GenBank accession numbers are given (Santos et al. 2009).

A total of 406 individuals for described (137) and undescribed (34-89) species of poison frogs and 12 outgroups (from Hyloidea) were used to estimate the phylogeny (Santos et al. 2009). The estimate of undescribed species (34-89) corresponds to the estimated minimum and maximum number of new species. Therefore, the described diversity of poison frogs (264 species) plus the diversity discovered by our analysis yields a maximum of353 (264 known + 89 maximum number of undescribed species), which is a better estimate of the true extant diversity. Of the 127 described poison frog species not sampled (Santos et al. 2009), we were able to identify their closest relative or species group in 92.1% of the cases (117 species). Thus, we are confidant that we have not missed any crucial lineage and that our conclusions will hold as more data are incorporated. Furthermore, the conservation status of the unsampled species is based on the Global Amphibian Assessment (IUCN et al. 2006) is as follows (Santos et al. 2009): 51.3% are data deficient, 16.6% have been described recently (no category), 28.9% are in one of four "threatened" categories, and 3.2% are of least concern.

The classification here partially follows that of Grant *et al*. (Grant et al. 2006). Species placements that conflict with this taxonomy are indicated as paraphyletic genera (e.g., *Colostethus* 1 and 2). Proposed taxonomic changes and corrections are explained in “Corrections to Taxonomy” (Dicussion). Our taxon

sample included species from throughout the distribution of dendrobatid frogs, with regions of higher diversity sampled more extensively (Santos et al. 2009) and the 117 species that were not sampled were assigned to a taxonomic group (Santos et al. 2009) and included in Speciation and Extinction Patterns Under Incomplete Taxon Sampling. Molecular data were generated using the same protocols indicated below. We included only the mitochondrial rRNA genes (12S and 16S sequences; ~2400 bp), from which 374 individuals (121 species) have complete sequences. GenBank sequence accession numbers are given (Santos et al. 2009); because some outgroup sequences will appear in other papers currently under review, their numbers are not listed. Although sequences from other genes are available in GenBank, these were not used because data from the data are highly incomplete; complete data for only 80 species were available. Moreover, simulation studies have indicated that large phylogenetic analyses including many terminals with incomplete sequences might bias branch length estimation, and cause topological inconsistencies due to unrealistic estimates of the rate of evolution (Lemmon et al. 2008).

Sequence Alignment, Data Partitioning, and Model Testing

Contigs were assembled using Sequencher 4.7 (GeneCodes 2006). Sequences were initially aligned using ClustalX 1.81 (Thompson et al. 1997) and manually adjusted to minimize informative sites using MacClade 4.08 (Maddison and Maddison 2001). The final matrices included 2688 characters (i.e., 2192 from mitochondrial genes, 495 from RAG-1) for the Amphibian Tree Matrix (ATM) and 2380 characters (mitochondrial genes) for the Poison Frog Tree Matrix

(PFTM). A total of 228 (ATM) and 113 (PGTM) ambiguously aligned characters were excluded. For the ATM, we divided the data into mitochondrial gene and RAG-1 partitions. For the PFTM, we used 12S rRNA, tRNA-Valine, and 16S rRNA partitions. The best model of nucleotide substitution for each partition was determined using ModelTest 3.7 (Posada and Buckley 2004; Posada and Crandall 1998). For the ATM, GTR+Γ+I and TrN+Γ+I were selected for the mitochondrial genes and RAG-1 segments, respectively. For the PFTM, GTR+Γ+I was selected for the 12S and 16S rRNA segments and the GTR+Γ for the tRNA-valine segment.

Phylogenetic Analysis

ATM and PFTM were analyzed with maximum likelihood (ML) methods under a genetic algorithm in GARLI 0.951 (Zwickl 2006) and with Bayesian sampling of tree space with MrBayes 3.1.2 (Huelsenbeck and Ronquist 2001; Ronquist and Huelsenbeck 2003). For the ATM analyses, the amphibian species were constrained to be monophyletic. For the GARLI analyses, a total of 40 independent runs were used to infer the best tree and 200 nonparametric bootstrap searches were used to estimate support for the nodes. For the MrBayes analyses, tree topology estimation, branch lengths, and Bayesian posterior probabilities (PP) were determined from five independent runs of four incrementally heated chains. Runs were performed for 35-45 x 10^6 generations under partitioned models using default settings as priors; the sampling frequency was 1 in 1000 generations. The convergence of the runs and the optimal burn-in was determined to be 1.238 x 10^6 (ATM) and 4.282 x 10^6 (PFTM) generations using MrConverge

(Lemmon et al. 2008). This program estimates the point where the likelihood score becomes stationary and the overall precision of the bipartition posterior probability is maximized.

Determination of Divergence Times

The strict molecular clock model was rejected from both ATM (χ^2 = 4762.6, df = 87, $p < 0.001$) and PFTM (χ^2 = 3822.6, df = 404, $p < 0.001$) datasets using a likelihood ratio test (LRT) that compared the best unconstrained GARLI trees to those estimated under a strict molecular clock. Therefore, a relaxed molecular clock Bayesian method in MULTIDIVTIME (Thorne and Kishino 2002) was used to estimate chronograms for the Amphibian Tree and the Poison Frog Tree.

For chronogram estimation, all taxa in the ATM dataset (Amphibian Chronogram) and a pruned PFTM dataset (Poison Frog Chronogram) were used. The pruned PFTM dataset excluded multiple individuals of the same species to improve computational efficiency. For each analysis (ATM and pruned PFTM), the aligned matrix and the rooted ML topologies without branch lengths were input into MULTIDIVTIME (Thorne and Kishino 2002). Branch length estimates under the F84+Γ model of molecular evolution and variance/covariance matrices were calculated using the BASEML and ESTBRANCHES components of PAML 3.15 (Yang 2003) and MULTIDIVTIME (Thorne and Kishino 2002) respectively. Calibration points (Santos et al. 2009), relaxed-clock model priors, and variance/covariance matrices were then input into MULTIDIVTIME (Thorne and Kishino 2002).

For the Amphibian Chronogram, three different sets of time constraints were used to assess the robustness of the dating estimates; these were based on paleogeography, vertebrate fossils, and amphibian fossil records (Santos et al. 2009). The ingroup tip-to-root distances needed for the estimation of the MULTIDIVTIME rtrate and rtratesd priors (Thorne and Kishino 2002) were calculated using TreeStat v1.2 (Rambaut and Drummond 2008). The relaxed-clock model priors were 344 MYA for the expected age between tip and root (rttm) and 20 MYA for its standard deviation (rttmsd). The rttm prior corresponds to the divergence of Amniota and Amphibia and is based on fossil and molecular analyses (Roelants et al. 2007; Ruta et al. 2003a; Ruta et al. 2003b; Zhang et al. 2005). The expected molecular evolution rate at the ingroup root node (rtrate) prior and its standard deviation (rtratesd) were estimated at 0.00345 substitutions/site/MY by dividing the median of ingroup tip-to-root distances by the rttm prior as suggested by the MULTIDIVTIME documentation (Thorne and Kishino 2002). The priors for the expected value of the Brownian motion constant υ (nu) (brownmean) and its standard deviation (brownsd) were estimated to be 0.058 by setting rttm * brownmean equal to 2.0 (on-line suggestion of Frank Rutschmann (Rutschmann 2005)). The bigtime parameter was set to twice the estimated time divergence of Amniota and Amphibia (i.e., 700 MYA). Markov chain (newk, othk, thek) and beta (minab) priors were set to default values. Each MCMC chain was run for 1×10^6 generations with sampling frequency of 1 per 100 generations and burn-in of the first 100,000 generations. All analyses were run twice to ensure convergence of the time estimates. The divergence time

estimated for each node of the amphibian chronogram was described by its mean age and 95% CI (Santos et al. 2009).

The Poison Frog Chronogram was estimated from the pruned PFTM dataset that included 224 individuals from 157 poison frog species (131 described and 26 undescribed) and 12 outgroups. The fossil record of Tertiary Neotropical frogs is minimal and no fossils of poison frogs have been found (Sanchíz 1998). For this reason, we used a three-part strategy to date the Poison Frog Chronogram. First, the expected ages and 95% CIs of the split of the Dendrobatidae from other Hyloidea and the age of the most recent common ancestor of this clade were estimated from the Amphibian Chronogram. Second, a list of geological time constraints (Santos et al. 2009) was developed based on paleogeological evidence (Santos et al. 2009). Third, ancestral area reconstruction was inferred and explained in section E. To test the overall accuracy of these approaches, three sets of progressively less inclusive time constraints were used (Santos et al. 2009). The relaxed-clock model priors were 71.4 MYA for the expected age between tip and root (rttm) and 18.6 MYA for its standard deviation (rttmsd). This value, estimated from the Amphibian Chronogram, corresponds to the mean age of the split between Dendrobatidae and its sister clade.. The expected value (rtrate) and standard deviation (rtratesd) priors were set to 0.0056 substitutions/site/MY. The priors for the expected value (brownmean) and its standard deviation (brownsd) of the Brownian motion constant υ (nu) were set to 0.2. These priors (rtrate, rtratesd, brownmean, and brownsd) were obtained similarly as in the Amphibian Chronogram (see above). The bigtime parameter

was set to three times the estimated age of the Dendrobatidae node from the Amphibian Chronogram (40 * 3 = 120 MYA). Markov chain priors (newk, othk, thek), beta prior (minab), and MCMC chain parameters were the same as for the Amphibian Chronogram. All analyses were run twice to ensure convergence of the time estimates. The divergence time estimated for each node of the Poison Frog Chronogram was described by its mean age and 95% CI (Santos et al. 2009) and major taxonomic events (Santos et al. 2009).

We assessed the robustness of the calibrations (Santos et al. 2009) with three approaches. First, we recalculated the chronogram by using penalized likelihood approach (PL) (Sanderson 2002) implemented in r8s (Sanderson 2003). Because the penalized likelihood method requires at least one fixed node age, the nodes were fixed for root of the poison frog tree at 42.9 MYA or for the major split between clades B+C+D and A at 36.3 MYA. These values correspond to the mean age for each node obtained by averaging the ages from the three estimates of the Amphibian Chronogram (Santos et al. 2009). We calculated the Poison Frog Chronogram with all constraints and then by removing one calibration constraint at a time (Santos et al. 2009). We use five different smoothing parameters (1, 10, 100, 500, and 1000), an additive scale for rate penalty, and 20 random starts to estimate the chronogram. The average of all runs without the respective constraint was used as the estimate of node age (Santos et al. 2009). Second, we recalculated the chronogram using the same parameters of the relaxed-clock Bayesian method but removing one calibration constraint at a time (Santos et al. 2009). Finally, we recalculated the Poison Frog Chronogram to

determine the effect of the combination of bigtime and rttmsd priors, which have been shown to have the substantial impact (Vieites et al. 2007), by changing the estimates of nodes to make them older or younger. We used the same rttmsd prior (18.6 MYA) and two bigtime prior values of 60 and 80 (Santos et al. 2009). Based on all tests, the estimates of 36 exemplar nodes that correspond to major phylogenetic events in the family (Santos et al. 2009) and the differences in MYA from the Poison Frog Chronogram node mean are provided (Santos et al. 2009). We found that all time estimates from each test were within two standard deviations of the mean of poison frog chronogram (Santos et al. 2009). The time estimates obtained by using the penalized likelihood method mostly were within one standard deviation from those estimated in the Poison Frog Chronogram. In the case of the tests done using the relaxed molecular clock Bayesian method, the removal of constraint A (2.4-15.0 MYA, which was assigned to nodes that correspond to dispersals between South America and Central America) was found to provide older time estimates for all nodes, especially those close to the root. The effect of changing the rttmsd/bigtime priors combination was negligible.

Ancestral Area Reconstruction

The reconstruction of ancestral areas of the poison frog clade was determined by three methods: a maximum-likelihood inference of geographic range evolution (Ree et al. 2005; Ree and Smith 2007; Ree and Smith 2008), dispersal-vicariance analysis (DIVA) (Ronquist 1997), and Bayesian analysis of ancestral areas (Brumfield and Edwards 2007; Pagel et al. 2004; Ronquist 2004). Ten areas (designated by letters) were delimited based on geological barriers,

areas of endemism (Duellman 1999; Gentry 1992; Stattersfield et al. 1998), and distribution maps (IUCN et al. 2006) (Fig. 2.1). The Andes were divided into four adjacent regions: Central Occidental Andes (H), Central Oriental Andes (G), North Oriental Andes (E), and North Occidental Andes (F). Northern and Central Andes are divided perpendicular to the southern limit of Carnegie Ridge (parallel 2°S) in southern Ecuador (Gutscher et al. 1999; Hungerbuhler et al. 2002). The Oriental and Occidental Andes are divided along the Interandean valleys that separate both parallel mountain chains. The Guiana Shield (B) and Brazilian Shield (K) regions are located in the eastern shoulder and center of South America, respectively. Both regions are ancient Precambrian plateaus with lowland tropical rainforest, dry forest, and cloud forests from 200-2800 m. The Venezuelan Highlands (D) region includes the current Caribbean costal cordilleras of Venezuela (Mérida, Cordillera de la Costa, and Paria peninsula) and Trinidad and Tobago Islands. Paleontological and stratigraphical evidence suggests that Venezuelan Highlands region had strong similarities to the western Amazonian Tertiary fossil fauna (Aguilera and Rodrigues de Aguilera 2004a; Aguilera and Rodrigues de Aguilera 2004b; Brochu 1997; Cozzuol 2006). However, the Venezuelan Highlands biogeographic distinctiveness is evidenced by the Miocene uplift (Diaz de Gamero 1995), episodic Miocene floodings, and the formation of the Llanos (Cooper et al. 1995), the separation from the Guiana Shield region by the current Orinoco river drainage and from the northern Andes by the Táchira depression. The Amazon Basin (C) region includes the river drainage and its extensive lowland tropical rainforest <300 m. The Central

America (J) region corresponds to the lowlands and highlands of western side of the Panama Land Bridge (PLB) to southern Nicaragua (northernmost distribution of poison frogs). The Chocó (I) region includes the eastern side of the PLB and the costal lowland tropical forest below 500 m of the Pacific Coast of Ecuador and Colombia on the western side of Andes. The Magdalena river drainage and the Gorgona Island were also included in the Chocó region based on the paleontological and biotic resemblance to the Chocó (Forero 1988; Guerrero 1997; Kerr 2005).

Ancestral area reconstructions, time of diversification, and rate of diversification estimates require a fully bifurcate tree (Magallon and Sanderson 2001; Nee 2001; Paradis 1997; Sanderson et al. 2004). We used the best GARLI tree to reconstruct the ancestral areas. Each species in the phylogeny was assigned to one or more regions based on distribution (Santos et al. 2009). For the first method, we estimated a dispersal-extinction-cladogenesis (DEC) model using Lagrange package (Ree and Smith 2007; Ree and Smith 2008). The DEC model is a continuous-time stochastic model for geographic range evolution in discrete areas, with maximum likelihood parameters estimated for rates of dispersal between areas (range expansion) and local extinction within areas (range contraction). The DEC model considers geographic scenarios of lineage divergence (including scenarios involving within-area speciation), allowing a widespread ancestral range to persist through a cladogenesis event as ancestral states at internal nodes on a phylogeny with observed species ranges at the tips. In all cases, ancestral ranges were assumed to include no more than two areas, the

maximum observed for extant species. Moreover, spatial and temporal constraints (e.g., area distances, dates of geological origin) may be imposed in the DEC model estimation, providing a more accurate estimation of the ancestral areas and hypothesis testing of specific geographic scenarios.

We tested three biogeographic scenarios based on the hypothesized origin of the group (Santos et al. 2009). First, the SM0 null model has all areas as equiprobable ancestral ranges and assigns them to be adjacent pairs (i.e., separated by one step in the matrix), plus the individual areas themselves. Second, the SM1 (center-of-origin model) favors an Amazon Basin origin of the poison frog clade and assigns all non-Amazonian areas to be adjacent to the Amazon Basin (i.e., separated by 1 step in the matrix) and non-adjacent to each other (i.e., separated by two steps). However, the one exception was to make the Chocó and Central America adjacent, because it is not possible to reach Central America without passing through the Chocó. Third, the SM2 model (stepping-stone model) assigns the rates of dispersal between areas to be inversely scaled by their relative distance and connectivity (e.g., the distance between Guiana Shield and Central America is four steps, so the rate of dispersal was constrained to be 0.25). Each analysis estimated the global rate of dispersal and local extinction on the phylogeny with species ranges at the tips, considering all possible range inheritance scenarios (ancestral states) at internal nodes without conditioning on any particular values. Then, the global rates were used to calculate and rank the likelihoods of all ancestral states at every internal node on the phylogeny. This is done by calculating the likelihood at the root of the tree, given the global rates,

with one node fixed at one ancestral range scenario, and all other nodes free to vary. The ML scores for all nodes are compared to the overall ML score of each geographic scenario under a "global" method of ML ancestral state reconstruction (Pagel 1999). The likelihood of each model was optimized against the observed ranges of species and their phylogenetic relationships, with differences greater than 2 log-likelihood units considered significant; the reconstruction with the worst score was rejected (Pagel 1999). Tests of the three hypotheses (SM0, SM1, and SM2) were repeated in both the complete ML phylogeny and chronogram (reduced number of taxa). All tests were repeated in both large ML phylogeny and chronogram including and excluding *Allobates alagoanus* whose phylogenetic position at the base of Clade A is not well supported (Santos et al. 2009). In all cases similar results were found, so the results excluding *A. alagoanus* are presented.

For the second method, we performed ancestral area reconstruction by dispersal-vicariance analysis using DIVA 1.1 (Ronquist 1997). DIVA assumes that speciation occurs as a consequence of vicariance and reconstructs these events at no cost. Therefore, the ancestral geographic distributions are reconstructed by minimizing the number of dispersal or extinction events necessary to explain the actual distribution pattern. Because we assigned all nine regions to favor dispersals equally, no single solution for the large tree was found (~16 x 10^6 possible reconstructions). Hence, this analysis is considered exploratory due to its limitations. DIVA, which is parsimony-based, only optimizes historical events on cladograms without regard to relative or absolute

time (i.e., branch lengths), and is less flexible about geographic lineage divergence scenarios (e.g., widespread ancestors are assumed to undergo vicariance); specific biogeographic hypotheses cannot be tested. In consequence, the strict consensus of the dispersal/vicariance events on >75% of all possible reconstructions was used as the best solution and mapped on the ML poison frog phylogeny (Santos et al. 2009).

For the third method, estimates of the values of states at ancestral nodes were derived by point estimates (log-likelihoods) using a maximum likelihood (ML) approach in BAYESMULTISTATE, a component of BAYESTRAITS (Pagel and Meade 2006; Pagel et al. 2004). The reduced chronogram (236 terminals) described in Section D1 was used for the analysis. We coded all terminal distributions under two alternatives, Amazonian Basin (C) origin, and non-Amazonian Basin origin (all other areas). We calculated the proportion of likelihood of both alternatives at each node with 10,000 samples under default parameters. The results were mapped onto the chronogram (Fig. 2.2). We also tested whether an Amazonian origin was present at each node by constraining the node to this state using the option "fossilizing" in BAYESMULTISTATE (Pagel and Meade 2006). The likelihoods of the constrained and unconstrained reconstructions were compared, and a difference of ≥ 2 log-likelihood units was considered significant; the model with the worse score was rejected (Pagel 1999).

Speciation and Extinction Patterns Under Incomplete Taxon Sampling

We calculated the tree imbalance of the ML poison frog phylogeny, the reduced-taxon chronogram, and the tree of each super-regions: the Amazon Basin

(region C), the Andes (regions E, F, G, and H), Chocó-Central America (regions I and J), and Guiana Shield-Venezuela-Brazilian Shield (regions B, D, and K). We used conservative imbalance metrics (Agapow and Purvis 2002; Blum and Francois 2006): I_C (Colless 1982), I_S (Mooers and Heard 1997), and *s* (Fill 1996; Semple and Steel 2003). All standardized indices and probability of rejecting the null model of each branch having the equal probability of splitting (Equal Markov Rate or ERM) were calculated using functions colless.test, sackin.test, and likelihood.test, implemented in the R package apTreeshape (Bortolussi et al. 2006).

An indirect estimate of diversification rates assuming incomplete taxon sampling was explored using the γ statistic (Pybus and Harvey 2000) and adjusted for actual phylogenies by excluding the distance between the most recent node to the present (i.e., g_n node of a phylogeny of size *n*), which does not come from the same distribution (Weir 2006). The adjusted γ statistic values were obtained from the Poison Frog Chronogram (all regions) and each tree of the four super-regions.

The adjusted γ statistic (Pybus and Harvey 2000; Weir 2006) was calculated using following functions of the R package LASER (Rabosky 2006): (1) the g_n node was excluded from the chronogram (i.e., entire family and major region subtrees) by using truncateTree function, (2) the γ statistic of the truncated tree was calculated using gamStat function, (3) a null-distribution of γ under a pure birth model was obtained by 10,000 Monte Carlo replicates using mccrTest.Rd. This function generates full size trees at the species level and prunes randomly terminals to the actual size of the empirical tree (i.e., simulates

incomplete taxon sampling), (4) the empirical γ statistic was adjusted by subtracting the mean value of the simulated null-distribution of γ, which is expected to be 0 (Weir 2006), and (5) the p-values of the adjusted γ statistics were computed from a normal distribution; values outside the ± 1.96 standard deviation boundaries are significantly different (alpha = 0.05) from the null pure birth expectation.

We tested for significant changes in diversification rate within the poison frog clade using a maximum likelihood methodology under the assumption of incomplete taxon sampling (Rabosky et al. 2007). First, we produced a genus-supraspecific level (GSPF chronogram) by pruning all but a single lineage per taxonomic group (Fig. 2.3) from the Poison Frog Chronogram, yielding a tree of 78 terminals. The total species richness per taxonomic group was assigned to each terminal based on previous taxonomic and phylogenetic studies (Coloma 1995; Duellman 2004; Grant et al. 2006; La Marca 1995 [1994]; Morales 2002 [2000]; Rivero 1988[1990]; Santos et al. 2003). Second, we estimated a constant diversification rate *r* (i.e., the difference between speciation, λ, and extinction, μ, rates) across the phylogeny using a maximum likelihood estimator that incorporates both known taxonomic diversity and phylogenetic data (Rabosky et al. 2007). We calculated the constant-rate model fit statistics (log likelihood and AIC score) and *r* using the fitNDR_1rate.Rd function of LASER (Rabosky 2006). Third, we tested for shifts in diversification rate within the poison frog phylogeny by comparing likelihood of the GSPF chronogram under constant and rate-flexible diversification models (Rabosky et al. 2007). Two alternative hypotheses

for rate-flexible model may explain the shifts in rate of diversification: (1) an increase within a particular clade (r_{CL}) from the ancestral diversification rate r (flexible-rate model) or (2) a clade-specific decrease (r_{CL}) from the ancestral diversification rate r (rate-decrease model) (Rabosky et al. 2007). We calculated both rate-flexible alternative model fit statistics, r and r_{CL} values using the fitNDR_2rate.Rd function of LASER (Rabosky 2006). The best fitting model was determined using a likelihood ratio test (LRT) between the constant-rate and the flexible-rate models (nested), and by ΔAIC scores between the flexible-rate and rate-decrease models (not nested). All analyses were performed under two extremes of the relative extinction rate ($a = \mu/\lambda$, $a = 0$ and $a = 0.99$) as a fixed parameter to determine the robustness of the results to variation in the extinction fraction (Raup 1985).

RESULTS

We reconstructed a maximum likelihood (ML) phylogeny from an extensive taxon sample (Santos et al. 2009), and a relaxed-clock Bayesian chronogram from a sub-sample of the previous (Thorne and Kishino 2002). The phylogeny is in general agreement with previous studies (Grant et al. 2006; Santos et al. 2003) and the significance of branch support is provided in Fig. 2.2 (for detailed support values see (Santos et al. 2009)). Although our taxon sampling is the most extensive for poison frogs (i.e., ~ 63.5% of the diversity in the family), we were concerned that incomplete taxon sampling might cause tree imbalance and introduce bias into divergence time estimation (Blum and Francois 2006; Heath et al. 2008). We assessed imbalance by testing the null model that

each branch has an equal probability of splitting (Equal Rate Markov or ERM) using three tree imbalance tree indices: Colless IC, Sackin IS, and likelihood shape s (see Materials and Methods). Overall, our results showed that the imbalance indices for all trees (i.e., ML, chronogram, and super-region phylogenies) have a tendency to depart from, but do not reject, the equal rates model (ERM). Therefore, our inferences about macroevolutionary events (e.g., ancestral area reconstruction, divergence times, and diversification rates) should not be affected significantly by incomplete taxon sampling.

Historical Biogeography of the Poison Frogs

The patterns of spatial and temporal distribution of poison frogs were inferred using dispersal-extinction-cladogenesis (DEC) modeling (Ree and Smith 2008). We compared three DEC models (i.e., a null and two alternatives) for ten areas (Fig. 2.1). The null model (SM0) assumes that spatial structure has no effect on biogeographic patterns of evolution. The alternative models either favor the Amazon Basin as a center-of-origin (SM1), or patterns of dispersal/vicariance that reflect the spatial arrangement or connectivity of biogeographic areas (a stepping-stone model; SM2). Our results strongly support the SM2 model over SM1 (large phylogeny $\Delta\ln(L) = 140.5$, $p < 0.001$; chronogram $\Delta\ln(L) = 48.6$, $p < 0.001$) and SM0 (large phylogeny $\Delta\ln(L) = 17.7$, $p < 0.001$; chronogram $\Delta\ln(L) = 0.5$NS, $p > 0.05$). The non-significant comparison of SM2 and SM0 for the chronogram alone is likely due to its reduced taxon sample.

The chronogram and a summary of the significant biogeographic events with confidence limits (Santos et al. 2009) from the stepping-stone model are

superimposed on the four major clades (Fig. 2.2). The most recent ancestor of Dendrobatidae was distributed in regions that correspond to the current Venezuelan Highlands and Northern Oriental Andes at 40.9 ± 5.4 million years ago (MYA). This ancestral range split into a Venezuelan Highlands ancestor of Clade A and an Andean ancestor (Clade B+C+D). The most recent ancestor of each major clade occurred during the Oligocene at 34.9 ± 5.4 MYA (Clade A), 30.9 ± 3.9 MYA (Clade B), 27.1 ± 3.2 MYA (Clade C), and 29.9 ± 4.0 MYA (Clade D). We inferred 14 dispersals into and 18 from the Amazon Basin to adjacent areas, including 3 major radiations and a single lineage extinction within Amazonia. We also found 5 cross-Andean dispersals, 5 dispersals from Northern to Central Andes, 6 dispersals from Northern Andes to Chocó, 4 dispersals from Chocó to the Andes, and 3 temporal phases of lineage dispersal with 2 interleaved periods of vicariant events between the Chocó and Central America (Fig. 2.2).

The diversity of Amazonian poison frogs (>70 species) resulted from 14 separate dispersals into this region, in three phases (Fig. 2.2). First, the two oldest dispersals originated independently from the Guiana Shield (23.8 MYA) and from the developing Andes (21.1 MYA), just before and during the existence of the Amazonian Miocene floodbasin. Second, a single dispersal from the Guiana Shield occurred 15.5 MYA, during a low sea-level period associated with reduction of the Miocene floodbasin system. Third, the 11 remaining dispersals from the Andes took place between (1.6-7.3 MYA) during the formation of the modern Amazon Basin river system. Ancestral area reconstructions using a Bayesian multistate procedure similarly support the recent multiple dispersals to

the Amazon Basin (Fig. 2.2). Thus, our results suggest that much of the extant Amazonian biodiversity results from relatively recent immigration of distinct lineages followed by in situ radiation during the last 10 MYA.

At least 18 dispersals from the Amazon Basin to other areas were found in three temporal phases. First, the earliest dispersals to the developing Chocoan lowlands (21.8 MYA) and the Andes (15.2 MYA) occurred during the establishment of the Miocene floodbasin system. Interestingly, for the present Chocoan lineage of Dendrobates pumilio (Fig. 2.2), our results suggest a Miocene overwater dispersal from Chocó to the developing Central America archipelago and the extinction of the Amazonian lineage ancestor at ~ 19.5 MYA during the formation of the Miocene floodbasin system. Second, dispersals to the Guiana Shield (1), the Venezuela Highlands (1) and the Andes (1) took place after the Miocene floodbasin system receded (8.8-10.8 MYA). Third, the 12 remaining dispersals were very recent (0.7-6.0 MYA), to the Guiana Shield (7), Andes (4), and Brazilian Shield (1). Thus, 16 out of 18 occurred <11 MYA, after the establishment of the current Amazonian geomorphology (Fig. 2.2).

At least four major diversifications occurred within Amazonia: (1) the Allobates trilineatus complex (26 species) is the oldest (14.0-15.1 MYA); the three remaining are more recent (5.4-8.7 MYA): (2) the Amazonian Ameerega (19 species), (3) the Dendrobates ventrimaculatus complex (15 species), and (4) the Allobates femoralis complex (9 species). Moreover, all four lineages entered the Guiana Shield area in the Pliocene (Fig. 2.2).

Species diversity in the Andes (71 species) resulted from a continuous diversification process since the late Eocene (Fig. 2.2). However, several Andean events were contemporaneous with establishment of the Amazon Basin. Five cross-Andean dispersals from Oriental to Occidental Andes (2.0-25.4 MYA), five dispersals from Northern to Central Andes (14.9-30.9 MYA), and six dispersals from the Northern Andes to the Chocoan lowlands (8.3-29.9 MYA) (Fig. 2.2) took place before the establishment of the Andes as a major geographic barrier during the Miocene–Pliocene boundary (Gregory-Wodzicki 2000). We also found five dispersals from the Chocó to North and Central Andes (1.1-6.6 MYA) (Fig. 2.2) that took place mostly in the Pliocene when the Andes were already established as a barrier. Our results indicate that lower montane transition zones between Andean and lowland environments (Chocó and Amazonia) promote diversification, as exemplified by the Amazonian Ameerega (Roberts et al. 2006) and the Chocoan Epipedobates.

Central American and Chocoan species (> 40) also show a complex pattern of diversification at the end of the Miocene. Ten dispersals from Chocó to Central America suggest a pattern of recurrent colonization and isolation in three phases (Fig. 2.2). First, the two oldest dispersals (8.3-12.1 MYA) from the Chocó overlap with a proposed earlier exchange of faunas during the late Miocene (Webb 1985). A single vicariant event at 6.8 MYA isolated the first wave of immigrants (i.e., ancestors of Phyllobates and Colostethus 1). Interestingly, the contemporaneous divergence of the Trinidad and Tobago species (Mannophryne trinitatis and M. olmonae) from Venezuelan relatives at 8.3 MYA suggests a

global period of high sea level. Second, six Pliocene dispersals from South America (3.2-5.4 MYA), immediately followed a proposed low sea-level period after 6.0 MYA (Coates and Obando 1996). Six vicariant events in the middle Pliocene (1.1-3.6 MYA) are concomitant with a second high sea-level period (1.5-3.0 MYA) that separated Central America from the Chocó (Coates and Obando 1996). Third, two dispersals in the late Pleistocene (0.5-2.2 MYA) are contemporaneous with the Great Faunal Interchange at 1.2 MYA (Coates and Obando 1996). Likewise, the endemic poison frog of Gorgona Island (Epipedobates boulengeri), located 50 km off the Pacific coast, was derived from a Chocoan ancestor 2.4 MYA during the same period. Our results strongly support the repeated dispersal of poison frogs into Central America across the PLB before its final Pliocene closure.

Similar results for the ancestral area reconstruction were obtained by dispersal-vicariance analysis (DIVA) (Ronquist 1997). However, DIVA provided unrealistic ancestral reconstructions for basal nodes (Santos et al. 2009), and a large number (i.e., ~16 x 106) of equally parsimonious reconstructions (see Material and Methods). Therefore, DIVA analyses were considered exploratory due to its algorithmic limitations (Ree et al. 2005; Ree and Smith 2008).

Lineage Diversification

We estimated diversification rates of the chronogram and super-region subtrees using the adjusted γ statistic to account for incomplete taxon sampling (Table 2.1) (Pybus and Harvey 2000; Weir 2006). The γ statistic compares the relative position of the nodes in a chronogram to that expected under the pure

birth model, and different values of γ characterize whether the diversification rate has increased ($\gamma > 0$), decreased ($\gamma < 0$), or remained constant ($\gamma = 0$) over time (Pybus and Harvey 2000). However, we emphasize that the γ statistic is an indirect estimation of the rate of diversification (Pybus and Harvey 2000), and our inferences from the γ statistic should be considered relative measures of the diversification. The Amazon Basin and the Central American-Chocó super-regions (Table 2.1) show significant positive values of γ, suggesting that the relative rate of speciation has increased over time compared to the entire family (all areas) and the Andes and Guiana-Venezuela super-regions (i.e., γ for these regions ~ 0). Simulations have suggested that significant positive values of γ have been associated with two alternatives, either increasing diversification or high extinction through time (Rabosky and Lovette 2008). The general absence of Tertiary frog fossils from lowland Neotropics (Sanchíz 1998) is intriguing, but it does not provide evidence for or against increases in extinction/diversification. Therefore, our inference of recent dispersals to Amazonia and the recent geological origin of the modern Neotropical rainforest (Hoorn 2006) might weigh in favor of a recent increase in diversification. Moreover, our results strongly suggest that the bulk of recent diversification in poison frogs might be due to rapid radiations in the Amazon Basin and the Central American-Chocó super-regions in the late Miocene. Alternatively, the relatively sparse sampling in both the Andes (i.e., 56.2 % of described species) and the Guiana-Venezuela (i.e., 40.5 % of described species) super-regions might have reduced the power to reject the

null of constant diversification rate. In either case, additional data from other Neotropical biota might be crucial to validate our results.

We further evaluated our claim of a significant increase in diversification in the Amazon Basin and the Central America-Chocó super-regions. We tested for significant changes in diversification rate at the genus-supraspecific level (GSPF chronogram and Fig. 2.3; see Material and Methods) under incomplete taxon sampling using maximum likelihood approach (Rabosky et al. 2007) with two extreme values of the extinction/speciation ratio (i.e., extinction rate fraction a = μ/λ, a = 0 and a = 0.99) (Table 2.2). The GSPF chronogram rejected the constant-rate model (all lineages with equal diversification rate) in favor of a variable rate model (at least one lineage has a significant higher or lower diversification rate) (Table 2.2). Additionally, the GSPF chronogram favored the variable-rate model with diversification rate change in one or more lineages (Fig. 2.3 and Table 2.3) over an alternative of retained elevated ancestral diversification rate (Table 2.2). However, we found possible spurious significant rate increases (i.e., nodes 2 and 9 of Fig. 2.3 and Table 2.2) that might be dependent on more inclusive lower nodes (i.e., 1 and 5 respectively). This "trickle-down effect" artifact can be explained by a significant rate increase detected in daughter clade being carried over to the adjacent parent clade.

The diversification rate increase within *Ameerega* is 3.23-fold (a = 0) to 7.55-fold (a = 0.99) higher than the rest of the GSPF chronogram (Fig. 2.3 and Table 2.3). Interestingly, *Ameerega* corresponds the most recent (i.e., 8.7 MYA) widespread radiation of poison frogs in the Amazon Basin after dispersal from the

Andes (Figs. 2.2 and 2.3) in the late Miocene. Other significant increases in the diversification rate include two in Amazonia, two in the Chocoan region, and one in the Andes (Fig. 2.3 and Table 2.3). Significant decreases in the rate of diversification correspond to the rare Guiana Shield endemic *Allobates* (0.0008-fold reduction) and the mostly Andean endemic Clade B (0.4851-fold reduction) (Fig. 2.3 and Table 2.3). Therefore, we found that Amazonian and Central American-Chocoan lineages significantly increased their diversification rate since the late Miocene, while the diversification rate in the Andean and Guianan-Venezuelan-Brazilian Shield lineages have been near constant with a tendency to slow-down since the Oligocene. However, we acknowledge that these super-regions (i.e., the Andes and the Guiana-Venezuela-Brazilian Shield) might be undersampled (Table 2.1) and conclusions about their near-constant rate of diversification need further validation

DISCUSSION

The unstable coexistence of lineages within a large community for extended periods of time has been hypothesized as a cause of Neotropical diversity (Hubbell 2001). However, our results suggest that such a model is incomplete; rather, the complex pattern of diversification is strongly intertwined with paleogeographic events. Our inferences about the past history of the poison frogs using ancestral area reconstructions and diversification analyses provide new insights on speciation and extinction patterns in the Neotropics. Three species richness patterns are potential explanations for the extant diversity differences among regions of the Neotropics: (1) high immigration into one

region after suitable geoclimatic conditions are established, (2) gradual *in situ* diversification of old endemic clades, regardless of the geoclimatic conditions, promoting species accumulation; or (3) rapid *in situ* diversification of endemic clades after favorable geoclimatic conditions are established. We found that all three patterns might apply to different areas depending on historical context.

All extant Amazonian species descended from 14 lineages that dispersed into the Amazon Basin, mostly after the Miocene floodbasin system receded. The recurrent immigrations that originated mostly in the adjacent Andes (species-richness pattern 1), combined with an increased rate of diversification, explain the high α–diversity of Amazonia. Later, from the Miocene-Pliocene boundary to the present, a rapid *in situ* diversification (pattern 3) gave rise to the extant Amazonian endemic biota. Therefore, most species in Amazonia originated in the last 10 MY. Moreover, lineages immigrating into Amazonia at < 8.0 MYA radiated rapidly, resulting in widespread species and young clades (e.g., *Ameerega*, *Allobates trilineatus*, *A. femoralis* and *Dendrobates ventrimaculatus* groups).

The diversity in the Chocoan-Central American super-region derived from scattered immigrations (pattern 1) from Andes to the early Chocoan rainforest during the late Miocene. However, starting at the Miocene-Pliocene boundary, significant orogenic events gave rise to the Central American archipelago (Coates et al. 2004; Coates and Obando 1996) followed by sea level fluctuations (Zachos et al. 2001), which provided the conditions for repeated dispersal and vicariance events in pre-Panamanian Land Bridge islands. Evidence of rapid *in situ*

diversification (pattern 3) is supported by the high genetic diversity observed among poison frogs and other lineages especially between Western and Eastern Panamá (Bermingham and Martin 1998; Wang et al. 2008; Zamudio and Green 1997). Interestingly, our results might explain the high β–diversity of other endemic clades within the Chocó-Central America super-region (Condit et al. 2002) as originating initially from long-distance dispersals between disconnected islands, with diversification later during isolation by high sea levels.

The Andes have undergone extended *in situ* diversification (pattern 2) since the late Eocene. However, our analyses also provided evidence of decline in the diversification rate since the middle Oligocene, which has important implications for history and conservation of the endemic Andean fauna. First, the Andes uplift at the Miocene–Pliocene boundary caused significant changes in the rate of diversification in the lowland transition zone. We found that several poison frog lineages distributed on one or both sides of the Andes had dispersed repeatedly before the Miocene uplift (i.e., five cross-Andean and five Northern to Central Andes migrations). Paleogeological evidence supports introgression of shallow seas across the northern Andes during the Miocene (Hoorn 1994), suggesting a historical connection between the Amazon Basin and the Chocó. Second, the Pliocene Andean uplift (>2000 masl) (Gregory-Wodzicki 2000) formed a significant barrier to dispersal, because no other cross-Andean dispersals were found. The uplift also was associated with dramatic ecological changes (Gregory-Wodzicki 2000) and a decrease in diversification rates. These results suggest a role for niche conservatism (Kozak and Wiens 2007; Wiens and

Graham 2005), in that some lineages may have gone extinct because of failure to adapt. Alternatively, despite greater sampling effort in the Andes region than in other areas, we failed to find some previously common Andean species (e.g., *Hyloxalus jacobuspetersi* and *H. lehmanni*). Consequently, it is difficult to separate a natural decrease in diversification rates from the current trend of amphibian species extinctions at high altitudes due to anthropogenic habitat alteration (Pechmann et al. 1991), increased UV radiation (Kiesecker et al. 2001), climate change (Pounds et al. 2006), or pandemic infection (Lips et al. 2008). In contrast, the montane transition zones of the Andes and adjacent lowlands (Chocó and Amazonia) have become centers of rapid cladogenesis (pattern 3), and species richness in these transition zones might be underestimated because many Neotropical lineages have been shown to contain several cryptic species (Hebert et al. 2004). Therefore, dispersals within or across the Andes diminished during the Pliocene, but diversification has intensified in the Andes-lowlands interface.

Although some of the oldest lineages of poison frogs originated in the Guiana Shield and the Venezuelan Highlands (>30 species), our results suggest extended *in situ* diversification (pattern 2) followed by a decline in the rate of diversification of endemic clades in both areas since the early Miocene. Along the same lines, the Guiana Shield has high poison frog endemism, which is mostly restricted to the summits of the sandstone tepuis (Señaris and MacCulloch 2005), while recent Amazonian poison frog immigrants occupy lowlands adjacent to the tepuis. Our results suggest that the decline of endemic Guianan diversity might be associated with ecological changes in habitat due to the collapse of the ancient

tepuis (Burnham and Graham 1999) and repeated dispersals from Amazonian lineages since the Pliocene. However, the diversity of poison frogs in the Guiana Shield is only beginning to be revealed (Señaris and MacCulloch 2005). In contrast, diversification in the Venezuelan region most likely reflects the oldest vicariant event in Dendrobatidae, at 40.9 MYA. The costal ranges of Mérida, Cordillera de la Costa, and Paria peninsula are species rich but their total area is less than 5% of that of the Amazon Basin. No lineage of this endemic fauna has dispersed out to other regions since the early radiation of the poison frog family in the late Eocene. However, Eocene floristic paleoecological reconstruction of the Venezuelan Highlands area showed that it was more diverse than at present (Jaramillo et al. 2006), suggesting that the ancestral habitat of poison frogs might have been lowland. The depauperate dendrobatid fauna of the Venezuelan llanos and Brazilian Shield plateau is puzzling, but might be related to Holocene aridity (Marchant and Hooghiemstra 2004).

The recurring dispersals to Amazonia suggests that a large part of dendrobatid diversity results from repeated immigration waves at <10.0 MYA, followed by a rapid *in situ* diversification after geoclimatic conditions suitable for a rainforest ecosystem were present. The biota of Amazonia was not isolated during the process of diversification, but finely intertwined with the development and export of biodiversity across the entire Neotropical realm. Poison frog diversity in the Chocoan-Central American super-region was significantly associated with formation of the Panamanian Land Bridge in the Pliocene. Repeated dispersals between disconnected islands followed vicariance by cyclic

high sea-level periods, promoted rapid *in situ* diversification and endemism of poison frog lineages. The extant Andean, Guianan, and Venezuelan Highlands fauna most likely originated after prolongated *in situ* diversification since the origin of the poison frog clade, but the pace of species formation within these areas has slowed down. Phylogenetic analyses on tropical biota such as birds (Fjeldså 1994) and the species-rich genus *Inga* (Richardson et al. 2001) as well as models of diversification (Moritz et al. 2000), have argued that the Amazon might accumulate older lineages; however, the origin of those lineages is not clear. Our results are the first to provide evidence, to our knowledge, of the major involvement of the Andes as a source of diversity of the Amazon. Because 23.5% of endemic Amazonian amphibian species are dendrobatids (i.e., ~70 of 298) (Duellman 2005), our results may generalize to other terrestrial biota. Moreover, these results provide a crucial broad spatiotemporal framework that, coupled with realistic phylogeny-based explanations of the current richness in Neotropics, explains why species occur where they do and how they came to get there. Thus, the major patterns of dispersals and radiations in the Neotropics were already set by the Miocene–Pliocene boundary, but the ongoing process of Neotropical radiation is occurring now, in the Chocó–Central America region and especially in the Amazonian rainforest.

Corrections to Taxonomy

Our phylogenetic analysis found results generally similar to previous phylogenetic hypotheses (Grant et al. 2006; Santos et al. 2003). For the purpose of this paper, some corrections to the Grant *et al.*'s *(Grant et al. 2006)* taxonomy

must be made in order to have a nomenclature concordant with well supported clades, and to avoid ambiguity and subsequent confusion in the literature of this family.

The monophyly of Dendrobatidae (*sensu* Noble 1926) (Noble 1926) has always been strongly supported by previous studies (Grant et al. 2006; Santos et al. 2003). The taxonomic split of Dendrobatidae into two families (i.e., Aromobatidae and Dendrobatidae) is unnecessary and adds no new information. Grant *et al.*'s (Grant et al. 2006) primary reason for the split is the inability to sequester alkaloids (i.e., chemical defense) in Allobatinae (Aromobatidae *sensu* Grant *et al*.). Very few species of Aromobatidae have been documented as being unable to sequester alkaloids, and many species of Colostethinae and Hyloxalinae are unable to do so (Daly et al. 1994; Myers et al. 1991). The restriction of Dendrobatidae to include only Colostethinae, Dendrobatinae, and Hyloxinae is rejected here, because (1) some of the putative synapomorphies are poorly defined, (2) the characterization of some Colostethinae and Hyloxinae as not able to sequester alkaloids is unfounded, because the chemical profile of the vast majority of species is lacking, (3) the alignment and phylogenetic analysis methods used are dubious (Wiens 2007), and (4) repeated mistakes in their molecular dataset were found (see below). For these reasons, the proposed split is not followed and we return Dendrobatidae to a single family that includes all members of both of the Grant *et al*.'s Dendrobatidae and Aromobatidae.

Grant *et al*. (Grant et al. 2006) redefined *Colostethus* to be monophyletic, but did not include the type species *C. latinasus* in their analysis. We found clear

paraphyly of Grant *et al.*'s (Grant et al. 2006) redefined *Colostethus* (indicated by *Colostethus* 1 and 2, each with high support), which paradoxically still renders *Colostethus* paraphyletic even after all the proposed taxonomic rearrangements to remove paraphyly. For the moment, we restrict *Colostethus* to the group of *C. latinasus* and allies (species in *Colostethus* 1 clade). *Colostethus* sensu lato is applied to the aggregate of species found in *Colostethus* 1 and 2 clades in our phylogeny.

Third, *Dendrobates* sensu lato (including *Adelphobates*, *Dendrobates*, *Excidobates*, *Minyobates*, *Oophaga*, and *Ranitomeya*) was found to be a well-supported monophyletic group (as it was previously); thus the splitting of *Dendrobates* into several genera is unnecessary (e.g., *Excidobates* (Twomey and Brown 2008)) and Grant *et al*. did not provide an unambiguous list of synapomorphies for their generic concepts. Some of the putative synapomorphies for genera used by Grant *et al*. (Grant et al. 2006) are ambiguous, and others are problematic; These include those with sequence errors (see below), those that are polymorphic intraspecifically (coloration pattern and alkaloid presence), poorly defined (e.g., advertisement call type), or undetermined in most species (e.g., larvae morphology, chromosome number, alkaloid profile, and type of parental care). Therefore, we synonymize *Adelphobates*, , *Excidobates*, *Minyobates*, *Oophaga*, and *Ranitomeya* in the genus *Dendrobates*.

Other minor changes are: (1) *Allobates craspedoceps* was found within *Hyloxalus*, so a new combination is proposed: *Hyloxalus craspedoceps*; (2) *Hyloxalus argyrogaster* was found with *Colostethus* sensu lato, so its new

combination is *Colostethus argyrogaster*, and (3) we were able to find remnant populations of *Allobates peruensis* (closely allied to *A. kingsburyi*); thus it is a valid name and not a *nomen dubium* as proposed by Grant *et al*. (Grant et al. 2006).

Some discrepancies between our results and those of Grant *et al*. (Grant et al. 2006) are explainable by mistakes in their molecular dataset. One set of mistakes possibly came from contamination. For example, the cytochrome oxidase (COX) sequence of *Allobates brunneus* (GenBank DQ502910) is identical by BLAST search to the paper wasp *Polistes dominulus* (GenBank DQ172914); similarly, the COX sequence of *Allobates femoralis* (GenBank DQ502733) is identical to Mediterranean sand smelt fish *Atherina hepsetus* (GenBank AY290810). Apparently, some tube mislabeling also occurred; as one example, the RAG-1 sequence of *Colostethus fraterdanieli* (GenBank DQ503373) is identical to *Phyllobates bicolor* (GenBank DQ503377) and not to other *C. fraterdanieli* RAG-1 sequences of the same population (GenBank DQ503371-2 and DQ503375). Although we used some sequences from Grant *et al*. (Grant et al. 2006) in our analysis, none yielded anomalous results. However, the possibility that other sequences not used by us might come from misidentified specimens remains. For these reasons, we suggest the sequences in Grant *et al*. (Grant et al. 2006) require thorough vetting through BLAST (http://www.ncbi.nlm.nih.gov/BLAST/) and other means.

Super-Region	Diversity		γ	*p*
	Total	Sampled		
Amazon Basin	76	61	2.192	0.028*
Andes	130	73	0.961	0.337
Central America-Chocó	73	62	3.054	0.002*
Guiana-Venezuela-Brazilian Shield	74	30	-0.012	0.991
All Areas	353	223	-0.662	0.508

Table 2.1: Results of the adjusted γ statistic (Pybus and Harvey 2000; Weir 2006) from the chronogram and subtrees of each of the super-regions, the total taxonomic diversity (described and undescribed species), the number of species sampled in the poison frog chronogram and super-regions, the adjusted γ statistic, and the probability of rejecting H_0: the pure birth expectation of exponential growth, $\gamma = 0$.

$a = \mu/\lambda$	Model	log *L*	LRT	ΔAIC[a]	$r = \lambda - \mu$	r_{CL}	λ	λ_{CL}
$a = 0$	constant-rate	-258.598	13.443*	9.444	0.1165	--	0.1165	--
	flexible-rate	-251.876	--	--	0.1096	0.3544	0.1096	0.3544
	rate-decrease	-255.813	--	7.874	0.1183	0.0001	0.1183	0.0001
$a = 0.99$	constant-rate	-275.286	7.475*	3.475	0.0033	--	0.3328	--
	flexible-rate	-271.549	--	--	0.0029	0.0219	0.2927	2.1851
	rate-decrease	-272.964	--	2.830	0.0041	0.0019	0.4093	0.1899

*The flexible-rate model is accepted over the constant-rate model ($\chi^2 > 3.84$, $p < 0.05$).
[a]ΔAIC values are the differences from the best model.

Table 2.2: Diversification rate estimates and fit under constant, flexible, and rate decrease model in poison frogs.

Node	Area	Event	Age MYA	log L	p	r	r_{CL}	r_{CL} / r
1	Amazon	increase	8.72	-251.876	<0.001	0.1096	0.3544	3.2336
2★	Andes-Amazon	increase	21.68	-253.645	0.001	0.1102	0.2800	2.5408
3	Chocó	increase	16.87	-255.586	0.014	0.1083	0.1765	1.6297
4	Guiana	slow-down	23.75	-255.813	0.018	0.1182	0.0001	0.0008
5	Amazon	increase	13.95	-255.967	0.022	0.1106	0.1943	1.7568
6	Andes-Amazon	increase	16.81	-256.142	0.027	0.1111	0.1972	1.7750
7	Andes	slow-down	30.92	-256.178	0.028	0.1212	0.0588	0.4851
8	Andes	slow-down	3.14	-256.574	0.044	0.1185	0.0241	0.2034
9★	Amazon	increase	15.16	-256.580	0.045	0.1110	0.1781	1.6045
10	Chocó	increase	13.15	-256.643	0.048	0.1117	0.1844	1.6509

Table 2.3: Significant shifts in diversification rate under the flexible-rate model with the lowest extinction fraction (a = 0). Node numbers correspond to Figure 2.3 and the ★ might be spurious due to a "trickle-down effect" (see Lineage Diversification section).

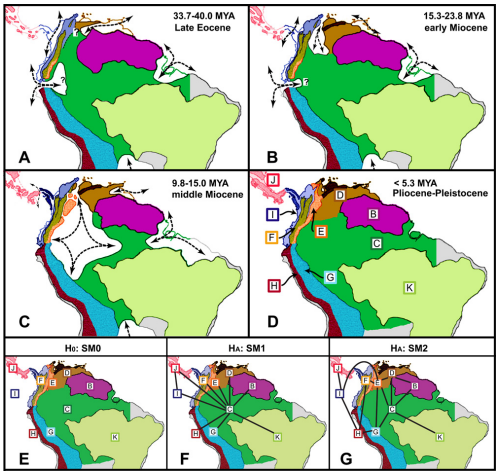

Figure 2.1: Biogeographic areas, extension of the floodbasin system or marine incursions (hatched arrows), and possible connections within Cenozoic paleogeographic maps of Central and South America, modified (Hoorn, 1994; Diaz de Gamero, 1995). Panels A-D correspond to paleogeographic reconstruction of northern South America. A: early to late Eocene; B: late Oligocene to middle Miocene; C: middle to late Miocene; and D: early Pliocene to the present. Uncertainties about the limit between biogeographic regions before the Pliocene are indicated by "?". The hypotheses about the spatial configuration of biogeographic areas on the origin of Neotropical diversity are indicated in the panels E-G. E: the null model (H_0: SM0), that assumes no spatial structure and equal rates of dispersal among all areas; F: the center-of-origin model (H_A: SM1), that assumes the Amazonia as the primary center of origin with widespread ancestral ranges constrained to include the Amazon Basin; and G: the stepping-stone model (H_A: SM2), that the assumes the historical spatial arrangement of biogeographic areas and constrains dispersals among geographically adjacent areas. The biogeographic areas used in the dispersal-extinction-cladogenesis (DEC) modeling are the Amazon Basin (C), Guiana Shield (B), Venezuelan Highlands and Trinidad and Tobago Islands (D), North Oriental Andes (E), North Occidental Andes (F), Central Oriental Andes (G), Central Occidental Andes (H), Chocoan rainforest, Magdalena Valley, and Gorgona Island (I), Central America west of the Gatun Fault Zone in Panamá (J) and the Brazilian Shield (K).

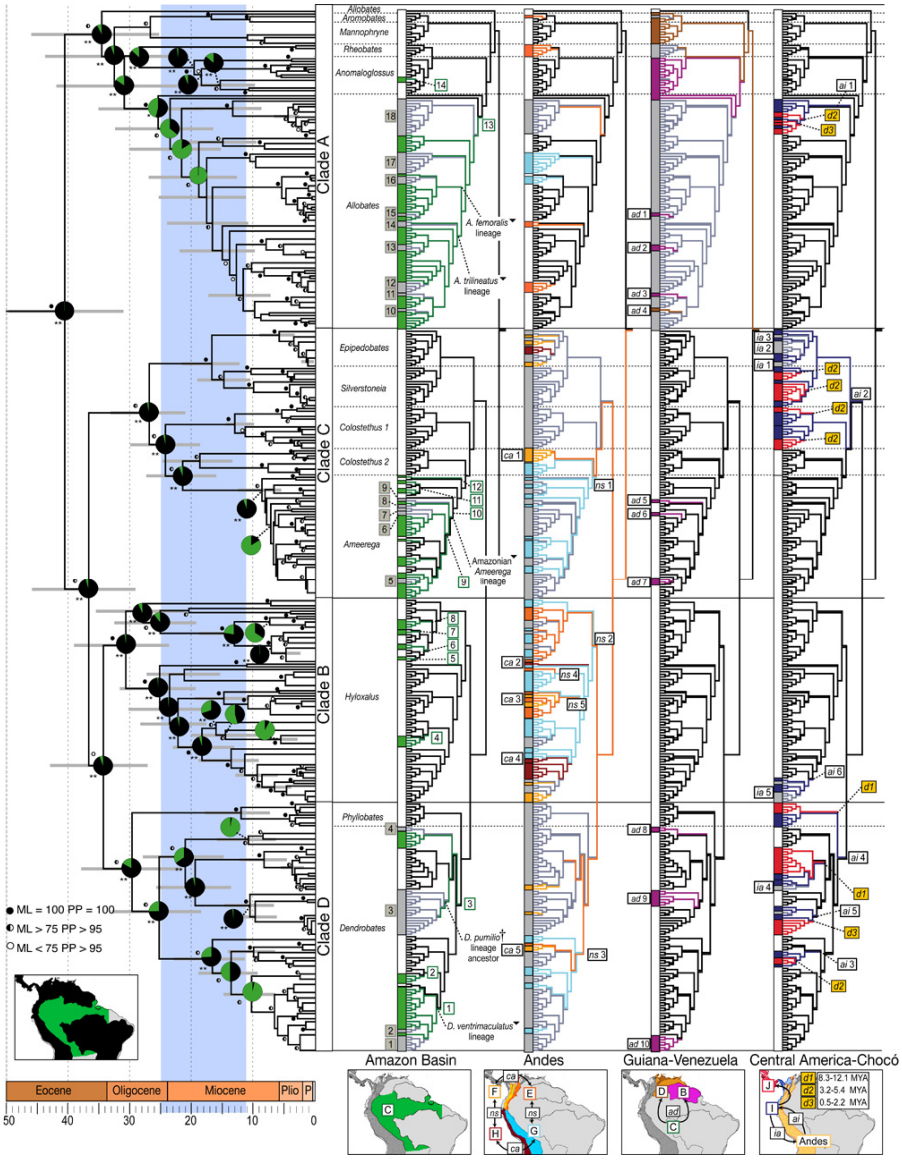
Clade A
Clade C
Clade B
Clade D
Allobates
Aromobates
Mannophryne
Rheobates
Anomaloglossus
Epipedobates
Silverstoneia
Colostethus 1
Colostethus 2
Ameerega
Hyloxalus
Phyllobates
Dendrobates
A. femoralis lineage
A. trilineatus lineage
Amazonian Ameerega lineage
D. pumilio lineage ancestor
D. ventrimaculatus lineage
ML = 100 PP = 100
ML > 75 PP > 95
ML < 75 PP > 95
Eocene
Oligocene
Miocene
Plio
P
50
40
30
20
10
0
Amazon Basin
Andes
Guiana-Venezuela
Central America-Chocó
d1 8.3-12.1 MYA
d2 3.2-5.4 MYA
d3 0.5-2.2 MYA
Andes

Figure 2.2: Box Chronogram and major biogeographic events of the poison frogs divided by major regions and inferred from the DEC (dispersal-extinction-cladogenesis) analysis. The green slice of the pie charts is the proportion of the likelihood associated with Amazonian reconstruction using Bayesian analysis of ancestral traits. The test results against the null hypothesis of an Amazonian ancestral state are indicated as * ($p < 0.05$) significant and ** ($p < 0.001$) highly significant. In the chronogram, support values from 200 non-parametric bootstrap replicates (ML), Bayesian posterior probabilities (PP), and the 95% CI of the estimated node age are also indicated. The major geographical events reconstructed using the SM2 model were mapped onto the ML phylogeny. The Amazon Basin subtree includes dispersals into Amazonia (numbered white squares), out of Amazonia (numbered gray squares), major lineage diversifications (5), and a lineage extinction (†). The Andes subtree includes cross-Andean (*ca* boxes) events, Northern-Southern Andean (*ns* boxes) dispersals, and the identification number of each event (Santos et al. 2009). The Guiana-Venezuela subtree includes dispersals toward this region from the Amazon Basin lineages (*ad* boxes) and the identification number of each event (Santos et al. 2009). The Central America-Chocó subtree indicates the three dispersals from Chocó and Central America (*d1*, *d2*, and *d3* yellow boxes), dispersals from the Andes to the Chocó (*ai* boxes), from the Chocó to the Andes (*ia* boxes) and the identification number of each event (Santos et al. 2009). For all subtrees, the tree branches and the rectangles at the tips of each tree are color coded as follows: (1) gray rectangles connected by gray branches mean extant lineages distributed in other areas different from the subtree region, but that descend from an ancestor distributed in the exemplified subtree region, (2) white rectangles connected by black branches indicate extant lineages distributed in other areas different from the subtree region, (3) color-coded rectangle and branches indicate extant lineages distributed in the exemplified subtree region. The duration of the Miocene floodbasin systems is indicated by blue-gray area. For detailed ancestral area reconstructions and date estimates with confidence intervals, see (Santos et al. 2009).

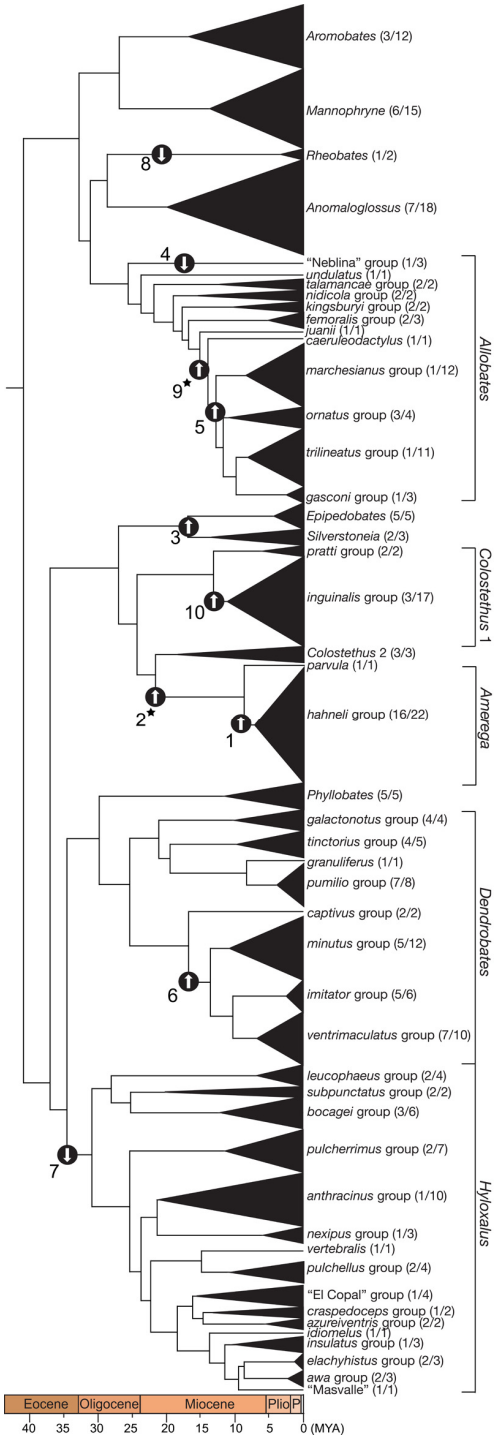
Aromobates (3/12)
Mannophryne (6/15)
Rheobates (1/2)
Anomaloglossus (7/18)
"Neblina" group (1/3)
undulatus (1/1)
talamancae group (2/2)
nidicola group (2/2)
kingsburyi group (2/2)
femoralis group (2/3)
luanii (1/1)
caeruleodactylus (1/1)
marchesianus group (1/12)
ornatus group (3/4)
trilineatus group (1/11)
gasconi group (1/3)
Allobates
Epipedobates (5/5)
Silverstoneia (2/3)
pratti group (2/2)
inguinalis group (3/17)
Colostethus 1
Colostethus 2 (3/3)
parvula (1/1)
hahneli group (16/22)
Amerega
Phyllobates (5/5)
galactonotus group (4/4)
tinctorius group (4/5)
granuliferus (1/1)
pumilio group (7/8)
captivus group (2/2)
minutus group (5/12)
imitator group (5/6)
ventrimaculatus group (7/10)
Dendrobates
leucophaeus group (2/4)
subpunctatus group (2/2)
bocagei group (3/6)
pulcherrimus group (2/7)
anthracinus group (1/10)
nexipus group (1/3)
vertebralis (1/1)
pulchellus group (2/4)
"El Copal" group (1/4)
craspedoceps group (1/2)
azureiventris group (2/2)
idiomelus (1/1)
insulatus group (1/3)
elachyhistus group (2/3)
awa group (2/3)
"Masvalle" (1/1)
Hyloxalus
1
2
3
4
5
6
7
8
9
10
Eocene
Oligocene
Miocene
Plio
P
40 35 30 25 20 15 10 5 0 (MYA)

Figure 2.3: The genus-supraspecific level tree (GSPF chronogram) of poison frogs with known taxonomic diversity (i.e., numbers within parentheses) and significant diversification rate changes for nodes or lineages from Table 2.3 (🙃 indicates rate increase, and 🙃 indicates rate decrease). Taxonomic diversity is indicated by the species sampled in our study (left number) and the total number of species described per group or genus (right number). The highest diversification increase (node 1) corresponds to the widespread *Ameerega* lineage that rapidly expanded into Amazonian since the late Miocene. The Andean-Amazonian increase (node 2) corresponds to the diversification of clade *Colostethus* 2 in the early Miocene. The Chocoan increases (nodes 3 and 10) correspond to the lowland radiation in western Colombian and Ecuadorian lowlands of *Colostethus* sensu lato, *Epipedobates*, and *Silverstoneia* during the middle Miocene and before the formation of the Panamanian Land Bridge. The Guiana decrease in the early Miocene (node 4) corresponds to the *Allobates* lineage of the Guianan tepuis. The Amazonian rate increases (nodes 5 and 9) correspond the largest radiation of *Allobates* since the Miocene to the Pliocene. The Andean-Amazonian increase (node 6) corresponds to the diversification of clade *Dendrobates* from the eastern Central Andean foothills into Amazonia since the early Miocene. The Andean decreases (nodes 7 and 8) correspond to a slow-down of the diversification of *Hyloxalus* (Clade B) and *Rheobates* (Clade A) lineages during the late Oligocene and Pliocene, respectively. The significant increases indicated by ★ next to nodes 2 and 9 might be dependent on deeper nodes (i.e., 1 and 5 respectively) and produced by a "trickle-down effect" (see Lineage Diversification section).

Chapter 3: Evolution of Complex Phenotypes in Poison Frogs: Scaling and Aposematism

INTRODUCTION

Biological systems can be described as an array of phenotypes derived by common ancestry, natural selection, and drift (Pigliucci and Preston 2004). Each phenotype is shaped by interactions with other traits at different levels, which provide epigenetic and emergent properties to the organism as a whole. Adaptive landscapes are structured from the plasticity among phenotypic traits (Van Buskirk and Steiner 2009) and polymorphic phenotypes are derived from genetic interaction (e.g., epistasis, codominance) (Whitlock et al. 1995). Therefore, the co-adapted functionality of multiple traits is likely to increase the complexity and diversity among living organisms. Here, we present a description of the phenotypic landscapes of aposematism and scaling (body mass and metabolic rates) as emergent complex traits in poison frogs using multivariate evolutionary comparative analyses. As well, we provide a phylogenetic analysis of metabolic rates in Anura.

Life-history traits associated with energy allocation for maintenance, growth, and reproduction are usually scaled to mass (Calder 1996). Scale has important ecological and evolutionary implications in the mechanistic and adaptive energy flux between individuals and their environment (Brown et al. 2000; Woodward and Hildrew 2002). Body size has definitive consequences for species abundance, interspecific competition, foraging ecology, social interactions, home range, life expectancy, generation time, and all metabolic processes (Dayan and Simberloff 2005; Moen and Wiens 2009; Schmidt-Nielsen 1984). Scale also has ecological and evolutionary implications above the

organism level in the generation of diversity and assemblage of ecosystems (Banavar et al. 1999; Brown et al. 2004).

Metabolism is the most significant life-history property; it is defined as the set of all biochemical reactions within an organism (Hulbert and Else 2000). Metabolic rates are tightly associated with body mass and heat production at different activity levels (Schmidt-Nielsen 1984). Basal metabolic rate (BMR) is the basic measure of the minimal energetic cost to sustain life and proportional to other metabolic rates (Hulbert and Else 2000). For ectotherm vertebrates (e.g., fish, amphibians, and reptiles), the minimal energetic cost of maintenance is called the resting metabolic rate (RMR); it is measured at rest, at controlled temperature, and in a post-absorptive status (Feder and Burggren 1992). At higher levels of activity, the energetic cost during activity is called active metabolic rate (AMR) under sustainable locomotion (e.g., endurance) or non-sustainable exercise (e.g., forced activity) (Feder and Burggren 1992). A common derivation of both measurements (e.g., difference or ratio) is the metabolic scope or the amount of energy provided by aerobic pathways for muscular activity (Schmidt-Nielsen 1984). However, most metabolic rate studies usually lack a phylogenetic perspective as well as knowledge of the association of metabolic rate with other traits, which required for understanding the evolution of complexity across the Tree of Life (Feder et al. 2000).

Since Darwin's time, few complex phenotypes have attracted so much attention on their evolution and maintenance as aposematism (Harlin and Harlin 2003). Aposematism is a deterrence strategy that is best described as an emergent trait derived from the significant association of warning signals (e.g., conspicuous coloration) and the presence of defense (e.g., noxious substances) (Marples et al. 2005; Servedio 2000). In the aposematic interaction, potential predators are expected to easily associate brightly colored prey with a costly or lethal meal and thus abstain from attack (Guilford 1988; Harlin and Harlin 2003). At least three

reasons make the evolution and maintenance of aposematism complex. First, the origin of defense might require a physiological capability to synthesize or sequester defensive compounds (Broom et al. 2005; Nishida 2002). Second, conspicuousness has to be effective and associated with the degree of defense of the prey by potential predators (Stevens 2007). Three, conspicuousness and defense might have to originate in simultaneously and require comparable energetic costs for maintenance (Blount et al. 2009). Under these conditions, the evolution of unpalatability is more likely to precede the origin of warning signals (Alatalo and Mappes 1996; Guilford 1988; Guilford and Dawkins 1993; Lindström 1999; Tullberg et al. 2000). However, the evolution of aposematism might be entangled with other traits (e.g., diet specialization, gregariousness, metabolism) and their associations might directly contribute to its maintenance and diversification (Ruxton and Sherratt 2006; Ruxton et al. 2004).

Complex phenotypes usually emerge from component trait covariation, selection, and environmental factors. For the origin of defense, some aposematic systems rely on xenobiotic metabolites usually derived from prey or symbionts and require dietary specialization (Darst et al. 2005; Santos et al. 2003). However, specialists are expected to have lower fitness than generalists unless the selection favors multiple adaptive peaks (Vantienderen 1991). Additionally, phenotypic specialization on a narrow prey range is energetically inefficient because of rejection of syntopic prey items (Robinson and Wilson 1998).

Amphibians are not an exception to the evolutionary implication of scale. The ecological implication of body size in amphibians has been documented for salamanders (Burton and Likens 1975) and frogs (Beard et al. 2002; Stewart and Woolbright 1996). In anurans, body size has mostly been studied in the context of community assemblage, niche partitioning (habitat and dietary), predation, and sexual selection (Duellman and Trueb 1986; Wells 2007). However, the evolutionary aspects of scale in anurans in a phylogenetic context are rarely

studied (Kozak et al. 2009; Moen and Wiens 2009). Few diverse lineages of anurans have been studied for multiple traits simultaneously.

Probably one of the best examples of a complex of traits in a single lineage of amphibians are the poison frogs (Dendrobatidae). Dendrobatids are an endemic Neotropical clade (~270 species) of small anurans (body mass ranges from ~0.1 to 10 g, 2 orders of magnitude). This group has a well-sampled phylogeny (Grant et al. 2006; Santos et al. 2009) and distinctive adaptations including conspicuous coloration, alkaloid sequestration, complex parental care, and diet specialization (Darst et al. 2005; Santos et al. 2003; Summers and Clough 2001; Summers and Earn 1999; Summers et al. 1999). Brightly colored species usually have skin alkaloids (~800 identified) derived by sequestration from specialized diet of ants and mites (Daly et al. 1994; Saporito et al. 2009). Physiologically, only seven species of poison frogs have been characterized metabolically, but without a broader context of the tendencies of the clade (Navas 1996a; Navas 1996b; Pough and Taigen 1990; Taigen and Pough 1985; Taigen and Pough 1983b). The implications of aerobic metabolism have been hypothesized to be associated with alkaloid sequestration and diet specialization (Pough and Taigen 1990; Taigen and Pough 1985; Taigen and Pough 1983b). However, a comprehensive phylogenetic approach that includes metabolism, aposematism, diet specialization, and scale under a single multivariate phylogenetic comparative analysis is lacking.

The main goal of our research is to provide the first integrative approach to the evolution of complexity in the poison frog clade. We have divided our effort into several objectives and specific tests of hypotheses. First, we provided of adequate background for the poison frogs by constructing a metanalysis of the metabolic physiology of anurans using phylogenetic comparative techniques. Our null hypothesis is that poison frogs as a clade do not differ from other anurans.

Second, we tested whether the evolution of higher aerobic capacity is associated with aposematism and diet specialization. For this purpose, we used a combination of multivariate regressions and bivariate comparative analyses (e.g., independent contrasts and general least squares analyses). Third, we reconstructed the evolutionary history of aposematism, diet specialization, and high aerobic capacity using maximum likelihood ancestral state reconstructions. Fourth, we implemented a new phylogenetic multivariate approach based on exploratory and confirmatory factor analyses to model the underlying phenotypic landscape of trait associations between aposematism, metabolism, and scale variables. We fitted seven alternative hypotheses and find the best model of phenotypic associations that explains our observed data based on a LTR likelihood ratio test for model fit. Our results revealed a complex network of multivariate correlations among the traits, and we propose a model of phenotypic integration of conspicuousness, alkaloid sequestration, diet specialization, and aerobic metabolism adaptations.

MATERIALS AND METHODS

Capture and Handling of Poison Frogs

We measured physiological parameters from 474 individuals of 55 species of poison frogs (Figure 3.1 and Table 3.1). Measurements from 49 species (454 individuals) were obtained from natural populations and the remaining six species (20 individuals) from captive bred individuals. Adult individuals from natural populations were collected by hand during the day, in pristine or secondary

growth habitats. Frogs were transported from the collection site to the field lab in plastic containers provided with humid substrate. In the lab, all animals were kept fully hydrated, fed ad libidum, and allowed to adjust to lab conditions (24.5-25.5 °C) for 1-2 weeks. Before the experiments, the animals were fasted for 2-3 days to ensure that they do not expend energy on digestion. Two physiological variables were measured: (1) resting metabolic rate (RMR, oxygen consumption while resting or VO2rest consumed/hour), and (2) active metabolic rate after non-sustainable exercise (AMR, oxygen consumption after forced activity or VO2active consumed/hour). All measurements were taken between 24.5-25.5 °C, during the day from 10:00h-18:00h (poison frogs are diurnal and crepuscular), and the same individual was measured between 2-3 times to estimate individual variability. Ambient water pressure was determined using a digital thermo-hygrometer (Mannix PTH8708). Animals were weighed before and after physiological measurements to the near 0.01 g with a digital balance (Ohaus Scout Pro Balance SP-202). Capture and handling of the animals were in concordance to the protocols under the animal care permit IACUC #05111001.

Measurement of the Physiological Parameters

We measured the rates of O2 consumption by constant-volume respirometry using O2 gas analyzer, scrubbing only water vapor with VCO2produced correction (Lighton 2008). We used ambient O2 as span gas, and O2 consumption estimated using manual bolus integration (Gomes et al. 2004; Lighton 2008; Navas 1996b). The experimental chambers (plexiglass or glass)

ranged in volume from 18-110 mL with enough volume to allow free movement of the individual. Between 4-6 hours before the experiment, the individuals were placed in their experimental chambers at standard temperature (24.5-25.5 °C) with incurrent ambient air at low flow rate and fully hydrated to reduce stress before the measurements. The effect of altitude of the field lab or origin of the experimental individuals (i.e., pet trade or natural population) did not affect the accuracy of our measurements (see Supplementary Methods).

Oxygen concentration was estimated using a field portable integrated oxygen analysis instrument (FoxBox, Sable Systems Inc.). The measurements were done to 0.001% resolution for O2 concentration, and barometric pressure compensation with accuracy at 0.1%. Before each measurement, the oxygen analyzer was calibrated to ambient O2 concentration (0.2095) and the mass flow controller was set to 200 mL/minute. Water vapor was scrubbed using anhydrous CaSO4 (Drierite, W. A. Hammond DRIERITE Co. LTD), and temperatures of the chamber and ambient were recorded using thermocouples during each measurement.

For the first parameter (RMR or VO2rest consumed/hour), fresh air was injected into the chamber and then it was hermetically closed for 1 hour. The frogs were kept at the control temperature, in a dark container, and constantly monitored for movement (data from frogs that moved were discarded). The measurement was repeated 2-3 times and the lowest measurement was used as an estimate of the resting metabolic rate (Table 3.2). For the second parameter (AMR or VO2active consumed/hour), fresh air was injected into the chamber and then it

was closed for 4 minutes. The chamber was manually rotated causing the frog to move (e.g., hop or walk) and forcing the individual to reach non-sustainable exercise level. The measurement was repeated 2-3 times with at least 1 day between experiments and the average was used as an estimate of the active metabolic rate (Table 3.2).

After each experiment, the air mixture from the chamber was injected into the flow-through respirometry system in a push mode configuration with the mass flow controller upstream, and the water vapor scrubber downstream of the chamber. The O2 concentration was recorded from the air exiting from the scrubber for 10 min at 0.5-sec intervals using the data logger FoxBoxDaemon for ExpeData ver 1.0.17 (Sable Systems Inc.). The volume of O2 consumed after the experiment (VO2comsumed) was determined using the standard equations for constant-volume respirometry (Bartholomew and Lighton 1986; Lighton 2008; Navas and Gomes 2001) (see Supplementary Methods). Data recorded were log-transformed and corrected for body weight, temperature, and barometric pressure to normalize distribution before analyses. Our estimates of O2 consumption were validated against a dry mixture of O2 and N2 in 24 different concentrations (range: 13.50-20.75% O2) as a reference for the manual bolus integration (Lighton 2008).

Aerobic metabolic scope (Scope) was calculated by the difference between AMR and RMR (Gatten et al. 1992). Scope provides an estimate of the amount of energy provided by aerobic pathways for muscular activity and the maximal rate at which oxygen used by the organism (Schmidt-Nielsen 1984).

Additionally, we calculated the factorial aerobic scope (AMR/RMR) as an estimate of the factor by which oxygen consumption increases with forced physical activity (Gatten et al. 1992).

The volume of O_2 consumed by the individual after the experiment ($V_{O2comsumed}$) was adjusted to STP conditions (standard conditions for temperature and pressure) and determined by the following equation (Lighton 2008; Vleck 1987):

$$V_{O2comsumed} = [V_{CH} (F'_{iO2} - F'_{eO2})]/[1 - F'_{eO2}(1 - RQ)]$$

where, V_{CH} is the volume of the experimental chamber, F'_{iO2} is the fractional concentration of O_2 at the beginning of the experiment, F'_{eO2} is the fractional concentration of O_2 within the chamber at the end of the experiment, and RQ is an approximation to $V_{CO2produced}$ in ~3% if 0.85 is assumed(Vleck 1987).

The estimations of the other parameters (excluding RQ) were determined with the following equations. The volume of the experimental chamber V_{CH} is determined by the following:

$$V_{CH} = V_{Initial} - (M_{individual}\, \rho_{indiviual}) - V_{iH2O}$$

where, $V_{Initial}$ is the volume in mL of the empty chamber, $M_{individual}$ is the mass of the individual in grams, $\rho_{indiviual}$ is the density of the organism and usually assumed to be 0.98 g/mL (Lighton 2008), and V_{iH2O} is the water pressure estimated from the ambient humidity.

The F'_{iO2} or fractional concentration of O_2 within the chamber at the beginning of each experiment was determined by

$F'_{iO2} = V_{iO2}/V_{CH}$

where, V_{iO2} is the volume of O_2 initially present at the beginning of the experiment and V_{CH} is volume of the experimental respirometry chamber.

The F'_{eO2} or fractional concentration of O_2 within the chamber at the end of each experiment was determined by

$$F'_{eO2} = (V_{iO2} - V_{O2comsumed})/(V_{CH} - V_{O2comsumed} + V_{CO2produced} - V_{H2O})$$

where, V_{iO2} is the volume of O_2 initially present at the beginning of the experiment, $V_{O2comsumed}$ is the volume of O_2 consumed by the individual after the experiment, V_{CH} is volume of the experimental respirometry chamber, $V_{CO2produced}$ is the volume of CO_2 produced by the individual after the experiment, and V_{H2O} is the water vapor lost by the individual after the experiment.

Anuran Metabolic Rates Metanalysis

We compared our physiological measurements of poison frogs against those of anurans as a clade. Physiology measurements (RMR and AMR) at 20°C and 25°C of 117 species of anurans were compiled to include those from Gatten et al. (1992) (Gatten et al. 1992) and new species reported after that review (Table 3.3). We tried to maximize the amount of statistical information for both RMR and AMR to accurately reflect the general trends in anurans. In general, most RMR methodologies are comparable and allowed us to combine them for statistical analyses (Gatten et al. 1992; Wells 2007). In contrast, AMR is

determined by two common experimental methodologies (hand or motor treadmill rotation) to achieve the level of physical activity required in maximizing the O2 consumption (Gatten et al. 1992). Different physiologists have advocated for one methodology over the other as more reliable approach to maximize O2 consumption (Rogowitz and Sánchez-Rivoleda 1999; Walsberg 1986; Wells 2007). Hand rotation accounts for > 70% of all the reports of AMR in anurans and most of motor rotation measurements came from mostly "walker frogs" especially bufonids (Gatten et al. 1992; Wells 2007). We compared the VO2active consumed/hour for both techniques and found a slight tendency ($F_{1,40} = 3.878$ $p = 0.056$NS) for higher rates of oxygen consumption at 20°C by animals that used the treadmill. However, we found not a significant effect ($F_{1,40} = 0.002$ $p = 0.961$NS) for different rates of oxygen consumption at 25°C by animals that used either the treadmill or the manual rotation. Therefore, we combined both motor and hand rotation AMR measurements in a single analysis.

Measurement of Conspicuousness

Our approach was based on the sampling coloration from scanned color photographs using a "pixel count " methodology (Summers and Clough 2001) (see explanation in Supplementary Methods). Our technique can be summarized: (1) we took color photographs with flash from the dorso-lateral side of the sampled species and their natural background (leaflitter); (2) the frog and leaflitter images were divided between 15-30 non-overlapping polygon samples of homogeneous color with Adobe PHOTOSHOP (Adobe 2008); (3) from each

polygon, we took the number of pixels, and the means from luminosity (brightness), and from each of the histograms of the primary colors (red, green, and blue, RGB); (4) we use a MANCOVA analysis of the luminosity (covariate) and the RGB channels to determine the predicted values for each RGB channel under constant luminosity; (5) a two-step likelihood cluster analysis was used to calculate the RGB coordinates (a 3-D coordinate) of the centroid of all leaflitter measurements; (6) the Euclidean distance between each frog polygon and the leaflitter centroids was used as a relative measurement of the conspicuousness of the polygon; (7) the proportion of pixels of the polygon to the total number sampled was multiplied to Euclidean distance, which provided a weighted contribution of the total conspicuousness of the frog; and (8) the total relative conspicuousness of the frog was determined by adding polygon the weighted color distances. Our methodology provides a continuous relative measurement of conspicuousness against a natural background environment (leaflitter) useful for the comparative analyses (Table 3.4). Alternatively, we also use a binary classification of the coloration by setting a cutoff for conspicuousness from values above the mean (i.e., 57.69) of the continuous color ranking.

Skin Alkaloid Profiles

Lipophilic skin alkaloid profiles were compiled from poison frog alkaloid published accounts (Daly et al. 1999; Daly et al. 2009; Darst et al. 2005; Saporito et al. 2007) and assessed (presence and concentration) from six species (20 skins) using thin layer chromatography (TLC; Table 3.4). The protocol for TLC was explained in detail on previous skin alkaloid assessments from poison frog skins

(Myers and Daly 1976) (Darst et al. 2005). We used five positive controls from methanol skin extracts of Dendrobates sylvaticus, Ameerega parvula, and A. bilinguis. Our negative controls included two methanol skin extracts of Hyloxalus maculosus and pure methanol (Figure 3.2). We failed to find alkaloids in skins of Allobates kingsburyi, Colostethus fugax, Epipedobates machalilla, Hyloxalus nexipus, and H. vertebralis. However, we found alkaloids in skins of Dendrobates captivus.

We divided the lipophilic skin alkaloid profiles into three variables: presence (categorical), concentration (continuous), and diversity (continuous) (Table 3.4). Alkaloid presence corresponds to proven ability of species to sequester lipophilic alkaloids. We scored as positive all species with skin alkaloids or those that have been experimentally demonstrated (e.g., artificial alkaloid feeding) to sequester alkaloids. We scored Hyloxalus azureiventris to be able to accumulate alkaloids based on the recent review of the arthropod dietary origin (Daly et al. 2009). Alkaloid concentration corresponds to abundance of lipophilic alkaloids detected in 100 mg of skin: 0 (no alkaloids detected), 1 (alkaloids present < 50 μg), 2 (alkaloids present > 50 and < 200 μg), and 3 (alkaloids present > 200 μg). We found significant amount of alkaloids in Dendrobates captivus (Figure 3.2) and assigned it level 3 after comparison with D. sylvaticus (+ control). Alkaloid diversity was determined by the total number of alkaloid classes found in at least one individual of the species sampled (Daly et al. 1999; Daly et al. 1987; Saporito et al. 2007).

Dietary Specialization

We determined the importance of dietary specialization on the aposematic interaction and physiology by measuring three variables: the percentage of ants and mites, the mean number of prey per individual, and niche breadth (Table 3.5). Dietary profiles, including percentage of ant and mites items and mean number of prey per individual, were compiled from gastrointestinal content surveys of poison frogs (Bonilla and La Marca 1996; Caldwell 1996; Darst et al. 2005; Silverstone 1975; Toft 1977; Toft 1980; Toft 1981; Valderrama-Vernaza et al. 2009). Niche breadth was estimated from raw diet data using the inverse Simpson's index (1949) formula (Pianka 1986; Simpson 1949) for eight dietary categories (i.e., ant and mites, coleopterans, orthopterans, collembolans, dipterans, isopterans, spiders, and larvae) which correspond to >85% of all described prey items of poison frogs (Bonilla and La Marca 1996; Caldwell 1996; Darst et al. 2005; Silverstone 1975; Toft 1977; Toft 1980; Toft 1981; Valderrama-Vernaza et al. 2009). Niche breath provides a complementary estimate of diet specialization by providing a continuous value from 0 (specialist in a single prey category) to 1 (all prey categories are equally included in the diet). For the binary discrete and regression analyses, we assigned to the specialist category if the species has diet > 70% of ants and mites and < 0.15 niche breadth values.

Phylogenetic Reconstruction

For the anuran metanalysis, we inferred a phylogeny of the anurans (PA) from 121 species of frogs (33 families) and 9 outgroups: 3 non-amphibians (lungfish, human, and chicken), 3 species of salamanders (3 families), 3 species of

caecilians (3 families) phylogeny (Figure 3.3 and Table 3.3). The molecular data included were the widely available mitochondrial rRNA genes (12S and 16S sequences; ~2400 bp). The molecular phylogeny of the poison frogs (PPF) was inferred from 54 species and 6 outgroups (Figure 3.1 and Table 3.1). We used six mitochondrial segments (12S and 16S rRNA genes; Val, Leu, and Met tRNA genes; ND2 and Cytb protein coding genes; total ~4.5 kb) and seven nuclear protein-coding genes BDNF, BMP2, NACA, NT3, POMC, TYR, ZEB2 (total ~5.0 kb). GenBank accession numbers and specimen information are given in Santos et al. (unpublished). Protocols of DNA extraction, PCR purification, and sequencing are provided in previous studies (Bossuyt et al. 2006; Darst and Cannatella 2004; Santos et al. 2003). All sequences amplified or retrieved from GenBank were validated by comparison to other anuran sequences using BLAST (http://www.ncbi.nlm.nih.gov/BLAST/). By this procedure, we were also able to identify and exclude contaminated or mislabeled submissions.

Contigs were assembled using Sequencher 4.7 (GeneCodes 2006), aligned using ClustalX 1.81 (Thompson et al. 1997) and manually adjusted to minimize informative sites using MacClade 4.08 (Maddison and Maddison 2001). The phylogeny of anurans (PA) was inferred from 1962 unambiguously aligned characters from the unpartitioned mitochondrial sequence matrix. The phylogeny of the poison frogs (PPF) was inferred from 8517 unambiguously aligned characters using unpartitioned and partitioned by gene sequence matrices. For both PA and PPF, we used a GTR+Γ+I model of nucleotide substitution model as determined by ModelTest 3.7 (Posada and Buckley 2004; Posada and Crandall

1998). PA and PPF were analyzed with maximum likelihood (ML) methods under a genetic algorithm in GARLI 0.960 (Zwickl 2006) and under a sequential and parallel ML-based inference in RAxML 7.0.4 (Stamatakis 2006). For the GARLI and RAxML analyses, a total of 50 independent runs were used to infer the best tree and 500 nonparametric bootstrap searches were used to estimate support for the nodes. Both programs gave similar topologies and we used the best trees (PA and PPF) inferred by the RAxML method for all comparative analyses. The PPF phylogeny used for the comparative analyses does not differ significantly from previous studies (Grant et al. 2006; Santos et al. 2003; Santos et al. 2009).

Statistical Methods

We used both continuous measurements and binary discrete categories of all variables. Data distributions of the continuous measurements were normalized using transformations such as log (allometric: body mass, AMR, RMR, and Scope), arcsine/square root (percentage: ants and mites % in diet), or power Box-Cox method (alkaloid concentration, diversity) to meet statistical assumptions (Felsenstein 1985; Garland 1992). Discrete binary scores were assigned for conspicuousness (0, cryptic; 1, brightly colored), alkaloid sequestration (0, unable; 1, able), diet specialization (0, generalist; 1, ant & mite specialist), Scope (0, negative residuals from regression against body size; 1, otherwise), and RMR (0, negative residuals from regression against body size; 1, otherwise).

We used three sets of comparative methods to determine the evolutionary associations between alkaloid profiles, conspicuousness, dietary specialization, metabolic parameters, phylogeny, and body mass. First, we used regression

analyses to determine the relationship between body size and metabolic parameters (AMR, RMR, and Scope). This method was also applied for the metanalysis of Anura. Second, we used bivariate scores for alkaloid sequestration, conspicuousness, dietary, RMR, and Scope to test for correlated evolution among pairs of traits using ML models (Pagel 1997). Third, we analyzed the degree to which continuous pair of traits in poison frogs covary with phylogeny using Generalized Least Squares (GLS) (Pagel 1997) and independent contrasts (Felsenstein 1985). Fourth, a novel multivariate approach that estimates the best path diagram of relationships among the continuous variables measured in poison frogs.

For the first method, we included conventional least squares regression (CLSR) and phylogenetic independent regression analysis based on independent contrasts (PIC) (Felsenstein 1985). For the CLSR, we used a general linear model to fit the relationships of AMR, RMR, Scope, and body mass. We used the standard linear model: log (AMR, RMR, or Scope) = a (allometric coefficient) + b (allometric exponent) x log Mass for allometric relationships (Schmidt-Nielsen 1984). In a complementary analysis, we included the categorical binary traits as dummy variables (0, 1) to test for the significance of conspicuousness, alkaloid sequestration, and diet specialization. We used the following linear model for allometric and categorical variables: log (AMR, RMR, or Scope) = a (allometric coefficient) + [b binary x categorical variable] + b (allometric exponent) x log Mass (Wiersma et al. 2007).

For the PIC analyses, we used the phylogeny of anurans (PA) and poison frogs (PPF); their branch lengths were log-transformed to standardize the contrasts (Garland Jr. et al. 1993; Garland et al. 1992). The PICs were calculated using PDAP:PTREE (Midford et al. 2005) module of Mesquite ver 2.9 (Maddison and Maddison 2009). The regression analyses based on PIC were fit through the origin (Garland et al. 1992) and significance of the regression coefficients were determined. Finally, we explored the effect of outlier contrasts or grade shifts on RMR, AMR, and Scope PIC allometric analyses (Felsenstein 1985; Harvey and Pagel 1991). For this purpose, we compared the estimates of regression coefficients (i.e., allomatric coefficient and exponent) and regression equation with and without the grade shift contrasts (Nunn and A. 2000). All CLSR and the regression based on PIC calculations were carried on using SPSS ver 16.0 (SPSS 2008) and the significance level of alpha was set to 0.05.

For the second method, we tested for correlated evolution among pairs of binary discrete traits using ML models (Pagel 1997) implemented in the BayesDiscrete module of BayesTraits ver 1.0 (Pagel and Meade 2006; Pagel and Meade 2007; Pagel et al. 2004). We ran 100 optimization attempts to find the best likelihood (i.e., mltries 100) for both the correlated and independent evolution model for each pair of traits. We compared both models using likelihood ratio (LRT) statistic of the likelihood difference of both models to approximate its significance (Pagel and Meade 2007). Additionally, estimates of the ancestral states at nodes were derived using the likelihood reconstruction module in Mesquite ver 2.9 (Maddison and Maddison 2009) and the ML approach in

BayesMultistate module of BayesTraits ver 1.0 (Pagel and Meade 2006; Pagel and Meade 2007; Pagel et al. 2004). For the reconstruction in Mesquite, we used the "mk1 model" (Lewis 2001) and the likelihoods of alternative states were reported as raw likelihoods. For the BayesMultistate, we calculated the proportion of likelihood of both alternative character states at each node with 5,000 samples under default parameters (Pagel and Meade 2006). Similar results were found in both analyses and only the Mesquite results are reported.

For the third method, we used continuous measurements of all traits with the exception alkaloid diversity and niche breadth. These variables were excluded due to collinearity with variables alkaloid concentration and percentage of ants and mites. First, we analyzed the degree to which pairs of continuous traits in poison frogs covary with phylogeny using Generalized Least Squares (GLS) (Pagel 1997) implemented in BayesContinuous module of BayesTraits ver 1.0 (Pagel and Meade 2006; Pagel and Meade 2007; Pagel et al. 2004). The GLS analysis was used to determine the evolutionary regression coefficient "λ" (Pagel 1993), which incorporates information about phylogenetic history. Therefore, the λ parameter varies from 0, if the trait evolution is completely independent of the phylogeny, to 1, if the trait covaries completely with the phylogeny (i.e., follows a Brownian motion process). We tested the estimated λ of each trait against a null hypothesis of phylogenetic independence (i.e., $\lambda = 0$) using a likelihood ratio test (LRT). We calculated the correlation coefficient among traits accounting for the phylogenetic inertia by estimating at the same time the λ parameter. We also tested the correlation coefficient among traits against the null hypothesis of

independence (i.e., r = 0) using a likelihood ratio test (LTR). We cross-validated our results by estimating phylogenetically independent contrasts and their correlation coefficients among traits using PDAP:PTREE (Midford et al. 2005) module of Mesquite ver 2.9 (Maddison and Maddison 2009).

For the fourth method, we used a multivariate approach based on variance-covariance matrix of the continuous traits inferred from the independent contrasts. The continuous variables (indicator variables) included were body size, RMR, conspicuousness, alkaloid concentration, alkaloid diversity, ant and mites percentage on diet, and mean number of prey per individual (log-prey). AMR and niche breadth were excluded due to collinearity with Scope and ant and mite percentage on diet, respectively. The set of species used (n = 20, see Table 3.1) are those with measurements from all variables. First, we determined if the assumptions of multivariate normality and linearity were met by the indicator variables by analyzing their distribution using SPSS ver 16.0 (SPSS 2008). Second, we calculated the variance and covariance matrix from the correlation matrix from the independent contrasts computed though the origin (Garland et al. 1992) and their standard deviations. Third, we performed an initial phylogenetic principal component analysis (PPCA) and phylogenetic principal axis factoring (PPFA) with Varimax orthogonal rotation. We found that two components that explained 77.9% of the variance (Table 3.6): (1) scale variables (58.8% of variance): body mass, AMR, and RMR; and (2) alkaloid sequestration variables (19.0% of variance): alkaloid profile (concentration and diversity), and ant and mite % in diet. Conspicuousness and log-prey cross-loaded in both without a clear

affiliation to either component. Fourth, we performed a variable relationships two-factor confirmatory factor analysis with model respecification using a Lagrange Multiplier test (Ullman 2007) in MPlus ver 5.1 (Muthén and Muthén 2008). We inferred alternative models for the poison frogs that include two types of variables: (1) latent variables, which are not directly observed or measurable but are rather inferred (e.g., scale and aposematism), and (2) indicator variables, which are observable and directly measurable (e.g., body mass, metabolic rates, color conspicuousness, alkaloid concentration). Seven models (Figure 3.6) were tested for different alternative associations between the latent (scale and aposematism) and the indicator variables (alkaloid profiles, body mass, conspicuousness, dietary profiles and metabolic rates). All models were fitted to the observed variance-covariance matrix and the models were ranked based on a chi-squared test, and three measurements of model fit: Bentler's Comparative Fit Index (CFI), Rucker-Lewis Index (TLI), and Standardized Root Mean-Square Residual (SRMR) (Brown 2006; Grace 2006). We used joint criteria to retain a model based on fit scores for CFI $\geq$ 0.96, TLI $\geq$ 0.96, and SRMR $\leq$ 0.10 and a non-significant chi-square goodness of fit test (Hu and Bentler 1999). Finally, we compared among the retained models for the most parsimonious answer based on a LTR approach derived by the difference between the chi-square values and the number of free parameters (Grace 2006).

RESULTS

Metabolic Parameters of Anurans and Poison Frogs

The metanalysis of physiological parameters among anurans (including 56 species measured at 20°C and 61 species measured at 25°C) showed a significant variability across the group (Figure 3.1 and Table 3.7). The conventional least squares regression (CLSR) and phylogenetic independent contrast (PIC) analyses showed a significant difference in the unit-mass intercepts (log a allometric coefficient) and allometric exponent (b) for the RMR versus AMR or Scope at both temperatures (Table 3.7). For anurans, the oxygen consumed per unit-mass (allometric coefficient) and the rate of oxygen consumption (allometric exponent) increase at higher temperatures (i.e., between 20°C to 25°C) and levels of activity (i.e., AMR versus RMR). We found that the allometric exponent of the AMR and Scope departed from the expected ~0.75. This result might reflect differences in the rate of oxygen consumption at different temperatures (Gatten et al. 1992). Alternatively, the quality of the data reported for anurans could be heterogeneous, which is reflected in the combined metanalysis approach (Borenstein et al. 2009).

We measured the RMR, AMR, and Scope of 474 individuals of 55 species of poison frogs (Figure 3.4 and Table 3.2). The conventional least squares regression (CLSR) determined a different in the unit-mass intercepts (log a constant) for the RMR versus AMR or Scope. For the RMR, this coefficient was 0.169 mlO2/h, while for AMR was 1.148 mlO2/h and for Scope was 0.964 mlO2/h. For the allometric exponent, CLSR determined similar for RMR, AMR, and Scope and 0.782 scaled to mass at 25±0.5°C. For poison frogs, the oxygen

consumed per unit-mass (allometric coefficient) increases and the rate of oxygen consumption (allometric exponent) is constant regardless of the level of activity (i.e., AMR versus RMR). The allometric exponent of the poison frogs is similar to other groups of vertebrates (White et al. 2006) and near the expected value of ~0.75 for other metabolic quarter-power allometric relationships (Brown et al. 2000; West et al. 1997).

The poison frog PIC analyses showed a similar trend for the RMR, AMR, and Scope regressions. However, the allometric exponents of AMR and Scope were slightly higher, but within the 95% CI of the CLSR estimates. The RMR of the poison frogs (allometric coefficient and exponent) overlaps with that of the anuran dataset at 25°C, but AMR and Scope differ in their allometric exponent from that of the anuran dataset at 25°C. Additionally, we found evidence that outlier contrasts (grade shifts) have occurred; they correspond to three origins of alkaloid sequestration (Ameerega clade, Epipedobates clade, and Hyloxalus azureiventris) and two significant body-size shifts between sister clades or species (Ameerega trivittata-Ameerega parvula clade, Dendrobates sylvaticus-D. pumulio) (Figure 3.5). After we removed the grade-shift contrasts and re-estimated the regression parameters and the allometric exponent was not significantly different from the estimated using CLSR (Figure 3.5 and Table 3.7). Therefore, poison frogs are similar to other anurans in their RMR, but differ in their AMR and Scope for anurans of similar size.

Scale, Metabolism, Aposematism, and Diet in Poison Frogs

Our regression analyses that incorporated dummy variables for conspicuousness, alkaloid sequestration, and diet specialization provided some insights about metabolic rates in poison frogs (Table 3.8 and Table 3.9). We found no significant effect of alkaloid sequestration, conspicuous coloration, or ant and mite diet specialization on the CLSR and PIC regression analyses of RMR (Table 3.8). Our results suggest that poison frogs share a similar minimal energetic cost of maintenance measured at rest regardless of being brightly colored, able to sequester alkaloids, or diet specialists. We found a significant effect of the ability to sequester alkaloids when included as a fixed effect in the allometric relationship of AMR, Scope, and body mass (Table 3.8). Frogs that were classified as brightly colored have also a significant increase in their AMR and Scope under the CLSR, but after removing the effect of phylogeny (PIC analyses) the effect was not significant (Table 3.8). The effect of diet specialization on ant and mites was found not to be significant from AMR, Scope, and body mass relationships (Table 3.8). Therefore, only the ability to sequester alkaloids was supported to have a significant increase in the aerobic metabolic capacity (i.e., ~37.4% for AMR and ~44.5% for Scope). Conspicuousness showed lack a significant effect on AMR and Scope, but only after accounting the phylogenetic inertia. We failed to find an effect of diet specialization on the allometric relationships between body mass and AMR and Scope. However, we found that the condition of homogeneity of slopes (i.e., assuming common slope) held was not held by diet specialization regressions (Table 3.9). More dietary

profiles are necessary to validate our results in terms of the effect of diet specialization on the allometric relationships.

Our analysis of the factorial aerobic scope (AMR/RMR) partially supported the results from the CLSR and PIC regression analyses. For conspicuousness, we found that the factorial aerobic scope of conspicuous (mean: 8.29 ± 0.57, n = 28) and cryptic species (mean 6.33 ± 0.55, n = 26) were significantly different (t = -2.448, P = 0.018). For alkaloid sequestration, we found that species that sequester alkaloids (mean: 8.50 ± 0.59, n = 22) and those that are unable (mean: 6.86 ± 0.73, n = 18) did not differ significantly (t = -1.761, P = 0.086). For diet specialization on ants and mites, the factorial scope from the specialists (mean: 7.95 ± 0.86, n = 11) and generalists (mean: 7.66 ± 0.98, n = 12) did not differ significantly (t = -0.223, P = 0.826). Therefore, the factorial scope supports an increase in oxygen consumption on brightly colored frogs regardless if they are able to sequester alkaloids or diet specialists.

For the pairwise correlation analyses of binary variables, we found significant pair associations ($P < 0.001$) between conspicuousness, alkaloid sequestration, and diet specialization (Table 3.10). Scope (mass corrected) was significantly associated with conspicuousness ($P < 0.001$), diet specialization ($P < 0.01$), and AMR ($P < 0.001$); but it was marginally non-significantly ($P \sim 0.05$) associated with alkaloid sequestration. No significant ($P > 0.05$) correlation was found between conspicuousness, alkaloid sequestration, or diet specialization with AMR (mass corrected) or RMR (mass corrected). AMR (mass corrected) and RMR (mass corrected) were not correlated ($P > 0.05$). Our results corroborated

the close correlation between alkaloid sequestration and conspicuousness (i.e., aposematism) in poison frogs (Santos et al. 2003; Summers and Clough 2001). The significant correlation between diet specialization and alkaloid sequestration supports the hypothesis of the dietary origin of poison frogs alkaloids (Daly et al. 1994; Saporito et al. 2009). The significant associations between Scope (mass corrected) with conspicuousness and diet specialization suggests a possible metabolic adaptation to the evolution of aposematism in poison frogs. However, the marginally non-significant association of Scope (mass corrected) and alkaloid sequestration suggests that higher aerobic capacity has a tendency to be associated with alkaloid sequestration. The non-significant association between AMR (mass corrected) and RMR (mass corrected) suggests that metabolic cost of resting and activity are decoupled and non-linear across poison frogs.

We found six origins of conspicuous coloration, four origins of alkaloid sequestration, and three origins of ant and mite specialization (Figure 3.5). Two of the origins of conspicuous coloration were not associated with alkaloid sequestration: Allobates zaparo, a Batesian mimic of Ameerega bilinguis and A. parvula (Darst and Cummings 2006), and Hyloxalus nexipus, brightly colored riparian frog. Four events represented a simultaneous origin of conspicuous coloration and alkaloid sequestration (i.e., aposematism): (1) Dendrobates+Phyllobates clade, (2) Hyloxalus azureiventris, (3) Epipedobates clade, and (4) Ameerega clade. Three of the origins of aposematism were associated with a simultaneous origin of diet specialization: (1) Dendrobates+Phyllobates clade, (2) Epipedobates clade, and (3) Ameerega clade.

However, the diet profile of the fourth origin of aposematism (i.e., H. azureiventris) is unknown as is its natural history and ecology (Lötters et al. 2000). High metabolic scope was found to originate several times: (1) in Allobates zaparo, (2) in Dendrobates+Phyllobates clade, (3) in Hyloxalus bocagei-H. sauli, (4) H. azureiventris, (5) H. toachi, (6) Silverstoneia-Epipedobates clade, and (7) Colostethus sensu lato-Ameerega clade. High metabolic scope originated simultaneously with two origins (Dendrobates+Phyllobates, and H. azureiventris) and preceded two origins (Epipedobates and Ameerega clades).

For the continuous trait correlation analyses, we found that all variables are not independent of the phylogeny ($\lambda > 0$), which supports the simultaneous estimation of this parameter and bivariate correlation coefficients (Table 3.11). We found significant pairwise associations ($P < 0.01$) between conspicuousness with alkaloid profiles (amount and diversity), diet specialization (ant and mites % in diet), prey number per individual (log-prey), body mass (log-weight), and active metabolic parameters (log-AMR, and log-Scope). Conspicuousness was not associated ($P > 0.05$) with resting metabolic rate (log-RMR). Alkaloid amount was significantly ($P < 0.01$) associated with alkaloid diversity, diet specialization, prey number per individual, body mass, and all metabolic parameters (log-RMR, log-AMR, and log-Scope). Alkaloid diversity was significantly ($P < 0.01$) correlated with diet specialization; but it was not associated ($P > 0.05$) with body mass or the metabolic parameters. Diet specialization was significantly ($P < 0.05$) associated with prey number per individual (log-prey), but it was not associated

($P > 0.05$) with body mass or the metabolic parameters. Prey number (log-prey) was significantly ($P < 0.05$) associated with body mass, and resting metabolism (log-RMR). Prey number was not associated ($P > 0.05$) with active metabolic parameters (log-AMR and log-Scope). Body mass was significantly associated ($P < 0.001$) with all metabolic parameters. Pairwise correlation analyses were significant ($P < 0.001$) between active (log-AMR and log-Scope) and resting (log-RMR) metabolic parameters. Our results suggest an interdependency of the aposematic variables (conspicuousness and alkaloid profiles), and diet profiles (ant and mite specialization, and prey number). Scale parameters such as body mass and the metabolic parameters show a strong interdependency. Surprisingly, scale parameters (body mass and metabolic parameters) are associated with aposematism variables (conspicuousness and alkaloid amount), but scale does not covary with alkaloid diversity or diet specialization.

Our multivariate analysis resulted in seven possible models (Figure 3.6) of the relationships among latent variables (i.e., scale and aposematism) and their indicator variables (conspicuousness, alkaloid profiles, diet specialization, body mass, and metabolic parameters). The best model (Figure 3.7) is supported by (1) its failure to reject the null (H0: observed data covariance matrix) with a $\chi 2 = 16.242$, ($df = 18$, $p = 0.576$); (2) fit indices: CFI = 1.000 (good fit if > 0.9), TLI = 1.022 (good fit if > 0.9), RMSEA < 0.001 (good model fit if < 0.05), and SRMR = 0.096 (good fit if < 0.08); and (3) its significantly low $\chi 2$ score against the alternative models (i.e., the next lowest score model was rejected with $\Delta\chi 2 = 5.607$, $\Delta df = 1$ and $p = 0.018$) (Figure 3.8).

The best model has a good fit to the observed data and most likely explains the relationships among observed and latent variables in poison frogs (Figure 3.7). The latent variable scale was significantly predicted (i.e., all regression coefficients > 0.40 and each with $p < 0.05$) by the indicator variables: body mass, RMR, Scope, and conspicuousness. The latent variable aposematism was significantly predicted (i.e., all regression coefficients > 0.45 and each with $p < 0.05$) by the indicator variables: alkaloid amount, alkaloid diversity, diet specialization in ants and mites, number of prey items per individual, and conspicuousness. Conspicuousness was the only variable that predicted simultaneously both scale and aposematism as latent variables. Scale and aposematism latent variables have a significant ($p < 0.05$) positive correlation of 0.514, supporting their dependency.

DISCUSSION

Comparison between Metabolic Rates of Anurans and Poison Frogs

Our metabolic characterizations for anurans and poison frogs for resting metabolic rate are in agreement with other ectotherms (Glazier 2005; White et al. 2006). Resting metabolic rate (RMR) and body mass was shown to be proportional and the allometric exponent ~0.77 for both anurans and poison frogs. Our results are in concordance with the metabolic allometry relationship (metabolic rate □ $Mass^{0.75}$) found in other groups across the Tree of Life (Hemmingsen 1960). For anurans, our estimates of the allometric exponent using CLSR were ~0.78 (20°C) and ~0.76 (25°C). Previous reports have shown

allometric coefficient were similar, but the exponent estimates were higher ~0.88 (20°C) (White et al. 2006), ~0.82 (20°C) and ~0.84 (25°C) (Gatten et al. 1992). The discrepancies between our estimated allometric exponent in anurans and those published may be related to the variability and quality of the data included in the metanalyses. However, our analyses suggest that the poison frog clade follows the 0.75-power law of metabolic allometric relationships as in most other organisms (West et al. 1997).

AMR and Scope between anurans and poison frogs were similar in their intercept, but different in their allometric exponent. Poison frogs have an allometric exponent of ~0.78, similar to the expected 0.75-power law of the metabolic allometric relationships (West et al. 1997). Anurans have an allometric exponent of ~1.00 (20°C and 25°C) for AMR and Scope. Therefore, our results suggest that, for anurans, as body mass increases the rate of oxygen increases faster than the constant increase expected in poison frogs. At least three alternative hypotheses might explain this discrepancy between anurans and poison frogs. First, poison frogs are relatively small frogs with body mass < 10 g compared to the significant variability across the anurans (0.1-500 g), and mass scale of anurans > 3 orders of magnitude has a significant impact on the AMR and aerobic scope. Second, anurans as a group are more diverse in aerobic metabolic pathways due to their life histories (e.g., aquatic, terrestrial, seasonal), reproductive strategies, long evolutionary history, and some heterogeneity of underlying power laws of metabolic rates (Wells 2007; White et al. 2006). Alternatively, poison frogs as a clade have comparable life histories (terrestrial

and diurnal), recent shared ancestry, and a common underlying 0.75-power allometric exponent. Third, the quality of the data used in the metanalysis of anurans is heterogeneous and some of the methodologies (e.g., manual/motor rotation, type of oxygen analyzer, animal body size correction) might not be truly comparable. By comparison, our experimental design and measurement equipment was the same for all the species analyzed.

Complex Phenotypes in Poison Frogs

Phenotypic integration can only be studied at the organismal level (Pigliucci and Preston 2004). Most phenotypic traits share some common evolutionary history as a direct effect of selection or byproduct of selection on other traits (Schlichting 2004). However, few biological systems are studied at multiple levels and phenotypic integration is rarely evidenced. By focusing on different aspects of the poison frog phenotypic diversity, we have attempted to reveal some aspects of the phenotypic integration, its ecological implications, and the evolutionary trends within this lineage of tropical amphibians.

Our goal was to identify different levels of integration using a multilevel approach to understand the evolution of conspicuousness, alkaloid sequestration ability (amount and diversity), dietary profiles (specialization on ants and mites), scale (body mass), and metabolic characterization (RMR, AMR, and Scope). First, we found support for aposematism in poison frogs as the association between brightly coloration, alkaloid sequestration, and diet specialization (Caldwell 1996; Daly et al. 1994; Darst et al. 2005; Santos et al. 2003; Summers and Clough 2001). Second, we also found that scale (body mass and active

metabolic parameters) is also associated with aposematism. However, resting metabolic rates is not associated with aposematism.

We found that most poison frogs have a similar energetic expense while resting after removing the effects of body mass. Similar RMRs across clade suggest that there might not be a significant metabolic cost of accumulation and resistance to xenobiotic alkaloids. Taigen and Pough (1983) (Taigen and Pough 1983b) showed a significant increase in the RMR for Dendrobates auratus (ant specialist and alkaloid sequestering specie), but their results might derive from their low sample size (one species). However, small or no metabolic cost of accumulation toxins has been document in some endotherm herbivores (Ianson and Murray 1996), mice (Bozinovic and Novoa 1997), and arthropods (Evans and Schmidt 1990).

Active metabolic parameters (AMR and Scope) were significantly associated with aposematism in poison frogs. Therefore, species that are conspicuously colored, able to sequester alkaloids, and diet specialists might have a higher aerobic capacity to generate energy for muscular activity. Taigen and Pough (1983) (Taigen and Pough 1983b) showed a similar result for Dendrobates auratus, but their limited sample size needed further confirmation. Our results for the factorial aerobic scope (AMR/RMR) only supported that brightly colored frogs have a significantly higher aerobic capacity. More data is necessary to determine if the association between factorial aerobic scope and other aposematism related variables (e.g., alkaloid profiles, and diet specialization).

The inclusion of binary categorical variables for conspicuousness, alkaloid sequestration, and diet specialization improved the fit and characterization of the metabolic allometric equations in poison frogs. The relationship between RMR and mass was not significantly affected after the inclusion of the conspicuousness, alkaloid sequestration, or diet specialization as fixed effects (all CLSR and PIC models: $P > 0.05$). Our results further confirm that most poison frogs do not differ in their RMR regardless if aposematic or not. In contrast, we found significant results for the AMR and Scope relationships allometric equations. The inclusion of alkaloid sequestration as fixed effect supported that frogs that were able to sequester alkaloids have a significant higher AMR and Scope than frogs that were unable (CLSR model: $P < 0.001$, and PIC model: $P < 0.05$). The increase in the expected aerobic capacity for the species that are able to sequester alkaloids by comparison of the allometric coefficient between species was ~37.4% (AMR) and ~44.5% (Scope) (Table 3.8). PIC analyses further validated the metabolic importance of the origin of alkaloid sequestration in Ameerega, Epipedobates, and Hyloxalus azureiventris. The origins of these lineages were consistent to grade shift events as an increases in the allometric coefficient without net change in allometric exponent for AMR and scope relationships (Figure 3.5). The absence of grade-shift at the node of Dendrobates+Phyllobates is puzzling and might be related to the overrepresentation of this clade in our analyses.

The inclusion of conspicuousness and diet specialization as fixed effects in the CLSR or PIC models for allometric equations of AMR and Scope were convoluted. In the CLSR analysis, frogs that were brightly colored have a

significant higher AMR and Scope (CLSR model: $P < 0.001$). In the PIC model, the inclusion of conspicuousness was not significant ($P > 0.05$) suggesting that the origin of bright coloration is not necessarily associated with a significant increase in the aerobic capacity after removing phylogenetic effect. Bright coloration without an association with alkaloid sequestration was found to occur at least twice in the poison frogs: (1) the Batesian mimicry of Allobates zaparo (Darst and Cummings 2006; Darst et al. 2006), and (2) Hyloxalus nexipus. Natural history of H. nexipus is largely unknown and further confirmation is necessary about its inability to sequester alkaloids.

Ants and mites are a significant component both in number, percentage, and volume of all prey items of poison frogs (Caldwell 1996; Darst et al. 2005). Additionally, the diet specialization of these prey items has been implicated as the xenobiotic source of the lipophilic alkaloids in defended poison frogs (Saporito et al. 2004; Saporito et al. 2009) (Darst et al. 2005; Takada et al. 2005). Diet specialization as a fixed effect did not have a significant effect on the AMR and Scope allometric regressions. However, the test of equal slopes was rejected and suggested a possible interaction between diet and mass terms in the CLSR analyses. Alternatively, the PIC analyses also rejected a significant effect of diet and the test of independent slopes was not rejected. Therefore, we found that both small and large poison frogs can be ant and mite specialists and they do not differ significantly in their active aerobic capacity. More poison frog diet profiles are necessary to validate our results.

Body size in poison frogs has only been explored in the positive association with conspicuous coloration (Hagman and Forsman 2003). Our analyses suggest a more complex involvement of scale in poison frogs. First, body size was significantly positive association with all metabolic parameters. Second, body mass was positively correlated with conspicuous coloration, which supports that larger frogs usually are more brightly colored (Hagman and Forsman 2003). Our results also corroborate other empirical and theoretical evidence favoring the increase effectiveness of warning signals with larger body sizes (Exnerová et al. 2003; Ruxton et al. 2004). Third, body mass was significantly associated with alkaloid amount, which supports that larger frogs usually have larger quantities of alkaloids. Our results are consistent with the evidence that most of the alkaloid diversity in poison frogs are of dietary origin (Daly et al. 1994), which accumulate in granular glands of their skins (Neuwirth et al. 1979) with apparent little or no biochemical modification (Daly et al. 2003; Saporito et al. 2003; Saporito et al. 2004). Moreover, our results supports that poison frogs act as effective alkaloid "capacitors" that concentrate xenobiotics from dietary sources. Therefore, large frogs act accumulate more alkaloids than smaller frogs. Fourth, body mass was not significantly associated with alkaloid diversity, which support multiple independent origins of the mechanisms of alkaloid sequestration. Fifth, body mass was not associated with dietary specialization, which supports that large to small poison frogs may be ants and mites specialists. Therefore, our analysis predicts that specialist large frogs might have to maximize their nutritional intake from specialist diet by ingesting a larger number prey. Some

evidence supports our prediction as specialist poison frogs are usually active predators with larger home ranges (Taigen and Pough 1983a), and readily reject available prey (e.g., orthopterans or coleopterans) (Toft 1977; Toft 1980; Toft 1981). Therefore, the persistence of diet specialization as co-adaption for chemical defense sequestration is most likely maintained by aposematism. We predict that diet specialization might dissolve if the selective advantage of aposematic interaction is lost.

Multivariate approach to the evolution of complex traits

Emergent phenotypes are derived from the plasticity, interactions, covariations, and constraints from underlying component traits (Pigliucci and Preston 2004). Poison frogs present a complex evolutionary history including repeated origins and dependent associations of scaling and aposematism related phenotypes. We found at least four correlated origins of bright coloration, alkaloid sequestration, and diet specialization. In poison frogs, the maintenance of the aposematism is highly dependent on the effectiveness of warning signal, the presence of defense (skin alkaloids), and regular supply of the dietary source of such xenobiotics (Daly et al. 1994; Darst et al. 2006; Santos et al. 2003). Our results suggest the addition of other factors to the establishment and effectiveness of the aposematism. The inclusion of larger body sizes, high aerobic capacity, and selective predation has been co-opted as additional phenotypic traits contributing to the effectiveness of aposematism.

Based on our results, we can propose a model for adaptive aposematic defense based on unambiguous warning signals (predator perspective conspicuous

coloration), effective alkaloid accumulation (efficient alkaloid sequestration and accumulation), efficient prey selection (foraging adaptation for capture and digestion of alkaloid-rich prey), and dependent on body mass (scale) and effective energy allocation for muscular activity (high aerobic scope).

Our model suggests direct and indirect effects between scaling and aposematism variables in poison frogs. In the case of the direct effects, we can consider the following prediction and inferences. First, we predict that selection in body size (scale) will directly affect the metabolic variables (Scope and RMR) and body mass. Second, selection on conspicuousness will simultaneously affect scale and aposematism. For example, we can predict that brightly colored frogs will have a direct increment in the efficiency of their warning signal as a byproduct of increasing their body size. Third, we predict the selection in aposematism will primary be derived from increase on the effectiveness of both chemical defense (alkaloids amount and diversity) and dietary specialization on alkaloid rich prey (ants and mites).

In the case of the indirect effects, we can consider the following predictions. First, we can infer that scale will affect indirectly alkaloid content and diversity as byproduct of an increase in body size. Second, scale will indirectly affect the dietary specialization by increasing the volume of prey items necessary to couple with the energetic and nutritional requirements in larger frogs. Third, alkaloid content (i.e., amount and diversity) will have indirect effect on increasing the metabolic rates due to the energetic cost of alkaloid sequestration, accumulation, and biochemical resistance.

Our data suggest an indirect metabolic cost of the chemical defense in poison frogs. Toxin resistance is usually achieved by directional selection on key protein sites that provide insensibility with suboptimal physiological efficiency (Daly et al. 1980; Wang and Wang 1998). In the poison frogs, alkaloids toxicity has been targeted to neuron and muscular ion channels (e.g., Ca+, K+, and Na+) causing lethal or sub-lethal impairment (Daly 1998; Daly et al. 1999). We predict that multiple mechanism of alkaloid sequestration might be operating. Further analyses at the genomic and preteomic level will allow describe such pathways and their individual metabolic cost.

Only analyses accounting for multiple variables simultaneously can reveal underlying patterns of evolution and evolutionary trends. In poison frogs, scale has a crucial effect in both metabolic and aposematic characteristics, as larger body size a directly correlated with better warning signals (conspicuousness), larger amounts of alkaloids (chemical defense), and higher metabolic parameters. However, scale is not associated with diet specialization and alkaloid diversity, suggesting active predation (more prey items per individual) in specialists and multiple alkaloid sequestering mechanisms. Our data suggest a metabolic cost of conspicuousness, and alkaloid sequestration and accumulation. More variables analyzed simultaneously provide a more fluid and complex phenotypic landscape of the evolutionary trends of poison frogs clade. Emergent properties in biological systems will become more apparent from multivariate approaches rather than single bivariate analyses.

Genus	Species	Museum	Country	Locality (sequences and physiology)	Altitude (m)	Other Localities (physiology)	Altitude (m)
Ademomera	*andreae*	QCAZ15998 (Outgroup)	Ecuador	Zamora Chinchipe: near Zamora	980	NA	
Bufo	*nebulifer*	(Outgroup)				NA	
Centrolene	*grandisonae*	QCAZ16512 (Outgroup)	Ecuador	Pichincha: Manuel Cornejo A (Tandapi), vía Atenas	950	NA	
Ceratophrys	*cornuta*	KU202561 (Outgroup)	Peru	Madre de Dios: Cusco Amazonico	200	NA	
Crossodactylus	*schmidti*	MLPA 1414 (Outgroup)	Argentina	Misiones:Aristobulo del Valle, Balneario Cunapiru	450	NA	
Lithodytes	*lineatus*	QCAZ16621 (Outgroup)	Ecuador	Morona Santiago: Méndez		NA	
Allobates	*femoralis*	QCAZSC19600	Ecuador	Sucumbios: Lumbaqui	260	Colombia: Leticia	83
Allobates	*insperatus*	QCAZ16533	Ecuador	Francisco de Orellana: Parque Nacional Yasuni-Estacion PUCE	230	--	
Allobates	*juanii*	TNHCFS4978	Colombia	Meta: Villavicencio, Villavicencio-Restrepo road	411	--	
Allobates	*kingsburyi*	QCAZ16523	Ecuador	Zamora Chinchipe: Rio Chicana	1085	Zamora Chinchipe: Panguitza	870
Allobates	sp. Tachira	TNHCFS5551	Venezuela	Tachira: road from San Cristobal to Rio Negro via el Pinal	529	--	
Allobates	*talamancae*	QCAZ16551	Ecuador	Pichincha: Rio Sabalo, ca. Pedro Vicente Maldonado	191	Panama: Lago Bayano Colombia: Quibdo	60 50
Allobates	*zaparo*	QCAZ16603	Ecuador	Napo: Jatun Sacha, vía Ahuano	390	--	
Ameerega	*bilinguis*	QCAZ25305	Ecuador	Sucumbios: Laguna Grande-Neotropic, Reserva de Producción Faunística Cuyabeno	260	Ecuador: Parque Nacional Yasuni-Estacion PUCE	230
Ameerega	*hahneli*	QCAZ19240	Ecuador	Francisco de Orellana: Parque Nacional Yasuni-Estacion PUCE	230	Ecuador: Canelos	631
Ameerega	*parvula*	QCAZ16584	Ecuador	Morona Santiago: near Mendez	550	Napo: Jatun Sacha, via Ahuano	390
Ameerega	*trivittata*	TNHCFS4966	Colombia	Amazonas: Leticia, Cerca Viva	83	--	
Anomaloglossus	sp. Ayacucho	TNHCFS5631	Venezuela	Amazonas: Puerto Ayacucho, Tobogan	81	--	
Aromobates	aff. *alboguttatus*	TNHCFS5541	Venezuela	Merida: Santa Cruz de Mora via Los Ranchos	1193	--	
Aromobates	*saltuensis*	TNHCFS5541	Venezuela	Tachira: San Felix, San Juan de Colon	751	--	
Colostethus	*fugax*	QCAZ16513	Ecuador	Morona Santiago: 2 km E Santiago	495	--	
Colostethus	*panamensis*	TNHCFS4810	Panama	Colon: Fort Sherman (Ci4)	189	--	
Colostethus	*pratti*	TNHCFS4807	Panama	Colon: Parque Nacional Portobello (CTC)	50	--	
Dendrobates	*auratus*	TNHCFS4811	Panama	Cocle: El Cope, Parque Nacional General de Division 'Omar Torrijos Herrera	782	Panama: Fort Sherman (Ci4)	189
Dendrobates	*bombetes*	TNHCFS4946	Colombia	Quindio: Barbas, Finlandia, Hacienda Lusitania	1958	Colombia: Buga, Buga-Buenaventura road	1610
Dendrobates	*captivus*	QCAZ27442	Ecuador	Zamora Chinchipe: near Panguitza	870	--	
Dendrobates	*claudiae*	KS9	Panama	Bocas del Toro: Isla Colon, Bocas del Drago	11	--	
Dendrobates	*duellmani*	QCAZ16559	Ecuador	Francisco de Orellana: Parque Nacional Yasuni-Estacion PUCE	230	--	
Dendrobates	*galactonotus*	TNHCFS4889	Brazil	Pet Trade	n.d.	--	
Dendrobates	*histrionicus*	TNHCFS4985	Colombia	Choco: Quibdo, La Troje	50	--	
Dendrobates	*lamasi*	JCS	Peru	Pet Trade	n.d.	--	
Dendrobates	*leucomelas*	TNHCFS5639	Venezuela	Amazonas: Puerto Ayacucho, Tobogan	81	--	
Dendrobates	*pumilio*	TNHCFS4814	Panama	Bocas del Toro: Isla Colon, Bocas del Drago (Dragomar)	11	--	
Dendrobates	sp. Quibdo	TNHCFS4943	Colombia	Choco: Quibdo, La Troje	50	--	
Dendrobates	*sylvaticus*	QCAZ16563	Ecuador	Esmeraldas: near Quingue	306	Ecuador: near Santo Domingo de los Colorados	604
Dendrobates	*tinctorius*	TNHC64416	Surinam	Pet Trade	n.d.	--	
Dendrobates	*truncatus*	TNHCFS4979	Colombia	Tolima: Mariquita, vereda Malabares	587	--	
Dendrobates	*ventrimaculatus*	QCAZ16566	Ecuador	Francisco de Orellana: Parque Nacional Yasuni-Estacion PUCE	230	Colombia: Leticia	83
Dendrobates	*virolinensis*	TNHCFS4950	Colombia	Santander: Virolin, Costilla de Fara	1767	--	
Epipedobates	*anthonyi*	QCAZ16597	Ecuador	Loja: Macará-Catacocha	1135	Ecuador: Pasaje-Girón	1512

Table 3.1: Collection data, museum numbers, and altitude of localities of the specimens used in the DNA amplification and physiological measurements.

Genus	Species	Museum	Country	Locality (sequences and physiology)	Altitude (m)	Other Localities (physiology)	Altitude (m)
Epipedobates	*boulengeri*	QCAZ16574	Ecuador	Esmeraldas: A 3 Km de Durango, road to San Lorenzo	253	--	
Epipedobates	*machalilla*	QCAZ16527	Ecuador	Manabi: Rio Ayampe	70	--	
Epipedobates	sp. F	QCAZ16590	Ecuador	Pichincha: Union del Toachi	694	Ecuador: Mindo	1525
Epipedobates	*tricolor*	QCAZ21977	Ecuador	Cotopaxi: Corazón-Moraspungo	1250	--	
Hyloxalus	*awa*	QCAZ16502	Ecuador	Esmeraldas: Laguna de Cubes, Montes del Mache.	350	Ecuador: Union del Toachi	694
Hyloxalus	*azueriventris*	KS32	Peru	San Martin: Cainarachi Valley	350	Pet Trade	
Hyloxalus	*bocagei*	QCAZ37259	Ecuador	Sucumbios: La Libertad road to La Virgen	1330	--	
Hyloxalus	*elachyhistus*	QCAZ16517	Ecuador	El Oro: Torata-Balsas road	640	--	
Hyloxalus	*maculosus*	QCAZ37262	Ecuador	Sucumbios: Lumbaqui	260	Ecuador: Hola Vida Reserve	631
Hyloxalus	*nexipus*	QCAZ16537	Ecuador	Morona Santiago: Indanza-San Miguel del Conchay	855	Ecuador: near Mendez	550
Hyloxalus	*sauli*	QCAZ16543	Ecuador	Francisco de Orellana: Parque Nacional Yasuni-Estacion PUCE	230	--	
Hyloxalus	*subpunctatus*	TNHCFS4957	Colombia	Boyaca: Chiquinquira	2575	--	
Hyloxalus	*toachi*	QCAZ16549	Ecuador	Carchi: Rio Baboso near Lita	534	Ecuador: Union del Toachi	694
Hyloxalus	*vertebralis*	QCAZ16553	Ecuador	Azuay: El Jordán (cerca a Paguancay)	2424	--	
Mannophryne	*collaris*	TNHCFS5507	Venezuela	Merida: El Estanquillo	1120	Venezuela: road from Pregonero to La Trampa	1192
Phyllobates	*aurotaenia*	TNHCFS4990	Colombia	Choco: Quibdo road to Pacuritas	50	--	
Phyllobates	*terribilis*	TNHC64420	Colombia	Pet Trade	n.d.	--	
Rheobates	*palmatus*	TNHCFS4955	Colombia	Boyaca: Villa de Leiva	2118	Colombia: Las Brisas	2005
Silverstoneia	*flotator*	TNHCFS4804	Panama	Cocle: El Cope, Parque Nacional General de Division 'Omar Torrijos Herrera	782	--	
Silverstoneia	*nubicola*	TNHCFS4942	Colombia	Choco: Quibdo, La Troje	50	--	

Table 3.1 (Cont): Collection data, museum numbers, and altitude of localities of the specimens used in the DNA amplification and physiological measurements.

Genus	Species	n	Weight (g)				VO_2rest consumed (mLO_2/h)				VO_2active consumed (mLO_2/h)				Aerobic Scope		Factorial
			Mean	SE	Min	Max	Mean	SE	Min	Max	Mean	SE	Min	Max	Raw	Mass-specific	Scope
Allobates	*femoralis*	6	1.246	0.103	0.940	1.570	0.223	0.031	0.135	0.355	1.104	0.228	0.613	2.159	0.881	0.707	4.942
Allobates	*insperatus*	4	0.551	0.041	0.430	0.605	0.082	0.018	0.056	0.133	0.609	0.030	0.535	0.678	0.527	0.956	7.459
Allobates	*juanii*	2	0.685	0.085	0.600	0.770	0.147	0.064	0.083	0.211	0.766	0.008	0.758	0.774	0.619	0.904	5.219
Allobates	*kingsburyi*	8	0.875	0.102	0.595	1.300	0.126	0.016	0.054	0.219	0.644	0.032	0.546	0.786	0.518	0.592	5.103
Allobates	sp. Tachira	6	0.585	0.013	0.540	0.620	0.168	0.019	0.100	0.217	0.593	0.071	0.366	0.805	0.425	0.726	3.520
Allobates	*talamancae*	5	0.880	0.087	0.605	1.150	0.080	0.014	0.049	0.126	0.714	0.050	0.578	0.797	0.634	0.720	8.890
Allobates	*zaparo*	10	1.615	0.133	1.010	2.510	0.299	0.029	0.163	0.458	1.919	0.108	1.381	2.535	1.620	1.003	6.422
Ameerega	*bilinguis*	11	0.949	0.077	0.570	1.515	0.180	0.011	0.128	0.260	0.974	0.051	0.691	1.213	0.794	0.837	5.408
Ameerega	*hahneli*	6	0.343	0.020	0.295	0.405	0.100	0.011	0.075	0.138	0.516	0.013	0.466	0.550	0.416	1.213	5.146
Ameerega	*parvula*	8	1.569	0.049	1.365	1.790	0.293	0.033	0.137	0.412	1.497	0.170	0.719	2.350	1.204	0.767	5.111
Ameerega	*trivittata*	3	5.512	0.994	4.515	7.500	0.964	0.178	0.785	1.320	6.632	0.924	5.523	8.468	5.668	1.028	6.879
Anomaloglossus	sp. Ayacucho	11	0.808	0.051	0.610	1.140	0.202	0.022	0.094	0.372	0.730	0.068	0.456	1.119	0.528	0.653	3.607
Aromobates	*aff. alboguttatus*	17	1.312	0.114	0.560	2.330	0.248	0.022	0.129	0.466	0.916	0.093	0.327	1.823	0.668	0.509	3.701
Aromobates	*saltuensis*	6	1.498	0.138	1.190	1.970	0.212	0.046	0.099	0.415	1.249	0.202	0.597	2.015	1.037	0.692	5.903
Colostethus	*fugax*	4	0.959	0.089	0.720	1.100	0.124	0.013	0.093	0.147	0.667	0.054	0.525	0.783	0.543	0.566	5.374
Colostethus	*panamensis*	5	0.973	0.093	0.693	1.167	0.096	0.004	0.088	0.109	1.159	0.085	0.971	1.412	1.063	1.092	12.122
Colostethus	*pratti*	12	0.806	0.031	0.657	0.950	0.111	0.008	0.072	0.179	1.133	0.051	0.669	1.324	1.022	1.268	10.203
Dendrobates	*auratus*	15	1.996	0.071	1.640	2.520	0.306	0.039	0.169	0.734	2.810	0.124	2.156	3.942	2.504	1.255	9.190
Dendrobates	*bombetes*	8	0.528	0.036	0.400	0.680	0.085	0.007	0.062	0.118	0.885	0.056	0.612	1.084	0.800	1.515	10.469
Dendrobates	*captivus*	6	0.484	0.025	0.405	0.565	0.087	0.014	0.061	0.154	0.602	0.039	0.487	0.719	0.515	1.064	6.952
Dendrobates	*claudiae*	1	0.217	--	--	--	0.060	--	--	--	0.652	--	--	--	0.592	2.728	10.822
Dendrobates	*duellmani*	7	0.414	0.030	0.340	0.520	0.095	0.012	0.060	0.138	0.686	0.060	0.487	0.916	0.591	1.428	7.252
Dendrobates	*galactonotus*	4	3.589	0.293	3.035	4.095	0.323	0.009	0.307	0.348	4.970	0.225	4.534	5.581	4.647	1.295	15.379
Dendrobates	*histrionicus*	4	3.320	0.119	3.140	3.670	0.205	0.021	0.167	0.257	2.496	0.301	1.788	3.105	2.291	0.690	12.156
Dendrobates	*lamasi*	2	0.390	0.070	0.320	0.460	0.068	0.015	0.054	0.083	1.074	0.062	1.011	1.136	1.006	2.579	15.683
Dendrobates	*leucomelas*	12	2.243	0.138	1.323	2.990	0.414	0.055	0.134	0.819	3.167	0.273	2.000	4.672	2.753	1.227	7.648
Dendrobates	*pumilio*	17	0.538	0.017	0.407	0.670	0.067	0.003	0.049	0.093	0.698	0.026	0.508	0.924	0.631	1.173	10.452
Dendrobates	sp. Quibdo	3	0.160	0.010	0.140	0.170	0.051	0.019	0.018	0.084	0.577	0.263	0.288	1.102	0.526	3.288	11.330
Dendrobates	*sylvaticus*	11	2.889	0.133	2.100	3.420	0.400	0.054	0.169	0.696	3.328	0.188	2.382	4.725	2.928	1.013	8.323
Dendrobates	*tinctorius*	8	5.037	0.358	4.110	6.310	0.549	0.051	0.402	0.832	5.983	0.767	2.788	9.798	5.434	1.079	10.889
Dendrobates	*truncatus*	12	1.573	0.115	1.080	2.170	0.188	0.016	0.119	0.283	1.926	0.111	1.353	2.581	1.738	1.105	10.263
Dendrobates	*ventrimaculatus*	7	0.345	0.056	0.140	0.550	0.134	0.044	0.027	0.306	0.661	0.098	0.389	1.033	0.527	1.528	4.950
Dendrobates	*virolinensis*	8	0.475	0.051	0.330	0.730	0.094	0.006	0.067	0.120	0.639	0.030	0.556	0.818	0.545	1.147	6.800
Epipedobates	*anthonyi*	10	1.062	0.052	0.750	1.410	0.197	0.009	0.159	0.255	1.207	0.036	1.025	1.409	1.010	0.951	6.130
Epipedobates	*boulengeri*	16	0.427	0.018	0.310	0.540	0.097	0.012	0.046	0.193	0.329	0.023	0.163	0.512	0.232	0.543	3.381
Epipedobates	*machalilla*	11	0.323	0.022	0.230	0.475	0.083	0.009	0.047	0.144	0.385	0.049	0.159	0.704	0.302	0.935	4.657
Epipedobates	sp. F	10	0.457	0.026	0.320	0.550	0.065	0.005	0.043	0.094	0.596	0.036	0.436	0.765	0.531	1.162	9.135
Epipedobates	*tricolor*	4	0.801	0.051	0.690	0.895	0.164	0.022	0.114	0.211	0.836	0.089	0.621	1.055	0.672	0.839	5.097
Hyloxalus	*awa*	10	0.915	0.050	0.730	1.280	0.121	0.005	0.093	0.152	0.653	0.038	0.532	0.853	0.532	0.581	5.398
Hyloxalus	*azueriventris*	4	1.018	0.063	0.905	1.165	0.208	0.026	0.133	0.250	1.309	0.017	1.273	1.354	1.101	1.082	6.296
Hyloxalus	*bocagei*	11	1.514	0.141	0.830	2.280	0.288	0.029	0.182	0.497	2.307	0.220	1.154	3.524	2.019	1.334	8.016
Hyloxalus	*elachyhistus*	28	0.958	0.054	0.550	1.640	0.248	0.019	0.114	0.450	0.840	0.060	0.352	1.432	0.592	0.618	3.387
Hyloxalus	*maculosus*	20	2.300	0.144	1.000	3.520	0.340	0.030	0.129	0.585	2.003	0.152	0.782	3.500	1.663	0.723	5.892
Hyloxalus	*nexipus*	3	1.066	0.181	0.705	1.263	0.264	0.092	0.124	0.438	1.236	0.084	1.147	1.403	0.972	0.912	4.684
Hyloxalus	*sauli*	3	1.703	0.313	1.080	2.055	0.331	0.093	0.165	0.488	2.365	0.206	1.999	2.713	2.034	1.194	7.152
Hyloxalus	*subpunctatus*	7	0.799	0.070	0.637	1.180	0.151	0.013	0.109	0.203	0.901	0.059	0.774	1.241	0.750	0.939	5.975
Hyloxalus	*toachi*	5	0.680	0.082	0.520	0.970	0.117	0.017	0.070	0.168	0.872	0.074	0.611	1.028	0.755	1.110	7.481
Hyloxalus	*vertebralis*	8	0.698	0.051	0.515	0.960	0.127	0.021	0.063	0.236	0.567	0.052	0.340	0.719	0.440	0.630	4.452
Mannophryne	*collaris*	35	1.833	0.144	0.620	4.420	0.362	0.042	0.086	1.007	1.502	0.159	0.444	4.399	1.140	0.622	4.151
Phyllobates	*aurotaenia*	3	2.017	0.447	1.290	2.830	0.184	0.074	0.096	0.332	1.347	0.252	0.940	1.809	1.163	0.577	7.329
Phyllobates	*terribilis*	5	6.013	0.125	5.715	6.365	0.787	0.113	0.588	1.202	5.092	0.101	4.783	5.381	4.305	0.716	6.467
Rheobates	*palmatus*	15	1.780	0.181	0.850	2.905	0.368	0.037	0.220	0.767	1.563	0.154	0.900	2.734	1.195	0.671	4.252
Silverstoneia	*flotator*	10	0.327	0.013	0.273	0.393	0.054	0.005	0.036	0.079	0.491	0.027	0.378	0.687	0.437	1.336	9.026
Silverstoneia	*nubicola*	7	0.371	0.032	0.270	0.470	0.043	0.003	0.031	0.055	0.636	0.048	0.422	0.770	0.593	1.598	14.885

Table 3.2: Metabolic measurements and body mass (mean, standard error, and range) of the poison frogs.

Family	Genus	species	1216S	V_{O2RES} (ml/h) 20°C	Mass (g)	V_{O2RES} (ml/h) 25°C	Mass (g)	V_{O2EX} (ml/h) 20°C	Mass (g)	V_{O2EX} (ml/h) 25°C	Mass (g)	Ref.
Lepidosirenidae	*Lepidosiren*	*paradoxa*	NC003342	--	--	--	--	--	--	--	--	
Phasianidae	*Gallus*	*gallus*	AP003319	--	--	--	--	--	--	--	--	
Hominidae	*Homo*	*sapiens*	AC000021	--	--	--	--	--	--	--	--	
Typhlonectidae	*Typhlonectes*	*natans*	NC002471	--	--	--	--	--	--	--	--	
Caeciliidae	*Gegeneophis*	*ramaswamii*	NC006301	--	--	--	--	--	--	--	--	
Rhinatrematidae	*Rhinatrema*	*bivittatum*	NC006303	--	--	--	--	--	--	--	--	
Hynobiidae	*Hynobius*	*formosanus*	NC008084	--	--	--	--	--	--	--	--	
Plethodontidae	*Eurycea*	*bislineata*	AY728217	--	--	--	--	--	--	--	--	
Ambystomatidae	*Ambystoma*	*mexicanum*	NC005797	--	--	--	--	--	--	--	--	
Alytidae	*Alytes*	*obstetricans*	*	--	--	--	--	--	--	--	--	
Alytidae	*Discoglossus*	*galganoi*	NC006690	--	--	--	--	--	--	--	--	
Alytidae	*Discoglossus*	*pictus*	*	1.142	30.71	--	--	8.166	30.70	--	--	Gatten et al. 1992
Arthroleptidae	*Arthroleptis*	*variabilis*	DQ283081	--	--	--	--	--	--	--	--	
Arthroleptidae	*Trichobatrachus*	*robustus*	AY843773	--	--	--	--	--	--	--	--	
Batrachophrynidae	*Caudiverbera*	*caudiverbera*	DQ283439	--	--	--	--	--	--	--	--	
Bombinatoridae	*Bombina*	*orientalis*	AY957562	0.149	2.62	0.340	3.79	1.230	2.60	--	--	Gatten et al. 1992 Secor et al. 2007
Brevicipitidae	*Callulina*	*kreffti*	AY326068	--	--	--	--	--	--	--	--	
Bufonidae	*Atelopus*	*peruensis*	AY819329 DQ158419	--	--	--	--	--	--	--	--	
Bufonidae	*Bufo*	*alvarius*	AY325984	--	--	--	--	--	--	--	--	
Bufonidae	*Bufo*	*americanus*	AY680206	1.377	27.00	2.937	40.40	28.053	27.00	34.098	40.40	Gatten et al. 1992
Bufonidae	*Bufo*	*bankorensis*	--	--	--	2.953	34.10	--	--	--	--	Hou and Huang 1999
Bufonidae	*Bufo*	*boreas*	AY325983	1.303	40.20	2.640	27.30	31.265	47.30	44.651	47.30	Gatten et al. 1992
Bufonidae	*Bufo*	*bufo*	AY325988	4.901	29.00	4.585	28.59	--	--	--	--	Gatten et al. 1992
Bufonidae	*Bufo*	*calamita*	--	0.511	8.67	--	--	6.777	8.70	--	--	Gatten et al. 1992

Table 3.3: Species of anurans and outgroups used for the phylogenetic inference and metanalysis of the metabolic parameters in Anura. Data include accession numbers, metabolic measurements, and references of physiological data.

Family	Genus	species	1216S	V_{O2RES} (ml/h) 20°C	Mass (g)	V_{O2RES} (ml/h) 25°C	Mass (g)	V_{O2EX} (ml/h) 20°C	Mass (g)	V_{O2EX} (ml/h) 25°C	Mass (g)	Ref.
Bufonidae	*Bufo*	*cognatus*	AY680231	1.290	63.80	1.930	67.50	42.280	28.00	51.761	27.10	Secor et al. 2007
Bufonidae	*Bufo*	*haematiticus*	AY680270	--	--	--	--	--	--	--	--	
Bufonidae	*Bufo*	*marinus*	AY325994	2.609	101.00	3.170	101.00	156.100	223.00	380.380	266.00	Gatten et al. 1992
Bufonidae	*Bufo*	*terrestris*	AY680222	15.100	102.00	2.243	19.80	--	--	--	--	Gatten et al. 1992
Bufonidae	*Bufo*	*viridis*	--	0.875	35.00	--	--	--	--	--	--	Gatten et al. 1992
Bufonidae	*Bufo*	*woodhousii*	AY680219	4.413	64.80	2.235	56.30	80.230	71.00	85.910	71.00	Gatten et al. 1992
Bufonidae	*Dendrophryniscus*	*minutus*	AY843582	--	--	--	--	--	--	--	--	
Bufonidae	*Melanophryniscus*	*stelzneri*	AY325999	--	--	--	--	--	--	--	--	
Centrolenidae	*Centrolene*	*prosoblepon*	AY843574	--	--	--	--	--	--	--	--	
Ceratobatrachidae	*Ceratobatrachus*	*guentheri*	DQ283198	--	--	--	--	--	--	--	--	
Ceratobatrachidae	*Ingerana*	*baluensis*	DQ283142	--	--	--	--	--	--	--	--	
Ceratophryidae	*Atelognathus*	*patagonicus*	AY843571	--	--	--	--	--	--	--	--	
Ceratophryidae	*Ceratophrys*	*calcarata*	--	--	--	2.967	55.50	--	--	--	--	Gatten et al. 1992
Ceratophryidae	*Ceratophrys*	*cranwelli*	AY843575	--	--	0.410	8.55	--	--	--	--	Grayson et al. 2005
Ceratophryidae	*Ceratophrys*	*ornata*	AY326013	--	--	--	--	--	--	--	--	
Ceratophryidae	*Lepidobatrachus*	*llanensis*	AY326019 (as sp.)	--	--	8.585	88.50	--	--	--	--	Gatten et al. 1992
Ceratophryidae	*Telmatobius*	*niger*	AY326015	--	--	--	--	--	--	--	--	
Cycloramphidae	*Alsodes*	*monticola*	AY326016	--	--	--	--	--	--	--	--	
Cycloramphidae	*Odontophrynus*	*americanus*	AY843704	0.549	15.24	--	--	8.786	15.20	--	--	Gatten et al. 1992
Cycloramphidae	*Rhinoderma*	*darwinii*	DQ283324	--	--	--	--	--	--	--	--	
Cycloramphidae	*Thoropa*	*miliaris*	DQ283331	--	--	--	--	--	--	--	--	
Dendrobatidae	*Allobates*	*femoralis*	AY364543	--	--	--	--	--	--	--	--	
Dendrobatidae	*Allobates*	*talamancae*	EU342516	0.053	0.87	--	--	0.255	0.87	--	--	Navas 1996
Dendrobatidae	*Hyloxalus*	*awa*	AY364544	--	--	--	--	--	--	--	--	
Dendrobatidae	*Colostethus*	*fugax*	AY364547	--	--	--	--	--	--	--	--	
Dendrobatidae	*Colostethus*	*panamansis*	EU342599	0.137	1.57	0.213	1.53	1.131	1.52	1.394	1.52	Gatten et al. 1992

Table 3.3 (Cont): Species of anurans and outgroups used for the phylogenetic inference and metanalysis of the metabolic parameters in Anura. Data include accession numbers, metabolic measurements, and references of physiological data.

Family	Genus	species	1216S	V_{O2RES} (ml/h) 20°C	Mass (g)	V_{O2RES} (ml/h) 25°C	Mass (g)	V_{O2EX} (ml/h) 20°C	Mass (g)	V_{O2EX} (ml/h) 25°C	Mass (g)	Ref.
Dendrobatidae	*Dendrobates*	*auratus*	AY326036	0.142	2.09	0.159	1.77	1.773	1.95	2.036	1.50	Gatten et al. 1992
Dendrobatidae	*Hyloxalus*	*subpunctatus*	EU342693	0.089	0.65	--	--	0.257	0.65	--	--	Navas 1996
Dendrobatidae	*Mannophryne*	*trinitatis*	EU342504	--	--	0.201	1.00	--	--	--	--	Gatten et al. 1992
Dendrobatidae	*Phyllobates*	*vittatus*	*	--	--	--	--	--	--	--	--	
Dendrobatidae	*Silverstoneia*	*nubicola*	EU342579	0.031	0.28	0.044	0.27	0.143	0.25	0.164	0.25	Gatten et al. 1992
Dicroglossidae	*Fejervarya*	*nicobariensis*	AY326062	--	--	0.256	2.60	--	--	--	--	Gatten et al. 1992
Dicroglossidae	*Hoplobatrachus*	*occipitalis*	DQ283059	--	--	--	--	--	--	--	--	
Dicroglossidae	*Limnonectes*	*magnus*	AY313706	1.402	34.20	--	--	--	--	--	--	Gatten et al. 1992
Dicroglossidae	*Occidozyga*	*martensii*	--	0.524	9.30	0.887	9.30	--	--	--	--	Gatten et al. 1992
Eleutherodactylidae	*Eleutherodactylus*	*coqui*	EF493539	0.179	4.06	--	--	1.193	4.10	--	--	Gatten et al. 1992
Heleophrynidae	*Heleophryne*	*purcelli*	AY326072	--	--	--	--	--	--	--	--	
Hemisotidae	*Hemisus*	*marmoratum*	AY326070	--	--	--	--	--	--	--	--	
Hylidae	*Acris*	*crepitans*	EF566971	--	--	0.329	1.86	--	--	--	--	Gatten et al. 1992
Hylidae	*Agalychnis*	*callidryas*	AY843563	0.337	5.65	--	--	2.993	5.70	--	--	Gatten et al. 1992
Hylidae	*Cyclorana*	*maini*	--	--	--	0.342	5.10	--	--	7.634	5.11	Gatten et al. 1992
Hylidae	*Cyclorana*	*platycephala*	--	--	--	1.007	21.90	--	--	--	--	Withers 1993
Hylidae	*Dendropsophus*	*labialis*	AY843635	0.730	7.45	--	--	3.129	7.45	--	--	Navas 1996
Hylidae	*Dendropsophus*	*microcephalus*	EF566945	0.080	0.67	--	--	0.311	0.67	--	--	Navas 1996
Hylidae	*Hyla*	*arenicolor*	AY843603	0.300	3.37	--	--	2.839	3.40	--	--	Gatten et al. 1992
Hylidae	*Hyla*	*chrysoscelis*	EF566948	0.437	3.90	--	--	5.382	5.47	--	--	Gatten et al. 1992
Hylidae	*Hyla*	*cinerea*	AY549327	0.560	3.82	0.459	4.50	--	--	--	--	Gatten et al. 1992
Hylidae	*Hyla*	*gratiosa*	EF566966	--	--	1.443	9.80	--	--	--	--	
Hylidae	*Hyla*	*versicolor*	EF566950	0.603	6.09	1.525	7.60	6.222	6.10	--	--	

Table 3.3 (Cont): Species of anurans and outgroups used for the phylogenetic inference and metanalysis of the metabolic parameters in Anura. Data include accession numbers, metabolic measurements, and references of physiological data.

Family	Genus	species	1216S	V_{O2res} (ml/h) 20°C	Mass (g)	V_{O2res} (ml/h) 25°C	Mass (g)	V_{O2ex} (ml/h) 20°C	Mass (g)	V_{O2ex} (ml/h) 25°C	Mass (g)	Ref.
Hylidae	*Phyllomedusa*	*sauvagei*	AY326045 (as *tomopterna*)	--	--	1.803	17.50	--	--	--	--	Gatten et al. 1992
Hylidae	*Pseudacris*	*crucifer*	AY291100	0.144	1.30	--	--	1.356	1.30	--	--	Gatten et al. 1992
Hylidae	*Pseudacris*	*nigrita*	AY291078	--	--	0.162	1.00	--	--	--	--	Gatten et al. 1992
Hylidae	*Pseudacris*	*regilla*	AY291112	0.166	2.76	--	--	0.745	2.76	--	--	Gatten et al. 1992
Hylidae	*Pseudacris*	*triseriata*	EF472157	0.269	1.13	0.112	0.94			--	--	Gatten et al. 1992
Hylidae	*Pseudis*	*paradoxa*	AY326032	--	--	--	--	--	--	--	--	
Hylidae	*Smilisca*	*fodiens*	AY843743	0.514	15.13	--	--	5.995	15.10	--	--	Gatten et al. 1992
Hylidae	*Trachycephalus*	*venulosa*	AY326048	--	--	--	--	--	--	--	--	
Hyperoliidae	*Hyperolius*	*marmoratus*	AY326069	0.067	1.00	0.361	1.39	--	--	--	--	Gräfe et al. 1992
Hyperoliidae	*Hyperolius*	*parallelus*	--	0.077	1.00	--	--	--	--	--	--	Gatten et al. 1992
Hyperoliidae	*Hyperolius*	*tuberilinguis*	--	0.068	1.00	--	--	--	--	--	--	Gatten et al. 1992
Hyperoliidae	*Hyperolius*	*viridiflavus*	FJ151059 (as *castaneus*)	0.083	0.88	0.458	1.58	0.663	0.90	--	--	Gräfe et al. 1992
Hyperoliidae	*Kassina*	*maculata*	--	0.280	5.80	0.370	5.67	--	--	--	--	Secor et al. 2007
Hyperoliidae	*Kassina*	*senegalensis*	FJ151067	0.228	3.02	--	--	2.481	3.00	--	--	Gatten et al. 1992
Hyperoliidae	*Kassina*	*weali*	--	0.318	6.25	--	--	4.120	6.30	--	--	Gatten et al. 1992
Leiopelmatidae	*Ascaphus*	*truei*	AJ871087	--	--	--	--	--	--	--	--	
Leiopelmatidae	*Leiopelma*	*archeyi*	*	--	--	--	--	--	--	--	--	
Leptodactylidae	*Adenomera*	*andreae*	AY364538	--	--	--	--	--	--	--	--	
Leptodactylidae	*Edalorhina*	*perezi*	AY843585	--	--	--	--	--	--	--	--	
Leptodactylidae	*Engystomops*	*pustulosus*	DQ337241	--	--	0.260	1.72	--	--	3.349	1.84	Gatten et al. 1992
Leptodactylidae	*Leptodactylus*	*fuscus*	DQ283404	--	--	0.587	5.10	--	--	--	--	Gatten et al. 1992
Leptodactylidae	*Leptodactylus*	*ocellatus*	DQ158417	--	--	--	--	--	--	--	--	
Leptodactylidae	*Leptodactylus*	*petadactylus*	AY326017	--	--	--	--	--	--	--	--	
Leptodactylidae	*Lithodytes*	*lineatus*	AY843690	--	--	--	--	--	--	--	--	

Table 3.3 (Cont): Species of anurans and outgroups used for the phylogenetic inference and metanalysis of the metabolic parameters in Anura. Data include accession numbers, metabolic measurements, and references of physiological data.

Family	Genus	species	1216S	V_{O2RES} (ml/h) 20°C	Mass (g)	V_{O2RES} (ml/h) 25°C	Mass (g)	V_{O2EX} (ml/h) 20°C	Mass (g)	V_{O2EX} (ml/h) 25°C	Mass (g)	Ref.
Leptodactylidae	*Pleurodema*	*brachyops*	AY843733	--	--	--	--	--	--	--	--	
Leptodactylidae	*Pseudopaludicola*	*falcipes*	AY843741	--	--	--	--	--	--	--	--	
Limnodynastidae	*Limnodynastes*	*salminii*	AY326071	--	--	0.573	6.82	--	--	--	--	Withers 1993
Mantellidae	*Aglyptodactylus*	*madagascariensis*	DQ283056	--	--	--	--	--	--	--	--	
Mantellidae	*Boophis*	*tephraeomystax*	DQ283032	--	--	--	--	--	--	--	--	
Mantellidae	*Laliostoma*	*labrosum*	DQ283057	--	--	--	--	--	--	--	--	
Mantellidae	*Mantella*	*nigricans*	DQ283034	--	--	--	--	--	--	--	--	
Megophryidae	*Megophrys*	*montana*	*	--	--	--	--	--	--	--	--	
Microhylidae	*Dyscophus*	*antonguilli*	EU341120	0.750	41.60	1.130	40.70	--	--	--	--	Secor et al. 2007
Microhylidae	*Elachistocleis*	*ovalis*	DQ283405	--	--	--	--	--	--	--	--	
Microhylidae	*Gastrophryne*	*olivacea*	AY326066	0.103	1.94	--	--	1.547	1.90	--	--	Gatten et al. 1992
Microhylidae	*Kaloula*	*pulchra*	NC006405	0.890	30.66	--	--	21.367	30.70	--	--	Gatten et al. 1992
Microhylidae	*Scaphiophryne*	*marmorata*	AY843751	--	--	--	--	--	--	--	--	
Myobatrachidae	*Crinia*	*parinsignifera*	EU443855	0.117	0.63	0.177	0.67	--	--	--	--	Gatten et al. 1992
Myobatrachidae	*Crinia*	*signifera*	EU443926	0.131	0.62	0.149	0.62	--	--	--	--	Gatten et al. 1992
Myobatrachidae	*Heleioporus*	*albopunctatus*	--	--	--	1.356	33.90	--	--	12.577	33.90	Withers 1993
Myobatrachidae	*Neobatrachus*	*centralis*	--	--	--	0.801	8.90	--	--	--	--	Gatten et al. 1992
Myobatrachidae	*Neobatrachus*	*fulvus*	--	--	--	1.154	11.90	--	--	--	--	Gatten et al. 1992
Myobatrachidae	*Neobatrachus*	*kunapalari*	AY843700 (as *sudelli*)	--	--	1.519	21.10	--	--	14.953	21.12	Withers 1993
Myobatrachidae	*Neobatrachus*	*pelobatoides*	--	--	--	1.040	8.00	--	--	6.593	8.03	Guppy and Withers 1999
Myobatrachidae	*Neobatrachus*	*sutor*	--	--	--	0.599	9.50	--	--	12.780	9.53	Gatten et al. 1992
Myobatrachidae	*Neobatrachus*	*wilsmorei*	--	--	--	1.515	18.70	--	--	--	--	Gatten et al. 1992
Myobatrachidae	*Notaden*	*nichollsi*	--	--	--	1.944	27.00	--	--	--	--	Withers 1993
Pelobatidae	*Pelobates*	*cultripes*	NC008144	--	--	--	--	--	--	--	--	
Pelodytidae	*Pelodytes*	*punctatus*	*	--	--	--	--	--	--	--	--	
Phrynobatrachidae	*Phrynobatrachus*	*natalensis*	DQ283414	--	--	--	--	--	--	--	--	

Table 3.3 (Cont): Species of anurans and outgroups used for the phylogenetic inference and metanalysis of the metabolic parameters in Anura. Data include accession numbers, metabolic measurements, and references of physiological data.

Family	Genus	species	1216S	V_{O2RES} (ml/h) 20°C	Mass (g)	V_{O2RES} (ml/h) 25°C	Mass (g)	V_{O2EX} (ml/h) 20°C	Mass (g)	V_{O2EX} (ml/h) 25°C	Mass (g)	Ref.
Pipidae	*Hymenochirus*	*boettgeri*	AY581623	--	--	--	--	--	--	--	--	
Pipidae	*Pipa*	*pipa*	*	--	--	--	--	--	--	--	--	
Pipidae	*Silurana*	*tropicalis*	NC006839	2.530	55.00	3.526	41.00	--	--	27.963	23.90	Gatten et al. 1992
Pyxicephalidae	*Afrana*	*fuscigula*	DQ283069	--	--	--	--	--	--	--	--	
Pyxicephalidae	*Pyxicephalus*	*adspersus*	--	14.220	562.30	18.500	500.00	344.000	400.00	--	--	Gatten et al. 1992
Pyxicephalidae	*Strongylopus*	*grayii*	DQ283068	--	--	--	--	--	--	--	--	
Ranidae	*Conraua*	*goliath*	DQ283132	--	--	18.860	251.00	--	--	--	--	Gatten et al. 1992
Ranidae	*Fejervarya*	*cancrivora*	--	1.041	20.45	1.577	20.45	--	--	--	--	Gatten et al. 1992
Ranidae	*Rana*	*arvalis*	--	2.887	17.00	4.769	17.00	--	--	--	--	Gatten et al. 1992
Ranidae	*Rana*	*aurora*	DQ283189	--	--	--	--	--	--	--	--	
Ranidae	*Rana*	*blythi*	--	--	--	4.373	88.70	--	--	--	--	Gatten et al. 1992
Ranidae	*Rana*	*catesbeiana*	DQ283257	5.614	228.20	8.650	292.00	21.320	26.00	--	--	Gatten et al. 1992
Ranidae	*Rana*	*chalconota*	DQ283139	--	--	0.391	4.10	--	--	--	--	Gatten et al. 1992
Ranidae	*Rana*	*clamitans*	DQ283185	--	--	2.701	32.50	1.984	4.00	--	--	Gatten et al. 1992
Ranidae	*Rana*	*erythraea*	DQ283138	0.781	19.00	1.625	19.00	--	--	--	--	Gatten et al. 1992
Ranidae	*Rana*	*esculenta*	--	4.394	45.30	4.195	50.32	--	--	--	--	Gatten et al. 1992
Ranidae	*Rana*	*galamensis*	DQ283058	--	--	--	--	--	--	--	--	
Ranidae	*Rana*	*palmipes*	DQ283384	--	--	--	--	--	--	--	--	
Ranidae	*Rana*	*pipiens*	*	1.521	34.80	3.276	42.00	16.520	28.00	27.108	50.20	Gatten et al. 1992
Ranidae	*Rana*	*ridibunda*	--	1.120	35.00	--	--	--	--	--	--	Gatten et al. 1992
Ranidae	*Rana*	*sylvatica*	DQ283387	1.098	12.67	0.648	6.00	9.462	12.70	--	--	Gatten et al. 1992
Ranidae	*Rana*	*temporaria*	AY326063	1.750	25.00	7.504	38.53	--	--	--	--	Gatten et al. 1992
Ranidae	*Rana*	*virgatipes*	--	--	--	1.015	7.00	--	--	--	--	

Family	Genus	species	1216S	V_{O2RES} (ml/h) 20°C	Mass (g)	V_{O2RES} (ml/h) 25°C	Mass (g)	V_{O2EX} (ml/h) 20°C	Mass (g)	V_{O2EX} (ml/h) 25°C	Mass (g)	Ref.
Rhinophrynidae	*Rhinophrynus*	*dorsalis*	*	--	--	--	--	--	--	--	--	
Scaphiopodidae	*Scaphiopus*	*couchii*	DQ283150	--	--	--	--	8.884	10.90	40.874	21.40	Gatten et al. 1992
Scaphiopodidae	*Scaphiopus*	*hurteri*	*	--	--	--	--	--	--	--	--	
Strabomantidae	*Pristimantis*	*bogotensis*	--	0.120	0.91	--	--	0.332	0.91	--	--	Navas 1996
Strabomantidae	*Pristimantis*	*diastema*	EU186682	--	--	--	--	--	--	--	--	Navas 1996

Table 3.3 (Cont): Species of anurans and outgroups used for the phylogenetic inference and metanalysis of the metabolic parameters in Anura. Data include accession numbers, metabolic measurements, and references of physiological data.

Genus	Species	Conspicuousness		Lipophilic Skin Alkaloids			Lipophilic Skin Alkaloid Diversity											
		Cont.	Bin.	Seq.	[ ]	Div.	MON	PTX	HTX	DHQ	3,5-P	3,5-I	5,8-I	5,6,8-I	QUI	TRI	BTX	Ref./ sampled
Allobates	*femoralis*	53.074	0	0	0	0	-	-	-	-	-	-	-	-	-	-	-	(Darst et al. 2006)
Allobates	*insperatus*	53.721	0	0	0	0	-	-	-	-	-	-	-	-	-	-	-	(Darst and Cannatella 2004)
Allobates	*juanii*	52.638	0	?	?	?	nd	nd	nd	nd	nd	nd	nd	nd	nd	nd	nd	--
Allobates	*kingsburyi*	53.328	0	0	0	0	-	-	-	-	-	-	-	-	-	-	-	(3 skins)
Allobates	sp. Tachira	24.179	0	?	?	?	nd	nd	nd	nd	nd	nd	nd	nd	nd	nd	nd	--
Allobates	*talamancae*	51.872	0	0	0	0	-	-	-	-	-	-	-	-	-	-	-	(Daly et al. 1994)
Allobates	*zaparo*	57.867	1	0	0	0	-	-	-	-	-	-	-	-	-	-	-	(Darst et al. 2006)
Ameerega	*bilinguis*	62.113	1	1	2	2	-	-	+	+	-	-	-	-	-	-	-	(Daly et al. 2009)
Ameerega	*hahneli*	38.212	0	1	2	2	-	-	+	+	-	-	-	-	-	-	-	(Daly et al. 1987)
Ameerega	*parvula*	60.255	1	1	2	4	-	+	+	+	-	-	+	-	-	-	-	(Daly et al. 1987)
Ameerega	*trivittata*	89.778	1	1	3	5	+	-	+	+	-	-	+	+	-	-	-	(Daly et al. 2009)
Anomaloglossus	sp. Ayacucho	33.281	0	?	?	?	nd	nd	nd	nd	nd	nd	nd	nd	nd	nd	nd	--
Aromobates	aff. *alboguttatus*	43.589	0	?	?	?	nd	nd	nd	nd	nd	nd	nd	nd	nd	nd	nd	--
Aromobates	*saltuensis*	23.456	0	?	?	?	nd	nd	nd	nd	nd	nd	nd	nd	nd	nd	nd	--
Colostethus	*fugax*	40.821	0	0	0	0	-	-	-	-	-	-	-	-	-	-	-	(5 skins)
Colostethus	*panamensis*	43.044	0	0	0	0	-	-	-	-	-	-	-	-	-	-	-	(Daly et al. 1994)
Colostethus	*pratti*	45.992	0	0	0	0	-	-	-	-	-	-	-	-	-	-	-	(Daly et al. 1994)
Dendrobates	*auratus*	89.171	1	1	3	10	+	+	+	+	+	+	+	+	+	+	-	(Daly et al. 1987)
Dendrobates	*bombetes*	67.145	1	1	2	5	-	+	-	+	-	-	+	+	+	-	-	(Daly et al. 1997)
Dendrobates	*captivus*	64.630	1	1	3	?	nd	nd	nd	nd	nd	nd	nd	nd	nd	nd	nd	(2 skins)

Abbreviations: Conspicuousness: Cons. = continuous, Bin. = binary (1, brightly; 0, cryptically colored); Lipophilic Skin Alkaloids: Seq. = ability to sequester (0, no; 1, yes), [ ] = concentration per 100 mg of skin (0, no alkaloids detected; 1, < 50 *µg*, 2, > 50 and < 200 *µg*; and 3, > 200 *µg*), Div. = number of structural classes. Diversity of lipophilic skin alkaloids of poison frogs (some grouped under a single structural classes for consistency): MON (Monocyclics), PXT (all pumiliotoxins classes: PTX, aPTX, hPTX, and Deoxy-hPTX), HTX (histrionicotoxins), DHQ (decahydroquinolines), 3,5-P (3,5-disubstituted pyrrolizidines), 3,5-I (3,5-disubstituted indolizidines), 5,8-I (5,8-disubstituted and dehydro-5,8 indolizidines), 5,6,8-I (5,6,8-trisubstituted indolizidines), QUI (4,6-disubstituted and 1,4-disubstituted quinolizidines), TRI (Tricyclics), and BTX (Batrachotoxins). ?, unknown; -, absent; +, present; and nd, no data.

Genus	Species	Conspicuousness		Lipophilic Skin Alkaloids			Lipophilic Skin Alkaloid Diversity											
		Cont.	Bin.	Seq.	[ ]	Div.	MON	PTX	HTX	DHQ	3,5-P	3,5-I	5,8-I	5,6,8-I	QUI	TRI	BTX	Ref./ sampled
Dendrobates	*claudiae*	77.153	1	1	2	6	+	+	-	+	+	-	+	-	+	-	-	(Daly et al. 1987)
Dendrobates	*duellmani*	74.567	1	?	?	?	nd	nd	nd	nd	nd	nd	nd	nd	nd	nd	nd	--
Dendrobates	*galactonotus*	82.880	1	1	3	7	-	+	+	+	+	-	+	+	-	+	-	(Daly et al. 2009)
Dendrobates	*histrionicus*	64.644	1	1	3	9	+	+	+	+	+	+	+	+	+	-	-	(Daly et al. 1987)
Dendrobates	*lamasi*	89.438	1	?	?	?	nd	nd	nd	nd	nd	nd	nd	nd	nd	nd	nd	--
Dendrobates	*leucomelas*	72.065	1	1	2	4	-	+	+	-	+	-	-	-	+	-	-	(Daly et al. 1987)
Dendrobates	*pumilio*	63.236	1	1	3	10	+	+	+	+	+	+	+	+	+	+	-	(Saporito et al. 2007)
Dendrobates	sp. Quibdo	65.783	1	1	1	3	-	+	-	-	+	-	+	-	-	-	-	(Daly et al. 1987)
Dendrobates	*sylvaticus*	63.055	1	1	3	6	-	+	+	+	-	-	+	+	+	-	-	(Daly et al. 1987)
Dendrobates	*tinctorius*	75.005	1	1	2	4	-	+	+	+	-	-	-	+	-	-	-	(Daly et al. 1987)
Dendrobates	*truncatus*	102.808	1	1	3	5	-	-	+	+	+	-	+	+	-	-	-	(Daly et al. 1987)
Dendrobates	*ventrimaculatus*	67.774	1	1	2	7	-	+	+	+	+	+	-	+	+	-	-	(Daly et al. 1987)
Dendrobates	*virolinensis*	57.892	1	?	?	?	nd	nd	nd	nd	nd	nd	nd	nd	nd	nd	nd	--
Epipedobates	*anthonyi*	74.186	1	1	3	4	-	+	-	-	-	-	+	+	+	-	-	(Daly et al. 1987)
Epipedobates	*boulengeri*	55.322	0	0	0	0	-	-	-	-	-	-	-	-	-	-	-	(Darst and Cannatella 2004)
Epipedobates	*machalilla*	59.140	1	0	0	0	-	-	-	-	-	-	-	-	-	-	-	(2 skins)
Epipedobates	sp. F	65.122	1	1	1	5	-	+	+	-	-	-	+	+	+	-	-	(Daly et al. 1987)
Epipedobates	*tricolor*	69.720	1	?	?	?	nd	nd	nd	nd	nd	nd	nd	nd	nd	nd	nd	--
Hyloxalus	*awa*	52.780	0	0	0	0	-	-	-	-	-	-	-	-	-	-	-	(Darst and Cumming s 2006)
Hyloxalus	*azueriventris*	68.512	1	1	1	?	nd	nd	nd	nd	nd	nd	nd	nd	nd	nd	nd	(Saporito et al. 2009)

Abbreviations: Conspicuousness: Cons. = continuous, Bin. = binary (1, brightly; 0, cryptically colored); Lipophilic Skin Alkaloids: Seq. = ability to sequester (0, no; 1, yes), [ ] = concentration per 100 mg of skin (0, no alkaloids detected; 1, < 50 *µg*, 2, > 50 and < 200 *µg*; and 3, > 200 *µg*), Div. = number of structural classes. Diversity of lipophilic skin alkaloids of poison frogs (some grouped under a single structural classes for consistency): MON (Monocyclics), PXT (all pumiliotoxins classes: PTX, aPTX, hPTX, and Deoxy-hPTX), HTX (histrionicotoxins), DHQ (decahydroquinolines), 3,5-P (3,5-disubstituted pyrrolizidines), 3,5-I (3,5-disubstituted indolizidines), 5,8-I (5,8-disubstituted and dehydro-5,8 indolizidines), 5,6,8-I (5,6,8-trisubstituted indolizidines), QUI (4,6-disubstituted and 1,4-disubstituted quinolizidines), TRI (Tricyclics), and BTX (Batrachotoxins). ?, unknown; -, absent; +, present; and nd, no data.

Genus	Species	Conspicuousness		Lipophilic Skin Alkaloids			Lipophilic Skin Alkaloid Diversity											
		Cont.	Bin.	Seq.	[ ]	Div.	MON	PTX	HTX	DHQ	3,5-P	3,5-I	5,8-I	5,6,8-I	QUI	TRI	BTX	Ref./ sampled
Hyloxalus	*bocagei*	42.288	0	?	?	?	nd	nd	nd	nd	nd	nd	nd	nd	nd	nd	nd	--
Hyloxalus	*elachyhistus*	49.151	0	0	0	0	-	-	-	-	-	-	-	-	-	-	-	(Daly et al. 1994)
Hyloxalus	*maculosus*	31.288	0	0	0	0	-	-	-	-	-	-	-	-	-	-	-	(Darst and Cannatella 2004)
Hyloxalus	*nexipus*	66.929	1	0	0	0	-	-	-	-	-	-	-	-	-	-	-	(3 skins)
Hyloxalus	*sauli*	38.131	0	0	0	0	-	-	-	-	-	-	-	-	-	-	-	(Darst and Cannatella 2004)
Hyloxalus	*subpunctatus*	54.270	0	?	?	?	nd	nd	nd	nd	nd	nd	nd	nd	nd	nd	nd	--
Hyloxalus	*toachi*	36.654	0	?	?	?	nd	nd	nd	nd	nd	nd	nd	nd	nd	nd	nd	--
Hyloxalus	*vertebralis*	32.728	0	0	0	0	-	-	-	-	-	-	-	-	-	-	-	(5 skins)
Mannophryne	*collaris*	39.034	0	?	?	?	nd	nd	nd	nd	nd	nd	nd	nd	nd	nd	nd	--
Phyllobates	*aurotaenia*	77.901	1	1	2	5	-	+	+	+	-	+	-	-	-	-	+	(Daly et al. 1987)
Phyllobates	*terribilis*	77.260	1	1	3	2	-	-	-	-	-	+	-	-	-	-	+	(Daly et al. 1987)
Rheobates	*palmatus*	25.686	0	?	?	?	nd	nd	nd	nd	nd	nd	nd	nd	nd	nd	nd	--
Silverstoneia	*flotator*	52.693	0	0	0	0	-	-	-	-	-	-	-	-	-	-	-	(Poulin et al. 2001)
Silverstoneia	*nubicola*	41.807	0	0	0	0	-	-	-	-	-	-	-	-	-	-	-	(Daly et al. 1978)

Abbreviations: Conspicuousness: Cons. = continuous, Bin. = binary (1, brightly; 0, cryptically colored); Lipophilic Skin Alkaloids: Seq. = ability to sequester (0, no; 1, yes), [ ] = concentration per 100 mg of skin (0, no alkaloids detected; 1, < 50 *µg*, 2, > 50 and < 200 *µg*; and 3, > 200 *µg*), Div. = number of structural classes. Diversity of lipophilic skin alkaloids of poison frogs (some grouped under a single structural classes for consistency): MON (Monocyclics), PXT (all pumiliotoxins classes: PTX, aPTX, hPTX, and Deoxy-hPTX), HTX (histrionicotoxins), DHQ (decahydroquinolines), 3,5-P (3,5-disubstituted pyrrolizidines), 3,5-I (3,5-disubstituted indolizidines), 5,8-I (5,8-disubstituted and dehydro-5,8 indolizidines), 5,6,8-I (5,6,8-trisubstituted indolizidines), QUI (4,6-disubstituted and 1,4-disubstituted quinolizidines), TRI (Tricyclics), and BTX (Batrachotoxins). ?, unknown; -, absent; +, present; and nd, no data.

Table 3.4: Continuous and binary measurements of conspicuousness and alkaloid profiles in the sampled poison frogs.

Genus	Species	n	Total Prey	Prey /indiv	Ants & Mites	Ortho.	Coleo.	Colle.	Dipte.	Isopt.	Aranae	Larvae	Other	Niche Breath	Ref.
Allobates	*femoralis*	15	60	4.000	0.367	0.000	0.117	0.033	0.083	0.017	0.050	0.033	0.300	0.750	(Darst et al. 2005)
Allobates	*insperatus*	12	74	6.167	0.514	0.000	0.068	0.068	0.014	0.000	0.095	0.081	0.162	0.352	(Darst et al. 2005)
Allobates	*juanii*	--	--	--	--	--	--	--	--	--	--	--	--	--	--
Allobates	*kingsburyi*	--	--	--	--	--	--	--	--	--	--	--	--	--	--
Allobates	sp. Tachira	--	--	--	--	--	--	--	--	--	--	--	--	--	--
Allobates	*talamancae*	19	262	13.900	0.305	0.019	0.046	0.263	0.149	0.015	0.027	0.027	0.149	0.614	(Caldwell 1996)
Allobates	*zaparo*	20	180	9.000	0.283	0.011	0.178	0.044	0.033	0.167	0.017	0.078	0.189	0.815	(Darst et al. 2005)
Ameerega	*bilinguis*	24	1676	69.833	**0.735**	0.013	0.000	0.013	0.001	0.036	0.004	0.180	0.018	0.106	(Darst et al. 2005)
Ameerega	*hahneli*	11	229	20.818	**0.808**	0.000	0.061	0.004	0.004	0.031	0.009	0.022	0.061	0.074	(Darst et al. 2005)
Ameerega	*parvula*	12	587	48.917	**0.841**	0.000	0.036	0.003	0.002	0.017	0.003	0.075	0.023	0.057	(Darst et al. 2005)
Ameerega	*trivittata*	--	--	77.200	0.593	0.000	0.071	0.018	0.018	0.035	0.018	0.212	0.035	0.211	(Toft 1977)
Anomaloglossus	sp. Ayacucho	--	--	--	--	--	--	--	--	--	--	--	--	--	--
Aromobates	aff. *alboguttatus*	104	1255	5.200	0.137	0.009	0.127	0.004	0.109	0.000	0.022	0.478	0.114	0.375	(Bonilla and La Marca 1996) [a]
Aromobates	*saltuensis*	--	--	--	--	--	--	--	--	--	--	--	--	--	--
Colostethus	*fugax*	--	--	--	--	--	--	--	--	--	--	--	--	--	--
Colostethus	*panamensis*	12	80	7.300	0.370	0.230	0.120	0.021	0.021	0.000	0.021	0.000	0.218	0.552	(Toft 1981)
Colostethus	*pratti*	8	26	5.100	0.060	0.780	0.090	0.000	0.000	0.000	0.000	0.000	0.070	0.088	(Toft 1981)
Dendrobates	*auratus*	23	4291	186.500	**0.946**	0.000	0.014	0.006	0.004	0.006	0.003	0.011	0.010	0.017	(Caldwell 1996)
Dendrobates	*bombetes*	--	--	--	--	--	--	--	--	--	--	--	--	--	--
Dendrobates	*captivus*	--	--	--	--	--	--	--	--	--	--	--	--	--	--
Dendrobates	*claudiae*	26	458	24.100	**0.810**	0.000	0.000	0.000	0.000	0.020	0.000	0.170	0.000	0.066	(Toft 1981) [b]
Dendrobates	*duellmani*	--	--	--	--	--	--	--	--	--	--	--	--	--	--
Dendrobates	*galactonotus*	--	--	--	--	--	--	--	--	--	--	--	--	--	--
Dendrobates	*histrionicus*	7	704	100.571	**0.933**	0.000	0.034	0.000	0.000	0.007	0.000	0.014	0.011	0.021	(Silverstone 1975)
Dendrobates	*lamasi*	--	--	--	--	--	--	--	--	--	--	--	--	--	--

Abbreviations: Ortho., orthopterans; Coleo., coleopterans; Colle., collembolans; Dipte., dipterans; Isopt., isopterans; Aranae, spiders. **Bold** indicate that ant & mite category was > 0.70. [a]. only females, [b]. as *minutus*, [c]. as *fulguritus*.

Genus	Species	n	Total Prey	Prey /indiv	Ants & Mites	Ortho.	Coleo.	Colle.	Dipte.	Isopt.	Aranae	Larvae	Other	Niche Breath	Ref.
Dendrobates	*leucomelas*	--	--	--	--	--	--	--	--	--	--	--	--	--	--
Dendrobates	*pumilio*	33	2783	84.400	**0.878**	0.000	0.008	0.070	0.004	0.001	0.000	0.015	0.024	0.041	(Caldwell 1996)
Dendrobates	sp. Quibdo	4	122	25.800	**0.970**	0.000	0.000	0.010	0.010	0.000	0.010	0.000	0.000	0.009	(Toft 1981) [c]
Dendrobates	*sylvaticus*	--	--	--	--	--	--	--	--	--	--	--	--	--	--
Dendrobates	*tinctorius*	--	--	--	--	--	--	--	--	--	--	--	--	--	--
Dendrobates	*truncatus*	--	--	--	--	--	--	--	--	--	--	--	--	--	--
Dendrobates	*ventrimaculatus*	5	354	70.800	**0.734**	0.000	0.008	0.006	0.011	0.000	0.006	0.215	0.020	0.101	(Caldwell 1996)
Dendrobates	*virolinensis*	165	8993	56.000	**0.884**	0.000	0.010	0.053	0.004	0.000	0.002	0.029	0.018	0.039	(Valderrama-Vernaza et al. 2009)
Epipedobates	*anthonyi*	10	288	28.800	**0.889**	0.004	0.031	0.004	0.024	0.000	0.010	0.017	0.021	0.037	(Darst et al. 2005)
Epipedobates	*boulengeri*	32	903	28.200	0.279	0.000	0.012	0.319	0.091	0.000	0.003	0.230	0.065	0.450	(Caldwell 1996)
Epipedobates	*machalilla*	--	--	--	--	--	--	--	--	--	--	--	--	--	--
Epipedobates	sp. F	--	--	--	--	--	--	--	--	--	--	--	--	--	--
Epipedobates	*tricolor*	--	--	--	--	--	--	--	--	--	--	--	--	--	--
Hyloxalus	*awa*	--	--	--	--	--	--	--	--	--	--	--	--	--	--
Hyloxalus	*azuriventris*	--	--	--	--	--	--	--	--	--	--	--	--	--	--
Hyloxalus	*bocagei*	--	--	--	--	--	--	--	--	--	--	--	--	--	--
Hyloxalus	*elachyhistus*	--	--	--	--	--	--	--	--	--	--	--	--	--	--
Hyloxalus	*maculosus*	22	241	10.955	0.216	0.000	0.079	0.000	0.017	0.008	0.017	0.556	0.108	0.251	(Darst et al. 2005)
Hyloxalus	*nexipus*	--	--	--	--	--	--	--	--	--	--	--	--	--	--
Hyloxalus	*sauli*	9	42	4.667	0.595	0.024	0.071	0.000	0.000	0.000	0.024	0.071	0.214	0.248	(Darst et al. 2005)
Hyloxalus	*subpunctatus*	--	--	--	--	--	--	--	--	--	--	--	--	--	--
Hyloxalus	*toachi*	--	--	--	--	--	--	--	--	--	--	--	--	--	--
Hyloxalus	*vertebralis*	--	--	--	--	--	--	--	--	--	--	--	--	--	--
Mannophryne	*collaris*	--	--	--	--	--	--	--	--	--	--	--	--	--	--

Abbreviations: Ortho., orthopterans; Coleo., coleopterans; Colle., collembolans; Dipte., dipterans; Isopt., isopterans; Aranae, spiders. **Bold** indicate that ant & mite category was > 0.70. [a]. only females, [b]. as *minutus*, [c]. as *fulguritus*.

Table 3.5: Dietary profiles of the sampled poison frogs including the number of individual reported, number prey per stomach (prey/individuals), percentage of individuals per prey category, and niche breadth.

	PCA			PAF		
	Comp-1	Comp-2	h^2	Factor-1	Factor-2	h^2
Log-Weight	**0.949**	0.078	0.907	**0.959**	0.103	0.931
Conspicuous	**0.720**	**0.469**	0.739	**0.644**	**0.504**	0.668
RMR	**0.943**	0.156	0.914	**0.937**	0.195	0.916
Scope	**0.915**	0.169	0.865	**0.892**	0.206	0.839
Alkaloid Conc.	**0.430**	**0.828**	0.870	**0.368**	**0.920**	0.981
Alkaloid Diver.	0.330	**0.794**	0.739	0.299	**0.750**	0.652
Ant & Mite	-0.130	**0.824**	0.696	-0.038	**0.586**	0.345
Log-Prey	**0.513**	**0.487**	0.500	**0.441**	**0.453**	0.400
% Variance	58.848	19.028		58.848	19.028	

Table 3.6: Factor loadings, communalities (h^2), and percents of variance explained from phylogenetic principal component analysis and principal axis factoring with Varimax orthogonal rotation. Bold indicates factor loadings > 0.330.

Group	Temp (C)	Metabolic measurement	*n*	Log a coefficient	Log M^b exponent	r^2	F	Mass (g)
Anura	20	RMR	56	-0.995^{***} (0.045)	0.782^{***} (0.038)	0.885	443.209^{***}	0.28 - 562.30
		RMR PIC	40	--	0.721^{***} (0.083)	0.655	96.618^{***}	0.28 - 228.20
	25	RMR	61	-0.775^{***} (0.044)	0.760^{***} (0.034)	0.892	488.472^{***}	0.27 - 500.00
		RMR PIC	39	--	0.751^{***} (0.059)	0.810	162.315^{***}	0.27 - 292.00
	20	AMR	39	-0.265^{***} (0.045)	1.084^{***} (0.040)	0.951	674.150^{***}	0.25 - 400.00
		AMR PIC	29	--	1.021^{***} (0.064)	0.900	299.106^{***}	0.25 - 223.00
	25	AMR	15	0.024^{NS} (0.091)	0.995^{***} (0.068)	0.934	211.714^{***}	0.25 - 266.00
		AMR PIC	12	--	1.039^{***} (0.098)	0.910	111.308^{***}	0.25 - 266.00
	20	Scope	28	-0.206^{**} (0.072)	0.957^{***} (0.066)	0.891	213.128^{***}	0.25 - 400.00
		Scope PIC	24	--	0.858^{***} (0.091)	0.796	89.905^{***}	0.25 - 43.60
	25	Scope	10	-0.079^{NS} (0.071)	1.017^{***} (0.055)	0.977	344.537^{***}	0.25 - 266.00
		Scope PIC	9	--	1.004^{***} (0.069)	0.964	212.516^{***}	0.25 - 266.00
Dendrobatidae	25±0.5	RMR	54	-0.771^{***} (0.018)	0.779^{***} (0.052)	0.815	119.144^{***}	0.16 - 6.01
		RMR PIC	53	--	0.846^{***} (0.065)	0.767	171.400^{***}	0.16 - 6.01
		RMR PIC (no outliers)	47	--	0.766^{***} (0.082)	0.657	87.929^{***}	0.16 - 6.01
		AMR	54	0.060^{**} (0.019)	0.782^{***} (0.053)	0.808	109.080^{***}	0.16 - 6.01
		AMR PIC	53	--	0.880^{***} (0.055)	0.830	253.138^{***}	0.16 - 6.01
		AMR PIC (no outliers)	47	--	0.818^{***} (0.068)	0.757	143.196^{***}	0.16 - 6.01
		Scope	54	-0.016^{NS} (0.022)	0.786^{***} (0.062)	0.756	79.945^{***}	0.16 - 6.01
		Scope PIC	53	--	0.889^{***} (0.064)	0.788	193.15^{***}	0.16 - 6.01
		Scope PIC (no outliers)	47	--	0.829^{***} (0.079)	0.703	108.685^{***}	0.16 - 6.01

Numbers in parenthesis are ± 1 SE. Significance is given by *, $P < 0.05$; **, $P < 0.01$; ***, $P < 0.001$. PIC (no outliers) correspond to grade shifts (see text).

Table 3.7: Metabolic parameters estimates for the log-log scaling relationships of resting metabolic rate (RMR, mL O2/hour), active metabolic rate (AMR, mL O2/hour), aerobic scope (Scope, mL O2/hour) and body mass (Mass, g) of anurans and poison frogs. Linear allometric equations in the form log(RMR, AMR, Scope) = log a (coefficient) + b (exponent) * log Mass. PIC denotes relationship derived from independent contrasts and n is number of species or independent contrasts.

Metabolic measurement	*n*	Log a constant	Log M_b exponent	Conspic-uousness	Lipophilic Alkaloids	Diet Specialist	r^2	F	Mass (g)
RMR	54	-0.776***	0.778***	0.010^{NS}	--	--	0.815	112.425***	0.16
		(0.026)	(0.052)	(0.037)					6.01
RMR PIC	53	--	0.847***	-0.007^{NS}	--	--	0.768	84.470***	0.16
			(0.065)	(0.016)					6.01
RMR	40	-0.812***	0.764***	--	0.038^{NS}	--	0.823	85.902***	0.16
		(0.034)	(0.060)		(0.046)				6.01
RMR PIC	39	--	0.857***	--	>0.001^{NS}	--	0.810	78.676***	0.16
			(0.069)		(0.019)				6.01
RMR^{a}	23	-0.809***	0.785***	--	--	0.060^{NS}	0.781	35.751***	0.16
		(0.047)	(0.095)			(0.071)			5.51
RMR PIC	22	--	0.744***	--	--	-0.005^{NS}	0.812	43.271***	0.16
			(0.085)			(0.021)			5.51
AMR	54	-0.012^{NS}	0.760***	0.138***	--	--	0.858	154.608***	0.16
		(0.023)	(0.046)	(0.032)					6.01
AMR PIC	53	--	0.878***	0.012^{NS}	--	--	0.832	126.560***	0.16
			(0.055)	(0.014)					6.01
AMR	40	-0.013^{NS}	0.769***	--	0.146***	--	0.880	136.177***	0.16
		(0.029)	(0.051)		(0.039)				6.01
AMR PIC	39	--	0.872***	--	0.036*	--	0.863	116.648***	0.16
			(0.059)		(0.017)				6.01
AMR^{a}	23	0.039^{NS}	0.733***	--	--	0.078^{NS}	0.810	42.714***	0.16
		(0.04)	(0.080)			(0.060)			5.51
AMR PIC	22	--	0.782***	--	--	0.010^{NS}	0.872	68.125***	0.16
			(0.073)			(0.018)			5.51
Scope	54	-0.101***	0.760***	0.164***	--	--	0.822	117.958***	0.16
		(0.027)	(0.054)	(0.038)					6.01
Scope PIC	53	--	0.886***	0.016^{NS}	--	--	0.792	97.219***	0.16
			(0.064)	(0.016)					6.01
Scope	40	-0.095**	0.773***	--	0.167***	--	0.856	109.563***	0.16
		(0.033)	(0.058)		(0.045)				6.01
Scope PIC	39	--	0.877***	--	0.043*	--	0.835	93.587***	0.16
			(0.067)		(0.019)				6.01
Scope^{a}	23	-0.036^{NS}	0.732***	--	--	0.086^{NS}	0.761	31.839***	0.16
		(0.046)	(0.093)			(0.069)			5.51
Scope PIC	22	--	0.792***	--	--	0.011^{NS}	0.851	57.304***	0.16
			(0.081)			(0.020)			5.51

Binary categories: conspicuousness (1 = brightly, or 0 = cryptically colored), lipophilic alkaloid (1 = able, or 0 = unable to sequester), diet specialist (1 = ants & mites, or 0 = generalist diet). Numbers in parenthesis are ± 1 SE. Common slope was not rejected for models ($P > 0.05$) with the exception diet CLSR analyses (^{a}) . Significance is given by *, $P < 0.05$; **, $P < 0.01$; ***, $P < 0.001$.

Table 3.8: Coefficients from general linear model analyses of the metabolic variables and associated traits of poison frogs. Metabolic parameters estimates for the log-log scaling relationships of resting metabolic rate (RMR, mL O2/hour), active metabolic rate (AMR, mL O2/hour), aerobic scope (Scope, mL O2/hour), binary categorical variable (conspicuousness, lipophilic alkaloids, diet specialist), and body mass (Mass, g) of anurans and poison frogs. Linear allometric equations in the form log(RMR, AMR, Scope) = log a (coefficient) + [bbinary x categorical variable] + b (exponent) * log Mass. PIC denotes relationship derived from independent contrasts and n is number of species or independent contrasts.

Metabolic measurement	Group	n	Log a (constant)	Log M_b (g)	Same Slope (*P*)	r^2	F	Mass (g)
RMR	Brightly colored	28	-0.766*** (0.025)	0.737*** (0.057)	0.116	0.864	165.831***	0.16-6.01
	Cryptically colored	26	-0.767*** (0.027)	0.937*** (0.116)	0.116	0.732	65.710***	0.32 -2.30
RMR	Alkaloid sequestration	22	-0.771*** (0.031)	0.721*** (0.066)	0.114	0.856	119.068***	0.16-6.01
	Alkaloid absent	18	-0.795*** (0.035)	0.959*** (0.138)	0.114	0.751	48.156***	0.32-2.30
RMR	>70% ants & mites in diet	11	-0.786*** (0.046)	0.575*** (0.106)	0.003	0.766	29.486***	0.16-3.32
	<70% ants & mites in diet	12	-0.823*** (0.037)	1.094*** (0.116)	0.003	0.899	88.637***	0.37-5.51
AMR	Brightly colored	28	0.127*** (0.023)	0.751*** (0.054)	0.376	0.881	191.65***	0.16-6.01
	Cryptically colored	26	-0.009^{NS} (0.023)	0.796*** (0.099)	0.376	0.731	65.214***	0.32-2.30
AMR	Alkaloid sequestration	22	0.134*** (0.026)	0.748*** (0.057)	0.135	0.896	171.917***	0.16-6.01
	Alkaloid absent	18	-0.004^{NS} (0.030)	0.866*** (0.121)	0.135	0.763	51.538***	0.32-2.30
AMR	>70% ants & mites in diet	11	0.088* (0.035)	0.569*** (0.081)	0.007	0.846	49.511***	0.16-3.32
	<70% ants & mites in diet	12	0.028^{NS} (0.037)	0.974*** (0.116)	0.007	0.876	70.371***	0.37-5.51
Scope	Brightly colored	28	0.063** (0.026)	0.755*** (0.060)	0.472	0.857	155.946***	0.16-6.01
	Cryptically colored	26	-0.100** (0.028)	0.780*** (0.121)	0.472	0.634	41.487***	0.32 -2.30
Scope	Alkaloid sequestration	22	0.073** (0.029)	0.753*** (0.062)	0.169	0.881	148.546***	0.16-6.01
	Alkaloid absent	18	-0.087* (0.037)	0.864*** (0.146)	0.169	0.687	35.190***	0.32-2.30
Scope	>70% ants & mites in diet	11	0.021^{NS} (0.041)	0.568*** (0.093)	0.021	0.806	37.273***	0.16-3.32
	<70% ants & mites in diet	12	-0.047^{NS} (0.046)	0.972*** (0.146)	0.021	0.816	44.363***	0.37-5.51

Numbers in parenthesis are ± 1 SE. Significance is given by *, $P < 0.05$; **, $P < 0.01$; ***, $P < 0.001$.

Table 3.9: Metabolic parameters estimates for the log-log allometric relationships of poison frogs and results for the test of equal slopes. Regressions are grouped by the binary categories of conspicuousness, alkaloid sequestration, and diet specialization. The metabolic parameters included resting metabolic rate (RMR, mL O2/hour), active metabolic rate (AMR, mL O2/hour), aerobic scope (Scope, mL O2/hour) and body mass (Mass, g) of anurans and poison frogs. Linear allometric equations in the form log(RMR, AMR, Scope) = log a (coefficient) + b (exponent) * log Mass. PIC denotes relationship derived from independent contrasts and n is number of species or independent contrasts.

Traits	Conspicuous		Lipophilic Alkaloids		Ant & Mite Specialists		AMR		Scope	
	LTR	*P*	LTR	*P*	LTR	*P*	LTR	*P*	LTR	*P*
Lipophilic alkaloids	27.538	<0.001	--	--	--	--	--	--	--	--
Ant & mite specialists	19.434	0.001	20.048	<0.001	--	--	--	--	--	--
AMR	6.914	0.140	6.375	0.1728	4.516	0.341	--	--	--	--
Scope	27.538	<0.001	9.303	0.054	13.922	0.008	37.417	<0.001	--	--
RMR	3.641	0.457	3.554	0.470	1.166	0.884	1.275	0.866	5.736	0.220

Table 3.10: Phylogenetic correlations based on the binary scoring of the ecological variables from metabolism (AMR, Metabolic Scope, and RMR-mass residuals), diet, conspicuousness, and skin alkaloids.

Traits		Conspicuous	Alkaloids Amount	Alkaloid Diversity	Ant & Mites % in Diet	Log-Prey	Log-Weight	Log-RMR	Log-AMR
	λ	*r*	*r*	*r*	*r*	*r*	*r*	*r*	*r*
Conspicuous	0.769***	--	--	--	--	--	--	--	--
n = 54	IC:	--	--	--	--	--	--	--	--
Alkaloids Amount	0.640***	0.623***	--	--	--	--	--	--	--
n = 40	IC:	0.607***	--	--	--	--	--	--	--
Alkaloid Diversity	0.595***	0.500***	0.753***	--	--	--	--	--	--
n = 39	IC:	0.391**	0.645***	--	--	--	--	--	--
Ant & Mites % in Diet	0.605**	0.492**	0.718***	0.660**	--	--	--	--	--
n = 22	IC:	0.211^{NS}	0.530***	0.466**	--	--	--	--	--
Log-Prey	1.000***	0.630**	0.822***	0.656**	0.489*	--	--	--	--
n = 22	IC:	0.621**	0.564**	0.423^{NS}	0.277^{NS}	--	--	--	--
Log-Weight	0.619***	0.320**	0.433**	0.177^{NS}	-0.044^{NS}	0.372^{NS}	--	--	--
n = 54	IC:	0.355**	0.457***	0.184^{NS}	0.028^{NS}	0.455**	--	--	--
Log-RMR	0.527**	0.262^{NS}	0.421**	0.123^{NS}	0.001^{NS}	0.426*	0.886***	--	--
n = 54	IC:	0.251^{NS}	0.424***	0.087^{NS}	0.018^{NS}	0.470*	0.876***	--	--
Log-AMR	0.508**	0.386**	0.475**	0.251^{NS}	0.071^{NS}	0.284^{NS}	0.906***	0.853***	--
n = 54	IC:	0.416***	0.505***	0.244^{NS}	0.119^{NS}	0.405^{NS}	0.911***	0.849***	--
Log-Scope	0.504**	0.398**	0.479**	0.271^{NS}	0.093^{NS}	0.259^{NS}	0.881***	0.799***	0.995***
n = 54	IC:	0.435***	0.515***	0.271^{NS}	0.142^{NS}	0.386^{NS}	0.888***	0.794***	0.995***

First row in the correlations is the GLS estimate and the second the independent contrasts (IC) estimate.
Significance is given by *, $P < 0.05$; **, $P < 0.01$; ***, $P < 0.001$.

Table 3.11: Evolutionary regression coefficient (λ) and phylogenetic correlations (*r*) based on the continuous measurements of the ecological variables from metabolism, diet, conspicuousness, and skin alkaloids.

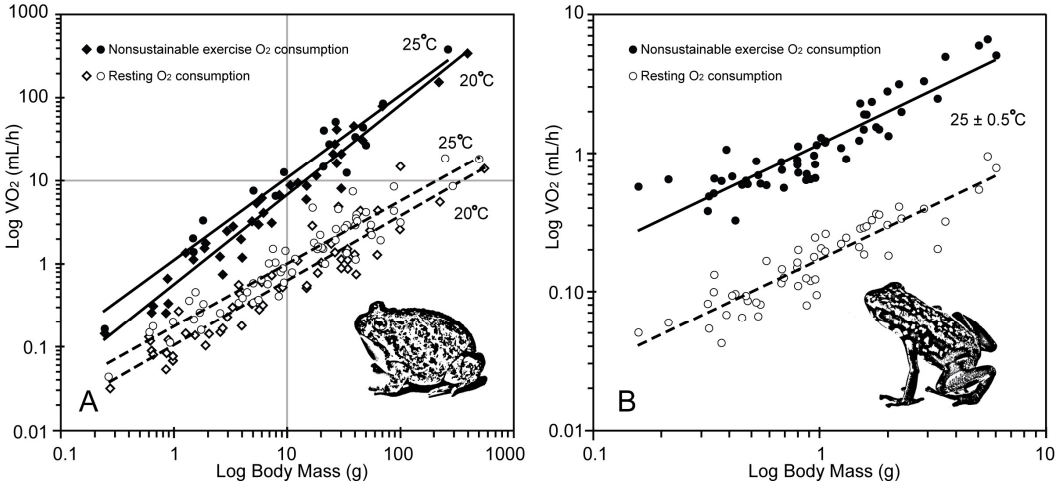

Figure 3.1: Active metabolic rate (AMR) and resting metabolic rate (RMR) as a function of body mass (g) in anurans and poison frogs. In Anurans (A), measurements correspond to 20°C (diamonds) and 25°C (circles). In poison frogs (B), only measurements at 25±0.5°C were obtained. Open diamonds or circles correspond to RMR and closed symbols correspond to AMR. The solid and dashed line is the result of the general linear model for AMR and RMR, respectively.

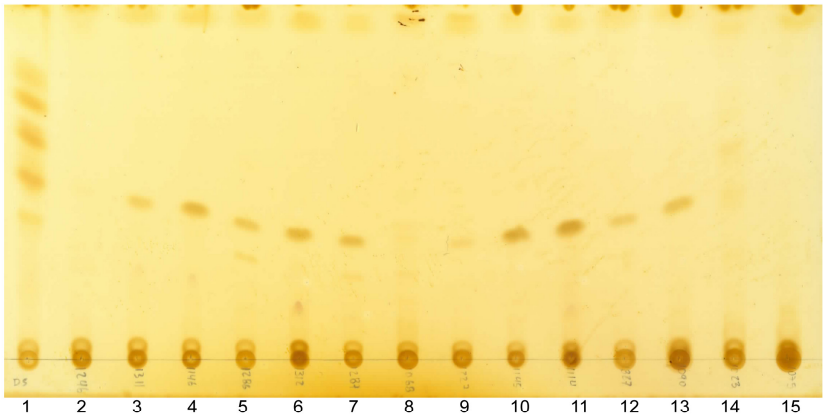

1 2 3 4 5 6 7 8 9 10 11 12 13 14 15

1 *Dendrobates sylvaticus* (+ control)
2 *Hyloxalus nexipus* (skin 1)
3 *Hyloxalus nexipus* (skin 2)
4 *Allobates kingsburyi* (skin 1)
5 *Colostethus fugax* (skin 1)
6 *Hyloxalus maculosus* (- control)
7 *Colostethus fugax* (skin 2)
8 *Epipedobates machalilla* (skin 1)
9 *Epipedobates machalilla* (skin 2)
10 *Allobates kingsburyi* (skin 2)
11 *Allobates kingsburyi* (skin 3)
12 *Colostethus fugax* (skin 3)
13 *Hyloxalus vertebralis* (skin 1)
14 Methanolic solvent (- control)
15 *Hyloxalus vertebralis* (skin 2)

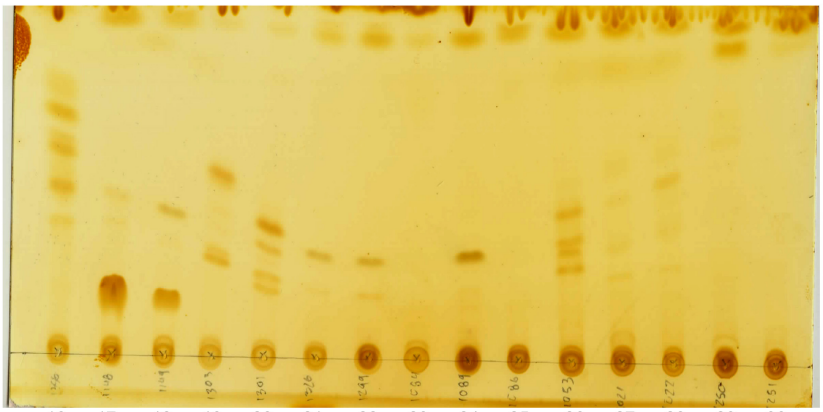

16 17 18 19 20 21 22 23 24 25 26 27 28 29 30

16 *Dendrobates sylvaticus* (+ control)
17 *Dendrobates captivus* (skin 1)
18 *Dendrobates captivus* (skin 2)
19 *Ameerega parvula* (+ control)
20 *Ameerega parvula* (+ control)
21 *Colostethus fugax* (skin 4)
22 *Colostethus fugax* (skin 5)
23 *Hyloxalus vertebralis* (skin 3)
24 *Hyloxalus vertebralis* (skin 4)
25 *Hyloxalus vertebralis* (skin 5)
26 *Ameerega bilinguis* (+ control)
27 *Epipedobates boulengeri* (- control)
28 *Hyloxalus maculosus* (- control)
29 Methanolic solvent (- control)
30 *Hyloxalus nexipus* (skin 3)

Figure 3.2: Thin layer chromatography (TLC) results of skin methanolic extracts of sampled poison frogs. We found alkaloids in skins of *Dendrobates captivus*. We fail to find skin alkaloids in *Allobates kingsburyi*, *Colostethus fugax*, *Epipedobates machalilla*, *Hyloxalus nexipus*, and *H. vertebralis*.

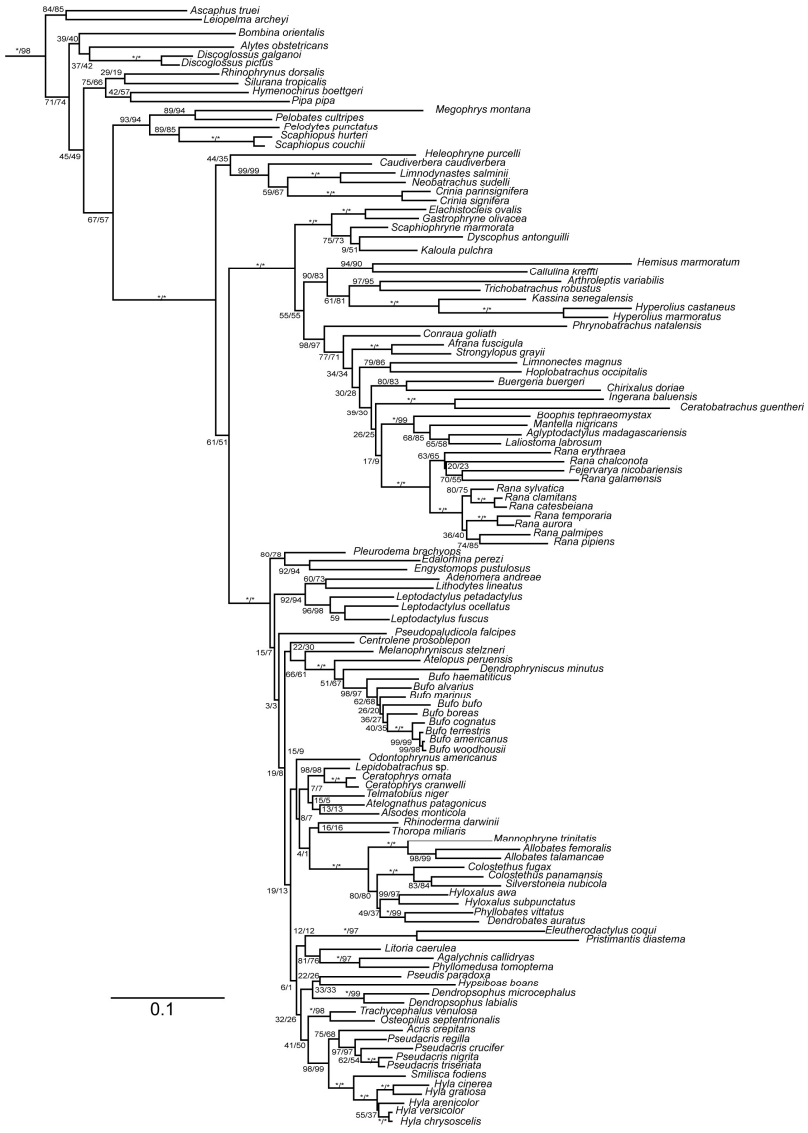

Figure 3.3: Maximum likelihood phylogeny of amphibians from 121 species of frogs (33 families). Support values in the phylogeny correspond to the summary of 500 ML non-parametric bootstraps estimated with GARLI (left) and RAxML (right). An asterisk indicates a support value of 100.

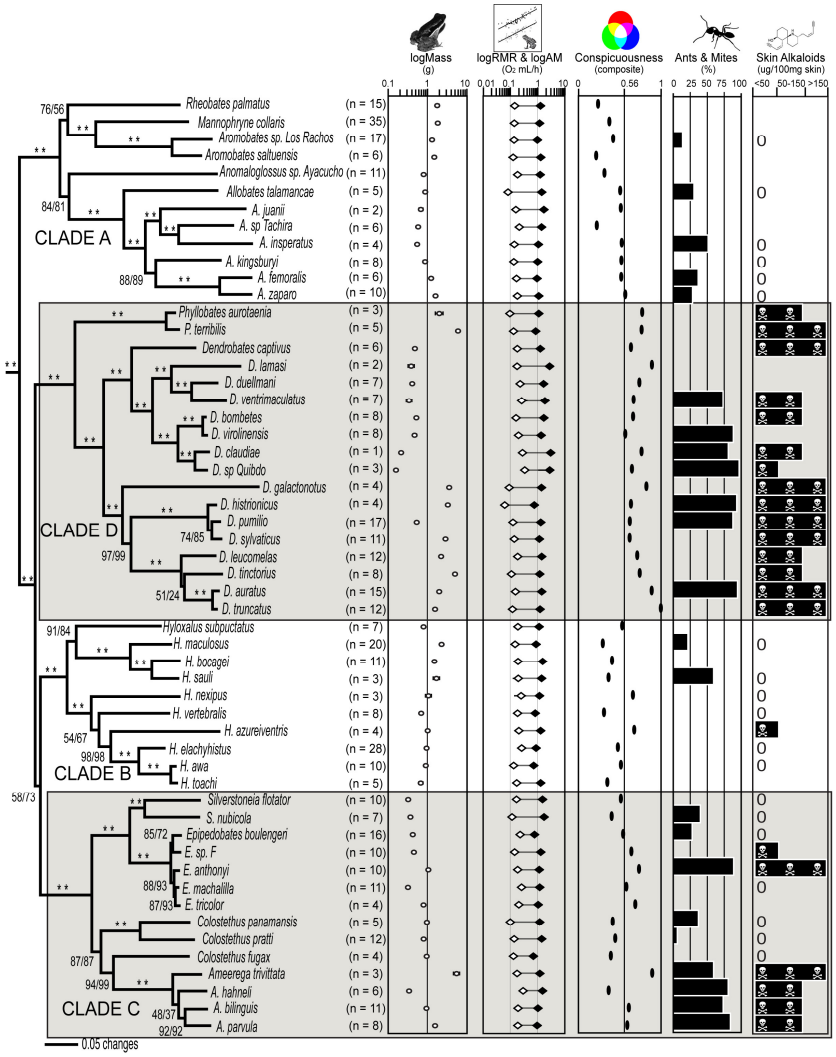

Figure 3.4: Phylogeny, number of individuals measured for metabolic parameters, body mass, RMR, AMR, Scope, conspicuousness, percentage of ants and mites in diet, and skin alkaloid concentrations used in the comparative analysis. Support values in the phylogeny correspond to the summary of 500 ML non-parametric bootstraps estimated with GARLI (left) and RAxML (right), * represents 100 support. Values 0 in the skin alkaloid column represent no alkaloids detected.

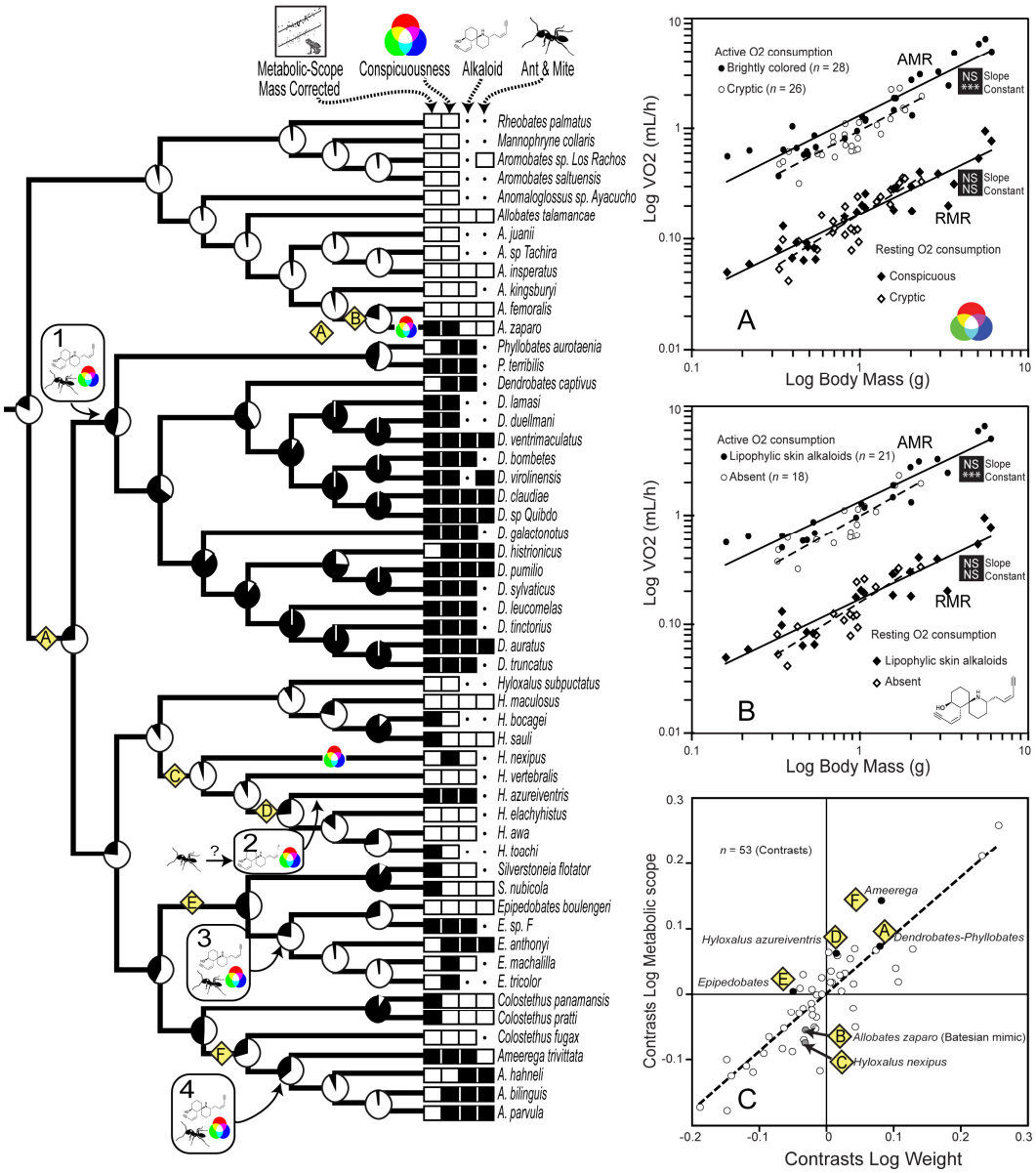
Metabolic-Scope Mass Corrected
Conspicuousness
Alkaloid
Ant & Mite
Rheobates palmatus
Mannophryne collaris
Aromobates sp. Los Rachos
Aromobates saltuensis
Anomaloglossus sp. Ayacucho
Allobates talamancae
A. juanii
A. sp Tachira
A. insperatus
A. kingsburyi
A. femoralis
A. zaparo
Phyllobates aurotaenia
P. terribilis
Dendrobates captivus
D. lamasi
D. duellmani
D. ventrimaculatus
D. bombetes
D. virolinensis
D. claudiae
D. sp Quibdo
D. galactonotus
D. histrionicus
D. pumilio
D. sylvaticus
D. leucomelas
D. tinctorius
D. auratus
D. truncatus
Hyloxalus subpuctatus
H. maculosus
H. bocagei
H. sauli
H. nexipus
H. vertebralis
H. azureiventris
H. elachyhistus
H. awa
H. toachi
Silverstoneia flotator
S. nubicola
Epipedobates boulengeri
E. sp. F
E. anthonyi
E. machalilla
E. tricolor
Colostethus panamansis
Colostethus pratti
Colostethus fugax
Ameerega trivittata
A. hahneli
A. bilinguis
A. parvula
Active O2 consumption
Brightly colored (n = 28)
Cryptic (n = 26)
AMR
NS Slope
*** Constant
NS Slope
NS Constant
RMR
Resting O2 consumption
Conspicuous
Cryptic
A
Log VO2 (mL/h)
Log Body Mass (g)
Active O2 consumption
Lipophylic skin alkaloids (n = 21)
Absent (n = 18)
AMR
NS Slope
*** Constant
NS Slope
NS Constant
RMR
Resting O2 consumption
Lipophylic skin alkaloids
Absent
B
Log VO2 (mL/h)
Log Body Mass (g)
n = 53 (Contrasts)
Ameerega
Hyloxalus azureiventris
Dendrobates-Phyllobates
Epipedobates
Allobates zaparo (Batesian mimic)
Hyloxalus nexipus
C
Contrasts Log Metabolic scope
Contrasts Log Weight

Figure 3.5: Maximum likelihood reconstructions and CLSR regression analyses of high aerobic scope, conspicuousness, and alkaloid sequestration in poison frogs. Positive character states are indicated by black boxes at the tips of the phylogeny: metabolic scope (positive residual after mass correction), conspicuousness (bright coloration), alkaloid sequestration (able to sequester), and diet specialization (ant and mite specialist). Unknown states are indicated by dots. The traced reconstructions over the phylogeny correspond to the aerobic scope after mass correction and the fraction of relative likelihood probability of high aerobic capacity (black) or low aerobic capacity (white). Rounded boxes indicate four origins of tandem evolution of bright coloration, alkaloid sequestration, and diet specialization. Two origins of bright coloration were not associated alkaloid sequestration and diet specialization and the conspicuousness icon indicates them. Plots of the CLSR regression including the categorical variables of (A) conspicuousness, and (B) alkaloid sequestration for AMR (circles) and RMR (diamonds) and body mass. Results from the homogeneity of slopes and similar intercept (constant) are indicated in the black box (***, $P < 0.001$; NS, $P > 0.05$). Plot of the PIC regression analysis (C) of the metabolic scope and body mass independent contrasts. Lettered diamond boxes correspond to node contrasts before the origin of bright coloration, alkaloid sequestration, and diet specialization.

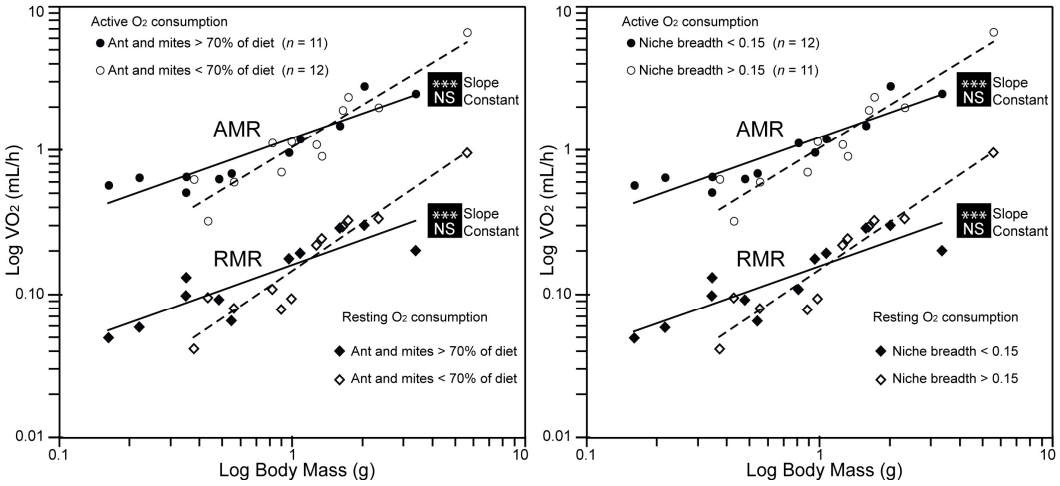

Figure 3.6: Plots of the CLSR regression including the categorical variables of diet specialization and niche breadth for AMR (circles) and RMR (diamonds) and body mass. Results from the homogeneity of slopes and similar intercept (constant) are indicated in the black box (***, $P < 0.001$; NS, $P > 0.05$).

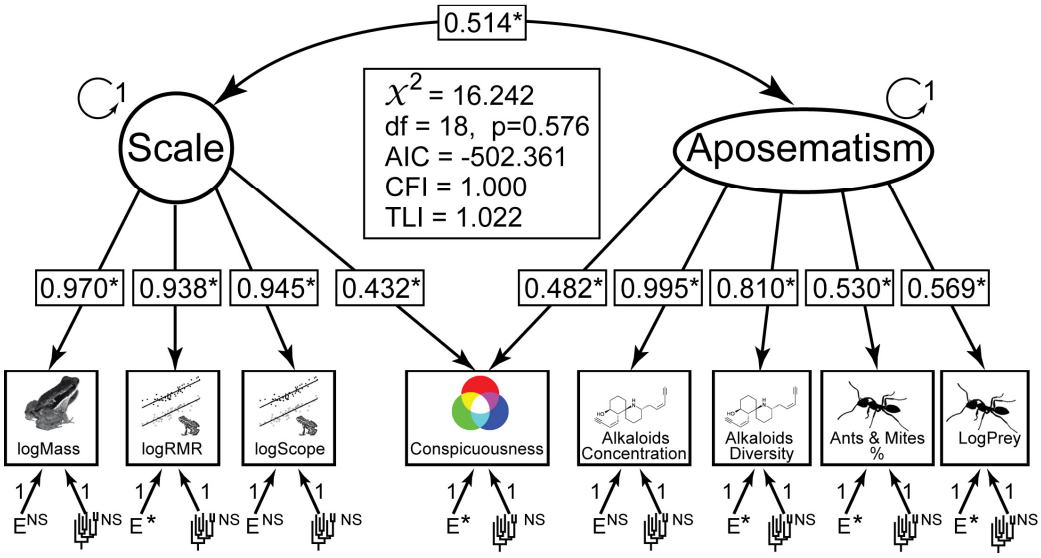

Figure 3.7: Multivariate model of relationships of scale and aposematism continuous traits in poison frogs using variance-covariance matrix derived from independent contrasts. Ellipses represent emergent (latent) variables measured by the observed (indicator) variables in squares. Lines connecting variables represent significant ($p < 0.05$) regression coefficients (single-headed arrows) and correlation (double-headed arrows). Scale (emergent variable) was predicted by four indicator variables: body mass (logMass), resting metabolic rate (logRMR), aerobic scope (logScope), and conspicuousness. Aposematism (emergent variable) was predicted by five indicator variables: conspicuousness, alkaloid amount, alkaloid diversity, ant and mites percentage in diet, and mean number of prey items per individual (logPrey). Variance of the emergent variables (circle) and the regression coefficients of the measurement error (E) and phylogenetic correction (tree) were set to 1, which allow the model to be estimable (overidentified).

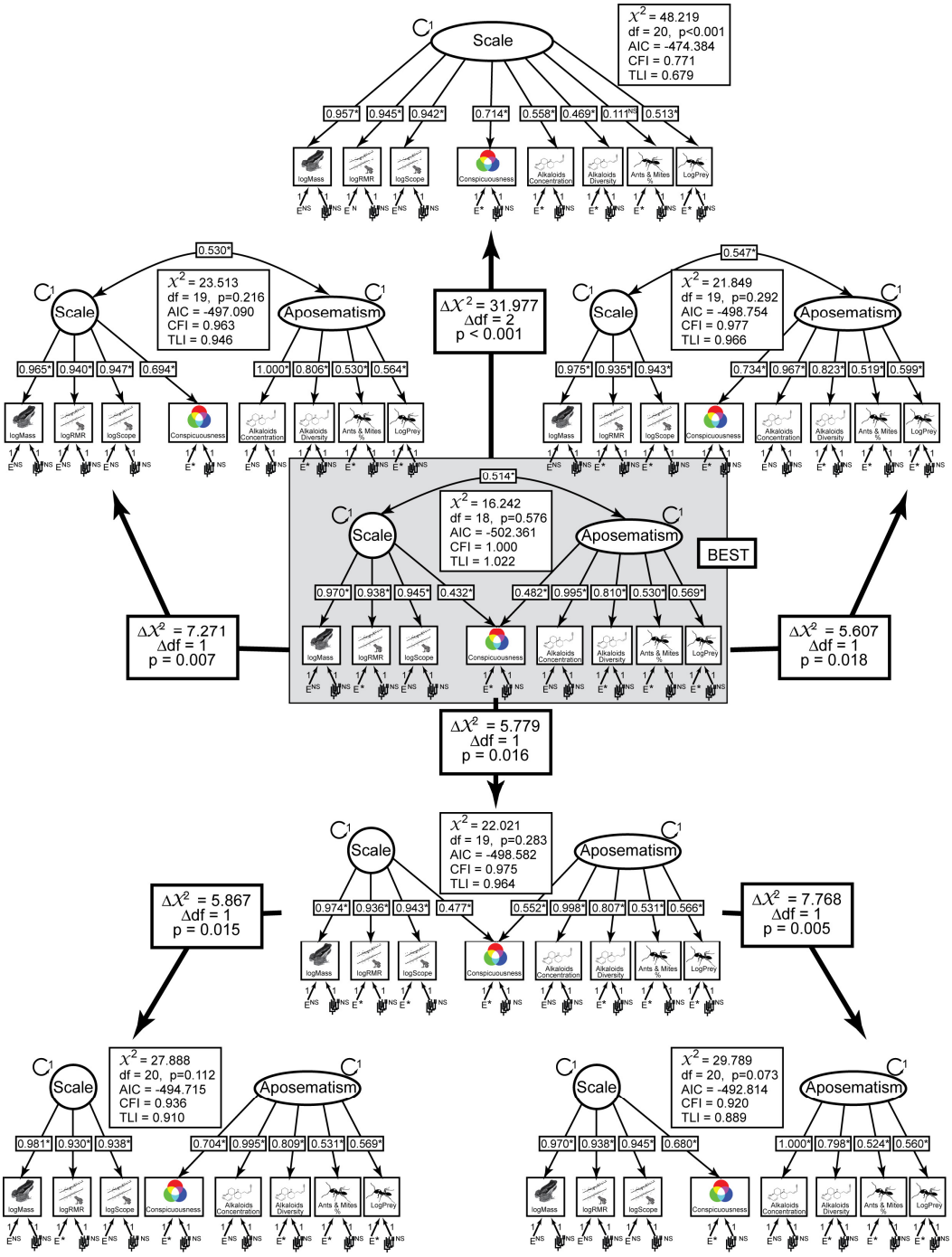
Scale
χ² = 48.219
df = 20, p<0.001
AIC = -474.384
CFI = 0.771
TLI = 0.679
0.957* 0.945* 0.942* 0.714* 0.558* 0.469* 0.111NS 0.513*
logMass logRMR logScope Conspicuousness Alkaloids Concentration Alkaloids Diversity Ants & Mites % LogPrey
ΔX² = 31.977
Δdf = 2
p < 0.001
0.530*
Scale
Aposematism
χ² = 23.513
df = 19, p=0.216
AIC = -497.090
CFI = 0.963
TLI = 0.946
0.965* 0.940* 0.947* 0.694*
1.000* 0.806* 0.530* 0.564*
0.547*
χ² = 21.849
df = 19, p=0.292
AIC = -498.754
CFI = 0.977
TLI = 0.966
0.975* 0.935* 0.943*
0.734* 0.967* 0.823* 0.519* 0.599*
0.514*
χ² = 16.242
df = 18, p=0.576
AIC = -502.361
CFI = 1.000
TLI = 1.022
BEST
0.970* 0.938* 0.945* 0.432*
0.482* 0.995* 0.810* 0.530* 0.569*
ΔX² = 7.271
Δdf = 1
p = 0.007
ΔX² = 5.607
Δdf = 1
p = 0.018
ΔX² = 5.779
Δdf = 1
p = 0.016
χ² = 22.021
df = 19, p=0.283
AIC = -498.582
CFI = 0.975
TLI = 0.964
0.974* 0.936* 0.943* 0.477*
0.552* 0.998* 0.807* 0.531* 0.566*
ΔX² = 5.867
Δdf = 1
p = 0.015
ΔX² = 7.768
Δdf = 1
p = 0.005
χ² = 27.888
df = 20, p=0.112
AIC = -494.715
CFI = 0.936
TLI = 0.910
0.981* 0.930* 0.938*
0.704* 0.995* 0.809* 0.531* 0.569*
χ² = 29.789
df = 20, p=0.073
AIC = -492.814
CFI = 0.920
TLI = 0.889
0.970* 0.938* 0.945* 0.680*
1.000* 0.798* 0.524* 0.560*

Figure 3.8: Results of the tests of multivariate model of relationships of scale and aposematism continuous traits in poison frogs using variance-covariance matrix derived from independent contrasts. Ellipses represent emergent (latent) variables measured by the observed (indicator) variables in squares. Lines connecting variables represent significant ($p < 0.05$) regression coefficients (single-headed arrows) and correlation (double-headed arrows). Diagrams include emergent variables: scale or aposematism. Indicator variables include: body mass (logMass), resting metabolic rate (logRMR), aerobic scope (logScope), and conspicuousness, alkaloid amount, alkaloid diversity, ant and mites percentage in diet, and mean number of prey items per individual (logPrey). Variance of the emergent variables (circle) and the regression coefficients of the measurement error (E) and phylogenetic correction (tree) were set to 1, which allow the model to be estimable (overidentified). Individual model fit indices and comparisons among models include X^2 score, AIC (Akaike's information criterion), CFI (Comparative Fit Index), and TLI (Rucker-Lewis Index). Comparisons between nested models uses a LTR approach p-value approximation from the difference of X^2 score and degrees of freedom (df).

Chapter 4: Higher active metabolic rates and faster molecular evolution in poison frogs

INTRODUCTION

Molecular evolution is the result of the combined effect of mutation rate, genetic drift, and natural selection (Graur and Li 2000). Rates of substitution are variable across lineages and genomes (e.g., nuclear, mitochondrial, or chloroplast) (Bromham 2009; Nabholz et al. 2009). Rapid accumulation of nucleotide changes has been associated to life history, biochemical, and physiological attributes at both organismal and cellular levels (Bromham and Penny 2003; Gillooly et al. 2005; Martin and Palumbi 1993). For example, small body size, rapid generation time, high basal or resting metabolic rate (BMR or RMR), and short lifespan have been associated with faster rates of molecular evolution (Welch et al. 2008). At the cellular level, proximity to the oxidative centers within the cell (e.g., inside mitochondria), error-prone mutation repair, or high DNA synthesis has also been associated with increased rate of nucleotide substitution (Galtier et al. 2009). Therefore, the variation on the molecular evolution might be multifactorial with variable contributions from life history, shared ancestry, and genomic properties of an organism.

At least three main hypotheses have been proposed to explain the variability in rates of molecular evolution among lineages and genomes. The generation time hypothesis proposes that the rate of molecular substitution is associated with the process of DNA synthesis per unit time (Ohta 1993; Smith

and Donoghue 2008). This model implies that higher molecular rates are associated with shorter generation times, faster accumulation of replication errors, and they are affecting both nuclear and organelle genomes (Bromham et al. 1996). Some complications of this model include: (1) variability in the number of germline DNA replications per lineage; (2) the mitochondrial genome appears to evolve 2-3 orders magnitude faster than the nuclear; (3) different synonymous/nonsynonymous substitutions among loci and genomes; and (4) lineages with similar generation times have dissimilar substitution rates (Bromham 2002; Martin 1999).

The longevity hypothesis implies a negative correlation between mutation rate and life span derived from higher resistance to oxidative damages (Nabholz et al. 2008). The predictions of this model include a higher substitution rate in the mitochondrial versus nuclear genome, variability in the mutation rate between functional domains of mitochondrial genes, and lower substitution rate in long-lived lineages (Galtier et al. 2009). However, the longevity model has some limitations including: (1) it applies mostly to the mitochondrial genome, but substitution rate variability of the nuclear loci is not explained; (2) the model has been applied only to endotherms; and (3) it assumes that selection for mechanisms to reduce oxidative damage is higher only in long-lived species.

The metabolic rate hypothesis correlates the mutation rate with the cellular aerobic respiration byproducts, the reactive oxidative radicals (ROS) (Martin and Palumbi 1993). However, this hypothesis implies that higher basal metabolic rates are associated with increases in the rate of molecular substitutions (Gillooly et al.

2005; Martin et al. 1992). This model has been criticized for the following reasons: (1) the basal or resting metabolic rates (BMR or RMR) are inaccurate measurements of the energy generation by organisms; (2) the oxygen intake might not directly associated with the production oxidative radicals; (3) DNA damage at the cellular level might be caused by other factors such as replication errors; (4) DNA repair efficiency is assumed to be similar across the Tree of Life; and (5) phylogenetic comparative analyses have rejected the association of BMR with the rates of molecular evolution (Bromham 2009; Lanfear et al. 2007; Seddon et al. 1998). Besides the shortcomings of all three hypotheses, the current view is that the variability of the substitution rate has multifactor causes that include oxidative damage from free radicals, inefficiency of DNA repair and replication, and the genome properties (e.g., organellar or nuclear).

At the organismal level, the substitution rate is associated at different degrees with scaling variables (metabolic rates, lifespan, generation, and body mass) (Bromham 2009). Metabolism is the energetic flux within an organism and based on the allocation of nutrients into growth, reproduction, and self-maintenance (Karasov and Martinez del Rio 2007). Metabolic rates have been found to correlate with body size, temperature, and most life history traits (e.g., generation time and reproduction rate) (Brown et al. 2004; Brown et al. 2000). Respirometry is usually the methodology to estimate the metabolic rates by calculating the heat production accounted by oxygen uptake at different activity levels (Schmidt-Nielsen 1984). Oxygen free radicals are common byproducts of energy production by aerobic respiration (Williams 1996). These free radicals

have been associated with cellular damage; increase the number of nucleotide substitutions; and higher rate genomic repair (Cortopassi and Wang 1996; Perez-Campo et al. 1998). Therefore, the association between metabolism and aerobic respiration allow to hypothesize that higher metabolic rates might be directly associated with increases the molecular substitution (Martin and Palumbi 1993).

Most analyses of the metabolic rate hypothesis are based on endotherms (Bromham 2009; Nabholz et al. 2008), but its predictions have been extended to ectotherms (Bromham 2002; Martin 1999). Specifically, ectotherm organisms might have lower molecular substitution rates if their BMR is low and have larger body size (Glazier 2005). However, few comparative analyses have rejected the association between BMR and substitution rates in some groups (e.g., Chelonia, Arthropoda and Mollusca) (Lanfear et al. 2007). Here, we analyzed these relationships using a well-known ectotherm clade, the poison frogs (Dendrobatidae). Dendrobatids are widespread Neotropical amphibians (~270 species) with diverse life history traits including parental care, aposematism, and diet specialization (Santos et al. 2003; Santos et al. 2009; Summers 2000). We compiled information about active and resting aerobic metabolism, body mass, and rates of molecular evolution of 8 mitochondrial and 7 nuclear loci. We used phylogenetic comparative analyzes based on phylogenetic independent contrasts (Felsenstein 1985) and generalized least squares (GLS) (Martins and Hansen 1997; Pagel 1997). These methods were used to estimate pairwise correlations between body mass and metabolic variables, with rates of molecular evolution. Additionally, we explored the relationship between nonsynonymous/synonymous

rates of the sampled loci and tested for the difference in metabolic parameters in poison frogs. Our results support the positive correlation of higher active metabolic parameters and faster rates of molecular evolution. We found no evidence of association with resting metabolic rate or body mass. Furthermore, we propose a modified metabolic hypothesis of molecular evolution for ectotherms based on active metabolic parameters.

MATERIALS AND METHODS

Metabolic Rates Data

Physiological parameters and body mass of 474 individuals from 55 species of poison frogs were compiled and results presented (Figure 4.1 and Table 4.1–4.4). Capture, handling, and experimental procedures are explained in detail in Santos et al. (in prep.) and follow the guidelines of the animal care permit (IACUC 05111001). Body mass were weighted before and after the physiological measurements to the near 0.01 g. Physiological measurements included four variables: (1) resting metabolic rate (RMR, oxygen consumption while resting or VO2rest consumed/hour), (2) active metabolic rate after non-sustainable exercise (AMR, oxygen consumption after forced activity or VO2active consumed/hour), (3) Aerobic metabolic scope (Scope) calculated by the difference between AMR and RMR (Gatten et al. 1992), and (4) factorial aerobic scope (AMR/RMR) as an estimate of the factor by which oxygen consumption increases with forced physical activity (Gatten et al. 1992). All measurements included were taken from animals fasting, at 24.5-25.5 °C of temperature, during the day from 10h00-

18h00, and measured between 1-3 times to get an estimate of individual variability.

Molecular Data

The molecular data included both mitochondrial and nuclear loci. Our mitochondrial data include six mitochondrial segments (total ~5.5 kb): 12S and 16S rDNA genes; Valine, Leucine, and Methionine tRNA genes (tRNAs V-L-M); NADH subunit 1 (ND1); NADH subunit 2 (ND2); and Cytochrome b (CYTB). The nuclear data include seven protein-coding segments (total ~5.0 kb): brain-derived neurotrophic factor (BDNF); bone morphogenetic protein 2 (BMP2); NCX1 sodium-calcium exchanger 1 (NACA); 3'-nucleotidase (NT3); proopiomelanocortin A (POMC); tyrosinase precursor (TYR); and zinc finger E-box binding homeobox 2 (ZFX). All segments were amplified from total genomic DNA using a list of primers and conditions provided in Table 4.5. Protocols of DNA extraction, PCR purification, and sequencing are provided in previous studies (Bossuyt et al. 2006; Darst and Cannatella 2004; Santos et al. 2003). Each individual segment was assembled using Sequencher 4.7 (GeneCodes 2006), automatically aligned using ClustalX 1.81 (Thompson et al. 1997) and adjusted manually to minimize informative sites using MacClade 4.08 (Maddison and Maddison 2001). GenBank accession numbers and specimen information are given in Santos et al. (unpublished). All sequences amplified were validated by comparison to other anuran sequences using BLAST (http://www.ncbi.nlm.nih.gov/BLAST/).

Phylogenetic analyses

We performed three sets of phylogenetic analysis: (1) a backbone phylogeny inferred from the supermatrix of all genes combined with the exception of ND1 (we were unable to sequence Allobates juanii segment due to a translocation), (2) a set of individual phylogenies inferred from each gene and the combined tRNAs; and (3) a codon position phylogenies inferred from matrices with 1st, 2nd, or 3rd nucleotide positions from the nuclear and mitochondrial protein coding genes. The supermatrix phylogeny of the poison frogs (SPPF) was inferred from the supermatrix that included 8517 unambiguously aligned characters and partitioned by gene. We used a GTR+Γ+I model of nucleotide substitution model for SPPF estimation as suggested by ModelTest 3.7 (Posada and Buckley 2004; Posada and Crandall 1998). Phylogeny estimation was performed using a maximum likelihood (ML) approach under a genetic algorithm in GARLI 0.960 (Zwickl 2006) and under a sequential and parallel ML based inference in RAxML 7.0.4 (Stamatakis 2006). For the SPPF, a total of 50 independent runs were used to infer the best tree and 500 nonparametric bootstrap searches were used to estimate support for the nodes. Both programs gave similar topologies and we considered the highest ML RAxML SPPF tree as our best estimate of the true phylogeny of the poison frogs. For the individual gene poison frog phylogenies (IGPFs) and codon position poison frog phylogenies (CPPFs), we used the more comprehensive GTR+Γ+I model of molecular evolution. We chose the GTR+Γ+I model to obtain a comparable substitution and rate matrix parameters for all IGPFs and CPPFs (Table 4.6). From each gene or codon

position, we obtained the parameter estimates from the best score tree of the 50 independent runs using a maximum likelihood (ML) approach in GARLI 0.960 (Zwickl 2006). We estimated the branch lengths of each IGPFs and CPPFs using the SPPF topology and the specific segment substitution parameters as constraints in PAUP 4.0 (Swofford 2000). We also estimated a nonsynonymous (dN) and synonymous (dS) distances constrained over the SPPF phylogeny for the combined CYTB+ND2 (mitochondrial distances) and all nuclear genes (nuclear distances) using CODEML module of PAML 4.2b (Yang 2007). The branch length from the tips (individual species) to the root were determined using TreeStat 1.2 (Rambaut and Drummond 2008) and used as measured of sequence divergence from the extant species to the last common ancestor of all poison frogs (Tables 4.7 and 4.8).

Comparative Analyses

Associations and covariances of pairwise comparisons among physiological measurements, body mass, and sequence divergence (tip-to-root distances) were evaluated using phylogenetic independent contrasts (PIC) (Felsenstein 1985) and generalized least squares (GLS) approach (Pagel 1997). First, we explored the life history data distributions and only body mass need to be log-transformed to meet with the statistical assumptions (Felsenstein 1985; Garland 1992). For the PIC and GLS analyses, we used the supermatrix phylogeny of poison frogs (SPPF) and we log-transform its branch lengths to standardize the contrasts (Garland Jr. et al. 1993; Garland et al. 1992). The PICs

were calculated in Mesquite 2.9 (Maddison and Maddison 2009) using PDAP:PTREE module (Midford et al. 2005). The regression analyses based on PIC were fit through the origin and the significance the regression coefficients was determined accordingly (Garland et al. 1992). No outliers were evidenced in the plots of the independent contrasts, which might have inflated the phylogenetic correlation coefficient (Harvey and Pagel 1991). For the GLS analyses, we estimated the pairwise trait covariation using BayesContinuous module of BayesTraits 1.0 (Pagel and Meade 2006; Pagel and Meade 2007; Pagel et al. 2004). We also included the evolutionary regression coefficient "λ" (Pagel 1993), which provides a measure of phylogenetic covariance. Each trait λ value is continuous measure of covariation from 0 (i.e., independent) to 1 (i.e., dependent) with the phylogeny. We tested the estimated λ from the null hypothesis of phylogenetic independence (i.e., $\lambda = 0$) using a likelihood ration test (LTR). We calculate the phylogenetic correlation coefficient between sequenced (genes, codon positions, dN, and dS distances), body mass, and physiological traits by simultaneously estimating at the λ parameter (i.e., accounting for the phylogenetic inertia). Finally, we determined the significance of the phylogenetic correlation coefficient by testing against the null hypothesis of independence (i.e., $r = 0$) using a likelihood ration test (LTR).

We estimates of the binary ancestral states for Scope at nodes were derived using the likelihood reconstruction module in Mesquite 2.9 (Maddison and Maddison 2009) and the ML approach in BayesMultistate module of BayesTraits 1.0 (Pagel and Meade 2006; Pagel and Meade 2007; Pagel et al.

2004). First, we log-transformed Scope and body mass to linearize their relationship. Second, we estimated a linear regression and saved the standardized residuals using SPSS 16.0 (SPSS 2008). Third, we assigned a binary category to all species based on high Scope (positive residuals) and low Scope (negative residuals). Fourth, the reconstruction was done using the "mk1 model" (Lewis 2001) in Mesquite and the likelihoods of alternative states were reported as raw likelihoods. For the BayesMultistate, we calculated the proportion of likelihood of both alternative character states at each node with 5,000 samples under default parameters (Pagel and Meade 2006). Similar results were found in both analyses and only the Mesquite results are reported.

Test of Variable Nonsynonymous/Synonymous Rate Ratio

We tested if nonsynonymous/synonymous rate ratio (ω = dN/dS) varied among branches of the poison frog phylogeny. We performed two test based on the Scope classification of the poison frogs. First, we used the binary classification based on standardized residuals (i.e., high or low Scope) of the ancestral states reconstruction. Second, we identified Dendrobates+Phyllobates (Clade D) as the lineage that have >50% of all high aerobic scope species and likely undergoing adaptive radiation under high active metabolic rates. We performed a one and two ω ratio models to each of the protein coding segments using the branch models option in the CODEML module of PAML 4.2b (Yang 2007). We tested two sets of comparisons: (1) one ω ratio for all poison frogs versus two ω ratios for high Scope (positive residuals) and low Scope species

(negative residuals); and (2) one ω ratio for all poison frogs versus two ω ratios for Clade D and the rest of the family (Clades A+B+C). We run both tests using codon data without assuming molecular clock (clock: 0), with codon frequencies estimated from the average nucleotide frequencies at the three codon positions (CodonFreq: 2), and including all sites (cleandata: 0). For each of the branch models, we used the following parameters: (1) one ω ratio model for all branches (model: 0, NSsites: 0, and fix_omega: 0), and (2) two ω ratios model for foreground (i.e., high Scope species or Clade D) and background (i.e., low Scope species or Clades A+B+C) branches (model: 2, NSsites: 0, and fix_omega: 0). We determined the best fitting model by comparing twice the difference in log-likelihood between models (LRT) approximation to $\chi 2$ distribution with 1 degree of freedom. Each model was run three times with starting ω = 0.4, 1.0, and 2.4 to avoid problems resulting from local optima.

RESULTS

Phylogeny, Body Mass, Metabolic Parameters, and Sequence Divergence

The supermatrix phylogeny (SPPF), Scope residuals (mass-corrected), body mass, AMR (mass-specific), RMR (mass-specific), and factorial scope of 54 species of poison frogs is presented (Figure 4.1). The SPPF phylogeny is not different from larger phylogenies of the poison frog family (Grant et al. 2006; Santos et al. 2009). In general, our phylogeny includes the four well-supported clades: A (Allobates, Anomaloglossus, Aromobates, Mannophryne, and Rheobates), B (Hyloxalus), C (Ameerega, Colostethus sensu lato, Epipedobates,

and Silverstoneia), and D (Dendrobates and Phyllobates). Body mass and physiological parameters (AMR, RMR, Scope, and factorial scope) presented a high interspecific and low intraspecific variability (Figure 4.1 and Table 4.4). Sequence divergence from the extant species to the last common ancestor of all poison frogs was estimated for each gene, codon position, nonsynonymous (dN), and synonymous (dS) substitution distances (mitochondrial, Table 4.7; nuclear, Table 4.8). Phylograms and boxplots (mean, IQRs, and range) for each gene, codon positions, and dN/dS distances were also estimated (Figure 4.2 and 4.3).

Active Metabolism and Sequence Divergence Association

We found evidence for a pairwise relationship between mass-specific active metabolic rate (AMR), Scope (Scope), factorial scope, with the substitution rate for nuclear or mitochondrial genes, codon positions, nonsynonymous (dN), and synonymous (dS) substitution distances (Table 4.1 and 4.2). The phylogenetic independent contrasts (IC) and GLS analyses showed a general agreement on the estimated correlation and their significance, but GLS was more conservative. First, both methods fail to find associations ($P > 0.05$) between body mass and resting metabolic rate (RMR) with the molecular evolution of the sampled loci, condon positions, and substitution distances. Therefore, increases in scale (body mass) or minimal energetic cost (i.e., BMR or RMR) are not associated with changes in the rate molecular substitution in both nuclear and mitochondrial loci analyzed. Second, both methods fail to find associations ($P > 0.05$) between the active metabolic parameters (AMR, Scope, and factorial scope) with the

following segments: tRNAs V-L-M combined, ND1, NACA, POMC and ZFX segments. Therefore, increases in aerobic metabolism are not associated with changes in the rate molecular substitution in some the mitochondrial and nuclear loci. Third, both methods find associations ($P < 0.05$) between some active metabolic parameters (AMR, Scope, or factorial scope) with the following segments: (1) 12S rDNA ribosomal subunit with factorial scope; (2) BMP2 with AMR and Scope; (3) NT3 with factorial scope; and (4) TYR with factorial scope. Fourth, the IC analyses were more liberal than the GLS and showed significant association ($P < 0.05$) for the following segments: (1) 12S rDNA ribosomal subunit with AMR, Scope, and factorial scope; (2) 16S rDNA ribosomal subunit with AMR, and Scope; (3) CYTB with Scope; (4) ND2 with factorial scope; (5) BMP2 with AMR and Scope; (6) NT3 with factorial scope; and (7) TYR with AMR, Scope, and factorial scope. Therefore, IC support that increases in aerobic metabolism are associated with increases in the rate molecular substitution in the ribosomal subunits, two of the proteins of the electron transport of the mitochondria, and some nuclear loci. Fifth, the GLS analysis only supported significant association ($P < 0.05$) between metabolic parameters and few segments: (1) 12S rDNA with factorial scope; (2) BDNF with AMR and Scope; (3) BMP2 with AMR and Scope; (4) NT3 with factorial scope; and (5) TYR with factorial scope. However, GLS indicated some tendency (i.e., $0.05 < P < 0.10$) for positive association for most of the significant correlations found with the IC analyses. Therefore, GLS is more conservative than IC analyses, but both support

increases in aerobic metabolism associated with faster rates of molecular substitution across mitochondrial and nuclear loci.

We found support for positive association ($P < 0.05$) of some codon positions and active metabolic parameters: (1) the IC analyses suggested that the second position of the mitochondrial protein coding genes CYTB and ND2 was associated with AMR, Scope, and factorial scope; and (2) both methods (IC and GLS) suggested that the third position of the nuclear protein coding genes was associated with AMR, Scope, and factorial scope. We found no association between the first codon positions with active metabolic parameters. Our data support the association between higher aerobic metabolic parameters and faster rates of substitution for second (mitochondrial) and third (nuclear) nucleotide position.

We found evidence of positive association ($P < 0.05$) between substitution distances and active metabolic parameters: (1) the IC analyses suggested that the nonsynonymous (dN) substitution distances of the mitochondrial protein coding genes CYTB and ND2 was associated with AMR and Scope; (2) the IC analyses suggested that the synonymous (dS) substitution distances of the mitochondrial protein coding genes was associated with factorial scope; (3) both methods (IC and GLS) suggested that nonsynonymous (dN) and synonymous (dS) substitution distances of the nuclear loci were associated with AMR, Scope, and factorial scope. Therefore, our data support the association between higher aerobic metabolic parameters and higher rates of nonsynonymous (dN) substitution distances in both nuclear and mitochondrial loci.

Variable Nonsynonymous/Synonymous Rate Ratio in Poison Frogs

We tested the variability of nonsynonymous/synonymous rate ratios (ω) in poison frogs. First, our estimates of the ω ratio of all genes analyzed (nuclear and mitochondrial) evidenced negative selection (i.e., $\omega < 1$). Second, we contrasted ω ratios of between high (positive residuals) or low (negative residuals) Scope species. Three loci (ND2, BMP2, and POMC) showed significant increase in the ω ratios of high Scope species that were 1.3-2.0 times more than low Scope counterparts (Table 4.3). Similarly, our analyses for the Dendrobates+Phyllobates (Clade D) against the remaining of the family (Clades A+B+C) supported the relationship between higher ω ratios in higher Scope species. Two main reasons support our conclusions: (1) Clade D contains > 59% (16/27 species) of all poison frogs with high aerobic metabolic scope after mass-correction; and (2) 83% (15/18 species) of the members included in Clade D have high aerobic metabolic scope compared to the other major clades of poison frogs. Our analyses suggested higher ω ratios (i.e., 1.2-2.0 times) for Clade D compared to the rest of the poison frogs (Table 4.3). Clade D has significantly higher ω ratios than the rest of poison frogs for mitochondrial genes (CYTB, ND1, and ND2) and three of the nuclear genes (BMP2, POMC, and ZFX). Four of the nuclear genes (BDNF, NACA, NT3, and TYR) did not show evidence of higher ω ratio across the poison frog family. Therefore, our results suggest a tendency to have higher ω ratio for groups or lineages (i.e., high Scope species or Clade D) to have higher active metabolic parameters. However, other selective forces might be affecting the ω ratio (e.g., functional constraints) regardless if the species analyzed have high Scope or not.

DISCUSSION

Molecular evolution is determined by the balance between mutation rate, substitution rate, and the likelihood of inheritance of molecular changes (Bromham 2009). Mutation rate is the speed at which sequence changes result from biochemical damage coupled with inefficient repair, DNA synthesis mistakes, or directed hypermutability (Bromham 2009; Graur and Li 2000; Pal et al. 2006). Thus, many factors synergistically influence the rate of molecular evolution at different levels of biological organization.

Ectotherms have been assumed to have low rates of molecular evolution, but this might be an underestimation (Seddon et al. 1998). More comparative analyses on ectotherm lineages (e.g., Chelonia, Arthropoda, and Mollusca) are showing substitution rates comparable to endotherms (Caccone et al. 2004; Lanfear et al. 2007). We also found a similar trend in poison frogs including significant variation in the rate of molecular substitutions across loci and genomes (mitochondrial versus nuclear). The mitochondrial protein coding genes have a higher transition to transversion (Ts/Tv) ratio of 3.8-4.2 compared to 1.5-3.0 of the nuclear loci (Table 4.3). The nuclear loci Ts/Tv ratios were comparable to nuclear loci among other vertebrates (Yang and Nielsen 1998). Therefore, poison frogs have a transition bias similar to other vertebrate mitochondrial DNA (Belle et al. 2005). We fail to find evidence for positive selection in both mitochondrial and nuclear protein coding genes. The rate of nonsynonymous/synonymous substitutions (ω) of each locus analyzed was < 1.0 suggesting negative selection

(Yang 1998). Therefore, the loci analyzed for poison frogs are within the variation among vertebrates in terms of their genomic origin and rate molecular evolution.

Our analyses revealed new and corroborated some of established relationships between metabolic parameters, body mass, and molecular evolution for ectotherms. First, we found that the substitution rate is poison frogs have a significant positive association with mass-specific active metabolic parameters (AMR, Scope, and factorial scope). To our knowledge, our results are the first demonstration of the association between the active energy production and the rate of molecular evolution in ectotherms. Second, we found no significant association between rates of substitution with mass-specific resting metabolic rate (RMR). Our results support the lack of association between resting metabolic rate and substitution rate found in endotherms (mammals and birds) and other ectotherms (marine and terrestrial invertebrates) (Lanfear et al. 2007). Third, we found no significant association between rates of substitution with body mass. Previous reports have suggested a negative association between body size and the rate of molecular evolution in endotherms (mammals) and ectotherms (reptiles) (Bromham 2002; Welch et al. 2008). Two reasons might explain the discrepancy with our results: (1) the body size of poison frogs ranges 1-2 orders of magnitude (i.e., 0.1-10 grams), and (2) we use robust comparative analyses (i.e., independent contrasts and GLS analyses). However, other life history traits (e.g., generation time, lifespan, and fecundity) might need to be explored in the context of molecular evolution in poison frogs.

We found a significant variation on the degree of associations between active metabolic parameters and substitution rate of the mitochondrial loci analyzed. We found that the rRNA subunits (i.e., 12S and 16S) were significantly ($P < 0.05$) associated with active metabolic parameters. Our results are not surprising as both mitochondrial genes are a mosaic of conserved (e.g., stems) and variable (e.g., loops) sequence motifs (Kjer 1995). Therefore, we expect different substitution rates to occur across these ribosomal genes based on their functionality and secondary structure in the ribosomal subunits (Hickson et al. 1996). We found that the Val, Leu, and Met tRNAs combined matrix was not significantly ($P > 0.05$) associated with active metabolic parameters. Our results might be partially explained by the relatively slow evolving mitochondrial tRNA genes (Pesole et al. 1999). We found that the CYTB, ND1 and ND2 genes were not significantly ($P > 0.05$) associated with most active metabolic parameters (CYTB was associated with Scope, and ND2 with factorial scope). The substitution rate among the protein-coding genes is highly dependent on the functionality of protein regions (Pesole et al. 1999) and they might be under strong purifying selection. Nuclear loci showed a significant variation on their relationships between molecular evolution and active metabolic parameters. Three segments (NACA, POMC, and ZFX) were not associated ($P > 0.05$) with active metabolic parameters. Four segments (BDNF, BMP2, NT3, and TYR) were associated ($P < 0.05$) with some of the active metabolic parameters. Thus, we found a significant variability in the association between the substitution rates and active metabolic parameters. Our results are not surprising as some nuclear and

mitochondrial genes vary on their substitution rate based on the purifying selection upon them (Hirsh and Fraser 2001; Meiklejohn et al. 2007). We expect that the substitution rate will be highly dependent on the likelihood of the oxidative radicals reaching the target genome (nuclear or mitochondrial), the mutation rate, and the DNA repair efficiency (Yakes and VanHouten 1997).

Our analyses of the codon positions and nonsynonymous/synonymous distances varied in their association with active metabolic parameters. For the mitochondrial codon positions, first and third were not associated ($P > 0.05$) while the second was associated ($P < 0.05$) with active metabolic parameters. Our results are in concordance with the expected frequency of changes for each the codon position under selection. Specifically, the first codon positions are non-degenerate sites (i.e., nucleotide changes causes aminoacid replacement) under strong negative selection (Graur and Li 2000; Rand and Kann 1998) and unlikely to be associated with active metabolic parameters. The second codon positions are non- to twofold degenerate sites (i.e., some nucleotide changes causes aminoacid replacements) under weaker purifying selection (Graur and Li 2000; Rand and Kann 1998) and likely to be associated with active metabolic parameters. The third codon positions are fourfold degenerate sites (i.e., nucleotide changes do not cause nucleotide replacement) under near neutral selection (Graur and Li 2000), saturated (i.e., multiple hits per site), and not associated with active metabolic parameters due to homoplasy. For the nuclear codon positions, first and second were not associated ($P > 0.05$) while the third was associated ($P < 0.05$) with active metabolic parameters. Our results for the nuclear loci are in concordance

with the expectations for slow evolving sequences under selection. Specifically, the first and second codon positions are under strong purifying selection (Graur and Li 2000) and unlikely to be associated with active metabolic parameters. The third codon positions are near neutral (Graur and Li 2000), not saturated, and likely to be associated with active metabolic parameters. Mitochondrial and nuclear nonsynonymous/synonymous sites was associated ($P < 0.05$) with active metabolic parameters. Nonsynonymous sites evolve slower than synonymous (Pesole et al. 1999), but our results suggest that both sites accumulate more changes with higher active metabolic parameters. Therefore, our data predicts that active metabolic parameter relationships with codon positions and nonsynonymous/synonymous distances will depend on the genome, natural selection, and level of saturation.

We found differences in the nonsynonymous/synonymous rate ratios (ω) between low and high Scope species. The contrast was more evident for the Dendrobates+Phyllobates (Clade D) against the rest of the family (Clade A+B+C). Six loci (3 mitochondrial and 3 nuclear) showed a significantly more nonsynonymous/synonymous substitutions in Clade D than the rest of poison frogs. The mitochondrial genes (CYTB, ND1, and ND2) are all involved in the electron transport chain and adapted to the metabolic demands of high aerobic capacity (Kurland and Andersson 2000). However, we found no evidence of positive selection (i.e., $\omega < 1$), which suggests that nonsynonymous changes might be into functionally homologous aminoacids (Yang 1998; Zhang et al. 2005). For the nuclear genes, we found evidence of two ω ratios for some genes

(BMP2, POMC, and ZFX) and only one ω ratio for others (BDNF, NACA, NT3, and TYR). Our results reflect the variability of the purifying selection expected across the nuclear genome (Yang and Nielsen 1998). Therefore, our results suggest that poison frogs have significant variability on the ω ratios, which might be related to active metabolic rates and other factors.

Three main hypotheses explain the variability in rates of molecular evolution among lineages and genomes: generation times, longevity, and metabolic rates. Our results support the metabolic rate hypothesis for poison frogs, which predicts a link between higher metabolic rates and faster molecular evolution (Martin et al. 1992{Gillooly, 2005 #10531). However, we propose a modified version based on mass-specific active metabolic rate (AMR) and not in the basal metabolic rate (BMR or RMR) for ectotherms. The use of active metabolic rates is supported for the following reasons: (1) AMR is a better estimate of the potential of energy generation by the species (Schmidt-Nielsen 1984); (2) AMR is closer to the actual energetic cost under natural conditions rather than the artificial resting state imposed to measure RMR (Gatten et al. 1992); and (3) AMR are species specific, requires actual empirical measurements, and they cannot be approximated by allometric proxies derived by body mass and temperature alone (e.g., Gillooly et al., 2005 (Gillooly et al. 2005)). Some assumptions of the AMR metabolic rate hypothesis are: (1) the oxygen intake during physical activity is associated with production of oxidative free radicals; (2) the cellular respiration during physical activity is associated with DNA damage at the cellular level; (3) DNA repair efficiency is dependent on AMR and

the actual energetic cost of life history traits (e.g., foraging ecology, home range, reproductive effort); and (4) the oxidative free radicals produced by AMR are responsible of both nuclear and mitochondrial mutation rates. Limitations of the AMR-metabolic rate hypothesis are also similar to those of the original based on BMR (Lanfear et al. 2007). Some of these limitations are: (1) mutation rates is directly associated metabolic rates; (2) mitochondrial respiration produces free radicals that damage both nuclear and mitochondrial genomes; and (3) oxidative radical production is not decoupled from oxygen intake during physical activity. Thus, we propose the AMR-metabolic rate hypothesis of substitution rate for ectotherms (e.g., poison frogs). However, molecular evolution is multifactorial and includes oxidative damage by free radicals, effectiveness of DNA repair, life history traits, and the loci of interest (e.g., organellar or nuclear). More data on generation time, fecundity, longevity, and other life history variables are necessary to understand the molecular evolution in poison frogs.

Molecular clocks or the constancy of rates of nucleotide substitutions across lineages and genes (Kumar and Hedges 1998) has been proposed as a derivation of the metabolic hypothesis of molecular evolution (Martin and Palumbi 1993). Our data suggest a significant variation on the rates of molecular evolution, which rejects a molecular clock. However, we found that active metabolic rates are more likely to influence the variation on the rate of molecular substitutions in poison frogs and possibly other ectotherms.

We found a significant increase in the rate of molecular evolution in poison frog species that have high active metabolic rates. Our results are robust

against phylogenetic non-independence due the general agreement between independent contrasts (IC) and phylogenetic generalized least squares (GLS) analyses. Our data show a great variability on the rate of substitutions depending on the loci. Mitochondrial ribosomal genes tend to have higher rates of substitution compared to tRNAs or the protein coding genes analyzed (CYTB, ND1, and ND2). Nuclear loci are under strong purifying selection, but showed high variability on rate of molecular evolution as expected. Some nuclear loci (BDNF, BMP2, NT3, and TYR) showed that their substitution rates are positively associated with active metabolic parameters. However, more loci (e.g., introns) are needed to validate our conclusions and the role of active metabolic parameters on molecular evolution. We proposed a modified version of the metabolic hypothesis based on the active metabolic rate. Physiological and genomic data of more poison frogs and other ectotherms are necessary to confirm our predictions.

Classification	Gene	Fragment		Log BodyMass (g)		VO^2_{active}/hour (mass-specific)		$VO^2_{resting}$/hour (mass-specific)		Metabolic Scope (mass-specific)		Factorial Scope	
		(bp)	*n*	*r*	*p*	*r*	*p*	*r*	*p*	*r*	*p*	*r*	*p*
Mitochondrial ribosomal	12S	921	IC:52	0.027	0.846	**0.291**	**0.033**	0.102	0.465	**0.316**	**0.020**	**0.396**	**0.003**
		Inv: 0.398	λ:1.00	-0.034	0.798	0.247	0.066	-0.037	0.787	0.259	0.053	**0.295**	**0.031**
	16S	1588	IC:52	0.092	0.508	**0.276**	**0.044**	0.076	0.584	**0.273**	**0.046**	0.187	0.175
		Inv: 0.363	λ:1.00	0.016	0.909	0.198	0.144	0.188	0.162	0.181	0.184	0.041	0.770
tRNAs	V-L-M	211	IC:52	0.095	0.496	0.014	0.918	0.010	0.942	0.013	0.925	0.021	0.878
		Inv: 0.186	λ:1.00	0.123	0.361	-0.092	0.500	0.081	0.552	-0.084	0.535	0.024	0.860
Mitochondrial protein	CytB	690	IC:52	0.077	0.579	0.257	0.061	0.021	0.882	**0.268**	**0.049**	0.223	0.105
		Inv: 0.436	λ:1.00	-0.146	0.280	0.168	0.214	0.029	0.830	0.171	0.208	0.144	0.289
	ND1	960	IC:51	0.098	0.481	0.239	0.085	0.108	0.442	0.230	0.098	0.118	0.400
		Inv: 0.403	λ:1.00	-0.119	0.384	0.224	0.100	0.134	0.340	0.219	0.109	0.120	0.381
	ND2	837	IC:52	0.113	0.415	0.190	0.174	0.182	0.193	0.224	0.106	**0.327**	**0.017**
		Inv: 0.239	λ:1.00	0.080	0.559	0.082	0.561	-0.149	0.277	0.111	0.429	0.247	0.072
Mitochondrial codon position	Pos1	509	IC:52	0.144	0.297	0.233	0.091	0.066	0.638	0.250	0.068	0.262	0.056
		Inv: 0.436	λ:1.00	0.083	0.540	0.161	0.257	-0.052	0.704	0.179	0.202	0.241	0.075
	Pos2	509	IC:52	0.027	0.845	**0.295**	**0.030**	0.151	0.276	**0.328**	**0.016**	**0.364**	**0.007**
		Inv: 0.522	λ:1.00	0.088	0.519	0.177	0.192	-0.097	0.475	0.201	0.138	0.254	0.059
	Pos3	509	IC:52	0.103	0.459	0.151	0.277	0.043	0.758	0.162	0.241	0.228	0.097
		Inv: 0.002	λ:1.00	-0.069	0.610	0.064	0.641	-0.048	0.724	0.073	0.591	0.165	0.233
Mitochondrial codon	dN	1527	IC:52	0.103	0.460	**0.310**	**0.023**	0.142	0.304	**0.342**	**0.011**	**0.414**	**0.002**
			λ:1.00	0.050	0.713	0.208	0.123	-0.110	0.420	0.233	0.084	**0.356**	**0.008**
	dS	1527	IC:52	0.051	0.716	0.257	0.060	0.121	0.384	**0.284**	**0.037**	**0.340**	**0.012**
			λ:1.00	-0.011	0.937	0.133	0.326	-0.063	0.643	0.148	0.275	0.220	0.106

Inv: estimated proportion of invariant sites. First line includes the independent contrasts results (IC). Second line includes the phylogenetic GLS results including λ (the evolutionary regression coefficient). Gene abbreviations: 12S and 16S rDNA genes (12S and 16S); Valine, Leucine, and Methionine tRNA genes (tRNAs V-L-M); NADH subunit 1 (ND1); NADH subunit 2 (ND2); and Cytochrome b (CYTB). Values in bold are significant $P < 0.05$.

Table 4.1: Correlations and significance of the mitochondrial genes, codon positions, and synonymous (dS) / nonsynonymous (dN) estimated substitution rates with body mass and aerobic metabolic traits.

Classification	Gene	Fragment (bp)		Log BodyMass (g)		VO^2_{active}/hour (mass-specific)		$VO^2_{resting}$/hour (mass-specific)		Metabolic Scope (mass-specific)		Factorial Scope	
			n	*r*	*p*	*r*	*p*	*r*	*p*	*r*	*p*	*r*	*p*
Nuclear protein	BDNF	606	IC:52	0.006	0.966	0.229	0.095	0.007	0.960	0.238	0.083	0.189	0.172
		Inv: 0.652	λ:0.89	0.012	0.929	**0.306**	**0.024**	-0.001	0.992	**0.323**	**0.018**	0.242	0.087
	BMP2	579	IC:52	0.102	0.466	**0.350**	**0.009**	0.199	0.150	**0.331**	**0.015**	0.119	0.392
		Inv: 0.363	λ:0.91	-0.113	0.404	**0.363**	**0.006**	0.239	0.076	**0.346**	**0.009**	0.100	0.463
	NACA	1248	IC:52	0.028	0.839	0.151	0.276	0.041	0.767	0.149	0.281	0.116	0.402
		Inv: 0.470	λ:0.99	-0.129	0.348	0.110	0.419	0.118	0.387	0.098	0.471	-0.011	0.934
	NT3	591	IC:52	0.021	0.882	0.133	0.339	0.201	0.144	0.168	0.225	**0.507**	**<0.001**
		Inv: 0.322	λ:1.00	-0.096	0.481	0.054	0.689	-0.195	0.150	0.083	0.542	**0.446**	**<0.001**
	POMC	480	IC:52	0.024	0.863	0.194	0.160	0.010	0.943	0.202	0.144	0.188	0.174
		Inv: 0.350	λ:0.99	-0.004	0.979	0.200	0.146	-0.076	0.575	0.217	0.113	0.237	0.078
	TYR	510	IC:52	0.043	0.759	**0.292**	**0.032**	0.076	0.585	**0.313**	**0.021**	**0.364**	**0.007**
		Inv: 0.351	λ:0.96	0.029	0.835	0.240	0.073	-0.011	0.937	0.253	0.059	**0.262**	**0.049**
	ZFX	930	IC:52	0.022	0.874	0.159	0.252	0.069	0.618	0.153	0.270	0.145	0.297
		Inv: 0.597	λ:0.99	-0.196	0.150	0.134	0.324	0.024	0.861	0.136	0.317	0.185	0.171
Nuclear codon position	Pos1	1648	IC:52	0.101	0.468	0.250	0.069	0.238	0.083	0.221	0.108	0.103	0.459
		Inv: 0.660	λ:0.99	-0.057	0.676	0.256	0.057	0.198	0.141	0.237	0.079	0.111	0.417
	Pos2	1648	IC:52	0.101	0.468	0.040	0.772	0.106	0.446	0.058	0.677	0.257	0.060
		Inv: 0.824	λ:1.00	-0.029	0.833	0.026	0.848	-0.042	0.764	0.028	0.835	0.175	0.198
	Pos3	1648	IC:52	0.178	0.199	**0.406**	**0.002**	0.056	0.688	**0.428**	**0.001**	**0.453**	**0.001**
		Inv: 0.001	λ:0.97	-0.133	0.327	**0.379**	**0.004**	-0.016	0.910	**0.399**	**0.002**	**0.390**	**0.003**
Nuclear codon	dN	4944	IC:52	0.013	0.926	**0.403**	**0.003**	0.066	0.634	**0.426**	**0.001**	**0.491**	**<0.001**
			λ:1.00	-0.089	0.513	**0.395**	**0.003**	-0.035	0.797	**0.415**	**0.001**	**0.438**	**0.001**
	dS	4944	IC:52	0.069	0.622	**0.356**	**0.008**	0.006	0.968	**0.367**	**0.006**	**0.389**	**0.004**
			λ:0.99	-0.147	0.281	**0.332**	**0.012**	0.043	0.752	**0.341**	**0.010**	**0.309**	**0.020**

Inv: estimated proportion of invariant sites. First line includes the independent contrasts results (IC). Second line includes the phylogenetic GLS results including λ (the evolutionary regression coefficient). Gene abbreviations: brain-derived neurotrophic factor (BDNF); bone morphogenetic protein 2 (BMP2); NCX1 sodium-calcium exchanger 1 (NACA); 3'-nucleotidase (NT3); proopiomelanocortin A (POMC); tyrosinase precursor (TYR); and zinc finger E-box binding homeobox 2 (ZFX). Values in bold are significant $P < 0.05$.

Table 4.2: Correlations and significance of the nuclear genes, codon positions, and synonymous (dS) / nonsynonymous (dN) estimated substitution rates with body mass and aerobic metabolic traits.

Genes	Ts/Tv (κ)	High Aerobic Metabolic Scope					*Dendrobates+Phyllobates*				
		2*ΔL	*P*	ω_0	ω_1	ω_1/ω_0	2*ΔL	*P*	ω_0	ω_1	ω_1/ω_0
CYTB	3.867	3.535	0.060	0.018	--	1.000	5.775	0.016	0.017	0.023	1.379
ND1	4.214	5.899	0.052	0.041	--	1.000	20.944	<0.001	0.036	0.054	1.515
ND2	4.454	10.760	0.001	0.055	0.072	1.307	6.333	0.012	0.059	0.073	1.241
BDNF	2.955	0.014	0.906	0.075	--	1.000	0.125	0.724	0.075	--	1.000
BMP2	2.172	5.881	0.015	0.034	0.073	2.128	4.881	0.027	0.038	0.077	2.027
NACA	2.437	0.184	0.668	0.033	--	1.000	0.019	0.890	0.033	--	1.000
NT3	2.407	1.747	0.186	0.114	--	1.000	0.479	0.489	0.114	--	1.000
POMC	1.551	7.222	0.007	0.075	0.138	1.830	7.872	0.005	0.080	0.156	1.945
TYR	2.058	1.016	0.313	0.081	--	1.000	0.872	0.350	0.081	--	1.000
ZFX	2.665	3.681	0.055	0.124	--	1.000	4.043	0.044	0.116	0.136	1.176

Gene abbreviations: Cytochrome b (CYTB); NADH subunit 1 (ND1); NADH subunit 2 (ND2); brain-derived neurotrophic factor (BDNF); bone morphogenetic protein 2 (BMP2); NCX1 sodium-calcium exchanger 1 (NACA); 3'-nucleotidase (NT3); proopiomelanocortin A (POMC); tyrosinase precursor (TYR); and zinc finger E-box binding homeobox 2 (ZFX). Transition/transversion ratio ($\kappa = Ts/Tv$). Likelihood Ratio Statistics (2*ΔL) is approximated by a χ^2 with 1 df. Nonsynonymous/synonymous rate ratio is ($\omega = dN/dS$), if only ω_0 (one ratio was favored) or ω_0 and ω_1 (two ratios was favored).

Table 4.3: Model test results and estimates of the nonsynonymous/synonymous rate of poison frogs.

Genus	Species	n	Weight (g)				VO_2rest consumed (mLO_2/h)				VO_2active consumed (mLO_2/h)				Aerobic Scope		Factorial
			Mean	SE	Min	Max	Mean	SE	Min	Max	Mean	SE	Min	Max	Raw	Mass-specific	Scope
Allobates	*femoralis*	6	1.246	0.103	0.940	1.570	0.223	0.031	0.135	0.355	1.104	0.228	0.613	2.159	0.881	0.707	4.942
Allobates	*inseperatus*	4	0.551	0.041	0.430	0.605	0.082	0.018	0.056	0.133	0.609	0.030	0.535	0.678	0.527	0.956	7.459
Allobates	*juanii*	2	0.685	0.085	0.600	0.770	0.147	0.064	0.083	0.211	0.766	0.008	0.758	0.774	0.619	0.904	5.219
Allobates	*kingsburyi*	8	0.875	0.102	0.595	1.300	0.126	0.016	0.054	0.219	0.644	0.032	0.546	0.786	0.518	0.592	5.103
Allobates	sp. Tachira	6	0.585	0.013	0.540	0.620	0.168	0.019	0.100	0.217	0.593	0.071	0.366	0.805	0.425	0.726	3.520
Allobates	*talamancae*	5	0.880	0.087	0.605	1.150	0.080	0.014	0.049	0.126	0.714	0.050	0.578	0.797	0.634	0.720	8.890
Allobates	*zaparo*	10	1.615	0.133	1.010	2.510	0.299	0.029	0.163	0.458	1.919	0.108	1.381	2.535	1.620	1.003	6.422
Ameerega	*bilinguis*	11	0.949	0.077	0.570	1.515	0.180	0.011	0.128	0.260	0.974	0.051	0.691	1.213	0.794	0.837	5.408
Ameerega	*hahneli*	6	0.343	0.020	0.295	0.405	0.100	0.011	0.075	0.138	0.516	0.013	0.466	0.550	0.416	1.213	5.146
Ameerega	*parvula*	8	1.569	0.049	1.365	1.790	0.293	0.033	0.137	0.412	1.497	0.170	0.719	2.350	1.204	0.767	5.111
Ameerega	*trivittata*	3	5.512	0.994	4.515	7.500	0.964	0.178	0.785	1.320	6.632	0.924	5.523	8.468	5.668	1.028	6.879
Anomaloglossus	sp. Ayacucho	11	0.808	0.051	0.610	1.140	0.202	0.022	0.094	0.372	0.730	0.068	0.456	1.119	0.528	0.653	3.607
Aromobates	*aff. alboguttatus*	17	1.312	0.114	0.560	2.330	0.248	0.022	0.129	0.466	0.916	0.093	0.327	1.823	0.668	0.509	3.701
Aromobates	*saltuensis*	6	1.498	0.138	1.190	1.970	0.212	0.046	0.099	0.415	1.249	0.202	0.597	2.015	1.037	0.692	5.903
Colostethus	*fugax*	4	0.959	0.089	0.720	1.100	0.124	0.013	0.093	0.147	0.667	0.054	0.525	0.783	0.543	0.566	5.374
Colostethus	*panamensis*	5	0.973	0.093	0.693	1.167	0.096	0.004	0.088	0.109	1.159	0.085	0.971	1.412	1.063	1.092	12.122
Colostethus	*pratti*	12	0.806	0.031	0.657	0.950	0.111	0.008	0.072	0.179	1.133	0.051	0.669	1.324	1.022	1.268	10.203
Dendrobates	*auratus*	15	1.996	0.071	1.640	2.520	0.306	0.039	0.169	0.734	2.810	0.124	2.156	3.942	2.504	1.255	9.190
Dendrobates	*bombetes*	8	0.528	0.036	0.400	0.680	0.085	0.007	0.062	0.118	0.885	0.056	0.612	1.084	0.800	1.515	10.469
Dendrobates	*captivus*	6	0.484	0.025	0.405	0.565	0.087	0.014	0.061	0.154	0.602	0.039	0.487	0.719	0.515	1.064	6.952
Dendrobates	*claudiae*	1	0.217	--	--	--	0.060	--	--	--	0.652	--	--	--	0.592	2.728	10.822
Dendrobates	*duellmani*	7	0.414	0.030	0.340	0.520	0.095	0.012	0.060	0.138	0.686	0.060	0.487	0.916	0.591	1.428	7.252
Dendrobates	*galactonotus*	4	3.589	0.293	3.035	4.095	0.323	0.009	0.307	0.348	4.970	0.225	4.534	5.581	4.647	1.295	15.379
Dendrobates	*histrionicus*	4	3.320	0.119	3.140	3.670	0.205	0.021	0.167	0.257	2.496	0.301	1.788	3.105	2.291	0.690	12.156
Dendrobates	*lamasi*	2	0.390	0.070	0.320	0.460	0.068	0.015	0.054	0.083	1.074	0.062	1.011	1.136	1.006	2.579	15.683
Dendrobates	*leucomelas*	12	2.243	0.138	1.323	2.990	0.414	0.055	0.134	0.819	3.167	0.273	2.000	4.672	2.753	1.227	7.648
Dendrobates	*pumilio*	17	0.538	0.017	0.407	0.670	0.067	0.003	0.049	0.093	0.698	0.026	0.508	0.924	0.631	1.173	10.452
Dendrobates	sp. Quibdo	3	0.160	0.010	0.140	0.170	0.051	0.019	0.018	0.084	0.577	0.263	0.288	1.102	0.526	3.288	11.330
Dendrobates	*sylvaticus*	11	2.889	0.133	2.100	3.420	0.400	0.054	0.169	0.696	3.328	0.188	2.382	4.725	2.928	1.013	8.323
Dendrobates	*tinctorius*	8	5.037	0.358	4.110	6.310	0.549	0.051	0.402	0.832	5.983	0.767	2.788	9.798	5.434	1.079	10.889
Dendrobates	*truncatus*	12	1.573	0.115	1.080	2.170	0.188	0.016	0.119	0.283	1.926	0.111	1.353	2.581	1.738	1.105	10.263
Dendrobates	*ventrimaculatus*	7	0.345	0.056	0.140	0.550	0.134	0.044	0.027	0.306	0.661	0.098	0.389	1.033	0.527	1.528	4.950
Dendrobates	*virolinensis*	8	0.475	0.051	0.330	0.730	0.094	0.006	0.067	0.120	0.639	0.030	0.556	0.818	0.545	1.147	6.800
Epipedobates	*anthonyi*	10	1.062	0.052	0.750	1.410	0.197	0.009	0.159	0.255	1.207	0.036	1.025	1.409	1.010	0.951	6.130
Epipedobates	*boulengeri*	16	0.427	0.018	0.310	0.540	0.097	0.012	0.046	0.193	0.329	0.023	0.163	0.512	0.232	0.543	3.381
Epipedobates	*machalilla*	11	0.323	0.022	0.230	0.475	0.083	0.009	0.047	0.144	0.385	0.049	0.159	0.704	0.302	0.935	4.657
Epipedobates	sp. F	10	0.457	0.026	0.320	0.550	0.065	0.005	0.043	0.094	0.596	0.036	0.436	0.765	0.531	1.162	9.135
Epipedobates	*tricolor*	4	0.801	0.051	0.690	0.895	0.164	0.022	0.114	0.211	0.836	0.089	0.621	1.055	0.672	0.839	5.097
Hyloxalus	*awa*	10	0.915	0.050	0.730	1.280	0.121	0.005	0.093	0.152	0.653	0.038	0.532	0.853	0.532	0.581	5.398
Hyloxalus	*azueriventris*	4	1.018	0.063	0.905	1.165	0.208	0.026	0.133	0.250	1.309	0.017	1.273	1.354	1.101	1.082	6.296
Hyloxalus	*bocagei*	11	1.514	0.141	0.830	2.280	0.288	0.029	0.182	0.497	2.307	0.220	1.154	3.524	2.019	1.334	8.016
Hyloxalus	*elachyhistus*	28	0.958	0.054	0.550	1.640	0.248	0.019	0.114	0.450	0.840	0.060	0.352	1.432	0.592	0.618	3.387
Hyloxalus	*maculosus*	20	2.300	0.144	1.000	3.520	0.340	0.030	0.129	0.585	2.003	0.152	0.782	3.500	1.663	0.723	5.892
Hyloxalus	*nexipus*	3	1.066	0.181	0.705	1.263	0.264	0.092	0.124	0.438	1.236	0.084	1.147	1.403	0.972	0.912	4.684
Hyloxalus	*sauli*	3	1.703	0.313	1.080	2.055	0.331	0.093	0.165	0.488	2.365	0.206	1.999	2.713	2.034	1.194	7.152
Hyloxalus	*subpunctatus*	7	0.799	0.070	0.637	1.180	0.151	0.013	0.109	0.203	0.901	0.059	0.774	1.241	0.750	0.939	5.975
Hyloxalus	*toachi*	5	0.680	0.082	0.520	0.970	0.117	0.017	0.070	0.168	0.872	0.074	0.611	1.028	0.755	1.110	7.481
Hyloxalus	*vertebralis*	8	0.698	0.051	0.515	0.960	0.127	0.021	0.063	0.236	0.567	0.052	0.340	0.719	0.440	0.630	4.452
Mannophryne	*collaris*	35	1.833	0.144	0.620	4.420	0.362	0.042	0.086	1.007	1.502	0.159	0.444	4.399	1.140	0.622	4.151
Phyllobates	*aurotaenia*	3	2.017	0.447	1.290	2.830	0.184	0.074	0.096	0.332	1.347	0.252	0.940	1.809	1.163	0.577	7.329
Phyllobates	*terribilis*	5	6.013	0.125	5.715	6.365	0.787	0.113	0.588	1.202	5.092	0.101	4.783	5.381	4.305	0.716	6.467
Rheobates	*palmatus*	15	1.780	0.181	0.850	2.905	0.368	0.037	0.220	0.767	1.563	0.154	0.900	2.734	1.195	0.671	4.252
Silverstoneia	*flotator*	10	0.327	0.013	0.273	0.393	0.054	0.005	0.036	0.079	0.491	0.027	0.378	0.687	0.437	1.336	9.026
Silverstoneia	*nubicola*	7	0.371	0.032	0.270	0.470	0.043	0.003	0.031	0.055	0.636	0.048	0.422	0.770	0.593	1.598	14.885

Table 4.4: Metabolic measurements and body mass (mean, standard error, and range) of the poison frogs.

Genes	Name	Sequence (5'-3')	Annealing
12S-ND2	MVZ59-L	ATAGCACTGAAAAYGCTDAGATG	45-48 °C
	12SJ-L	AAAGGTTTGGTCCTAGCCTT	
	12L1-L	AAAAAGCTTCAAACTGGGATTAGATACCCCACTAT	
	12SA-L	AAACTGGGATTAGATACCCCACTAT	
	12SF-H	CTTGGCTCGTAGTTCCCTGGCG	
	H29616-H	GAGGGTGACGGGCGGTGTGT	
	H29616-L	ACACACCGCCCGTCACCCTC	
	12SM-L	GGCAAGTCGTAACATGGTAAG	
	12SK-H	TCCGGTGTGCTTACCATGTTACGA	
	tRNAval-H	GGTGTAAGCGARAGGCTTTKGTTAAG	
	16SH-H	GCTAGACCATGATGCAAAAGGTA	
	16SC-L	GTRGGCCTAAAAGCAGCCAC	
	16SDB-L	CGCCTGTTTATCAAAAACAT	
	16SA-H	ATGTTTTTGATAAACAGGCG	
	16SD-H	CTCCGGTCTGAACTCAGATCACGTAG	
	16S-frog[a]	TTACCCTRGGGATAACAGCGCAA	
	tMet-frog[a]	TTGGGGTATGGGCCCAAAAGCT	
	ND1(a1)-L	TACCCACGATTTCGRTAYGAYCA	
	ND1(a2)-L	TACCCACGATTTCGNTAYGA	
	L5556a-H	CTTAGGGCTTTGAAGGCYCTT	
	tRNAW6313-H	CTCYTGYTTAGRGCTTTGAAGGC	
	H5934-H	AGRGTGCCAATGTCTTTGTGRTT	
CYTB	CytbDen3-L	AAYATYTCCRYATGATGRAAYTTYGG	45-48 °C
	CytbDen1-H	GCRAANAGRAAGTATCATTCNGGYTTRAT	
BDNF	BDNF_F1	ACCATCCTTTTCCTKACTATGG	52 °C
	BDNF_R1	CTATCTTCCCCTTTTAATGGTC	
BMP2	BMP2_F7	AGACTATTGGACACCAGACTGGTACATCATA	52 °C
	BMP2_R3	CRCAYCCCTCCACRACCATGTCTTGATA	
NACA	CXCR4-G[b]	AGCAACAGTGGAARAANGC	52 °C
	CXCR4-H[b]	GTAATGGARATCCAYTTATG	
	CXCR4-L[b]	GGGTTAAGGCARCARTGRAA	
	CXCR4-N[b]	GGTCATGGGTTATCARAARAARTC	
NT3	NTF3_R3	ACATTGRGAATTCCAGTGTTTGTCGTCA	52 °C
	NTF3_F3	TCTTCCTTATCTTTGTGGCATCCACGCTA	
POMC	POMCF1	ATATGTCATGASCCAYTTYCGCTGGA	52 °C
	POMCR1	GGCRTTYTTGAAWAGAGTCATTAGW	
TYR	DendroTYRFl	TGCCAAGATGTTGTCCTGTC	52 °C
	DendroTYRrM	CTCTCCARTCCCAGMAGGGG	
	TYRC[c]	GGCAGAGGAWCRTGCCAAGATGT	
	TYRG[c]	TGCTGGCRTCTCTCCARTCCCA	
ZFX	ZFHX1B_F1[d]	TAYGARTGYCCAAACTGCAAGAAACG	52 °C
	ZFHX1B_R3	TCTCRGAAAGTACCGAYGACARCAGGAG	

[a]Wiens *et al.* (2005), [b]Roelants *et al.* (2007), [c] Bossuyt and Milinkovitch (2000), [d]Townsend *et al.* (2008)

Table 4.5: Primers and conditions used to amplify mitochondrial and nuclear segments.

	Ribosomal		tRNA	Protein Coding			Codon		
Parameter	12S	16S	VLM	CYTB	ND1	ND2	Pos1	Pos2	Pos3
AC	7.1879	6.4246	2.7644	0.5726	0.2077	0.2349	0.7939	4.1028	0.1641
AG	15.0329	15.1341	14.2868	19.3678	10.1492	7.1459	5.7806	6.1643	10.1358
AT	10.8702	9.3126	2.1838	1.7431	0.2614	0.3622	1.7885	1.7302	0.3120
CG	0.0973	0.5114	0.0141	1.1572	0.4015	0.6639	0.4005	3.9421	0.2900
CT	50.0684	52.6833	25.0095	11.6038	2.3197	2.6497	6.0859	15.0350	3.6549
A	0.3422	0.3807	0.3253	0.2763	0.3112	0.3279	0.3142	0.1862	0.3231
C	0.2254	0.2065	0.2082	0.3695	0.3148	0.3147	0.2563	0.2930	0.3370
G	0.1782	0.1417	0.1601	0.0670	0.0537	0.0564	0.1598	0.1137	0.0511
T	0.2542	0.2711	0.3064	0.2873	0.3203	0.3011	0.2696	0.4071	0.2888
α-shape	0.6272	0.7366	0.3975	0.4448	0.6319	0.6172	1.2888	0.5533	1.8415
Invariant	0.3981	0.3634	0.1858	0.4359	0.4033	0.2394	0.4360	0.5216	0.0017

	Protein Coding							Codon		
Parameter	BDNF	BMP2	NACA	NT3	POMC	TYR	ZFX	Pos1	Pos2	Pos3
AC	0.8899	1.8714	2.8354	0.9910	1.7742	1.1935	1.1784	3.0136	3.0239	1.4105
AG	4.6915	4.7411	6.0707	5.0316	3.0323	3.5650	4.5078	2.6903	8.8941	5.7027
AT	0.8025	0.8003	1.7094	1.0197	1.0688	0.5852	1.0847	1.3606	1.3411	1.0174
CG	0.7818	1.0858	1.3804	1.7591	0.8371	0.7047	0.8183	0.6378	3.7716	1.0720
CT	6.5096	7.5127	13.1813	7.3074	9.7695	4.7969	4.9498	4.7401	6.2962	7.1766
A	0.3165	0.3051	0.3068	0.3265	0.3914	0.2478	0.3336	0.3354	0.3511	0.2673
C	0.2165	0.2133	0.1845	0.2230	0.1862	0.2564	0.1994	0.1892	0.2050	0.2222
G	0.2529	0.2231	0.2195	0.2288	0.2254	0.2221	0.2009	0.2966	0.1782	0.1988
T	0.2142	0.2585	0.2891	0.2217	0.1971	0.2738	0.2661	0.1789	0.2656	0.3117
α-shape	0.8111	0.6163	0.7601	0.6355	1.1971	0.7450	0.7218	0.7867	0.9592	0.8896
Invar	0.6525	0.3626	0.4705	0.3218	0.3495	0.3508	0.5967	0.6605	0.8243	0.0014

Table 4.6: Model parameter specification for mitochondrial and nuclear genes and codon positions under GTR+Γ+I model of molecular evolution.

Genus	species	12S	16S	tRNA-VLM	CYTB	ND1	ND2	Pos1	Pos2	Pos3	dN	dS
Allobates	*femoralis*	0.2769	0.4334	0.4073	0.8438	0.7060	0.9350	0.2833	0.1469	2.7193	0.0779	2.0065
Allobates	*insperatus*	0.2815	0.4045	0.3528	0.8219	0.7675	0.9944	0.3271	0.1651	2.5747	0.0826	2.1355
Allobates	*juanii*	0.2407	0.4317	0.3370	0.7722	--	1.0270	0.3404	0.1494	2.7292	0.0780	2.0100
Allobates	*kingsburyi*	0.2474	0.3615	0.3872	0.7945	0.6297	0.9519	0.2646	0.1364	2.9696	0.0710	1.8185
Allobates	sp. Tachira	0.2545	0.3931	0.3722	0.6768	0.8192	0.8286	0.2426	0.1274	2.4837	0.0732	2.1358
Allobates	*talamancae*	0.2237	0.3633	0.3556	0.7439	0.5703	0.7526	0.2550	0.1133	2.5200	0.0792	2.1043
Allobates	*zaparo*	0.2830	0.4254	0.3939	0.7935	0.7270	1.0021	0.2752	0.1452	2.7989	0.0695	2.0343
Ameerega	*bilinguis*	0.2250	0.3337	0.1789	0.6390	0.6552	0.7792	0.2267	0.0922	2.7309	0.0853	2.2349
Ameerega	*hahneli*	0.2182	0.3485	0.1593	0.6241	0.6537	0.7572	0.2438	0.0886	2.5535	0.0722	2.1080
Ameerega	*parvula*	0.2251	0.3453	0.1778	0.6312	0.6818	0.7847	0.2200	0.1037	2.6720	0.0958	2.5001
Ameerega	*trivittata*	0.2158	0.3444	0.1505	0.6101	0.6133	0.7330	0.2496	0.0973	2.3982	0.0905	2.3528
Anomaloglossus	sp. Ayacucho	0.2449	0.3331	0.4301	0.7985	0.6895	0.7839	0.2904	0.0955	2.7184	0.0815	2.1068
Aromobates	*saltuensis*	0.2121	0.3203	0.3837	0.6389	0.6266	0.7754	0.2350	0.0999	2.2708	0.0655	1.9260
Aromobates	*aff. alboguttatus*	0.2314	0.3485	0.3967	0.6935	0.6785	0.8036	0.2563	0.0955	2.4200	0.0739	2.1556
Colostethus	*fugax*	0.2144	0.3372	0.1763	0.5548	0.6682	0.6976	0.2308	0.0692	2.2573	0.0743	1.9984
Colostethus	*panamensis*	0.2331	0.2901	0.2336	0.6071	0.5903	0.7512	0.2443	0.0759	2.3866	0.0691	1.7674
Colostethus	*pratti*	0.2294	0.3199	0.2237	0.6019	0.6108	0.7017	0.2422	0.0951	2.1002	0.0790	2.0328
Dendrobates	*auratus*	0.1951	0.3523	0.2960	0.5229	0.6896	0.8049	0.2294	0.0825	2.4893	0.0769	1.9872
Dendrobates	*bombetes*	0.1931	0.3511	0.1285	0.6731	0.7482	0.6650	0.2143	0.0730	2.3525	0.0673	1.7159
Dendrobates	*captivus*	0.1851	0.3443	0.1692	0.5269	0.6981	0.6624	0.2122	0.0515	2.1432	0.0780	2.0783
Dendrobates	*claudiae*	0.2042	0.3738	0.1453	0.6141	0.7887	0.6984	0.2531	0.0722	2.1971	0.0641	1.8877
Dendrobates	*duellmani*	0.2171	0.3916	0.1715	0.6295	0.8189	0.6995	0.2108	0.0778	2.3436	0.0575	1.7069
Dendrobates	*galactonotus*	0.2761	0.4009	0.2556	0.6287	0.7808	0.9105	0.2853	0.1244	2.8942	0.0752	1.9333

Genus	species	12S	16S	tRNA-VLM	CYTB	ND1	ND2	Pos1	Pos2	Pos3	dN	dS
Dendrobates	*histrionicus*	0.2276	0.3415	0.2492	0.6049	0.6828	0.8454	0.2700	0.0828	2.5852	0.0834	1.9490
Dendrobates	*lamasi*	0.2565	0.4170	0.1351	0.7914	0.8202	0.8286	0.2683	0.1137	2.6721	0.0921	2.1362
Dendrobates	*leucomelas*	0.1769	0.3556	0.2794	0.5384	0.6871	0.7579	0.2316	0.0850	2.3595	0.0799	1.8746
Dendrobates	*pumilio*	0.2448	0.3473	0.2190	0.6247	0.7076	0.8298	0.2536	0.0816	2.6396	0.0846	1.9756
Dendrobates	sp. Quibdo	0.2022	0.3566	0.1441	0.6390	0.7479	0.6828	0.2239	0.0784	2.2901	0.0746	1.7606
Dendrobates	*sylvaticus*	0.2443	0.3503	0.2486	0.6135	0.6972	0.8483	0.2660	0.0817	2.6335	0.0853	1.9909
Dendrobates	*tinctorius*	0.2020	0.3476	0.2943	0.5391	0.8046	0.8346	0.2504	0.0838	2.5224	0.0868	2.0214
Dendrobates	*truncatus*	0.1883	0.3473	0.2851	0.5026	0.7036	0.8197	0.2406	0.0780	2.4780	0.0822	1.9245
Dendrobates	*ventrimaculatus*	0.2237	0.4067	0.1468	0.6935	0.7967	0.6887	0.2367	0.0800	2.3296	0.0782	1.8369
Dendrobates	*virolinensis*	0.1971	0.3533	0.1230	0.6881	0.7177	0.6715	0.2143	0.0728	2.4100	0.0773	1.8195
Epipedobates	*anthonyi*	0.1813	0.3344	0.1919	0.5640	0.6551	0.6883	0.2051	0.0639	2.2638	0.0649	1.9088
Epipedobates	*boulengeri*	0.1821	0.3256	0.2161	0.5731	0.6840	0.6805	0.2200	0.0663	2.2631	0.0791	2.2974
Epipedobates	*machalilla*	0.1765	0.3324	0.1919	0.5837	0.6637	0.6914	0.2012	0.0663	2.2835	0.0656	1.9285
Epipedobates	sp. F	0.1782	0.3198	0.1978	0.5877	0.6661	0.6782	0.2115	0.0687	2.2774	0.0764	2.2233
Epipedobates	*tricolor*	0.1801	0.3314	0.1978	0.5930	0.6684	0.6893	0.2051	0.0712	2.2758	0.0777	2.2604
Hyloxalus	*awa*	0.1573	0.3174	0.1242	0.5071	0.6514	0.7201	0.2311	0.0540	2.3487	0.0668	1.9329
Hyloxalus	*azueriventris*	0.2165	0.3721	0.3478	0.6212	0.8883	--	0.3430	0.1462	2.3035	0.0657	1.9299
Hyloxalus	*bocagei*	0.1980	0.3051	0.1536	0.6358	0.7147	0.6717	0.2143	0.0800	2.5822	0.0767	2.1430
Hyloxalus	*elachyhistus*	0.1356	0.2987	0.1237	0.5153	0.5748	0.6256	0.2051	0.0543	2.2985	0.0877	2.1495
Hyloxalus	*maculosus*	0.1868	0.3245	0.1795	0.5134	0.6506	0.6388	0.1762	0.0634	2.2838	0.0682	1.7414
Hyloxalus	*nexipus*	0.1971	0.3081	0.1808	0.5286	0.6795	0.7459	0.2154	0.0685	2.5302	0.0670	1.5985
Hyloxalus	*sauli*	0.1964	0.3145	0.1188	0.6235	0.7104	0.6633	0.2066	0.0796	2.5604	0.0689	1.6387
Hyloxalus	*subpunctatus*	0.1677	0.2650	0.1226	0.4929	0.5878	0.5274	0.1817	0.0440	1.9588	0.0834	1.9490

Genus	species	12S	16S	tRNA-VLM	CYTB	ND1	ND2	Pos1	Pos2	Pos3	dN	dS
Hyloxalus	*toachi*	0.1673	0.3197	0.1360	0.5131	0.6757	0.7008	0.2231	0.0517	2.3165	0.0733	2.1227
Hyloxalus	*vertebralis*	0.1641	0.2736	0.1168	0.5543	0.6380	0.6792	0.1925	0.0569	2.5559	0.0696	2.0369
Mannophryne	*collaris*	0.1911	0.3268	0.2615	0.6928	0.5418	0.6285	0.2335	0.0726	2.3758	0.0682	1.7414
Phyllobates	*aurotaenia*	0.1653	0.3126	0.2222	0.5635	0.6780	0.5938	0.2146	0.0811	1.8387	0.0670	1.5985
Phyllobates	*terribilis*	0.1643	0.3289	0.2053	0.5319	0.6779	0.6515	0.2351	0.0717	1.8751	0.0689	1.6387
Rheobates	*palmatus*	0.1958	0.2973	0.3378	0.6380	0.7442	0.7447	0.2578	0.0943	2.5383	0.0691	1.7674
Silverstoneia	*flotator*	0.2165	0.3235	0.2339	0.6916	0.7330	0.8023	0.2347	0.0798	2.9730	0.0853	2.2349
Silverstoneia	*nubicola*	0.1983	0.3331	0.2172	0.5651	0.6872	0.7148	0.2118	0.0692	2.5569	0.0743	1.9984

Table 4.7: Sequence divergence (branch length) from the mitochondrial genes codon positions, and nonsynonymous (dN) / synonymous (dS) substitutions of extant species to the last common ancestor of all poison frogs.

Genus	species	BDNF	BMP2	NACA	NT3	POMC	TYR	ZFX	Pos1	Pos2	Pos3	dN	dS
Allobates	*femoralis*	0.0263	0.0588	0.0632	0.0611	0.0710	0.1346	0.0410	0.0254	0.0140	0.1368	0.0087	0.1312
Allobates	*insperatus*	0.0187	0.0584	0.0680	0.0602	0.0700	0.1311	0.0473	0.0251	0.0120	0.1434	0.0085	0.1288
Allobates	*juanii*	0.0187	0.0509	0.0585	0.0583	0.0802	0.1243	0.0461	0.0231	0.0120	0.1355	0.0071	0.1094
Allobates	*kingsburyi*	0.0206	0.0495	0.0541	0.0504	0.0575	0.1210	0.0424	0.0219	0.0114	0.1207	0.0066	0.1033
Allobates	sp. Tachira	0.0169	0.0563	0.0652	0.0637	0.0680	0.1288	0.0528	0.0269	0.0133	0.1397	0.0088	0.1089
Allobates	*talamancae*	0.0169	0.0578	0.0576	0.0652	0.0582	0.1383	0.0386	0.0201	0.0093	0.1380	0.0086	0.1018
Allobates	*zaparo*	0.0275	0.0606	0.0625	0.0606	0.0710	0.1424	0.0422	0.0254	0.0127	0.1405	0.0084	0.1035
Ameerega	*bilinguis*	0.0255	0.0427	0.0724	0.0522	0.0829	0.1121	0.0348	0.0247	0.0127	0.1316	0.0100	0.1155
Ameerega	*hahneli*	0.0273	0.0496	0.0699	0.0602	0.0786	0.1183	0.0361	0.0267	0.0120	0.1355	0.0083	0.1023
Ameerega	*parvula*	0.0291	0.0445	0.0707	0.0542	0.0852	0.1124	0.0360	0.0234	0.0120	0.1362	0.0088	0.1326
Ameerega	*trivittata*	0.0255	0.0457	0.0665	0.0485	0.0842	0.1144	0.0361	0.0261	0.0120	0.1283	0.0080	0.1213
Anomaloglossus	sp. Ayacucho	0.0203	0.0657	0.0501	0.0616	0.0723	0.1177	0.0404	0.0290	0.0055	0.1275	0.0067	0.1039
Aromobates	*saltuensis*	0.0164	0.0513	0.0626	0.0495	0.0632	0.1165	0.0368	0.0257	0.0062	0.1272	0.0090	0.1128
Aromobates	*aff. alboguttatus*	0.0182	0.0528	0.0591	0.0495	0.0660	0.1056	0.0373	0.0244	0.0075	0.1238	0.0083	0.1023
Colostethus	*fugax*	0.0218	0.0435	0.0556	0.0524	0.0623	0.0991	0.0350	0.0193	0.0141	0.1125	0.0115	0.1318
Colostethus	*panamensis*	0.0312	0.0417	0.0541	0.0604	0.0685	0.0977	0.0379	0.0228	0.0114	0.1187	0.0047	0.0767
Colostethus	*pratti*	0.0312	0.0431	0.0580	0.0545	0.0610	0.1169	0.0376	0.0225	0.0094	0.1251	0.0097	0.1064
Dendrobates	*auratus*	0.0315	0.0534	0.0548	0.0665	0.1122	0.1131	0.0435	0.0284	0.0130	0.1396	0.0100	0.1106
Dendrobates	*bombetes*	0.0292	0.0424	0.0579	0.0731	0.0870	0.1065	0.0484	0.0284	0.0116	0.1346	0.0069	0.1064
Dendrobates	*captivus*	0.0239	0.0499	0.0581	0.0592	0.0849	0.1020	0.0410	0.0264	0.0130	0.1259	0.0082	0.0978
Dendrobates	*claudiae*	0.0340	0.0498	0.0553	0.0634	0.0850	0.1073	0.0471	0.0277	0.0103	0.1347	0.0076	0.0923
Dendrobates	*duellmani*	0.0273	0.0537	0.0553	0.0595	0.0825	0.1178	0.0471	0.0263	0.0084	0.1381	0.0090	0.1119
Dendrobates	*galactonotus*	0.0323	0.0580	0.0575	0.0997	0.1070	0.1440	0.0436	0.0319	0.0188	0.1530	0.0077	0.1174

Genus	species	BDNF	BMP2	NACA	NT3	POMC	TYR	ZFX	Pos1	Pos2	Pos3	dN	dS
Dendrobates	*histrionicus*	0.0238	0.0439	0.0513	0.0716	0.0875	0.1134	0.0447	0.0264	0.0130	0.1280	0.0113	0.1164
Dendrobates	*lamasi*	0.0219	0.0595	0.0576	0.0653	0.0853	0.1140	0.0483	0.0255	0.0097	0.1422	0.0123	0.1265
Dendrobates	*leucomelas*	0.0315	0.0595	0.0566	0.0703	0.1056	0.1135	0.0447	0.0310	0.0136	0.1403	0.0130	0.1341
Dendrobates	*pumilio*	0.0256	0.0439	0.0538	0.0735	0.0942	0.1112	0.0468	0.0277	0.0124	0.1328	0.0119	0.1218
Dendrobates	sp. Quibdo	0.0318	0.0637	0.0561	0.0616	0.0894	0.1157	0.0421	0.0283	0.0103	0.1394	0.0124	0.1275
Dendrobates	*sylvaticus*	0.0292	0.0457	0.0538	0.0716	0.0897	0.1094	0.0459	0.0283	0.0124	0.1318	0.0118	0.1216
Dendrobates	*tinctorius*	0.0297	0.0628	0.0557	0.0665	0.1036	0.1183	0.0472	0.0303	0.0131	0.1421	0.0132	0.1368
Dendrobates	*truncatus*	0.0315	0.0534	0.0548	0.0665	0.1100	0.1131	0.0435	0.0284	0.0130	0.1390	0.0127	0.1314
Dendrobates	*ventrimaculatus*	0.0237	0.0616	0.0578	0.0614	0.0847	0.1123	0.0471	0.0263	0.0090	0.1409	0.0122	0.1260
Dendrobates	*virolinensis*	0.0274	0.0406	0.0579	0.0712	0.0870	0.1109	0.0484	0.0284	0.0116	0.1339	0.0120	0.1238
Epipedobates	*anthonyi*	0.0218	0.0379	0.0644	0.0497	0.0561	0.1525	0.0298	0.0261	0.0127	0.1228	0.0094	0.1175
Epipedobates	*boulengeri*	0.0236	0.0397	0.0627	0.0523	0.0626	0.1375	0.0298	0.0255	0.0121	0.1206	0.0101	0.1275
Epipedobates	*machalilla*	0.0200	0.0379	0.0627	0.0485	0.0583	0.1415	0.0310	0.0248	0.0133	0.1172	0.0092	0.1150
Epipedobates	sp. F	0.0218	0.0415	0.0636	0.0524	0.0711	0.1398	0.0310	0.0248	0.0121	0.1263	0.0105	0.1324
Epipedobates	*tricolor*	0.0255	0.0415	0.0660	0.0485	0.0561	0.1415	0.0323	0.0255	0.0133	0.1234	0.0103	0.1303
Hyloxalus	*awa*	0.0201	0.0581	0.0537	0.0427	0.0528	0.1176	0.0404	0.0226	0.0087	0.1196	0.0097	0.1189
Hyloxalus	*azueriventris*	0.0182	0.0449	0.0499	0.0587	0.0638	0.1379	0.0374	0.0248	0.0094	0.1215	0.0095	0.1197
Hyloxalus	*bocagei*	0.0257	0.0418	0.0487	0.0426	0.0722	0.1253	0.0313	0.0201	0.0067	0.1197	0.0101	0.1221
Hyloxalus	*elachyhistus*	0.0201	0.0465	0.0549	0.0446	0.0550	0.1133	0.0372	0.0233	0.0094	0.1131	0.0089	0.1313
Hyloxalus	*maculosus*	0.0239	0.0385	0.0427	0.0407	0.0775	0.1302	0.0252	0.0181	0.0054	0.1134	0.0059	0.0925
Hyloxalus	*nexipus*	0.0182	0.0403	0.0508	0.0424	0.0596	0.1204	0.0413	0.0226	0.0067	0.1169	0.0095	0.0967
Hyloxalus	*sauli*	0.0239	0.0459	0.0436	0.0426	0.0773	0.1323	0.0264	0.0194	0.0061	0.1170	0.0095	0.0961
Hyloxalus	*subpunctatus*	0.0257	0.0457	0.0587	0.0423	0.0729	0.1157	0.0365	0.0255	0.0087	0.1212	0.0113	0.1164

Genus	species	BDNF	BMP2	NACA	NT3	POMC	TYR	ZFX	Pos1	Pos2	Pos3	dN	dS
Hyloxalus	*subpunctatus*	0.0257	0.0457	0.0587	0.0423	0.0729	0.1157	0.0365	0.0255	0.0087	0.1212	0.0093	0.1121
Hyloxalus	*toachi*	0.0201	0.0484	0.0554	0.0427	0.0571	0.1245	0.0446	0.0246	0.0100	0.1206	0.0089	0.1105
Hyloxalus	*vertebralis*	0.0182	0.0357	0.0555	0.0522	0.0881	0.1016	0.0400	0.0261	0.0088	0.1178	0.0059	0.0925
Mannophryne	*collaris*	0.0189	0.0498	0.0544	0.0474	0.0598	0.0996	0.0354	0.0231	0.0103	0.1119	0.0095	0.0967
Phyllobates	*aurotaenia*	0.0219	0.0328	0.0488	0.0654	0.0763	0.1077	0.0361	0.0249	0.0065	0.1172	0.0095	0.0961
Phyllobates	*terribilis*	0.0201	0.0328	0.0504	0.0635	0.0763	0.1056	0.0361	0.0249	0.0065	0.1164	0.0047	0.0767
Rheobates	*palmatus*	0.0188	0.0322	0.0464	0.0420	0.0567	0.1092	0.0304	0.0230	0.0058	0.1000	0.0100	0.1155
Silverstoneia	*flotator*	0.0218	0.0342	0.0541	0.0623	0.0701	0.1333	0.0426	0.0247	0.0140	0.1216	0.0115	0.1318
Silverstoneia	*nubicola*	0.0275	0.0360	0.0624	0.0845	0.0701	0.1408	0.0388	0.0292	0.0154	0.1320	0.0093	0.1121

Table 4.8: Sequence divergence (branch length) from the nuclear codon positions, and nonsynonymous (dN) / synonymous (dS) substitutions of extant species to the last common ancestor of all poison frogs.

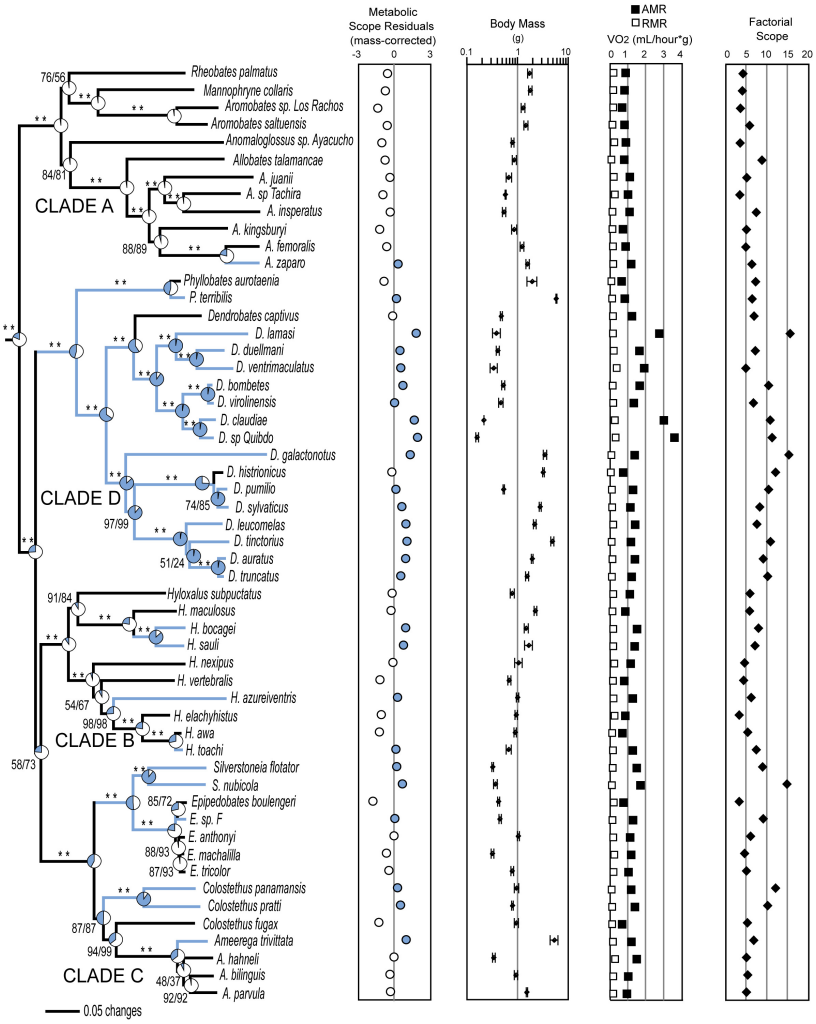

Figure 4.1: Phylogeny of the poison frogs, Scope (standardized residuals), body mass, RMR, AMR, and factorial metabolic scope of the poison frogs. Aerobic metabolic scope standardized residuals were determined by linear regression of the log-metabolic scope versus log-body mass. Ancestral reconstructions of low and high Scope were traced over the supermatrix phylogeny and total raw likelihood are indicated by pie charts (blue, high Scope; and white, low Scope). Support values in the phylogeny correspond to the summary of 500 maximum likelihood non-parametric bootstraps estimated with GARLI (left) and RAxML (right), * represents 100 support.

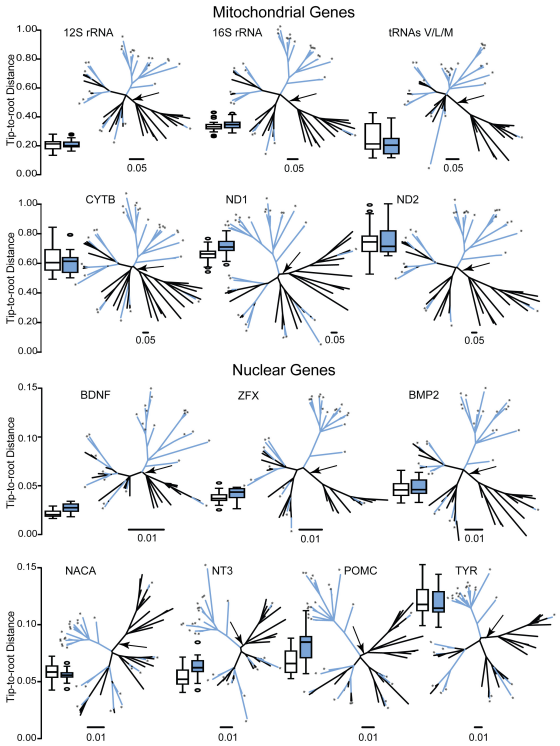

Figure 4.2: Box plots of the tip-to-root branch length and phylograms from each of the genes of the mitochondrial and nuclear loci. Blue boxplots and branches with stars on their tips represent a species with high Scope (positive residuals) determined after regressing Scope with body mass. White boxplots and black branches represent a species with low aerobic scope (negative residuals). Arrow indicates the position of the root of the tree. Mitochondrial gene abbreviations are 12S and 16S rDNA genes (12S and 16S); Valine, Leucine, and Methionine tRNA genes (tRNAs V-L-M); NADH subunit 1 (ND1); NADH subunit 2 (ND2); and Cytochrome b (CYTB). Nuclear gene abbreviations are brain-derived neurotrophic factor (BDNF); bone morphogenetic protein 2 (BMP2); NCX1 sodium-calcium exchanger 1 (NACA); 3'-nucleotidase (NT3); proopiomelanocortin A (POMC); tyrosinase precursor (TYR); and zinc finger E-box binding homeobox 2 (ZFX).

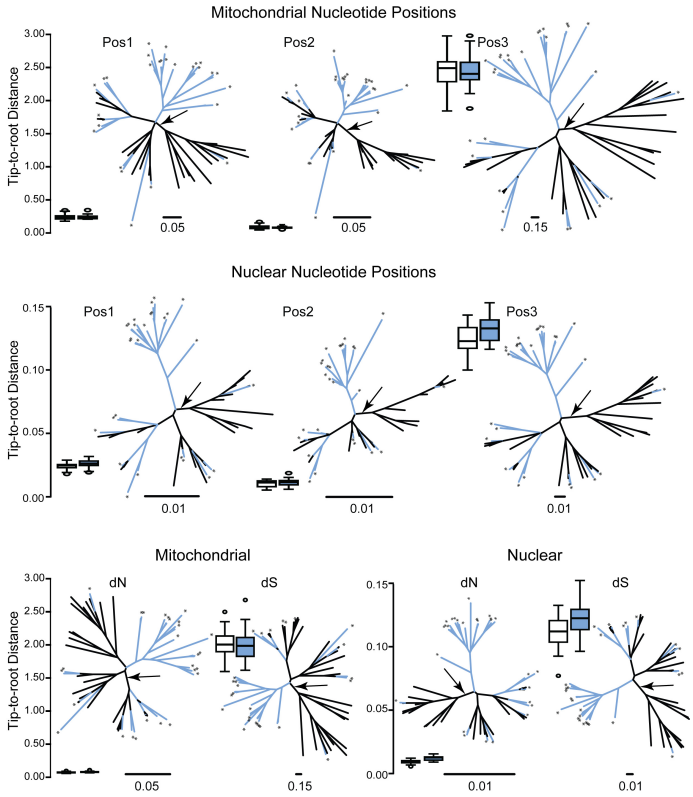

Figure 4.3: Box plots of the tip-to-root branch length and phylograms from the codon positions, nonsynonymous (dN) and synonymous (dS) substitution distances of the mitochondrial and nuclear loci. Codon positions for the mitochondrial loci correspond to the CYTB and ND2 combined sequence matrices. Codon positions for the nuclear loci are for the all genes combined sequence matrices. Blue boxplots and branches with stars on their tips represent a species with high aerobic scope (positive residuals) determined after regressing Scope with body mass. White boxplots and black branches represent a species with low aerobic scope (negative residuals). Arrow indicates the position of the root of the tree.

Bibliography

Adobe. 2008. Adobe Photoshop CS4. Adobe Systems Incorporated, San Jose.

Agapow, P. M., and A. Purvis. 2002. Power of eight tree shape statistics to detect nonrandom diversification: A comparison by simulation of two models of cladogenesis. Syst Biol 51:866-872.

Aguilera, O., and D. Rodrigues de Aguilera. 2004a. Amphi-American Neogene sea catfishes (Siluriformes, Ariidae) from northern South America. Pp. 29-48 *in* M. R. Sanchez-Villagra and J. A. Clack, eds. Fossils from the Miocene Castillo Formation, Venezuela: Contributions in Neotropical Paleontology. Special Papers in Paleontology. The Palaeontological Association.

Aguilera, O., and D. Rodrigues de Aguilera. 2004b. New Miocene otolith-based sciaenid species (Pisces, Perciformes) from Venezuela. Pp. 49-59 *in* M. R. Sanchez-Villagra and J. A. Clark, eds. Fossils from the Miocene Castillo Formation, Venezuela: Contributions in Neotropical Paleontology. Special Papers in Paleontology. The Paleontological Association.

Alatalo, R. V., and J. Mappes. 1996. Tracking the evolution of warning signals. Nature 382:708-710.

Almendáriz, A. 1987. Contribución al conocimiento de la herpetofauna centroriental Ecuatoriana. Revista Politécnica, Quito 12:144-177.

Alroy, J. 2002. How many named species are valid? Proc Natl Acad Sci U S A 99:3706-3711.

Banavar, J. R., A. Maritan, and A. Rinaldo. 1999. Size and form in efficient transportation networks. Nature 399:130-132.

Bartholomew, G. A., and J. R. B. Lighton. 1986. Oxygen consumption during hover-feeding in free-ranging *Anna* hummingbirds. J. Exp. Biol. 123:191-199.

Beard, K. H., K. A. Vogt, and A. Kulmatiski. 2002. Top-down effects of a terrestrial frog on forest nutrient dynamics. Oecologia 133:583-593.

Belle, E. M. S., G. Piganeau, M. Gardner, and A. Eyre-Walker. 2005. An investigation of the variation in the transition bias among various animal mitochondrial DNA. Gene 355:58-66.

Bermingham, E., and A. P. Martin. 1998. Comparative mtDNA phylogeography of neotropical freshwater fishes: testing shared history to infer the evolutionary landscape of lower Central America. Mol. Ecol. 7:499–517.

Bickler, P. E., and L. T. Buck. 2007. Hypoxia tolerance in reptiles, amphibians, and fishes: life with variable oxygen availability. Ann Rev Physiol 69:145-170.

Blount, J. D., M. P. Speed, G. D. Ruxton, and P. A. Stephens. 2009. Warning displays may function as honest signals of toxicity. Proc R Soc Lond B Biol Sci 276:871-877.

Blum, M. G. B., and O. Francois. 2006. Which random processes describe the tree of life? A large-scale study of phylogenetic tree imbalance. Syst Biol 55:685-691.

Bonilla, J. P., and E. La Marca. 1996. Hábitos alimentarios de Nephelobates alboguttatus (Anura, Dendrobatidae) en una selva nublada andina de Venezuela. Revista de Biologia Tropical 44:827-833.

Borenstein, M., L. V. Hedges, J. P. T. Higgins, and H. R. Rothstein. 2009. Introduction to Meta-Analysis. John Wiley & Sons, Ltd, Padstow, UK.

Bortolussi, N., E. Durand, M. Blum, and O. Francois. 2006. apTreeshape: statistical analysis of phylogenetic tree shape. Bioinformatics 22:363-364.

Bossuyt, F., R. M. Brown, D. M. Hillis, D. C. Cannatella, and M. C. Milinkovitch. 2006. Phylogeny and biogeography of a cosmopolitan frog radiation: Late Cretaceous diversification resulted in continent-scale endemism in the family Ranidae. Syst. Biol. 55:579-594.

Bossuyt, F., and M. C. Milinkovitch. 2000. Convergent adaptive radiations in Madagascan and Asian ranid frogs reveal covariation between larval and adult traits. Proc. Nat. Acad. Sci. 97:6585-6590.

Bozinovic, F., and F. F. Novoa. 1997. Metabolic costs of rodents feeding on plant chemical defenses: a comparison between an herbivore and an omnivore. Comp Biochem Physiol A Physiol 117:511-514.

Brochu, C. 1997. Morphology, fossils, divergence timing, and the phylogenetic relationships of Gavialis. Syst Biol 46:479-522.

Bromham, L. 2002. Molecular clocks in reptiles: Life history influences rate of molecular evolution. Mol Bio Evol 19:302-309.

Bromham, L. 2009. Why do species vary in their rate of molecular evolution? Biol Lett 5:401-404.

Bromham, L., and D. Penny. 2003. The modern molecular clock. Nat Rev Genet 4:216-224.

Bromham, L., A. Rambaut, and P. H. Harvey. 1996. Determinants of rate variation in mammalian DNA sequence evolution. J Mol Evol 43:610-621.

Broom, M., M. P. Speed, and G. D. Ruxton. 2005. Evolutionarily stable investment in secondary defences. Functional Ecology 19:836-843.

Brown, J. H., J. F. Gillooly, A. P. Allen, V. M. Savage, and G. B. West. 2004. Toward a metabolic theory of ecology. Ecology 85:1771-1789.

Brown, J. H., G. B. West, and B. J. Enquist. 2000. Scaling in biology: patterns, processes, causes, and consequences. Pp. 1-24 *in* J. H. B. a. G. B. West, ed. Scaling in Biology. Oxford University Press, New York, NY.

Brown, T. A. 2006. Confirmatory Factor Analysis for Applied Research. The Guildford Press, New York, NY.

Brumfield, R. T., and S. V. Edwards. 2007. Evolution into and out of the Andes: a Bayesian analysis of historical diversification in *Thamnophilus* antshrikes. Evolution 61:346-367.

Burnham, R. J., and A. Graham. 1999. The history of neotropical vegetation: New developments and status. Ann. Mo. Bot. Gard. 86:546-589.

Burton, T. M., and G. E. Likens. 1975. Energy flow and nutrient cycling in salamander populations in the Hubbard Brook Experimental Forest, New Hampshire. Ecology 56:1068-1080.

Bush, M. B. 1994. Amazonian speciation - a necessarily complex model. J. Biogeogr. 21:5-17.

Caccone, A., G. Gentile, C. E. Burns, E. Sezzi, W. Bergman, M. Ruelle, K. Saltonstall, and J. R. Powell. 2004. Extreme difference in rate of mitochondrial and nuclear DNA evolution in a large ectotherm, Galapagos tortoises. Mol Phylogenet Evol 31:794-798.

Calder, W. A., III. 1996. Size, Function, and Life History. Dover Publications, Inc., Mineola.

Caldwell, J. P. 1996. The evolution of myrmecophagy and its correlates in poison frogs (family Dendrobatidae). J. Zool., London 240:75-101.

Clough, M., and K. Summers. 2000. Phylogenetics systematics and biogeography of the poison frogs: evidence from mitochondrial DNA sequences. Biol. J. Linn. Soc. 70:515-540.

Coates, A. G., L. S. Collins, M. P. Aubry, and W. A. Berggren. 2004. The geology of the Darien, Panama, and the late Miocene-Pliocene collision of the Panama arc with northwestern South America. Geol. Soc. Am. Bull. 116:1327-1344.

Coates, A. G., and J. A. Obando. 1996. The geological evolution of the Central American Isthmus. Pp. 21-56 *in* J. B. C. Jackson, A. F. Budd and A. G. Coates, eds. Evolution and Environment in Tropical America. The University of Chicago Press.

Colless, D. H. 1982. Review of phylogentics: Phylogenetics: The Theory and Practice of Phylogenetic Systematics, by E. O. Wiley. Syst Zool 31:100-104.

Coloma, L. A. 1995. Ecuadorian frogs of the genus *Colostethus* (Anura:Dendrobatidae). Misc. Publ. Mus. Nat. Hist. Univ. Kansas 87:1–72.

Condit, R., N. Pitman, E. G. Leigh, J. Chave, J. Terborgh, R. B. Foster, P. Nunez, S. Aguilar, R. Valencia, G. Villa, H. C. Muller-Landau, E. Losos, and S. P. Hubbell. 2002. Beta-diversity in tropical forest trees. Science 295:666-669.

Cooper, M. A., F. T. Addison, R. Alvarez, C. M., R. H. Graham, A. B. Hayward, S. Howe, J. Martinez, J. Naar, R. Penas, A. J. Pulham, and A. Taborda. 1995. Basin development and tectonic history of the Llanos basin, Eastern Cordillera, and middle Magdalena Valley, Colombia. Am Assoc Pet Geol Bull 79:1421-1443.

Cortopassi, G. A., and E. Wang. 1996. There is substantial agreement among interspecies estimates of DNA repair activity. Mech Ageing Dev 91:211-218.

Cozzuol, M. A. 2006. The Acre vertebrate fauna: Age, diversity, and geography. J S Am Earth Sci 21:185-203.

Daly, J. W. 1998. Thirty years of discovering arthropod alkaloids in amphibian skin. J. Nat. Prod. 61:162-172.

Daly, J. W., H. M. Garraffo, P. Jain, T. F. Spande, R. R. Snelling, C. Jaramillo, and A. S. Rand. 2000a. Arthropod-frog connection: decahydroquinoline and pyrrolizidine alkaloids common to microsympatric myrmicine ants and dendrobatid frogs. J. Chem. Ecol. 26:73-85.

Daly, J. W., H. M. Garraffo, C. Jaramillo, and A. S. Rand. 1994a. Dietary source for skin alkaloids of poison frogs (Dendrobatidae)? J. Chem. Ecol. 20:943-955.

Daly, J. W., H. M. Garraffo, and T. F. Spande. 1999. Alkaloids from amphibian skins. Pp. 1-161 *in* S. W. Pelletier, ed. Alkaloids: chemical and biological perspectives. Pergamon Press, New York.

Daly, J. W., H. M. Garraffo, T. F. Spande, V. C. Clark, J. Y. Ma, H. Ziffer, and J. F. Cover. 2003. Evidence for an enantioselective pumiliotoxin 7-hydroxylase in dendrobatid poison frogs of the genus Dendrobates. Proc. Nat. Acad. Sci. 100:11092-11097.

Daly, J. W., H. M. Garraffo, T. F. Spande, M. W. Decker, J. P. Sullivan, and M. Williams. 2000b. Alkaloids from frog skin: the discovery of epibatidine and the potential for developing novel non-opioid analgesics. Nat. Prod. Rep. 17:131-135.

Daly, J. W., F. Gusovsky, C. W. Myers, M. Yotsu-Yamashita, and T. Yasumoto. 1994b. First occurrence of tetrodotoxin in a dendrobatid frog (*Colostethus inguinalis*), with further reports for the bufonid genus *Atelopus*. Toxicon 32:279-285.

Daly, J. W., T. Kaneko, J. Wilham, H. M. Garraffo, T. F. Spande, A. Espinosa, and M. A. Donnelly. 2002. Bioactive alkaloids of frog skin: combinatorial bioprospecting reveals that pumiliotoxins have an arthropod source. Proc. Nat. Acad. Sci. 99:13996-14001.

Daly, J. W., C. W. Myers, J. E. Warnick, and E. X. Albuquerque. 1980. Levels of batrachotoxin and lack of sensitivity to its action in poison-dart frogs (*Phyllobates*). Science 208:1383-1385.

Daly, J. W., C. W. Myers, and N. Whittaker. 1987. Further classification of skin alkaloids from neotropical poison frogs (Dendrobatidae), with a general survey of toxic/noxious substances in the Amphibia. Toxicon 25:1023-1095.

Daly, J. W., S. I. Secunda, H. M. Garraffo, T. F. Spande, A. Wisnieski, and J. F. Cover. 1994c. An uptake system for dietary alkaloids in poison frogs (Dendrobatidae). Toxicon 32:657-663.

Daly, J. W., S. I. Secunda, H. M. Garraffo, T. F. Spande, A. Wisnieski, C. Nishihira, and J. F. Cover Jr. 1992. Variability in alkaloid profiles in neotropical poison frogs (Dendrobatidae): genetic versus environmental determinants. Toxicon 30:887-898.

Daly, J. W., N. Ware, R. A. Saporito, T. F. Spande, and H. M. Garraffo. 2009. N-Methyldecahydroquinolines: An Unexpected Class of Alkaloids from Amazonian Poison Frogs (Dendrobatidae). J. Nat. Prod. Article ASAP DOI: 10.1021/np900094v Publication Date (Web): 11 May 2009

Darst, C. R., and D. C. Cannatella. 2004. Novel relationships among hyloid frogs inferred from 12S and 16S mitochondrial DNA sequences. Mol. Phylogenet. Evol. 31:462-475.

Darst, C. R., and M. E. Cummings. 2006. Predator learning favours mimicry of a less-toxic model in poison frogs. Nature 440:208-211.

Darst, C. R., M. E. Cummings, and D. C. Cannatella. 2006. A mechanism for diversity in warning signals: conspicuousness versus toxicity in poison frogs. Proc. Nat. Acad. Sci. U.S.A. 103:58252-5857.

Darst, C. R., P. A. Menendez-Guerrero, L. C. Coloma, and D. C. Cannatella. 2005. Evolution of dietary specialization and chemical defense in poison frogs (Dendrobatidae): a comparative analysis. Am. Nat. 165:56-69.

Dayan, T., and D. Simberloff. 2005. Ecological and community-wide character displacement: the next generation. Ecol Lett 8:875-894.

Diaz de Gamero, M. L. 1995. The changing course of the Orinoco River during the Neogene: a review. Palaeogeog. Palaeoclim. Palaeoecol. 123:385-402.

Dobler, S. 2001. Evolutionary aspects of defense by recycled plant compounds in herbivorous insects. Basic and Applied Ecology 2:15-26.

Duellman, W. E. 1999. Distribution patterns of amphibians in South America. Pp. 255-328 *in* W. E. Duellman, ed. Patterns of Distribution of Amphibians: A global perspective. The Johns Hopkins University Press, Baltimore.

Duellman, W. E. 2004. Frogs of the genus *Colostethus* (Anura; Dendrobatidae) in the Andes of Northern Peru. Scientific Papers, Natural History Museum, The University of Kansas 35:1-49.

Duellman, W. E. 2005. Biogeography. Pp. 433. Cusco Amazonico: The Lives of Amphibians and Reptiles in an Amazonian Rainforest. Cornell University Press, Ithaca, New York.

Duellman, W. E., and L. Trueb. 1986. Biology of Amphibians. McGraw-Hill, New York.

Evans, D. L., and J. O. Schmidt. 1990. Insect Defenses: Adaptive Mechanisms and Strategies of Prey and Predators., State University of New York Press.

Exnerová, A., E. Landová, P. Stys, R. Fuchs, M. Prokopová, and P. Cehláriková. 2003. Reactions of passerine birds to aposematic and non-aposematic firebugs (Pyrrhocoris apterus, Heteroptera). Biol J Linn Soc 78:517-525.

Feder, M. E., A. F. Bennett, and R. B. Huey. 2000. Evolutionary physiology. Ann Rev Ecol Syst 31:315-341.

Feder, M. E., and W. Burggren. 1992. Environmental physiology of the amphibians. Pp. 646. University of Chicago Press, Chicago.

Felsenstein, J. 1985. Phylogenies and the comparative method. Am Nat 125:1-15.

Fill, J. A. 1996. On the distribution of binary search trees under the random permutation model. Random Struct Algor 8:1-25.

Fisher, R. A. 1958. The genetical theory of natural selection. Dover Publications, New York.

Fjeldså, J. 1994. Geographical patterns for relict and young species of birds in Africa and South America and implications for conservation priorities. Biodivers. Conserv. 3:207-226.

Ford, L. S., and D. C. Cannatella. 1993. The major clades of frogs. Herp. Monogr. 7:94-117.

Forero, E. 1988. Botanical exploration and phytogeography of Colombia: past, present, and future. Taxon 37:561-566.

Frost, D. R., T. Grant, J. Faivovich, R. H. Bain, A. Haas, C. F. B. Haddad, R. O. De Sa, A. Channing, M. Wilkinson, S. C. Donnellan, C. J. Raxworthy, J. A. Campbell, B. L. Blotto, P. Moler, R. C. Drewes, R. A. Nussbaum, J. D. Lynch, D. M. Green, and W. C. Wheeler. 2006. The amphibian tree of life. Bull. Am. Mus. Nat. Hist. 297:1-370.

Futuyma, D., and G. Moreno. 1988. The evolution of ecological specialization. Ann. Rev. Ecol. Syst. 19:207-233.

Galtier, N., R. W. Jobson, B. Nabholz, S. Glemin, and P. U. Blier. 2009. Mitochondrial whims: metabolic rate, longevity and the rate of molecular evolution. Biol Lett 5:413-416.

Garland Jr., T., A. W. Dickerman, C. M. Janis, and J. A. Jones. 1993. Phylogenetic analysis of covariance by computer simulation. Syst Biol 42:265-292.

Garland, T., Jr, P. H. Harvey, and A. R. Ives. 1992. Procedures for the analysis of comparative data using phylogenetically independent contrasts. Syst Biol 41:18-32.

Garland, T., Jr. 1992. Rate tests for phenotypic evolution using phylogenetically independent contrasts. Am. Nat. 140:509-519.

Gatten, R. E., K. J. Miller, and R. J. Full. 1992. Energetics at rest and during locomotion. Pp. 646 *in* M. E. Feder and W. W. Burggren, eds. Environmental Physiology of the Amphibians. The University of Chicago, Chicago.

GeneCodes. 2006. Sequencher. Gene Codes Corp., Ann Arbor, MI. USA.

Gentry, A. H. 1992. Tropical forest biodiversity - Distributional patterns and their conservational significance. Oikos 63:19-28.

Gillooly, J. F., A. P. Allen, G. B. West, and J. H. Brown. 2005. The rate of DNA evolution: Effects of body size and temperature on the molecular clock. Proc Natl Acad Sci U S A 102:140-145.

Glazier, D. S. 2005. Beyond the '3/4-power law': variation in the intra- and interspecific scaling of metabolic rate in animals. Biol Rev Camb Philos Soc 80:611-662.

Gomes, F. R., J. G. Chaui-Berlinck, J. E. Bicudo, and C. A. Navas. 2004. Intraspecific relationships between resting and activity metabolism in anuran amphibians: influence of ecology and behavior. Physiol. Biochem. Zool. 77:197-208.

Grace, J. B. 2006. Structural Equation Modeling and Natural Systems. Cambridge University Press, Cambridge, UK.

Grant, T., D. R. Frost, J. P. Caldwell, R. Gagliardo, C. F. B. Haddad, P. J. R. Kok, B. D. Means, B. P. Noonan, W. Schargel, and W. C. Wheeler. 2006. Phylogenetic systematics of dart-poison frogs and their relatives (Anura: Athesphatanura: Dendrobatidae). Bull. Amer. Mus. Nat. Hist. 299:1-262.

Graur, D., and W.-H. Li. 2000. Fundamentals of Molecular Evolution. Sinauer Associates, Inc., Sunderland, MA.

Gregory-Wodzicki, K. M. 2000. Uplift history of the Central and Nothern Andes: a review. Geol. Soc. Am. Bull. 112:1091-1105.

Guerrero, J. 1997. Stratigraphy, sedimentary environments, and the Miocene uplift of the Colombian Andes. Pp. 15-43 *in* R. F. Kay, R. H. Madden, R. L. Cifelli and J. J. Flynn, eds. Vertebrate Paleontology in the Neotropics. Smithsonian Institution Press, Washington, D. C.

Guilford, T. 1988. The evolution of conspicuous coloration. Am. Nat. 131 Suppl.:S7-S21.

Guilford, T., and M. S. Dawkins. 1993. Receiver psychology and the design of animal signals. Trends in Neurosciences 16:430-436.

Gutscher, M. A., J. Malavielle, S. Lallemand, and J. Y. Collot. 1999. Tectonic segmentation of the North Andean margin: impact of the Carnegie Ridge collision. Earth Planet. Sci. Lett. 170:155-156.

Hagman, M., and A. Forsman. 2003. Correlated evolution of conspicuous coloration and body size in poison frogs (Dendrobatidae). Evolution 57:2904-2910.

Harlin, C., and M. Harlin. 2003. Towards a historization of aposematism. Evol. Ecol. 17:197-212.

Harvey, P. H., and M. D. Pagel. 1991. The Comparative Method in Evolutionary Biology. Oxford University Press, Oxford.

Heath, T. A., D. J. Zwickl, J. Kim, and D. M. Hillis. 2008. Taxon sampling affects inferences of macroevolutionary processes from phylogenetic trees. Syst Biol 57:160-166.

Hebert, P., E. Penton, J. Burns, D. Janzen, and W. Hallwachs. 2004. Ten species in one: DNA barcoding reveals cryptic species in the neotropical skipper butterfly Astraptes fulgerator. Proc Natl Acad Sci U S A 101:14812-14817.

Hemmingsen, A. M. 1960. Energy metabolism as related to body size and respiratory surfaces, and its evolution. Rep. Steno Memorial Hospital Nordisk Insulinlaboratorium 9:1-110.

Hickson, R. E., C. Simon, A. Cooper, G. S. Spicer, J. Sullivan, and D. Penny. 1996. Conserved sequence motifs, alignments, and secondary structure for the third domain of animal 12S rRNA. Mol Biol Evol 13:150-169.

Hirsh, A. E., and H. B. Fraser. 2001. Protein dispensability and rate of evolution. Nature 411:1046-1049.

Hoorn, C. 1994. An environmental reconstruction of the paleo-Amazon River system (Middle-Late Miocene, NW Amazonia). Palaeogeog. Palaeoclim. Palaeoecol. 112:187-238.

Hoorn, C. 2006. The birth of the mighty Amazon. Sci. Am. 294:52-59.

Hu, L., and P. M. Bentler. 1999. Cutoff criteria for fit indexes in covariance structure analysis: conventional criteria versus new alternatives. Structural Equation Modeling: A Multidisciplinary Journal 6:1-55.

Hubbell, S. P. 2001. The Unified Neutral Theory of Biodiversity and Biogeography. Princeton University Press, Princeton, NJ.

Huelsenbeck, J. P. 1991. When are fossils better than extant taxa in phylogenetic analysis? Syst. Zool. 40:458-469.

Huelsenbeck, J. P., D. M. Hillis, and R. Jones. 1996. Parametric bootstrapping in molecular phylogenetics: applications and performance. Pp. 19-45 *in* J. D. Ferraris and S. R. Palumbi, eds. Molecular Zoology: advances, strategies, and protocols. Wiley-Liss, New York.

Huelsenbeck, J. P., and F. P. Ronquist. 2001. MRBAYES: Bayesian inference of phylogenetic trees. Bioinformatics 17:754-755.

Hulbert, A. J., and P. L. Else. 2000. Mechanisms underlying the cost of living in animals. Ann Rev Physiol 62:207-235.

Hungerbuhler, D., M. Steinmann, W. Winkler, D. Seward, A. Eguez, D. E. Peterson, U. Helg, and C. Hammer. 2002. Neogene stratigraphy and Andean geodynamics of southern Ecuador. Earth-Sci. Rev. 57:75-124.

Ianson, G. R., and A. H. Murray. 1996. The energy costs of ingestion of naturally occuring nontannin plant phenolics by sheep. Physiol Zool 69:532-546.

IUCN, C. International, and NatureServe. 2006. Global Amphibian Assessment. <www.globalamphibians.org>. Downloaded on 4 May 2006.

Jaramillo, C., M. J. Rueda, and G. Mora. 2006. Cenozoic plant diversity in the Neotropics. Science 311:1893-1896.

Kaandorp, R. J. G., F. P. Wesselingh, and H. B. Vonhof. 2006. Ecological implications from geochemical records of Miocene Western Amazonian bivalves. J S Am Earth Sci 21:54-74.

Karasov, W. H., and C. Martinez del Rio. 2007. Physiological Ecology: How Animals Process Energy, Nutrients, and Toxins. Princeton University Press, Princeton, NJ.

Kerr, A. C. 2005. La Isla de Gorgona, Colombia: A petrological enigma? Lithos 84:77-101.

Kiesecker, J., A. Blaustein, and L. Belden. 2001. Complex causes of amphibian population declines. Nature 410:681-684.

Kjer, K. M. 1995. Use of rRNA secondary structure in phylogenetic studies to identify homologous positions: an example of alignment and data presentation from the frogs. Mol Phylogenet Evol 4:314-330.

Knowlton, N., and L. A. Weigt. 1998. New dates and new rates for divergence across the Isthmus of Panama. Proc. R. Soc. Lond. B 265:2257–2263.

Koch, P. B., B. Behnecke, and R. H. ffrench-Constant. 2000. The molecular basis of melanism and mimicry in a swallowtail butterfly. Curr. Biol. 10:591-594.

Komárek, S. 1998. Mimicry, aposematism and related phenomena in animals and plants. Bibliography 1800-1990. Vesmír, Prague.

Kozak, K. H., R. W. Mendyk, and J. J. Wiens. 2009. Can parallel diversification occur in sympatry? Repeated patterns of body-size evolution in coexisting clades of North American salamanders. DOI: 10.1111/j.1558-5646.2009.00680.x. Evolution

Kozak, K. H., and J. J. Wiens. 2007. Climatic zonation drives latitudinal variation in speciation mechanisms. Proc R Soc Lond B Biol Sci 274:2995-3003.

Kumar, S., and S. B. Hedges. 1998. A molecular timescale for vertebrate evolution. Nature 392:917-920.

Kurland, C. G., and S. G. E. Andersson. 2000. Origin and evolution of the mitochondrial proteome. Microbiol Mol Biol Rev 64:786-+.

La Marca, E. 1995 [1994]. Taxonomy of the frogs of the genus Mannophryne (Amphibia; Anura: Dendrobatidae). Publ. Asoc. Amigos Donana 4:1-75.

Lanfear, R., J. A. Thomas, J. J. Welch, T. Brey, and L. Bromham. 2007. Metabolic rate does not calibrate the molecular clock. Proc Natl Acad Sci U S A 104:15388-15393.

Latrubesse, E. M., J. Bocquentin, C. R. Santos, and C. G. Ramonell. 1997. Paleoenvironmental model for the late Cenozoic southwestern Amazonia: paleontology and geology. Acta Amazonica 27

Lemmon, A. R., J. M. Brown, K. Stanger-Hall, and E. C. Moriarty-Lemmon. 2008. The effect of missing data on phylogenetic estimates obtained by

maximum-likelihood and bayesian inference. (in press). Syst. Biol.:(in press).

Lewis, P. O. 2001. A likelihood approach to estimating phylogeny from discrete morphological character data. Syst Biol 50:913-925.

Lighton, J. R. B. 2008. Measuring Metabolic Rates: a Manual fo Scientists. Oxford University Press, New York, NY.

Lindström, L. 1999. Experimental approaches to studying the initial evolution of conspicuous aposematic signalling. Evolutionary Ecology 13:605-618.

Lindström, L., R. V. Alatalo, J. Mappes, M. Riipi, and L. Vertainan. 1999. Can aposematic signals evolve by gradual change? Nature 397:249-251.

Lips, K., J. Diffendorfer, and J. Mendelson. 2008. Riding the wave: Reconciling the roles of disease and climate change in amphibian declines. PLoS Biol 6:441-454.

Lovejoy, N. R., J. S. Albert, and W. G. R. Crampton. 2006. Miocene marine incursions and marine/freshwater transitions: Evidence from Neotropical fishes. J. South Am. Earth. Sci. 21:5-13.

Lötters, S., K. H. Jungfer, and A. Widmer. 2000. A new genus of aposematic poison frog (Amphibia: Anura: Dendrobatidae) from the upper Amazon basin with notes on its reproductive behaviour and tadpole morphology. Jhrh. Ges. Naturk. Württemberg 156:233-243.

Maddison, D. R., and W. P. Maddison. 2000. MacClade 4: Analysis of phylogeny and character evolution. Version 4.0. Sinauer Associates, Sunderland, Massachusetts.

Maddison, W. P., and D. R. Maddison. 2001. MacClade 4: analysis of phylogeny and character evolution. Sinauer Associates, Sunderland, Massachusetts, USA.

Maddison, W. P., and D. R. Maddison. 2009. Mesquite: a modular system for evolutionary analysis. http://mesquiteproject.org.

Magallon, S., and M. J. Sanderson. 2001. Absolute diversification rates in angiosperm clades. Evolution 55:1762-1780.

Mallet, J., and M. Joron. 1999. Evolution of diversity in warning color and mimicry: polymorphisms, shifting balance, and speciation. Ann. Rev. Ecol. Syst. 30:201-33.

Marchant, R., and H. Hooghiemstra. 2004. Rapid environmental change in African and South American tropics around 4000 years before present: a review. Earth Sci Rev 66:217-260.

Marples, N. M., D. J. Kelly, and R. J. Thomas. 2005. Perspective: the evolution of warning coloration is not paradoxical. Evolution 59:933-940.

Martin, A. P. 1999. Substitution rates of organelle and nuclear genes in sharks: Implicating metabolic rate (again). Mol Bio Evol 16:996-1002.

Martin, A. P., G. J. P. Naylor, and S. R. Palumbi. 1992. Rates of mitochondrial-dna evolution in sharks are slow compared with mammals. Nature 357:153-155.

Martin, A. P., and S. R. Palumbi. 1993. Body size, metabolic rate, generation time, and the molecular clock. Proc Natl Acad Sci U S A 90:4087-4091.

Martins, E., and T. F. Hansen. 1997. Phylogenies and the comparative method: a general approach to incorporating phylogenetic information into the analysis of interspecific data. Am Nat 149:646-667.

Meiklejohn, C. D., K. L. Montooth, and D. M. Rand. 2007. Positive and negative selection on the mitochondrial genome. Trends Genet. 23:259-263.

Midford, P. E., T. J. Garland, and W. P. Maddison. 2005. PDAP Package of Mesquite.

Moen, D. S., and J. J. Wiens. 2009. Phylogenetic evidence for competitively driven divergence: body-size evolution in caribbean treefrogs (Hylidae: Osteopilus). Evolution 63:195-214.

Mooers, A. O., and S. B. Heard. 1997. Evolutionary process from phylogenetic tree shape. Q Rev Biol 72:31-54.

Morales, V. R. 2002 [2000]. Sistematica y biogeografia del grupo *trilineatus* (Amphibia, Anura, Dendrobatidae, *Colostethus*) con description de once nuevas especies. Publicaciones de la Asociacion de Amigos de Doñana 13:1-59.

Moritz, C., J. L. Patton, C. J. Schneider, and T. B. Smith. 2000. Diversification of rainforest faunas: An integrated molecular approach. Ann. Rev. Ecol. Syst. 31:533-563.

Muthén, B. O., and L. K. Muthén. 2008. Mplus (Version 5), (1998-2006). Los Angeles, CA.

Myers, C. W., and J. W. Daly. 1976. Preliminary evaluation of skin toxins and vocalizations in taxonomic and evolutionary studies of poison-dart frogs (Dendrobatidae). Bull. Am. Mus. Nat. Hist. 157:173-262.

Myers, C. W., J. W. Daly, H. M. Garraffo, A. Wisnieski, and J. F. Cover, Jr. 1995. Discovery of the Costa Rican poison frog *Dendrobates granuliferus* in sympatry with *Dendrobates pumilio*, and comments on the taxonomic use of skin alkaloids. American Museum Novitates 3144:1-21.

Myers, C. W., A. Paolillo O., and J. W. Daly. 1991. Discovery of a defensively malodorous and nocturnal frog in the family Dendrobatidae: phylogenetic significance of a new genus and species from the venezuelan Andes. Am. Mus. Novit. 3002:1-33.

Myers, N., R. A. Mittermeier, C. G. Mittermeier, A. B. da Fonseca, and J. Kent. 2000. Biodiversity hotspots for conservation priorities. Nature 403:853-858.

Nabholz, B., S. Glemin, and N. Galtier. 2008. Strong variations of mitochondrial mutation rate across mammals - the longevity hypothesis. Mol Bio Evol 25:120-130.

Nabholz, B., S. Glemin, and N. Galtier. 2009. The erratic mitochondrial clock: variations of mutation rate, not population size, affect mtDNA diversity across birds and mammals. BMC Evol Biol 9

Navas, C. A. 1996a. Implications of microhabitat selection and patterns of activity on the thermal ecology of high elevation neotropical anurans. Oecologia 108:617-626.

Navas, C. A. 1996b. Metabolic physiology, locomotor performance, and thermal niche breadth in Neotropical anurans. Phys. Zool. 69:1481-1501.

Navas, C. A., and F. R. Gomes. 2001. Time in captivity as a confunding variable in herpetological research: an example from the metabolic physiology of treefrogs (Scinax). Herpetol. Rev. 32:228-230.

Nee, S. 2001. Inferring speciation rates from phylogenies. Evolution 55:661-668.

Neuwirth, M., J. W. Daly, C. W. Myers, and L. W. Tice. 1979. Morphology of the granular secretory glands in skin of poison-dart frogs (Dendrobatidae). Tissue & Cell 11:755-771.

Nishida, R. 2002. Sequestration of defensive substances from plants by Lepidoptera. Ann. Rev. Ent. 47:57-92.

Noble, G. K. 1926. The pectoral girdle of the brachycephalid frogs. Am. Mus. Novit. 230:1-14.

Nunn, C. L., and B. R. A. 2000. Allometric slopes and independent contrasts: A comparative test of Kleiber's law in primate ranging patterns. Am Nat 156:519-533.

Ohta, T. 1993. An examination of the generation-time effect on molecular evolution. Proc Natl Acad Sci U S A 90:10676-10680.

Pagel, M. 1993. Seeking the evolutionary regression coefficient: an analysis of what comparative methods measure. J. Theor. Bio. 164:191–205.

Pagel, M. 1997. Inferring evolutionary processes from phylogenies. Zoologica Scr. 26:331-348.

Pagel, M. 1999. The maximum likelihood approach to reconstructing ancestral character states of discrete characters on phylogenies. Syst. Biol. 48:612-622.

Pagel, M., and A. Meade. 2006. Bayesian analysis of correlated evolution of discrete characters by reversible-jump Markov chain Monte Carlo. (www.evolution.rdg.ac.uk.). Am. Nat. 167:808-825.

Pagel, M., and A. Meade. 2007. BayesTraits Manual. http://www.evolution.rdg.ac.uk/BayesTraits.html. School of Biological Sciences. University of Reading, Reading, UK.

Pagel, M., A. Meade, and D. Barker. 2004. Bayesian estimation of ancestral character states on phylogenies. Syst Biol 53:673-684.

Pal, C., B. Papp, and M. J. Lercher. 2006. An integrated view of protein evolution. Nat Rev Genet 7:337-348.

Paradis, E. 1997. Assessing temporal variations in diversification rates from phylogenies: estimation and hypothesis testing. Proc. R. Soc. Lond., B, Biol. Sci. 264:1141-1147.

Patton, J. L., and M. N. F. da Silva. 1998. Rivers, refuges and ridges: the geography of speciation of Amazonian mammals *in* D. J. Howard and S. H. Berlocher, eds. Endless Forms: Species and Speciation. Oxford University Press, New York.

Pechmann, J. H. K., D. E. Scott, R. D. Semlitsch, J. P. Caldwell, L. J. Vitt, and J. W. Gibbons. 1991. Declining amphibian populations: The problem of seperating human impacts from natural fluctuations. Science 253:825-940.

Perez-Campo, R., M. Lopez-Torres, S. Cadenas, C. Rojas, and G. Barja. 1998. The rate of free radical production as a determinant of the rate of aging: evidence from the comparative approach. J Comp Physiol B 168:149-158.

Pesole, G., C. Gissi, A. De Chirico, and C. Saccone. 1999. Nucleotide substitution rate of mammalian mitochondrial genomes. J Mol Evol 48:427-434.

Pianka, E. R. 1986. Ecology and Natural History of Desert Lizards: Analyses of the Ecological Niche and Community Structure. Princeton University Press, Princeton, NJ.

Pigliucci, M., and K. Preston. 2004. Phenotypic Integration: Studying the Ecology and Evolution of Complex Phenotypes. Oxford University Press, New York, NY.

Pitman, N. C. A., J. W. Terborgh, M. R. Silman, P. Nunez, D. A. Neill, C. E. Ceron, W. A. Palacios, and M. Aulestia. 2001. Dominance and distribution of tree species in upper Amazonian terra firme forests. Ecology 82:2101-2117.

Pollock, D. D., D. J. Zwickl, J. A. McGuire, and D. M. Hillis. 2002. Increased taxon sampling is advantageous for phylogenetic inference. Syst Biol 51:664-671.

Posada, D., and T. R. Buckley. 2004. Model selection and model averaging in phylogenetics: advantages of the AIC and Bayesian approaches over likelihood ratio tests. Syst. Biol. 53:793-808.

Posada, D., and K. A. Crandall. 1998. Modeltest: testing the model of DNA substitution. Bioinformatics 14:817-818.

Pough, F. H., and T. Taigen. 1990. Metabolic correlates of the foraging and social-behavior of dart-poison frogs. Anim. Behav. 39:145-155.

Pounds, J., M. Bustamante, L. Coloma, J. Consuegra, M. Fogden, P. Foster, E. La Marca, K. Masters, A. Merino-Viteri, R. Puschendorf, S. Ron, G. Sanchez-Azofeifa, C. Still, and B. Young. 2006. Widespread amphibian extinctions from epidemic disease driven by global warming. Nature 439:161-167.

Pybus, O. G., and P. H. Harvey. 2000. Testing macro-evolutionary models using incomplete molecular phylogenies. Proc. R. Soc. Lond., B, Biol. Sci. 267:2267-2272.

Rabosky, D. L. 2006. LASER: a maximum likelihood toolkit for detecting temporal shifts in diversification rates. Evol Bioinform Online 2:257-260.

Rabosky, D. L., S. C. Donnellan, A. L. Talaba, and I. J. Lovette. 2007. Exceptional among-lineage variation in diversification rates during the radiation of Australia's most diverse vertebrate clade. Proc R Soc Lond B Biol Sci 274:2915-2923.

Rabosky, D. L., and I. J. Lovette. 2008. Explosive evolutionary radiations: decreasing speciation or increasing extinction throught time? Evolution doi:10.1111/j.1558-5646.2008.00409.x:1-10.

Rambaut, A., and A. J. Drummond. 2008. TreeStat v1.2 (http://tree.bio.ed.ac.uk/software/treestat/), Edinburgh, U.K.

Rambaut, A., and N. C. Grassly. 1997. Seq-Gen: an application for the Monte Carlo simulation of DNA sequence evolution along phylogenetic trees. Comput Appl Biosci 13:235-238.

Rand, D. M., and L. M. Kann. 1998. Mutation and selection at silent and replacement sites in the evolution of animal mitochondrial DNA. Genetica 102-3:393-407.

Raup, D. M. 1985. Mathematical-models of cladogenesis. Paleobiology 11:42-52.

Ree, R. H., B. R. Moore, C. O. Webb, and M. J. Donoghue. 2005. A likelihood framework for inferring the evolution of geographic range on phylogenetic trees. Evolution 59:2299-2311.

Ree, R. H., and S. A. Smith. 2007. Lagrange: software for likelihood analysis of geographic range evolution. <http://code.google.com/p/lagrange>.

Ree, R. H., and S. A. Smith. 2008. Maximum-likelihood inference of geographic range evolution by dispersal, local extinction, and cladogenesis. Syst Biol 57:4-14.

Richardson, J. E., R. T. Pennington, T. D. Pennington, and P. M. Hollingsworth. 2001. Rapid diversification of a species-rich genus of neotropical rain forest trees. Science 5538:2242-2245.

Rivero, J. A. 1988[1990]. Sobre las relaciones de las especies del genero *Colostethus* (Amphibia, Dendrobatidae). Mem. Soc. Cien. Nat. La Salle 18:3-32.

Roberts, J. L., J. L. Brown, R. von May, W. Arizabal, R. Schulte, and K. Summers. 2006. Genetic divergence and speciation in lowland and montane peruvian poison frogs. Mol Phylogenet Evol 41:149-164.

Robinson, B. W., and D. S. Wilson. 1998. Optimal foraging, specialization, and a solution to Liem's paradox. Am Nat 151:223-235.

Roelants, K., D. J. Gower, M. Wilkinson, S. P. Loader, S. D. Biju, K. Guillaume, L. Moriau, and F. Bossuyt. 2007. Global patterns of diversification in the history of modern amphibians. Proc. Nat. Acad. Sci. U.S.A. 104:887-892.

Rogowitz, G. L., and J. Sánchez-Rivoleda. 1999. Locomotor performance and aerobic capacity of the cave coquí, Eleutherodactylus cooki. Copeia 1999:40-48.

Ronquist, F. 1997. Dispersal-vicariance analysis: a new approach to the quantification of historical biogeography. Syst. Biol. 46:195-203.

Ronquist, F. 2004. Bayesian inference of character evolution. Trends Ecol. Evol. (Amst.) 19:475-481.

Ronquist, F., and J. P. Huelsenbeck. 2003. MRBAYES 3: Bayesian phylogenetic inference under mixed models. Bioinformatics 19:1572-1574.

Ruta, M., M. Coates, and H. Ibarra-Vidal. 2003a. Bones, molecules and crown-tetrapod origins. *in* P. C. J. Donoghue and M. P. Smith, eds. Telling the Evolutionary Time: Molecular Clocks and the Fossil Record. Taylor & Francis., London.

Ruta, M., M. I. Coates, and D. L. J. Quicke. 2003b. Early tetrapod relationships revisited. Biol. Rev. Camb. Philos. Soc. 78:251-345.

Rutschmann, F. 2005. Bayesian dating step-by-step manual (version 1.5, July 2005). http://www.plant.ch/software.html/bayesiandating1.5.pdf.

Ruxton, G. D., and T. N. Sherratt. 2006. Aggregation, defence and warning signals: the evolutionary relationship. Proc. R. Soc. 273:2417-2424.

Ruxton, G. D., T. N. Sherratt, and M. P. Speed. 2004. Avoiding Attack: The Evolutionary Ecology of Crypsis, Warning Signals & Mimicry. Oxford University Press, Oxford.

Sanchíz, B. 1998. Salientia. Verlag Dr. Friedrich Pfeil, München.

Sanderson, M. J. 2002. Estimating absolute rates of molecular evolution and divergence times: A penalized likelihood approach. Mol Biol Evol 19:101-109.

Sanderson, M. J. 2003. r8s: inferring absolute rates of molecular evolution and divergence times in the absence of a molecular clock. Bioinformatics 19:301-302.

Sanderson, M. J., J. L. Thorne, N. Wikstrom, and K. Bremer. 2004. Molecular evidence on plant divergence times. Am. J. Bot. 91:1656-1665.

Santos, J. C., L. A. Coloma, and D. C. Cannatella. 2003. Multiple, recurring origins of aposematism and diet specialization in poison frogs. Proc. Nat. Acad. Sci. U.S.A. 100:12792-12797.

Santos, J. C., L. A. Coloma, K. Summers, J. P. Caldwell, R. Ree, and D. C. Cannatella. 2009. Amazonian amphibian diversity is primarily derived from late Miocene Andean lineages. PLoS Biology 7:e56 doi:10.1371/journal.pbio.1000056.

Saporito, R. A., M. A. Donnelly, R. L. Hoffman, H. M. Garraffo, and J. W. Daly. 2003. A siphonotid millipede (*Rhinotus*) as the source of

spiropyrrolizidine oximes of dendrobatid frogs. J. Chem. Ecol. 29:2781-2786.

Saporito, R. A., M. A. Donnelly, P. Jain, H. M. Garraffo, T. F. Spande, and J. W. Daly. 2007. Spatial and temporal patterns of alkaloid variation in the poison frog Oophaga pumilio in Costa Rica and Panama over 30 years. Toxicon 50:757-778.

Saporito, R. A., H. M. Garraffo, M. A. Donnelly, A. L. Edwards, J. T. Longino, and J. W. Daly. 2004. Formicine ants: An arthropod source for the pumiliotoxin alkaloids of dendrobatid poison frogs. Proc. Nat. Acad. Sci. 101:8045-8050.

Saporito, R. A., T. F. Spande, H. M. Garraffo, and M. A. Donnelly. 2009. Arthropod alkaloids in poison frogs: A review of the 'dietary hypothesis'. Heterocycles 79:277-297.

Schlichting, C. 2004. The diversity of complexity. Pp. 443 *in* M. a. K. Pigliucci, Preston, ed. Phenotypic Integration: Studying the Ecology and Evolution of Complex Phenotypes. Oxford University Press, New York, NY.

Schmidt-Nielsen, K. 1984. Scaling: Why is animal size so important? Cambridge University Press, Cambridge.

Seale, D. B. 1987. Amphibia. Pp. 467-552 *in* T. J. a. F. J. Pandian, Vernberg, ed. Animal Energetics: Bivalvia through Reptilia. Academic Press, Inc., San Diego, CA.

Seddon, J. M., P. R. Beaverstock, and A. Georges. 1998. The rate of mitochondrial 12S rRNA gene evolution is similar in freshwater turtles and marsupials. J Mol Evol 46:460-464.

Semple, C., and M. Steel. 2003. Phylogenetics. Oxford University Press, Oxford, UK.

Sepkoski, J. J. 1997. Biodiversity: Past, present, and future. J Paleontol 71:533-539.

Servedio, M. R. 2000. The effects of predator learning, forgetting, and recognition errors on the evolution of warning coloration. Evolution 54:751-763.

Señaris, J. C., and R. MacCulloch. 2005. Amphibians. Pp. 9-23 *in* T. Hollowell and R. P. Reynolds, eds. Checklist of the Terrestrial Vertebrates of the Guiana Shield. Bulletin of the Biological Society of Washington, Washington.

Sillén-Tullberg, B. 1988. Evolution of gregariousness in aposematic butterfly larvae: a phylogenetic analysis. Evolution 42:293-305.

Silverstone, P. A. 1975. A revision of the poison-arrow frogs of the genus *Dendrobates* Wagler. Science Bulletin, L.A. Cty. Nat. Hist. Mus.:1-55.

Simpson, E. H. 1949. Measurement of diversity. Nature 163:688.

Smith, S. A., and M. J. Donoghue. 2008. Rates of molecular evolution are linked to life history in flowering plants. Science 322:86-89.

SPSS. 2008. SPSS for Windows, Rel. 16.0.2 (April 10th, 2008), Chicago.

Stamatakis, A. 2006. RAxML-VI-HPC: Maximum likelihood-based phylogenetic analyses with thousands of taxa and mixed models. Bioinformatics 22:2688–2690.

Stattersfield, A. J., M. J. Crosby, A. J. Long, and D. C. Wege. 1998. Endemic Bird Areas of the World. BirdLife International, Cambridge, UK.

Stevens, M. 2007. Predator perception and the interrelation between different forms of protective coloration. Proc R Soc Lond B Biol Sci 274:1457-1464.

Stewart, M. M., and L. L. Woolbright. 1996. Amphibians. Pp. 273-320 *in* D. P. a. R. B. Reagan, Waide, ed. The Food Web of a Tropical Rain Forest. University Of Chicago Press, Chicago, IL.

Summers, K. 2000. Mating and aggressive behaviour in dendrobatid frogs from Corcovado National Park, Costa Rica: A comparative study. Behaviour 137:7-24.

Summers, K., and M. Clough. 2001. The evolution of coloration and toxicity in the poison frog family (Dendrobatidae). Proc. Nat. Acad. Sci. 98:6227-6232.

Summers, K., and D. J. D. Earn. 1999. The cost of polygyny and the evolution of female care in poison frogs. Biol. J. Linn. Soc. 66:515-538.

Summers, K., L. Weigt, P. Boag, and E. Bermingham. 1999. The evolution of female parental care in poison frogs of the genus *Dendrobates*: Evidence from mitochondrial DNA sequences. Herpetologica 55:254-270.

Swofford, D. L. 2000. PAUP* Phylogenetic analysis using parsimony (*and other methods), version 4.0b.8a. Sinauer., Sunderland, Massachusetts.

Swofford, D. L., G. J. Olsen, P. J. Waddell, and D. M. Hillis. 1996. Phylogenetic inference. Pp. 407-514 *in* D. M. Hillis, C. Moritz and B. K. Mable, eds. Molecular systematics. Sinauer Associates, Sunderland, Massachusetts.

Taigen, T., and F. H. Pough. 1983a. Prey preference, foraging behavior, and metabolic characteristics of frogs. Am Nat 122:509-520.

Taigen, T., and F. H. Pough. 1985. Metabolic correlates of anuran behavior. Amer. Zool. 25:987-997.

Taigen, T. L., and F. H. Pough. 1983b. Prey preference, foraging behavior, and metabolic characterstics of frogs. Amer. Nat. 122:509-520.

Takada, W., T. Sakata, S. Shimano, Y. Enami, N. Mori, R. Nishida, and Y. Kuwahara. 2005. Scheloribatid mites as the source of pumiliotoxins in dendrobatid frogs. J Chem Ecol 31:2403–2415.

Thompson, J. D., T. J. Gibson, F. Plewniak, F. Jeanmougin, and D. Higgins. 1997. The Clustal X window interface: flexible strategies for multiple sequence alignment aided by quality analysis tools. Nucleic Acids Res. 25:4876-4882.

Thorne, J. L., and H. Kishino. 2002. Divergence time and evolutionary rate estimation with multilocus data. Syst. Biol. 51:689-702.

Toft, C. A. 1977. Partition of Food in a Community of Tropical Frogs. Pp. 63. Princeton University, Princeton, NJ.

Toft, C. A. 1980. Feeding ecology of thirteen syntopic species of anurans in a seasonal tropical environment. Oecologia (Berl.) 45:131-141.

Toft, C. A. 1981. Feeding ecology of Panamanian litter anurans: Patterns of diet and foraging mode. J. Herpetol. 15:139-144.

Toft, C. A. 1995. Evolution of diet specialization in poison-dart frogs (Dendrobatidae). Herpetologica 51:202-216.

Townsend, T. M., E. R. Alegre, S. T. Kelley, J. J. Wiens, and T. W. Reeder. 2008. Rapid development of multiple nuclear loci for phylogenetic analysis using genomic resources: An example from the squamate reptile Tree of Life project. Mol Phylogenet Evol 47:129-142.

Tullberg, B. S., O. Leimar, and G. Gamberale-Stille. 2000. Did aggregation favour the initial evolution of warning coloration? A novel world revisited. Anim. Behav. 59:281-287.

Twomey, E., and J. L. Brown. 2008. Spotted poison frog: rediscovery of the lost species and a new genus (Anura: Dendrobatidae) from Northwestern Peru. Herpetologica 64:121-137.

Ullman, J. B. 2007. Structural Equation Modeling *in* B. G. L. S. Tabachnick, Fidell, ed. Using Multivariate Statistics. Pearson Education, Inc., Boston, MA.

Valderrama-Vernaza, M., P. Ramírez-Pinilla, and V. H. Serrano-Cardozo. 2009. Diet of the Andiean frog Ranitomeya virolinensis (Athesphatanura: Dendrobatidae). J Herpetology 43:114-123.

Van Buskirk, J., and U. K. Steiner. 2009. The fitness costs of developmental canalization and plasticity. J Evol Biol 22:852-860.

Vantienderen, P. H. 1991. Evolution of generalists and specialists in spatially heterogeneous environments. Evolution 45:1317-1331.

Vences, M., F. Glaw, and W. Böhme. 1998. Evolutionary correlates of microphagy in alkaloid-containing frogs (Amphibia: Anura). Zool. Anz. 236:217-230.

Vences, M., J. Kosuch, S. Lötters, A. Widmer, K.-H. Jungfer, J. Köhler, and M. Veith. 2000. Phylogeny and classification of poison frogs (Amphibia: Dendrobatidae), based on mitochondrial 16S and 12S ribosomal RNA gene sequences. Mol. Phyl. Evol. 15:34-40.

Vieites, D. R., M. S. Min, and D. B. Wake. 2007. Rapid diversification and dispersal during periods of global warming by plethodontid salamanders. Proc Natl Acad Sci U S A 104:19903-19907.

Vleck, D. 1987. Measurement of O2 consumption, CO2 production, and water vapor production in a closed system. J Appl Physiol 62:2103-2106.

Walsberg, G. E. 1986. Comparison of two techniquesfor estimating the maximum aerobic capacity of amphibians. Herpetologica 42:389-394.

Wang, I., A. Crawford, and E. Bermingham. 2008. Phylogeography of the Pygmy Rain Frog (Pristimantis ridens) across the lowland wet forests of isthmian Central America. Mol Phylogenet Evol 47:992-1004.

Wang, S. Y., and G. K. Wang. 1998. Point mutations in segment I-S6 render voltage-gated Na+ channels resistant to batrachotoxin. Proc Natl Acad Sci U S A 95:2653-2658.

Webb, S. D. 1985. Late Cenozoic mammal dispersal between the Americas. Pp. 357-386 *in* F. G. Stehli and S. D. Webb, eds. The Great American Biotic Interchange. Plenum Press, New York.

Weir, J. T. 2006. Divergent timing and patterns of species accumulation in lowland and highland neotropical birds. Evolution 60:842-855.

Welch, J. J., O. R. P. Bininda-Emonds, and L. Bromham. 2008. Correlates of substitution rate variation in mammalian protein-coding sequences. BMC Evol Biol 8

Wells, K. D. 2007. The Ecology and Behavior of Amphibians. University Of Chicago Press, Chicago IL, USA.

West, G. B., J. H. Brown, and B. J. Enquist. 1997. A general model for the origin of allometrical scaling laws in biology. Science 276:122-126.

White, C. R., N. R. Phillips, and R. S. Seymour. 2006. The scaling and temperature dependence of vertebrate metabolism. Biol Lett 2:125-127.

Whitlock, M. C., P. C. Phillips, F. B. G. Moore, and S. J. Tonsor. 1995. Multiple fitness peaks and epistasis. Ann Rev Ecol Syst 26:601-629.

Wiens, J. J. 2007. Review of "The amphibian tree of life" by Frost et al. Q. Rev. Biol. 82:55–56.

Wiens, J. J., and M. J. Donoghue. 2004. Historical biogeography, ecology and species richness. Trends Ecol. Evol. 19:639-644.

Wiens, J. J., J. W. Fetzner, C. L. Parkinson, and T. W. Reeder. 2005. Hylid frog phylogeny and sampling strategies for speciose clades. Syst Biol 54:719-748.

Wiens, J. J., and C. H. Graham. 2005. Niche conservatism: Integrating evolution, ecology, and conservation biology. Annu Rev Ecol Syst 36:519-539.

Wiersma, P., A. Munoz-Garcia, A. Walker, and J. B. Williams. 2007. Tropical birds have a slow pace of life. Proc Natl Acad Sci U S A 104:9340-9345.

Williams, R. J. P. 1996. From dihydrogen to dioxygen: evolution of biological oxidation-reduction. Pp. 109-141 *in* H. Baltscheffsky, ed. Origin and Evolution of Biological Energy Conversion. VCH Publishers, Inc., New York, NY.

Wilson, E. O. 1988. Biodiversity. National Academy Press, Washington, D.C. USA.

Withers, P. C., and S. S. Hillman. 1983. The effects of hypoxia on pulmonary function and maximal rates of oxygen consumption in two anuran species. J Comp Physiol 152B:125-129.

Woodward, G., and A. G. Hildrew. 2002. Body-size determinants of niche overlap and intraguild predation within a complex food web. J Anim Ecol 71:1063-1074.

Yachi, S., and M. Higashi. 1998. The evolution of warning signals. Nature 394:882-884.

Yakes, F. M., and B. VanHouten. 1997. Mitochondrial DNA damage is more extensive and persists longer than nuclear DNA damage in human cells following oxidative stress. Proc Natl Acad Sci U S A 94:514-519.

Yang, Z. 1998. Likelihood ratio tests for detecting positive selection and application to primate lysozyme evolution. Mol Bio Evol 15:568-573.

Yang, Z. 2003. PAML: phylogenetic analysis by maximum likelihood. (http://abacus.gene.ucl.ac.uk/software/paml.html). University College London, London.

Yang, Z. 2007. PAML 4: a program package for phylogenetic analysis by maximum likelihood. Mol Bio Evol 24:1586-1591.

Yang, Z. H., and R. Nielsen. 1998. Synonymous and nonsynonymous rate variation in nuclear genes of mammals. J Mol Evol 46:409-418.

Zachos, J., M. Pagani, L. Sloan, E. Thomas, and K. Billups. 2001. Trends, rhythms, and aberrations in global climate 65 Ma to present. Science 292:686-693.

Zamudio, K. R., and H. W. Green. 1997. Phylogeography of the bushmaster (*Lachesis muta*: Viperidae): implications for neotropical biogeography, systematics, and conservation. Biol. J. Linn. Soc. Lond. 62:421-442.

Zhang, J., R. Nielsen, and Z. Yang. 2005a. Evaluation of an improved branch-site likelihood method for detecting positive selection at the molecular level. Mol Bio Evol 22:2472-2479.

Zhang, P., H. Zhou, Y. Q. Chen, Y. F. Liu, and L. H. Qu. 2005b. Mitogenomic perspectives on the origin and phylogeny of living amphibians. Syst. Biol. 54:391-400.

Zwickl, D. 2006. Genetic algorithm approaches for the phylogenetic analysis of large biological sequence datasets under the maximum likelihood criterion. www.bio.utexas.edu/faculty/antisense/garli/Garli.html. The University of Texas at Austin.

Vita

Juan Carlos Santos was born in Quito, Ecuador, on September 4th 1977. He is one of the three sons of Ernesto Santos and Sara García. He lived in his native city since his childhood. His love for living things was inspired by his visits with his father to the cloud forests in the Eastern Andean Foothills. His parents gave him, since early childhood, free access to books including Science and History. His love for basic sciences and the unselfish support from his parents influenced him to follow the path of Academia. He graduated from the San Gabriel High School in 1995 and he went for a full year visit to the US. In 1996, he studied Biology at the Pontificia Universidad Católica del Ecuador. He earned a B.A. in Biology in 2002 under the direction of Luis Coloma. In the fall of 2002 he entered the Program of Ecology, Evolution and Behavior at the University of Texas at Austin under the supervision of David Cannatella. He was a teaching assistant for Genetics and Biostatistics courses. He met his wife Natalia Biani in Austin and together, they have been sharing their love for Nature. He conducted his doctorate fieldwork in Ecuador, Perú, Colombia, Panamá, and Venezuela.

Permanent address: Ventura Aguilera N57-11 y Anonas, Quito, Pichincha, Ecuador.

This dissertation was typed by the author.